

ADVERTIMENT. L'accés als continguts d'aquesta tesi queda condicionat a l'acceptació de les condicions d'ús establertes per la següent llicència Creative Commons:  <https://creativecommons.org/licenses/?lang=ca>

ADVERTENCIA. El acceso a los contenidos de esta tesis queda condicionado a la aceptación de las condiciones de uso establecidas por la siguiente licencia Creative Commons:  <https://creativecommons.org/licenses/?lang=es>

WARNING. The access to the contents of this doctoral thesis it is limited to the acceptance of the use conditions set by the following Creative Commons license:  <https://creativecommons.org/licenses/?lang=en>

Tesi doctoral
Programa de doctorat en Microbiologia

Juny 2024

UAB
**Universitat Autònoma
de Barcelona**

Universitat Autònoma de Barcelona
Departament de Genètica i de Microbiologia

Institut de Ciències del Mar
Departament de Biologia Marina i Oceanografia

Unravelling protist trophic relationships at the microscale:
Insights from chemotactic interactions and responses to light-stress events

Queralt Güell Bujons

Departament de Biologia Marina i Oceanografia
Institut de Ciències del Mar (ICM-CSIC)

Directors:

Rafel Simó Martorell

Departament de Biologia Marina i Oceanografia
Institut de Ciències del Mar (ICM-CSIC)

Albert Calbet Fabregat

Departament de Biologia Marina i Oceanografia
Institut de Ciències del Mar (ICM-CSIC)

Tutor acadèmic:

Jordi Mas Gordi

Departament de de Genètica i de Microbiologia
Universitat Autònoma de Barcelona (UAB)



June 3rd 2024

During the realization of this thesis, Queralt Güell Bujons was hired through the SUMMIT project, funded by the European Research Council Advanced Grant (ERC-2018-ADG-834162) to RS. Further funding was provided by Grant PID2020-118645RB-I00 to A.C funded by the Ministerio de Ciencia e Innovación (MCIN)/AEI/ 10.13039/501100011033. The ICM-CSIC is supported by the 'Severo Ochoa Centre of Excellence' (CEX2019-000928-S).

A les d'abans i a les de després

*I a la meva xarxa de suport
Imprescindible*

"In nature nothing exists alone"
-Rachel Carson, *Silent Spring* (1962)

ACKNOWLEDGMENTS/AGRAÏMENTS

La biosfera marina funciona gràcies a una xarxa de relacions entre organismes de tot tipus que dona vida als oceans. Entre tot el reguitzell d'interaccions existents, la cooperació és fonamental i ubiqua al sistema marí. Aquest principi també s'aplica a la nostra vida quotidiana i per tant a la realització d'un doctorat. El fonament del meu doctorat és doncs també una xarxa de connexions. La meva xarxa és molt extensa i diversa, conté molts nodes i pilars que es mereixen un agraïment exhaustiu. Comencem.

El primer node és també l'inici d'aquesta història doctoral, la persona que va decidir escollir-me i confiar en mi per aquest projecte. Rafel, gràcies per molt. Per acompanyar-me en aquest camí de ben a prop, per escoltar sempre les meves idees, per ser-hi colze a colze omplint falcons i baixant escales corrents (a 30°C i també a 0°C). Per donar-me l'oportunitat de viure somnis. Gràcies per tantes converses científiques on he après més que mai i he crescut com a investigadora. Per tot el que m'has explicat, amb paciència i amabilitat. I gràcies també per les converses més humanes, sobre escalada, sobre nosaltres, sobre la vida en general.

Les gràcies continuen en direcció al meu altre node científic, per l'Albert, que m'ha contagiats la seva fascinació per aquests protistes microscòpics que amb prou feines coneixia quan vaig arribar a l'ICM. Gràcies per les reunions eternes, al despatx o al laboratori, i per haver-me ensenyat a cuidar i entendre aquestes bestioles extraordinàries. També donar les gràcies a l'Enric, per ajudar-me sempre que li he demanat, per escoltar-me i donar-me ànims els dies de desànim.

Gràcies a l'Idan i a la Medea, per treballar plegats en el capítol 1 d'aquesta tesi, per tot el que m'han ensenyat i per tot el que han aportat.

I si avancem en els capítols, apareix l'ISCA i l'aventura australiana on cal agrair al Justin Seymour però especialment al Jean-Baptiste Raina. Thank you, JB! For teaching me through Zoom the unteachable, for all the continuous support online and in Sydney, for giving me the chance to travel halfway across the world to learn and work at your lab.

Però si la majoria d'experiments d'aquesta tesi han sigut possibles, és gràcies a la Yaiza i la Marta. Per la disposició a ajudar sempre, per les hores de suport, per ensenyar-me tantes coses i ser font de solucions de tot tipus de problemes. I aquí hi afegeixo l'Elena, per fer que la tesi en si hagi sigut possible, per facilitar de manera enorme la burocràcia, els viatges i els entrebancs que han anat apareixent en aquest camí.

Els nodes a l'ICM és multipliquen molt fàcilment. La cooperació és la base del funcionament d'aquest ecosistema que et dona l'oportunitat de conèixer persones fantàstiques. Les campanyes oceanogràfiques em venen a la memòria com els meus moments preferits. Són un submón on la ciència emergeix i fructifica com mai però també un ecosistema on la cooperació és bàsica i les relacions científiques es transformen en humanes. Fran, Eli, Elisa, Dolors, Magda, Ari, Ana, Marta, Yaiza, Rafel, sou un equip formidable, humanament i científicament. Quina sort, haver compartit campanyes amb vosaltres. Però hi ha moltes persones més que l'aventura d'aquest doctorat m'ha permès conèixer i anomenar com a amics. *Viejagente mindungui* és una super xarxa de suport de tot tipus, emocional, científic, burocràtic que sempre està disponible i que t'acompanya en la boja aventura de fer un doctorat. Tinc la sort d'haver compartit laboratori amb amics, Clàudia, Deju, sou molt més que companys de feina i sense la vostra ajuda, converses i ànims això hauria sigut molt més dur. La sort continua amb els companys de despatx, Ari, Marta, Lucía, Alan i els moments compartits. Marta i Ari, gràcies pel suport, pel bateig de submarinisme i per escoltar sempre. Marina, Aleix, Patri, Joan, Miguel, Sara, Guillem, amics i tots els companys viejagente en aquest viatge. Quina sort trobar-vos! Ana i Ari, us valoro enormement, heu sigut família antàrtica i molt molt més. Sandra, de companya de pis a bizcocho i amiga estimada, que feliç de compartir-te. Adri, vida paral·lela, suport de tot tipus, la connexió que em va obrir la porta a tot això i que segueix obrint-me la porta i despertant la meva curiositat pel món i la lluita. Que m'escolta

i m'aconsella. A tots, amics, que seguim trobant-nos i compartint moments, que seguim ajudant-nos i rient junts. Us estimo.

Però la meva xarxa no s'acaba a l'ICM, es ramifica i s'escampa per moltes bandes. La meva relació amb la microbiologia va començar a la UAB. I a part de descobrir els fascinant món dels microorganismes vaig tenir la sort de trobar-me amb persones precioses que avui en dia encara m'acompanyen. Persones amb qui obrir-se de bat a bat és lo més fàcil del món, on sentir-te entès passa sense buscar-ho. Dani, Anna B, Anna S, Eva, Ferran, Marc, Núria, Rosanna, Quim, Meri, Andrés, Konsti, sou part de la meva família, ja ho sabeu. Andrés i Konsti, you were also part of my great Austrian family, a family that shared house, cars, sweat, climbing hours, tears of joy and notthatmuchjoy. El que va unir Àustria i el roadtrip, no ho separarà ningú!

I la xarxa creix i colonitza altres territoris, santpedorencs i santpedorenques de La Famiglia, contenta de compartir-vos. Lluís i Montse, gràcies per la contínua disposició a ajudar i a ser-hi. I llavors hi ha totes aquelles persones que la vida t'ha portat a conèixer i que s'han quedat, han crescut amb tu i s'han convertit en pilars. Alba, Miki, si algú m'ha vist créixer i m'ha fet de germans adoptius, sou vosaltres. Felicíssima de seguir sentint-vos tant a prop més de 10 anys després i de veure com la família creix. Alba, les birres/cafès/vins a Vic aquests últims mesos han sigut miraculoses i un bon flotador en aquesta etapa de final de tesis, gràcies amiga! Albert, gràcies per travessar corrents mitja Barcelona per fer un cafè curtet i per escoltar tant i tant bé. Nil, per seguir dinant mentre tenim converses transcendents. Maria, Leire, sou imprescindibles a la meva terrasseta, amigues, gràcies pels moments intensos, bons i dolents, per tot lo compartit. Adri, Cris gràcies per la vostra habitació de convidats i per la vostra companyia, espero que seguim trobant moments per compartir la vida. I a l'amiga que està lluny però que sento tant tant a prop, Núria, gràcies per parlar amb mi sempre amb les comportes ben obertes, per entendre'm i sostenir-me tal com jo ho intento amb tu. Per no tenir tabús ni filtres, que passin els anys, que aquí seguirem.

I ja per anar acabant, els fonaments, la família. Tiets i tietes, iaia, avis, cosins. Tots junts formeu una xarxa indestructible. Em recarregueu les piles, em feu sentir acompanyada i molt molt afortunada de tenir-vos. Raquel, tot i lo bé que van les plantetes, em quedo amb les converses i amb les teves abraçades. Txell, els teus whatsapps arriben i si, tens tota la raó, la merda compartida fa menys pudor. Gràcies per ser-hi! Però a més, no tothom presenta els seus amics com a part de la seva família. Jo he tingut aquesta sort. Els Buvas són l'Albert, la Mireia, el David, la Joana, la Sara, el Ferran, la Clàudia, el Jordi i el Bernat. Familiars de primer grau, polítics o amics de tota la vida. És igual. El més important és que sempre hi sou, que sou zona de confort màxima i que espero tenir-vos sempre al meu costat. Gràcies per ser-hi, per riure i plorar, per donar forces, per cagar-se amb el que calgui i per l'entusiasme a celebrar qualsevol cosa.

I per acabar, la base de tot, els pilars principals. Pare, mare, no sé ni per on començar a donar-vos les gràcies. Sempre he pensat que vingués el que vingués no m'enfonsaria mai, perquè vosaltres sou a sota cada cop que caic. Us estimo moltíssim. Ferran, germà, millor amic, psicòleg, company de pis i en general company d'aventures. Ets imprescindible. Ets un regal. I el meu refugi. I l'altre refugi, l'últim pilar, però no pas el menys important. Jordi, company de rutina, company de vida. Gràcies per la tranquil·litat, per les forces, per la companyia contínua, per treure'm un somriure quan sembla impossible, per cuidar-nos mútuament, per ser un oasis dins del caos, per ajudar-me a baixar els ploms i a respirar quan tot es complica.

CONTENTS

SUMMARY	5
RESUM	6
RESUMEN	7
GENERAL INTRODUCTION	8
Planktonic food webs in the marine biosphere	8
Heterogeneity at the microscale	9
Unicellular eukaryotes	12
Microzooplankton grazing and its drivers	14
Methodological perspectives: Chemotaxis, microzooplankton grazing, and phytoplankton fitness	19
HYPOTHESES AND OBJECTIVES	23
CHAPTER 1 – THE CHEMOTACTIC BEHAVIOURAL RESPONSE OF MARINE HERBIVORE PROTISTS TO DMSP AND RELATED COMPOUNDS	26
INTRODUCTION	27
MATERIALS AND METHODS	29
RESULTS	32
DISCUSSION	39
REFERENCES	42
SUPPLEMENTARY INFORMATION	46
CHAPTER 2 – THE IN-SITU CHEMOTAXIS ASSAY (ISCA) AS A TOOL TO EXAMINE MICROPLANKTON CHEMOTAXIS	66
INTRODUCTION	67
MATERIALS AND METHODS	69
RESULTS	74
DISCUSSION	82
REFERENCES	86
SUPPLEMENTARY INFORMATION	90
CHAPTER 3 – EXPLORING THE DYNAMICS OF LIGHT STRESS AND GRAZING INTERACTIONS IN NATURAL COMMUNITIES AND MODEL SYSTEMS	93
INTRODUCTION	94
MATERIALS & METHODS	98
RESULTS	107
3.1 Light-stress treatments and responses of four phytoplankton assemblages	107
3.2 Microzooplankton grazing on light-stressed and non-stressed phytoplankton	114
3.3 Influence of grazing on phytoplankton recovery from light-stress	118
3.4 The relationship of light stress and grazing in a model system: <i>G. dominans</i> grazing on <i>I. galbana</i>	127
DISCUSSION	132
REFERENCES	140
SUPPLEMENTARY INFORMATION	147
3.1: Light-stress treatments and responses of four phytoplankton assemblages	148
3.2: Microzooplankton grazing on light-stressed and non-stressed phytoplankton	149

3.3 Influence of grazing on phytoplankton recovery from light-stress	150
3.4. The relationship of light stress and grazing in a model system: <i>G. dominans</i> grazing on <i>I. galbana</i>	155
GENERAL DISCUSSION	159
The healthy herds hypothesis	159
The plankton interactome	160
Cell aggregation. Benefit or drawback?	161
From micro to macro. A global perspective of microscale processes and their connection with biogeochemical cycles	163
Microbial plankton research beyond genomic data	166
GENERAL REFERENCES	167
CONCLUSIONS	177
ANNEX I	179

SUMMARY

Marine microbial life dominates the Earth's oceans, dictating the energy and matter flow within marine trophic networks. Chemical gradients, influenced by individual physiological responses and trophic interactions, link connections and responses at the ecosystem level to environmental disturbances. Therefore, understanding trophic relationships requires studying chemically based interactions and their environmental drivers. This thesis aims at further exploring the feeding behaviour of heterotrophic protists, the main grazers of primary production. Two major potential drivers of selective grazing are studied: chemotaxis and environmental stress. In **chapter 1** we used the microcapillary technique and image analysis tools to characterize the chemotactic behaviour of three heterotrophic protists (*Oxyrrhis marina*, *Karlodinium armiger*, and *Gyrodinium dominans*) towards the phytoplankton-derived compounds dimethylsulfoniopropionate (DMSP), dimethylsulfide (DMS), and acrylate. Amongst the many metabolites acting as infochemicals in the marine system, DMSP and its degradation compounds are notably significant due to their widespread abundance in the ocean, their role in phytoplankton responses to physiological stress and their chemotactic potential. While chemoattraction by DMSP was observed in the three protists, DMS induced weaker and variable responses and acrylate did not induce neither repulsion nor consistent attraction. Additionally, the chemotactic response to DMSP revealed distinct behaviours related to the protists' feeding strategies. In the presence of prey-signalling cue but absence of actual prey, *O. marina* and *K. armiger* aggregation around the DMSP source can be linked to their ability for osmotrophic uptake of DMSP. Conversely, the strict phagotroph *G. dominans*, which is not able to take up DMSP, used this compound only as signal for prey search, ultimately switching to ballistic swimming to promptly leave the cue patch. **Chapter 2** explored the chemotactic potential of DMSP and derived compounds in natural communities, using a device for in situ chemotaxis assays. Methodological artefacts and lack of consistent responses, hindered the characterization of the role of these metabolites in *in situ* conditions. In **chapter 3**, the impact of sunlight-derived physiological stress of the prey on grazing, and vice-versa, were examined. We monitored the photosynthetic efficiency and the DMSP release of phytoplankton assemblages, and microzooplankton grazing rates. The characterization of the phytoplankton response to high light exposure (including UV) revealed the importance of the previous light-history of the community in determining the impact of high irradiance on photosynthetic efficiency. Likewise, community composition was the main factor determining DMSP release upon light-stress. Interestingly, light-stress induced faster phytoplankton consumption by microzooplankton in natural communities. However, the opposite pattern was observed in a model system with cultured strains (the dinoflagellate *G. dominans* feeding on the haptophyte *Isochrysis galbana*). We then aimed to explore whether grazing influenced the phytoplankton recovery from light-stress using three approaches: (i) the dilution of natural communities, (ii) the addition of a cultivated grazer (*G. dominans*) to natural communities, and (iii) the addition of a cultivated grazer (*G. dominans*) to a cultivated phytoplankton population (*I. galbana*). In all experiments, after alleviating light-stress, recovery of the photochemical efficiency to >65% of its value before the stress was achieved within 3 to 8 hours. Faster grazing was accompanied by faster recovery of the photosynthetic efficiency across most of the experiments. Preferential grazing on the stressed prey individuals, probably mediated by the release of DMSP or other chemoattractants, is the best explanation behind the positive influence of grazing on recovery from stress. However, the observation of the same pattern in the model system, where grazing was faster on non-stressed prey, suggests the implication of other factors. Overall, this thesis provides new insights regarding the role of chemotaxis and light-stress events in trophic interactions at the microscale.

RESUM

Els microorganismes són imprescindibles per la vida als oceans, on regulen el flux d'energia i matèria a través de les xarxes tròfiques. Els gradients químics, modulats per les respostes fisiològiques individuals i les interaccions tròfiques, enllacen les connexions i les respostes dels ecosistemes amb les pertorbacions ambientals. Aquesta tesi té com principal objectiu aprofundir en el comportament i els hàbits alimentaris dels protistes heteròtrofs. Concretament, hem estudiat dos factors involucrats en la depredació selectiva: la quimiotaxi i l'estrès lumínic. Al **capítol 1** hem utilitzat microcapil·lars i eines d'anàlisi d'imatges per caracteritzar el comportament quimiotàctic de tres protistes heteròtrofs (*Oxyrrhis marina*, *Karlodinium armiger* i *Gyrodinium dominans*) vers tres compostos: dimetilsulfoniopropionat (DMSP), dimetilsulfur (DMS) i acrilat. Aquests compostos són coneguts per la seva presència generalitzada a l'oceà, per les seves funcions fisiològiques i pel seu potencial quimiotàctic. Mentre el DMSP ha mostrat una atracció química significativa en tots tres protistes, el DMS només ha provocat respostes febles i variables. L'acrilat no ha provocat ni atracció ni repulsió de manera consistent en cap dels tres organismes. En resposta als gradients de DMSP, els organismes han mostrat comportaments quimiotàctics diferents, relacionats amb l'estratègia alimentària de cadascun. L'agregació d' *O. marina* i de *K. armiger* al voltant de la font de DMSP en absència de presa real respon a la seva capacitat d'incorporació osmotròfica de DMSP. Per contra, *G. dominans*, fagòtrof estricte sense capacitat d'incorporació de DMSP, utilitza aquest compost només com a senyal en la recerca de presa i, en absència d'aquesta, acaba abandonant la font de DMSP. En el **capítol 2** hem explorat el potencial quimiotàctic del DMSP, el DMS i l'acrilat en comunitats naturals, utilitzant un dispositiu dissenyat per experiments de quimiotaxi *in situ*. Els artefactes metodològics i la manca de respostes consistents han dificultat la caracterització del paper d'aquests compostos en condicions naturals. Al **capítol 3** hem examinat l'impacte de l'estrès fisiològic de les preses sobre la depredació i viceversa. Durant els experiments, monitoritzàvem l'eficiència fotosintètica i l'alliberament de DMSP de les comunitats fotosintètiques, i les taxes de depredació del microzooplàncton. La caracterització de la resposta del fitoplàncton a irradiàncies altes (incloent-hi la llum UV) ha revelat la importància de la història lumínica de la comunitat en determinar l'abast de l'estrès en l'eficiència fotosintètica. Altrament, la composició taxonòmica de la comunitat era el factor determinant principal en l'alliberament de DMSP a causa de l'estrès lumínic. Tal com esperàvem, l'estrès lumínic induïa un consum més ràpid del fitoplàncton en comunitats naturals. Per contra, un sistema model amb organismes de cultiu (*G. dominans* vs *Isochrysis galbana*) mostrava el patró oposat. Hem explorat també si la depredació influïa en la recuperació de l'eficiència fotosintètica, utilitzant tres mètodes: (i) la tècnica de dilucions seriades amb comunitats naturals, (ii) l'addició d'un depredador cultivat (*G. dominans*) a comunitats naturals, i (iii) l'addició d'un depredador cultivat (*G. dominans*) a una cultiu fotosintètic (*I. galbana*). En tots els experiments, l'eficiència fotosintètica es recuperava fins assolir almenys el 65% de l'eficiència original (pre-estrès) en un termini de 3-8 hores. Les taxes de depredació més altes coincidien amb una recuperació més ràpida de l'eficiència fotosintètica en la majoria dels experiments. La depredació preferencial de les preses estressades, probablement induïda per l'alliberament de DMSP o altres compostos quimiotàctics, és l'explicació més plausible a la influència de la depredació en la recuperació de l'estrès. Tanmateix, l'observació d'aquesta mateixa influència en el sistema model, malgrat que mostrava un patró de depredació oposat, suggereix la implicació d'altres factors. En conjunt, aquesta tesi aporta una nova perspectiva sobre el paper de l'estrès lumínic i la quimiotaxi en les interaccions tròfiques a la microescala.

RESUMEN

Los microorganismos son imprescindibles para la vida en los océanos, dónde regulan el flujo de energía y materia de las redes tróficas marinas. Los gradientes químicos, modulados por las respuestas fisiológicas individuales y las interacciones tróficas, entrelazan las conexiones y las repuestas de los ecosistemas con las perturbaciones ambientales. Esta tesis tiene como objetivo explorar el comportamiento y los patrones alimentarios de los protistas heterótrofos. Concretamente, hemos estudiado dos factores involucrados en la depredación selectiva: la quimiotaxis y el estrés ambiental lumínico. En el **capítulo 1** se utilizaron microcapilares y herramientas de análisis de imágenes para caracterizar el comportamiento quimiotáctico de tres protistas heterótrofos (*Oxyrrhis marina*, *Karlodinium armiger* y *Gyrodinium dominans*) hacia tres compuestos: dimetilsulfoniopropionato (DMSP), dimetilsulfuro (DMS) y acrilato. La importancia de estos metabolitos se debe a su abundancia generalizada en el océano, sus funciones fisiológicas y su potencial quimiotáctico. Mientras que el DMSP indujo una quimioatracción significativa en los tres protistas, el DMS solo motivó respuestas débiles y variables. El acrilato no impulsó de forma consistente ni repulsión ni atracción. En respuesta a los gradientes de DMSP, los organismos demostraron comportamientos quimiotácticos diferentes, ligados a su estrategia alimentaria. La agregación de *O. marina* y *K. armiger* alrededor de la fuente de DMSP en ausencia de presa real, responde a su capacidad osmotrófica de obtención de DMSP. Contrariamente, el fagótrofo estricto *G. dominans* incapaz de absorber DMSP, utiliza este compuesto solo como señal de búsqueda y termina abandonando la fuente de DMSP después de una búsqueda infructuosa. El **capítulo 2** exploramos el potencial quimiotáctico del DMSP y sus compuestos derivados en comunidades naturales, utilizando un dispositivo para ensayos de quimiotaxis *in situ*. Los artefactos metodológicos y la falta de respuestas consistentes dificultaron la caracterización del papel de estos metabolitos en condiciones naturales. En el **capítulo 3**, examinamos el impacto del estrés fisiológico de las presas en la depredación y viceversa. En los experimentos monitorizamos la eficiencia fotosintética y la liberación de DMSP de las comunidades y las tasas de depredación del microzooplancton. La caracterización de la respuesta del fitoplancton a irradiancias altas (incluyendo luz UV) reveló la importancia del historial lumínico de la comunidad para determinar el impacto en la eficiencia fotosintética. En cambio, la composición de la comunidad fue el principal factor influyente en la liberación de DMSP ante el estrés lumínico. Como hipotetizamos, el estrés lumínico indujo un consumo más rápido del fitoplancton en comunidades naturales. Sin embargo, se observó el patrón opuesto en un sistema modelo con cultivos (*G. dominans* vs *Isochrysis galbana*). Exploramos también si la depredación influía en la recuperación del fitoplancton del estrés lumínico utilizando tres escenarios: (i) diluciones seriadas de comunidades naturales, (ii) la adición de un depredador cultivado (*G. dominans*) a comunidades naturales, y (iii) la adición de un depredador cultivado (*G. dominans*) a un cultivo de fitoplancton (*I. galbana*). En todos los experimentos, la eficiencia fotoquímica se recuperó hasta alcanzar como mínimo el 65% de la eficiencia original (pre-estrés) en un tiempo de 3 a 8 horas. Las tasas de depredación altas coincidieron con una recuperación más rápida de la eficiencia fotosintética en la mayoría de los experimentos. La depredación preferencial de los individuos estresados, probablemente mediada por la liberación de DMSP u otros quimioatrayentes, es la mejor explicación detrás la influencia de la depredación en la recuperación del estrés. Sin embargo, la observación de la misma influencia en el sistema modelo, donde el patrón de depredación resultó opuesto, sugiere la implicación de otros factores. En general, esta tesis proporciona nuevos conocimientos sobre el papel de la quimiotaxis y del estrés lumínico en las interacciones tróficas de la microescala.

GENERAL INTRODUCTION

The oceans cover 70% of the Earth's surface, extending over $3.6 \cdot 10^8 \text{ km}^2$ (Charette & Smith, 2010). The marine realm is thus the largest ecosystem on Earth, dominated by microbial life. The first observations of microscopic organisms in seawater were made by Antonie van Leeuwenhoek in the early 17th century. His pioneer microscopic observations were documented in his letters to the Royal Society of London, including the famous letter on the protozoa from 1677 (Lane, 2015). Four centuries later, we now refer to the marine microbiome to emphasize the importance of microbial life in oceanic waters, where microbes surpass multicellular organisms in both biomass and diversity (Bar-On & Milo, 2019). Hence, as stated by Pomeroy et al. (2007) "Earth's Ocean is most certainly a sea of microbes". Marine microorganisms account for two-thirds of the biomass of all marine organisms (Bar-On & Milo, 2019), are responsible of half the primary production on Earth (Falkowski, 2012), influence the ocean's atmosphere and climate processes (Charlson et al., 1987; Simó, 2001; Worden et al., 2015), and regulate global biogeochemical cycles (Falkowski et al., 2008). Consequently, the importance of marine microbes cannot be disputed.

Planktonic food webs in the marine biosphere

The flow of energy and matter across food webs is the key to understanding any ecosystem (Pomeroy, 1974). The historical comprehension of oceanic trophic relations as linear food chains, from diatoms through copepods to fishes and whales, began to evolve when microorganisms and the organic matter continuum were acknowledged (Azam, 1998; Azam et al., 1983; Pomeroy et al., 2007; Pomeroy, 1974). Pomeroy's conceptual model (Pomeroy, 1974) described additional pathways from where the energy flow circulated, establishing the conception of food webs. The complexity of the novel model was complemented by Azam and collaborators' work with the definition of the microbial loop in 1983 (Azam et al., 1983). The new paradigm set the grounds for the current vision of trophic webs.

CO₂ is fixed into organic matter by phytoplankton, channelled through heterotrophic protists to metazoan zooplankton and higher trophic level carnivores. However, microbes are involved in many other pathways of the food web triggered by the existence of a diverse pool of organic material and the evolution of complex multi-faceted interactions (Worden et al., 2015). Patches of dissolved organic matter, colloids, organic gels, polymers, and alive and inert particles of multiple forms are all encompassed in the organic matter continuum (Azam, 1998; Stocker, 2012). Particulate material varies widely in size, ranging from micrometres to millimetres, and its composition strongly depends on its origin, containing organic and inorganic compounds in concentrations orders of magnitude higher than the surrounding media (Alldredge & Silver, 1988; Isao et al., 1990). Particles can be described as alive material (cells) or inert aggregates such as faecal pellets or marine snow. In both cases, their rich nutritional environment attracts microbes and triggers colonization processes implying hydrolysis and diffusion effects (Kiørboe, 2000; Kiørboe et al., 2003; Stocker & Seymour, 2012). The leaked material generates gradients and contributes to the dissolved pool of organic matter, characterised by its diversity and dynamism. Particles have their associated particle-sphere, the region immediately around the particle where DOM accumulates through metabolic transformations, active exudation, and leakage processes (Seymour et al., 2017). Plumes of substrates from zooplankton excretions increase bulk concentration in localised gradients (Peduzzi & Herndl, 1992). Nutrient patches generated by cell lyses or sloppy feeding processes establish hot spots of organic material (Smriga et al., 2016; S. L. Strom et al., 1997). Viruses, parasites, bacteria, protists, fungi, and phages contribute to the generation and continuous transformation of this pool (Worden et al., 2015). Microbial interactions driven by multiple trophic and metabolic capacities allow the recirculation of carbon and nutrients through the microbial loop, facilitating remineralization processes, new assimilation of inorganic elements into organic matter, and energy transfers to higher trophic levels (Pomeroy et al., 2007; Worden et al., 2015).

The current paradigm introduces several other layers of complexity centred on microbial connectivity and ecological drivers (Azam & Malfatti, 2007; Worden et al., 2015). Firstly, the leakage of chemicals and the widespread microbial sensing abilities, set chemical interactions as one key element governing food webs (Pohnert et al., 2007; Stocker, 2012). Secondly, environmental perturbations shape microbial responses (Kuhlich et al., 2024) as well as the dynamics of chemical communication (Taylor & Stocker, 2012; Thornton, 2014). Hence, the paradigm established by Pomeroy in (1974) and Azam et al. in (1983) needs to be continuously complemented, describing the drivers and the dynamics of microbial trophic interactions (Figure 1).

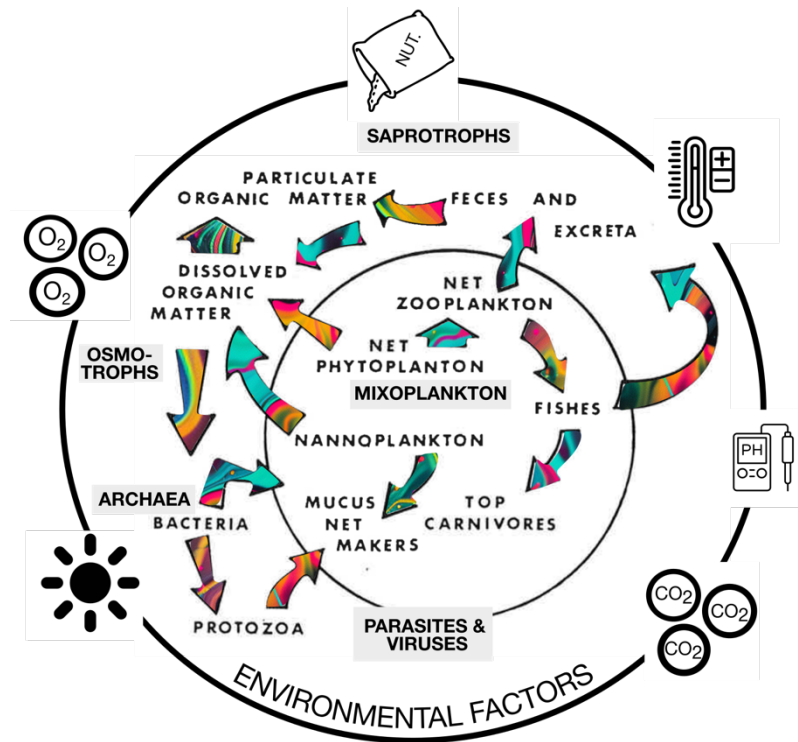


Figure 1. Trophic interactions and its drivers. The paradigm proposed by Pomeroy (1974) has been modified to highlight the importance of two drivers: chemical gradients prompting feeding relationships along the trophic network (colourful arrows) and environmental factors influencing food web dynamics (from left to right): sunlight, oxygenation, nutrient concentration, temperature, pH and CO_2 concentration. Additional food web members and feeding mechanism not recognised at Pomeroy's paradigm were also included: parasites, viruses, archaea, osmotrophs and saprotrophs.

Heterogeneity at the microscale

Ecosystems inherently consist of a multi-scale interconnected structure, from genes and metabolic pathways to populations and interactive communities, that ensures the persistence of systemic properties (productivity, diversity, resource recycling, space occupation), and altogether conforms the base of global biosphere dynamics (Cordero & Datta, 2016). Each layer of complexity needs to be examined and understood within its specific context. Thus, to study the role of microorganisms in trophic webs, spatial and temporal scales need to be adapted to the microbial perspective. Microbes perceive their surrounding environment as a patchy landscape dictated by the heterogeneity of resources and environmental conditions (Azam, 1998). Patchiness, typical in most ecosystems, is crucial for maintaining biological diversity (Levin, 1994) and triggering interactions (Stocker, 2012). The heterogeneous distribution of nutritional resources described by Azam (1998) initiated the research on the microbial behavioural responses to this heterogeneity (Figure 2A). It became evident that microscale heterogeneity generates activity hot spots (Cordero & Datta, 2016), that transforms the chemical seascape while contributing to maintain the heterogeneity (Stocker, 2012) (Figure 2B).

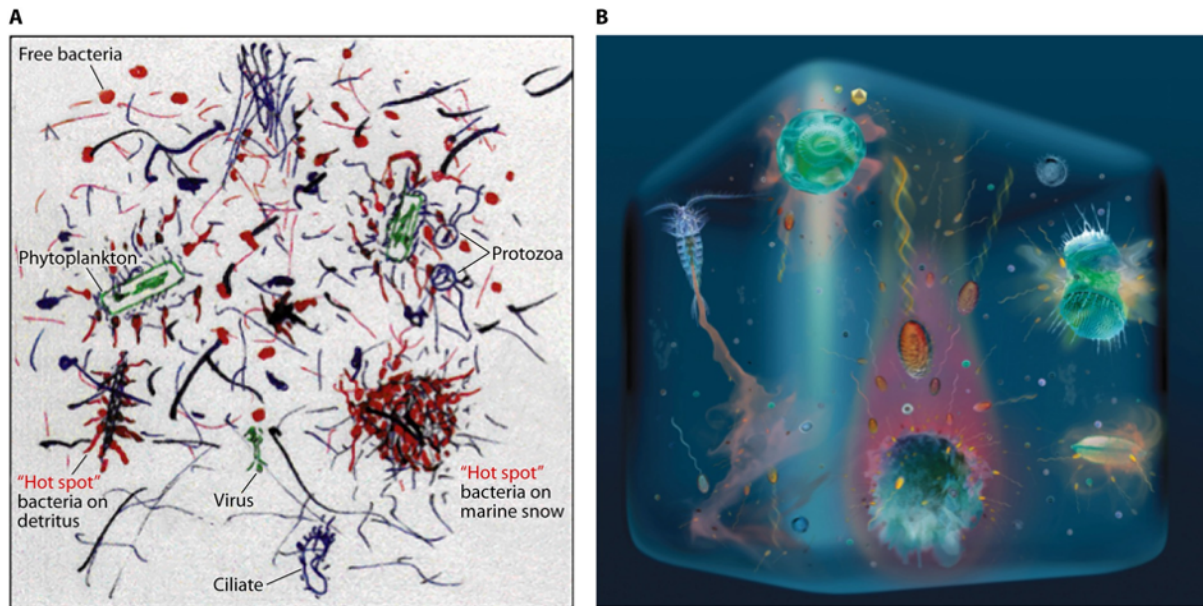


Figure 2. The heterogeneous ocean microscale. Two representations of the heterogeneity of resources and its close connection with microbial dynamics. **A.** Impressionist version of the microbial loop published in Azam (1998) illustrating the organic matter continuum and the occurrence of hotspots including both organic material and microbes. **B.** Artistic representation published in Stocker (2012) of microscale chemical gradients induced by microbial processes representing excretion plumes, phycosphere interactions, lysis events and snow particles.

Clusters of bacteria and other microbes were one of the first proof of the existence of nutrient/chemical patches triggering aggregation and heterogeneous spatial distribution (Blackburn & Fenchel, 1999). The challenge of direct visualization of the dissolved patches was overcome by reporting the symmetry of clusters and the dispersion rate, typical of point-source of substrates (Blackburn & Fenchel, 1999). Nowadays, the microarchitecture of these systems accumulates a comprehensive array of descriptors from various approaches, measuring chemical, physical, and biological features (Alldredge & Cohen, 1987; Flintrop et al., 2018; Guadayol et al., 2021; Seymour et al., 2010; Stocker & Seymour, 2012).

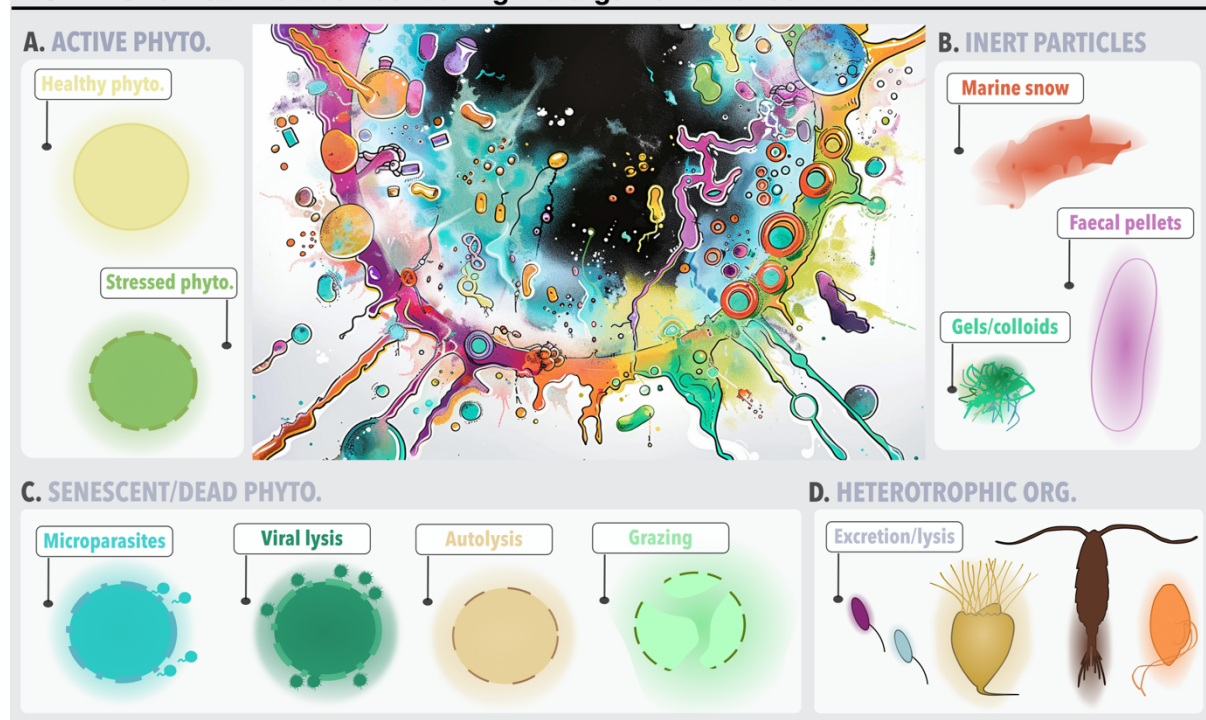
One key aspect of heterogeneity in the microscale is its physical microarchitecture. Its existence within the turbulent ocean is possible due to flow dynamics at this scale. Microscale interactions occur within a diffusion-governed environment. The diffusion boundary layer (DBL) is defined as the region adjacent to a surface, cell, or aggregate, where turbulence is quenched, and transport is characterised by low fluid velocities resulting in low Peclet numbers (Stocker & Seymour, 2012). Hence, molecular diffusion prevails over advection as the primary mode of transport. The efficiency of mixing and dispersion within the DBL is shaped by the Batchelor scale, which characterizes the size of turbulent eddies. Typical Batchelor scales in marine conditions range between 30-300 μm (Guasto et al., 2012). Thus, microscale gradients will be influenced differently depending on the size of the patch and the in-situ Batchelor scale, determining the balance between diffusion and turbulent mixing (Taylor & Stocker, 2012).

The chemical and biological microarchitectures of each microenvironment also determine the ecological processes occurring at the microscale. Species composition and chemical environment influence each other and govern the dynamics of interactive networks. Microscale communities are transient, controlled by migration patterns, feeding behaviours, and motility capabilities (Cordero & Datta, 2016). All these traits are strongly influenced by chemical gradients (Brown et al., 2019; Hay, 2009). The heterogeneous environment relies on ubiquitous gradients generated from each microenvironment and thereby provides spatial information to microbes about resource location. Therefore, sensing and directional motility are two crucial abilities advantageous to microorganisms to exploit transient nutritious resources (Stocker et al., 2008). An assorted set of directional movement responses (-taxes) have been

acknowledged in microbes as a reaction to surrounding stimuli (Stocker & Seymour, 2012). Chemotaxis refers specifically to the capacity to modulate the directional motility response as a reaction to a chemical gradient. If cells also regulate their swimming speed, the term chemokinesis is also appropriate. Chemotaxis is a widespread ability, greatly studied in bacterial ecology (Keegstra et al., 2022), but also relevant for microplankton (Brown et al., 2019; Pohnert et al., 2007) and higher trophic level organisms (Hay, 2009). Accordingly, chemically-mediated regulation impacts on multiple behaviours such as feeding, metamorphosis processes, shelter and settlement, sexual reproduction, symbiosis, and infection (Brown et al., 2019; Hay, 2009). In the microscale, it mediates in prey-predator and host-parasite interactions, allelopathy behaviour, and aggregation patterns (Brown et al., 2019). The pervasive influence of chemotaxis in the microbial world is possible thanks to the great variability of compounds and gradients existing in the sea (Stocker, 2012). Microscale chemical gradients vary in terms of chemical composition but also regarding their temporal stability and spatial distribution. The main factor dictating the chemical composition of gradients is the source of dissolved metabolites (Moran et al., 2022). Although chemical transformations are ensured through microbe colonization and aggregation (Cordero & Datta, 2016), the active or passive release from different resources will define the concentration and composition of each hot spot (BOX 1). While phytoplankton exudation processes generate steady chemical gradients in the phycosphere, other chemical environments are much unsteady. Nutrient patches of high concentration, cell lysis events, and sloppy feeding or excretion processes of motile organisms are characterised by highly unstable strong gradients (Stocker, 2012). Since chemical landscapes in the microscale are ephemeral and restricted by spatiotemporal patterns, all mechanisms optimizing arrival are enforced.

The spatial distribution of resources will control microbial aggregation patterns inducing the assembly of communities and thus their emergent ecological functions (Gralka et al., 2020). Nutrient patches induce aggregation, transforming the patch into a rich community of different trophic-level organisms (Cordero & Datta, 2016; Gralka et al., 2020). In these communities, besides nutrient uptake, predatory relationships develop, which enhance remineralization processes and boost the carbon flux by the microbial loop.

BOX 1. Chemical metabolites fuelling the organic matter continuum



Seawater is composed by an heterogenous distribution of resources ranging from particles to colloids and dissolved material composing the organic matter continuum (Azam, 1998). The continuous transformation of these resource hot-spots fuels the dissolved pool of matter and directs biogeochemical cycles (Worden et al., 2015; Moran et al., 2022). Highly diverse and dynamic composition is achieved by contributions from multiple live and dead sources intermingled in microbial interactions. Degradation and transformation of these sources by biotic and abiotic factors directly sustain the pervasive chemical gradients of the microscale, crucial to microorganisms to locate and exploit the patchy food landscape. Therefore, the organic matter continuum and its chemical environment is dependent on the different contributing sources. This box summarizes the main inputs of dissolved microbial metabolites in the marine carbon cycle.

A. Active photosynthetic phytoplankton: the kind of metabolites derived from this source depend on the phytoplankton physiological state and the release mechanisms. Healthy phytoplankton cells passively leak metabolites due to molecular diffusion of low molecular weight compounds with hydrophobic properties (Moran et al., 2022). The active excretion of specific molecules has also been detected and related to allelopathic, defence, symbiotic or mating interactions (Brown et al., 2019). Phytoplankton subjected to physiological or environmental stressors also rely on carbon export. Nutrient limitation or high irradiance can induce unbalanced growth conditions triggering the active export of excess fixed carbon, known as photosynthetic overflow (Stefels et al., 2007). However, UV radiation and other stressors can also compromise membrane integrity, allowing the passive diffusion of other metabolites (Vincent and Neale, 2000).

B. Inert particles. The release of partly digested organic matter in egested particles like copepod faecal pellets induce the dissolution of metabolites by abiotic factors or microbial transformations (Poulsen et al., 2011; Tang, 2001). Marine snow particles or other aggregates also contain gradients of DOM and act as point sources for protists, bacteria and higher trophic level organisms (Flintrop et al., 2018; Steiner et al., 2019; Kiørboe, 2000; Kiørboe et al., 2003).

C. Senescent/dead phytoplankton. Infective agents as parasites or viruses are important contributors in the liberation of endometabolites from phytoplankton cells (Klawonn et al., 2021; Suttle, 2007). Cell lysis can also be induced in senescence cells activating autocatalytic death processes triggered by different stressors (Bidle, 2015). Grazing relations also transform phytoplankton cells in smaller particles and dissolved metabolites during sloppy feeding mechanisms (Strom et al., 1997).

D. Heterotrophic organisms, from bacteria to protists and zooplankton are also able to fuel the dissolved pool by active excretion mechanisms responding to several biological functions (defence, mating, habitat finding, symbiosis interactions, grazing) and passive leakage through grazing or lysis events (Moran et al., 2022).

Unicellular eukaryotes

“Protist” is the term used to designate unicellular eukaryotes. Their high diversity is characterised by a wide collection of different sizes, morphologies, genetic repertoire, and ecological and trophic functions (Caron et al., 2012). Their phylogeny places them in every supergroup within the domain Eukarya (Keeling & Burki, 2019; Obiol Plana, 2022). In marine food webs, we can find protists representing all trophic modes, namely primary producers, strict heterotrophs, mixotrophs, osmotrophs, and saprotrophs, as well as related to symbiotic and parasitic interactions (Worden et al., 2015). Primary production and heterotrophy are the two major ecological roles. Although photo-autotrophy is easily identified by the detection of chloroplasts, the characterization of photosynthetic protists is not straightforward. High diversity, low number of cultured representatives, and missing information on phytoplankton physiology hinder the knowledge of natural photosynthetic communities (Worden et al., 2015). The discovery of mixotrophic protists, able to combine photo-autotrophy, osmo-heterotrophy and phago-heterotrophy, complicated the picture even further. Apart from constitutive mixoplankton (i.e., organisms possessing their own chloroplasts), non-constitutive species are able to ingest photosynthetic prey and retain and use their chloroplast (Duarte Ferreira et al., 2021). Photosynthetic protists are found in almost all supergroups within the domain Eukarya; archaeplastida, alveolates, stramenopiles, rhizaria and discicristates groups include photosynthetic forms (Caron et al., 2012) (Figure 3). The high phytoplankton diversity, related to either physiological or morphological characteristics, causes their dependence on different nutrient inputs and their different responses to changes in abiotic factors (Worden et al., 2015). Hence, nutrient limitation, high irradiance conditions, or changes in CO₂ levels will not influence equally all phytoplankton species (Beardall et al., 2009; Cooney

et al., 2019; Sobrino et al., 2014; Vincent & Neale, 2000). The spatial distribution and the composition of photosynthetic communities are shaped by environmental conditions, top-down and bottom-up controls. Top-down controls by predators and related trophic interactions have implications also in diversity and community assembly (Chase et al., 2002; Gralka et al., 2020). Herbivore protists are the major predators of phytoplankton in most areas and ecosystems (Calbet, 2008; Calbet & Landry, 2004; Schmoker et al., 2013). “Microzooplankton” is the term routinely used to encompass all grazers smaller than 200 μm . Despite their significant importance in marine trophic interactions, microzooplankton have received minor attention, resulting in important gaps of knowledge commonly described as the microzooplankton black box (Calbet, 2008). Microzooplankton constitute an essential building block of marine food webs. They are crucial predators over primary producers (Calbet & Landry, 2004; Schmoker et al., 2013), connect the energy and carbon flux from phytoplankton to mesozooplankton (Calbet & Saiz, 2005), and significantly contribute to the microbial loop and nutrient remineralization (Sherr & Sherr, 2002). The potential components of microzooplankton communities encompass a wide variety of groups, flagellates, dinoflagellates, ciliates, acantharids, radiolarians, foraminiferans, rotifers and several meroplankton forms that spread within the different phylogenetic breadths (Figure 3).

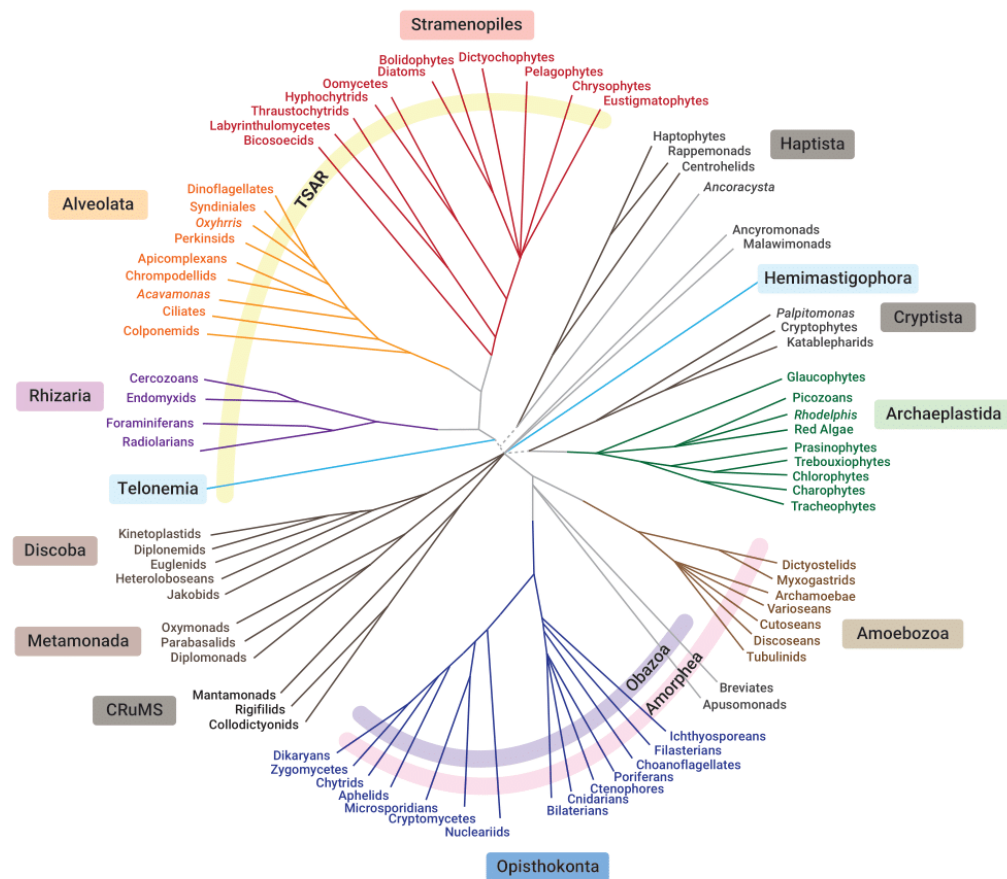


Figure 3. Eukaryotic phylogenetic scheme. Phylogenetic breadth of protists within the domain Eukarya based on phylogenomic studies and morphological and cell biological information. Adapted by Aleix Obiol based on Keeling & Burki (2019) (Keeling & Burki, 2019; Obiol Plana, 2022)

Microzooplankton grazing and its drivers

Microzooplankton (<200 μm) are the major predators in marine microbial ecosystems, consuming about 49-77% of daily primary production (Schmoker et al., 2013). However, high variability in consumption rates and predominant species occurs between different regions (Calbet, 2008; Calbet & Landry, 2004; Schmoker et al., 2013). The microzooplankton grazing impact in polar and sub-polar habitats falls typically in the lower range (53-57%) of daily consumption of primary production (PP) (Schmoker et al., 2013). The low consumption percentages are also highly variable and largely influenced by seasonal differences (Froneman et al., 1997; Schmoker et al., 2013). In temperate environments, the observed variability can be attributed to the diversity of geographic areas (oceanic, coastal, and estuarine) and the seasonal differences existing in these regions. The variability is such that the percentages of daily PP consumption can vary from 40% to 110% (Schmoker et al., 2013). Contrarily, tropical waters are much more stable regarding environmental annual cycles. These habitats accumulate the highest microzooplankton grazing rates, which can account for over 100% of the daily PP (Paterson et al., 2007). Generally, the differences in grazing rates between habitats and seasons are explained by the dynamics of planktonic community composition (Calbet, 2008; Lawrence & Menden-Deuer, 2012).

The prey preferences and feeding mode of the different microzooplankton groups encompass a diverse array of options. Three main feeding modes have been described in heterotrophic protists: interception, diffusion and raptorial feeding (Jeong et al., 2010). In interception and diffusion feeding, protists either generate currents or rely on diffusion to deliver prey into their opening structure. Raptorial feeding relies on the active search and capture of prey cells via three mechanisms: direct engulfment, pallium and peduncle feeding. Direct engulfment allows grazers to ingest the prey through the opening structure, generally limiting its feeding to smaller prey (although with exceptions). Contrarily, peduncle and pallium feeding enable protists to predate on larger cells (Jeong et al., 2010) via an extensible structure that either sucks the prey contents (peduncle) or digests the prey in the extruded sac (pallium) (García-Oliva & Wirtz, 2022). These two latter mechanisms allow the consumption of a wider prey range from dinoflagellates to naupliar states and chain-forming diatoms (Jeong et al., 2010; Sherr & Sherr, 2002). However, bacteria and small-size prey are not effectively targeted.

Flagellates are important bacterivorous typically found in the pico- (0.2 -2 μm) and nanoplankton range (2-20 μm). Ciliates and dinoflagellates (20-200 μm) are considered the main strict microzooplankton groups in terms of abundance and trophic importance (Calbet, 2008). Since ciliates mostly feed via feeding currents directed to their oral opening, they are more restricted to small-sized prey. On the contrary, the three feeding mechanisms described for dinoflagellates (pallium and tube feeding, and direct engulfment) allow them to target a wider range of sizes. Besides the selectivity dictated by the feeding mode, selective grazing relies on prey variability. Apart from distinctive attributes associated with different prey species, such as morphology or motility patterns, the same species can vary in terms of physiology and biochemical composition (Cooney et al., 2019; Meunier et al., 2012; Stefels, 2000), morphology (Gebühr et al., 2021), chemical signature (Archer et al., 2010; Thornton, 2014) and motile behaviour (Hessen et al., 1997) as a response to stressors. This intra-species variability is often a response to environmental conditions including biological, physical, and chemical drivers. Therefore, prey communities are diverse and dynamic, inducing selective grazing responses and the modulation of trophic relationships. This introduction focuses on two important drivers shaping selective grazing interactions: chemical signals and light as an environmental stressor.

Drivers (I): Chemical interactions

Food acquisition in raptorial feeding can be described in six steps: searching, contact, capture, processing, ingestion, and digestion (Montagnes et al., 2008). Chemical interactions occur in several of these steps with prevailing influence in the searching and handling time through dissolved cues and in food processing via surface receptors (Harvey et al., 2013; Roberts et al., 2011). Although the chemotactic ability of protists has been long recognised (Jennings, 1906; Spero, 1984), comprehension

of the influence of chemical signals in protists trophic interactions is far from complete. The heterogeneous distribution of resources in the microscale establishes chemotaxis as one key feature for surviving in a spatially and temporally dynamic environment (Stocker & Seymour, 2012). Hence, chemotactic-driven trophic relationships are widespread within the food web, impacting the majority of microscale interactions (Figure 4).

Swimming behaviour and motility patterns are crucial for responding to chemical gradients and optimizing the search for food resources (Stocker & Seymour, 2012). Encounter rates between prey and predators depend on size, swimming speed, motility patterns and turbulent flow (Gerritsen, 1980; Visser & Kiørboe, 2006). However, increasing the chances of finding prey also augments the probability of being found by the predators. Therefore, swimming patterns are vital to survive on the microscale and directly influence trophic relationships. “Run and tumble” and “helical klinotaxis” are two key mechanisms involved in chemotactic swimming responses (Fenchel & Blackburn, 1999). While the first one is described more for bacteria and smaller protists, helicoidal swimming influences the responses of larger cells. Helical motion defines the swimming pattern as an helicoidal path, characterised by spiral movements following a straight axis accomplished by both translational and rotational components. The term klinotaxis defines the ability to sense the direction and intensity of a stimulus to accurately orient the swimming direction (Crenshaw, 1993). The orientation is accomplished by changing the rotational components and causing a bending in the axis that changes the swimming direction (Fenchel & Blackburn, 1999). More convoluted paths cause shorter longitudinal displacement but optime spatial sampling and orientation. This ability also enables swimming in circular paths in order to stay within an interesting patch (Deuer & Grünbaum, 2006; Fenchel, 2001).

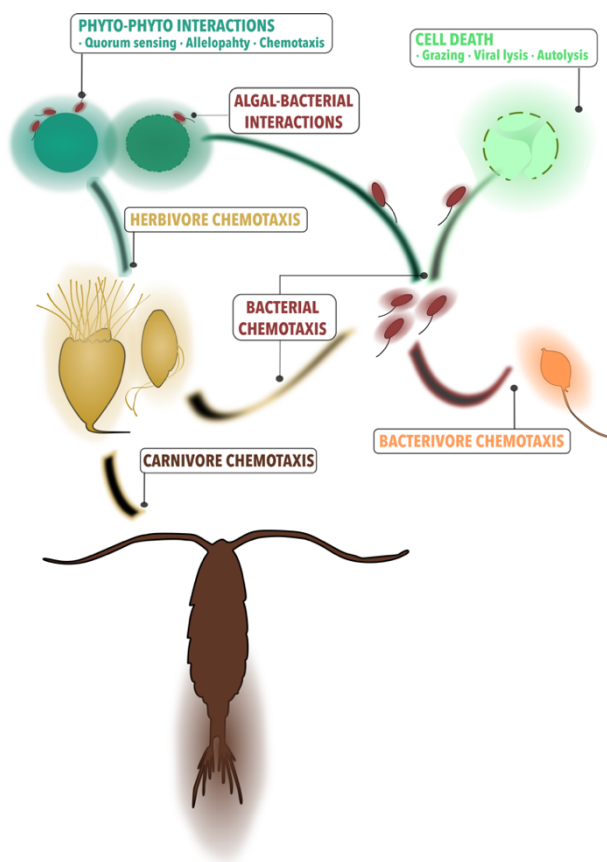


Figure 4. Chemotactic trophic interactions. The diagram illustrates how chemotaxis influences organisms' interactions at different trophic levels. The chemical gradients generated by each trophic block can trigger bacterivore, herbivore and carnivore chemotaxis, involving sensing a chemical gradient and swimming towards it to locate the preferred prey. Phytoplankton are represented at the top (green hues) together with bacteria (red). Flagellates (orange) and herbivore protists (yellow) are in the intermediate level targeting either phytoplankton or bacteria (respectively). Copepods are illustrated at the bottom level (dark brown).

The small volume and the dynamism characteristic of chemical gradients hinder the examination of their composition (Stocker, 2012). An extensive list of signals has been identified and tested in chemotactic experiments, usually focused on one predator population (Brown et al., 2019; Harvey et al., 2013; Kuhlisch et al., 2024; Pohnert et al., 2007). However, interactions are at least bidirectional and thus characterised by a complex and diverse chemical environment comprising a mixture of infochemicals originating from both interactive partners (Kuhlisch et al., 2024; Roberts et al., 2011; Smetacek, 2001). Depending on whether the focus is on the prey or the predator, we can distinguish between kairomones (i.e., chemical signals benefiting only the receiver) and phytoplankton chemical defences (Pohnert et al., 2007). Within the extensive group of kairomones including peptides, proteins, dissolved gases, and carbohydrates; a group of organic sulphur compounds stands out.

Organic sulphur is present in plants in a collection of different cellular components, including amino acids, vitamins, and some lipids (Stefels, 2000). However, in the marine sulphur cycle dimethylsulfoniopropionate (DMSP) emerges as a key element (Simó, 2001) (Figure 5). This metabolite is produced internally (DMSPp) by an extensive variety of marine phytoplankton and many bacteria (Keller et al., 1989; Zheng et al., 2020). Its physiological roles (osmolyte, cryoprotector, antioxidant, photosynthetic surplus) link its production and exudation to nutritional and environmental conditions, such as nitrogen and other nutrients availability and sunlight irradiance (Archer et al., 2010, 2018; Simó, 2001; Stefels et al., 2007; Sunda et al., 2002). However, we still lack understanding of the controls of DMSP synthesis, the dynamics of its cellular concentrations, and the triggers of its exudation. DMSP as a response to stressors may differ between communities of high and low DMSP producers, and the type and intensities of stressors (McParland & Levine, 2019; Stefels et al., 2007). When DMSP enters the dissolved pool via cell lysis or exudation processes, it acts as a chemical signal to prokaryotic and eukaryotic organisms (Seymour et al., 2010), modulating trophic relations (Edgcomb, 2021; Simó et al., 2018; Strom et al., 2020). DMSP can also be osmotrophically taken up and assimilated into cellular compounds by bacteria, phytoplankton, and microzooplankton (Kiene et al., 2000; Ruiz-González et al., 2012; Saló et al., 2009). Its accumulation in faecal or other particulate material defines these particles as other point-sources of dissolved DMSP (Steiner et al., 2019; Tang, 2001). Following the sulphur cycle, DMSP is converted to dimethylsulfoxide (DMSO) by green microalgae and bacteria (Thume et al., 2018). However, the most studied conversion is the generation of dimethyl sulphide (DMS) (and acrylate) via DMSP-lyase enzymes present in phyto- and bacterioplankton species (Alcolombri et al., 2015; Hopkins et al., 2023). Volatile DMS is metabolised by bacteria, photo-oxidised and ventilated into the atmosphere. Tropospheric DMS is crucial for aerosol formation, influencing the formation of cloud condensation nuclei and thus enhancing cloud albedo (Simó, 2001). The DMSP-lyase also generates acrylate, whose role in ecological relationships is not clear. Acrylate has been postulated as a microzooplankton repellent in bulk additions (Wolfe et al., 1997) and in high concentrations (Breckels et al., 2011). In bacterial interactions, it is described as an anti-predatory defence (Teng et al., 2021), as an antibacterial compound (Sieburth, 1960; Slezak et al., 1994), and also as a nutritive metabolite for bacteria (Raina et al., 2009; Tyssebotn et al., 2017; Xue et al., 2022).

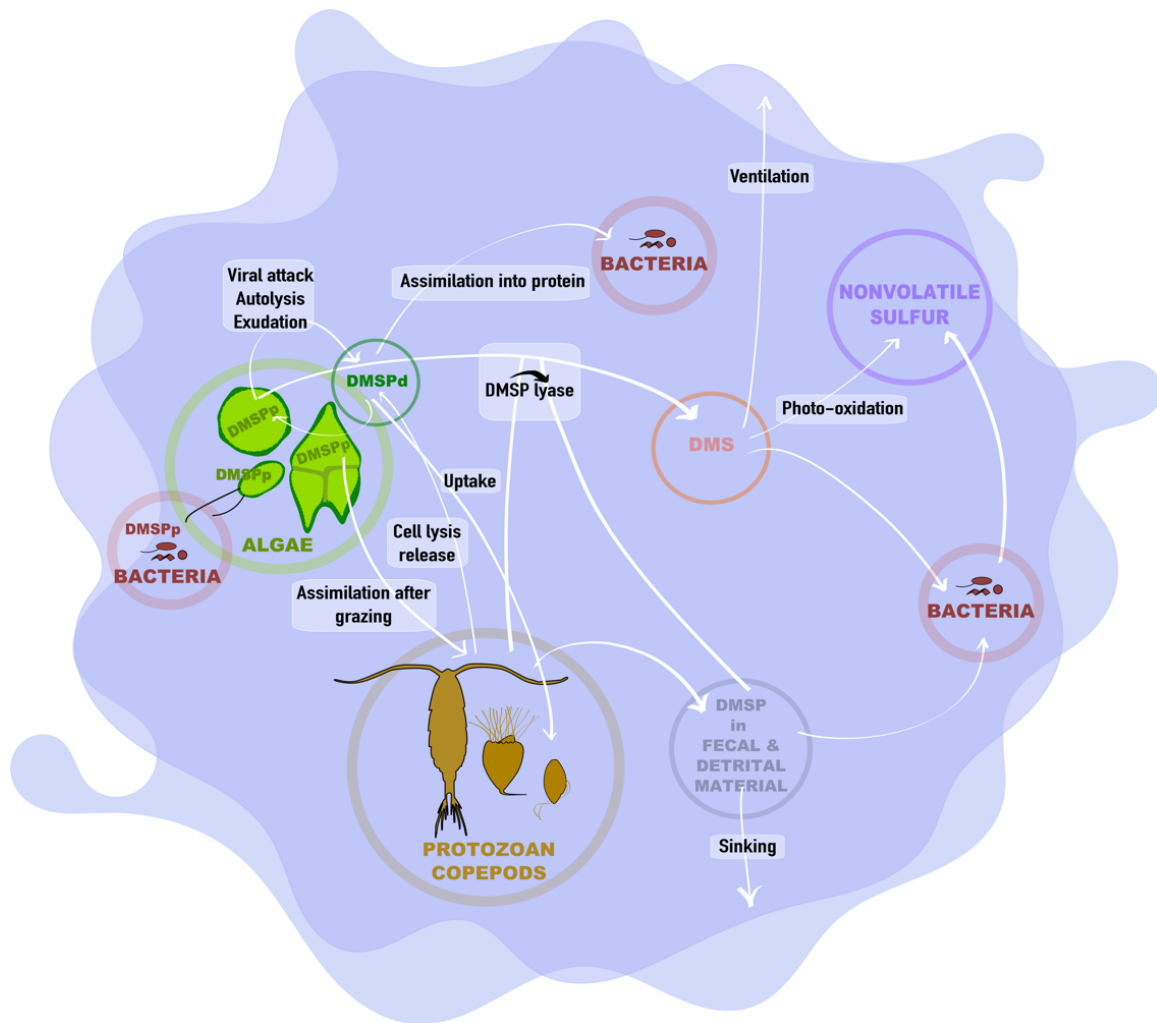


Figure 5. The organic sulphur cycle. DMSP production by algae and bacteria initiates the DMSP/DMS cycle described in the figure. Particulate DMSP (DMSPp) can either be directly taken up and assimilated by higher trophic level predators, released into the dissolved pool (DMSPd) by various process or converted into DMS by DMSP lyases. DMSP dissolved can also be taken by bacteria, phytoplankton or microzooplankton to satisfy sulphur, carbon or physiological requirements. The evolved DMS can in turn be transformed to non-volatile sulphur compounds by bacteria and photo-oxidation processes, or ventilated to the atmosphere (Hopkins et al., 2023).

DMSP and related compounds have also been suggested as triggers of tri-trophic interactions (Pohnert et al., 2007; Steinke et al., 2002). The generated DMS during microzooplankton grazing events might elicit the attraction of copepods feeding on herbivore protists, thus reducing grazing pressure over the initial phytoplankton prey. This chain of events would represent an indirect defence mechanism induced by the algae production of DMSP converted to DMS during grazing (Pohnert et al., 2007). DMS can also influence higher trophic levels and top predators, generating attractive plumes for seals, penguins or birds (Cunningham et al., 2008; Kowalewsky et al., 2006; Nevitt, 2008).

Drivers (II): Light as an environmental stressor

Environmental perturbations impact communities and generate diverse responses triggering the formation of various interactions and aggregations (Gralka et al., 2020). Consequently, environmental drivers are key regulators of ecosystem functioning including food web relationships. From all the environmental regulators, solar radiation singularity is characterised by its beneficial but also detrimental effects. Sunlight triggers primary production allowing the generation of the resources needed by heterotrophic microbes. Hence, light shapes the distribution, feeding, and growth of microzooplankton. Light and darkness periodicity determine the development of diel cycles in organisms

that adapt their physiology and behaviour accordingly (Arias et al., 2020). In microzooplankton, light triggers feeding and takes part in digestive processes (Arias et al., 2020; Jakobsen & Strom, 2004; Strom, 2001; Tarangkoon & Hansen, 2011). However, light excess and specially UV wavelengths, causes major damages in all organisms through direct and indirect effects (Vincent & Neale, 2000). The following direct effects have been described in aquatic organisms: genetic alterations, pigment and protein damage, photosynthesis and respiration inhibition, impacts on carbon allocation, nutrient uptake, nitrogen fixation and cell motility. Indirect effects are mediated by the generation of the listed reactive oxygen species (ROS): hydroxide peroxide, hydroxyl and superoxide radicals, and membrane lipid peroxides. Additionally, the photochemical conversion of some organics into more toxic forms also contributes to the indirect damages induced by UV radiation (Vincent & Roy, 1993).

From all these effects, photosynthesis inhibition has important implications in phytoplankton leakage and exudation processes, contributing to resource patchiness at the microscale (Cherrier et al., 2015; Fuentes-Lema et al., 2015; Thornton, 2014). High irradiance and UV can impact photosynthesis in several ways. Transient inhibition triggers a downregulation effect, managed through dissipation mechanisms such as fluorescence or heat emission (Tyystjärvi, 2013). However, stronger impacts can lead to structural changes affecting the molecular complex of photosystem II (Vincent & Neale, 2000; Vincent & Roy, 1993). Nonetheless, aquatic organisms display variability in their responses depending on several abiotic and biotic factors (Vincent & Neale, 2000). The biotic variables are related to the organism or community experiencing the harmful light conditions. Avoidance, screening, quenching and repair strategies will define the efficiency of protection and the extent of the potential damage (Vincent & Neale, 2000; Vincent & Roy, 1993). All these protective traits are closely linked to the light exposure history and pre-acclimation of the organism/community (Cooney et al., 2019; Zagarese & Helbling, 2003). However, the intensity, spectral irradiance, and duration of the exposure also play crucial roles in defining the outcome of the detrimental interaction (Vincent & Neale, 2000). Thus, the net stress depends on the balance between the damage mechanisms and the repair and protection strategies. The different responses of phytoplankton species to light stress induce physiological and chemical variability within the prey community (Archer et al., 2018; Cooney et al., 2019; Fuentes-Lema et al., 2015; Hessen et al., 1997; Nahon et al., 2010; Strom et al., 2020; Sunda et al., 2002). The ability of microzooplankton to rapidly sense and react to this diversity can have important effects on prey-predator interactions.

Culture-based studies documented contradictory and complex responses in grazing interactions between light-stressed phytoplankton and microzooplankton (De Lange & Lüring, 2003; Strom et al., 2020). Results pointing to either increased or decreased grazing can be found in current literature. On one side, nanoflagellates grazing on *Synechococcus* was reduced with UV-A and UV-B treatments, and the extent of grazing suppression was related with irradiance and duration of the exposure (Ochs, 1997; Ochs & Eddy, 1998). On the other side, higher grazing rates of copepods on diatom cultures exposed to high UV radiation have been found (Fields et al., 2011). Studies testing different combinations of prey and predators confirm multi-faceted responses and dependence on species-specific interactions and the surrounding conditions as the most realistic scenario (De Lange & Lüring, 2003; Strom et al., 2020). The difficulties of working with complex natural communities and the multi-faceted responses obtained with cultures, narrow our knowledge about light stress effects on trophic interactions.

DMSP and its related compounds have been extensively linked to high-light conditions, as they play hypothetical roles in protective mechanisms (Stefels, 2000; Stefels et al., 2007; Sunda et al., 2002) and climate regulation (Simó, 2001). DMS concentration in the upper mixed layer has been shown to be dependent of light effects on plankton communities (Simó & Pedrós-Alió, 1999), causing a DMS-irradiance correlation (Galí et al., 2013; Vallina & Simó, 2007). The role of DMSP in light-stress events has been related to its antioxidant properties (Sunda et al., 2002) and its function as metabolic overflow in unbalanced growth conditions such as high irradiance treatments (Archer et al., 2010; Darroch et al., 2015; Stefels et al., 2007). However, the connection of DMSP with light stress is complex and defined

by different processes that should be inspected individually. Firstly, DMSP synthesis in stress conditions might be dependent on basal DMSP concentrations, which are highly different between high and low DMSP producing taxa (Stefels et al., 2007). DMSP synthesis studies have provided contrasting results, documenting UV-mediated inhibition in natural communities (Archer et al., 2018) but increased cell-specific production in some microalgae cultures (Archer et al., 2010; Darroch et al., 2015; Sunda et al., 2002). However, changes in internal DMSP concentrations might not be directly comparable with the results of actual DMSP synthesis proven by the stable-isotopes approach (Archer et al., 2018; Stefels et al., 2009). Additionally, the phytoplankton response to light stress by increased exudation of DOC (and DMSP) (Cherrier et al., 2015; Fuentes-Lema et al., 2015; Stefels et al., 2007; Thornton, 2014) requires a separate examination. The higher DOC and DMSP exudation under high irradiance conditions observed in cultures (Archer et al., 2010; Darroch et al., 2015; Thornton, 2014) and natural communities (Cherrier et al., 2015; Thornton, 2014) is also supported by the larger DMS production observed in high-light incubations (Galí et al., 2013). Overall, despite the substantial literature available regarding DMSP as a response to stress conditions such as high irradiance, the multi-faceted roles of DMSP require more experiments to fully understand the controls and dynamics involved.

Methodological perspectives: Chemotaxis, microzooplankton grazing, and phytoplankton fitness

Studying microzooplankton selective grazing can be approached from multiple angles. This section introduces the methodological perspectives relevant to examining the interaction of chemotaxis and light stress with trophic interactions at the microscale.

Chemotaxis

The study of microbial chemotaxis began in the 1960s by the pioneering investigations of Julius Adler, inspired by the nineteenth-century research on bacterial taxis (Hazelbauer, 2012). This leading researcher also published the first method, the capillary assay, originally developed by Wilhelm Pfeffer in the 1880s (Adler, 1973; Pfeffer, 1884). The simplicity of the method lied in placing a glass microcapillary filled with a chemical solution in a bacterial suspension. Chemotaxis was either confirmed by observations under a microscope (Pfeffer, 1884) or by plating the cells accumulated inside the capillary in agar for subsequential colony counting (Adler, 1973). The first capillary-based studies with protists emerged in the 1980s, confirming chemotaxis responses to a range of amino acids, sugars, and nutritious mixtures such as yeast extract triggered in dinoflagellates and ciliates (Leick & Helle, 1983; Levandowsky et al., 1984; Spero, 1984). Nowadays, the capillary method is considered a traditional technique that has undergone multiple modifications and inspired novel configurations (Breckels et al., 2011; Fenchel, 2001; Martel, 2006). Additionally, the method foundation (i.e the qualitative or quantitative observation of the attracted cells) has been replicated in other configurations. Pipette tips (Ayo et al., 2010; Kóhidai et al., 1995) and maze structures (Ayo et al., 2009; Sibbald et al., 1987) have been developed and tested with ciliates and flagellates responding to multiple compounds. The idea behind all these methods is the creation of a point source of the chemical that triggers chemotactic reactions that can be either quantified afterwards or directly observed while happening. However, most of these devices do not reproduce natural flow speeds or turbulence events and induce artificial patterns of contact between the organisms, the device, and the chemical solution (Zimmer & Butman, 2000).

Another group of methods uses agarose and agar-based structures as point sources (Korolik & Ottemann, 2018; Wiggins & Rappoport, 2010). Similarly to the capillary method, the diffusing chemical generates cell aggregations that can be later observed and quantified.

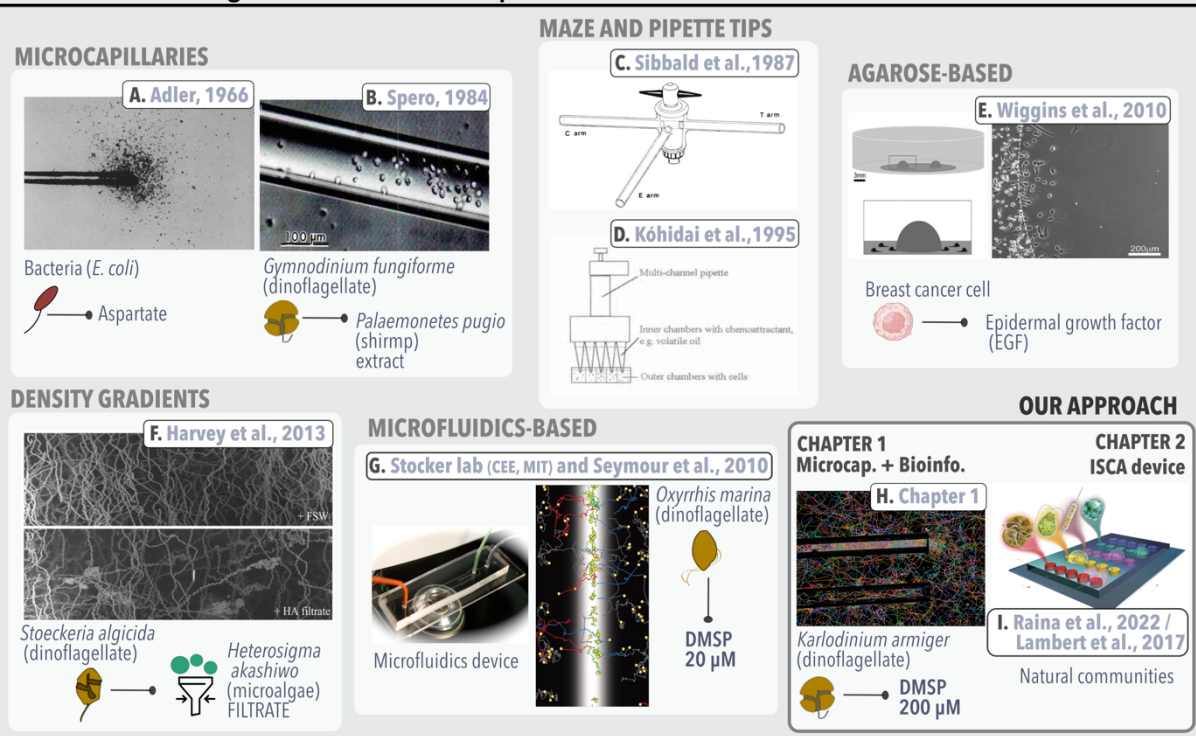
More recently, microscopic and bioinformatic techniques have allowed the examination of chemotactic behaviour in much more detail (Deuer & Grünbaum, 2006; Harvey et al., 2013; Seymour et al., 2010). Experimental setups that encompass larger temporal and spatial scales provide more comprehensive information on factors driving protist distribution and the spatial correlations between prey and predator

induced by chemical signals (Deuer & Grünbaum, 2006; Harvey et al., 2013). These setups create stable differentiated layers of chemical filtrates by a salinity gradient where chemotactic behaviour is described by recording 3D motility patterns. The first qualitative descriptions of chemotactic swimming behaviours accomplished by microscopic observations (Fenchel, 2001; Fenchel & Blackburn, 1999) laid the groundwork for the complex, detailed, quantitative analysis achieved today by bioinformatic computations. Current technology has enabled the development of microfluidic systems where both the chemical gradient and the microbial response can be meticulously controlled and analysed (Kiørboe & Jackson, 2001; Seymour et al., 2010). Microfluidic devices control the dynamics of the chemical patch diffusion applying at the same time microscopy setups to record the organism's behaviour and its swimming traits.

All these methods share one crucial drawback: their application is optimised for culture systems and laboratory conditions. As previously mentioned, microbial behaviour is significantly influenced by environmental conditions and complex biological interactions (Kuhlisch et al., 2024). Laboratory experiments exclude natural variability and poorly reflect real in-situ conditions. As a response to all these limitations, the in-situ chemotaxis assay (ISCA) was developed (Lambert et al., 2017). The microfluidic-based device generates microgradients from an array of wells into the surrounding in-situ environment. Chemotactic microbes responding to the diffused chemicals swim inside the wells and get trapped. Multiple techniques can be applied to the final content of the wells to quantify and characterize the responding community (Lambert et al., 2017; Raina et al., 2022). This device represents a pioneering advance in chemotactic methodology for in-situ analyses allowing efficient testing of chemicals and detailed characterization of microbial chemotactic communities.

A graphical summary of some of the principal methodologies used in chemotaxis experiments along the years is available in BOX 2.

BOX 2. Methodologies for chemotaxis experiments



The box illustrates a selection of methodologies used in chemotaxis experiments from the 1960s until today.

- A. The first capillary assay developed to study bacterial chemotaxis to aspartate (Adler, 1966).
- B. Microcapillary tubes prepared from glass pipettes to observe the chemotactic behaviour of *Gymnodinium fungiforme* towards an extract from the shrimp *Palaemonetes pugio* (Spero, 1984).
- C. T-maze apparatus used to test chemosensory abilities of heterotrophic microflagellates to bacterial compounds (Sibbald et al., 1987).
- D. Capillary assay based on multi-channel pipettes to examine chemotactic responses of ciliates towards volatile oils (Kóhidai et al., 1995).
- E. Agarose spot assay used to prove chemotaxis and chemokinesis in cancer cells (Wiggins & Rappoport, 2010).
- F. Stable density gradients of *Heterosigma akashiwo* filtrates to observe dinoflagellates chemo-responses with video and image analysis (FSW: filtered seawater, HA: *Heterosigma akashiwo* filtrate) (Harvey et al., 2013)
- G. Microfluidic device from the Stocker lab (CEE, MIT) used in chemotactic experiments with different cultured organisms towards DMSP (Seymour et al., 2010).
- H. Microcapillary assay coupled with imagen analysis and bioinformatic tools used in chapter 1 of this thesis.
- I. ISCA device developed by Lambert et al., (2017) to test chemotaxis in-situ natural communities. The device has been used for metagenomic analysis of chemotactic communities (Raina et al., 2022) and in chapter 2 of this thesis.

Microzooplankton grazing

The vast majority of studies of protist grazing have been conducted with monocultures in laboratory conditions due to the difficulties in identifying and characterizing the high diversity of protists and their behaviours in the natural environment (Weisse et al., 2016). Functional and numerical responses are the key metrics used to examine protists functional biology. The functional response described in the 1960s by the ecologist C.S. Holling (Holling, 1965), relates ingestion rates and prey concentration to quantify predator-prey interactions. The most established response for protists matches the Type II model, describing an initial increase of ingestion rates as prey concentration increases until reaching prey saturation conditions from where maximum ingestion and searching rates remain constant (Kjørboe et al., 2018). Also related to the quantity of ingested prey, the numerical response describes the growth rate of the predators following the same function observed in grazing interactions (Weisse et al., 2016). The description of these parameters contributed greatly to the description of protist functional biology. However, as occurred with chemotactic experiments, the use of functional and numerical responses is mostly restricted to monocultures and lab conditions. Hence, although culture-based studies try to mimic environmental conditions to observe protist responses, natural communities and actual in-situ dynamics are left out of the picture (Weisse et al., 2016). However, studying microzooplankton grazing in natural communities was hindered by the difficult identification of the involved organisms and the impossibility of separating prey and predators by size. The implementation of the dilution technique by Landry & Hassett (1982) overcame this last difficulty. This breakthrough triggered the quantification of grazing in natural communities allowing further understanding of microbial food webs and the role of protists in carbon and energy transfers. Although becoming the most used method, several drawbacks have been described. Trophic cascades (Calbet & Saiz, 2013), mixotrophy (Duarte Ferreira et al., 2021), top-down controls (Schmoker et al., 2013), grazing overestimation (Dolan, & McKeon, 2005), dilution effects on phytoplankton growth (Stoecker et al., 2015) and non-monotonic functional responses (Abrams, 2022) are some of the non-considered factors that can interfere with the dilution technique results. However, since no proper alternative is available, it is still widely used in the field.

Phytoplankton fitness

Chemical gradients and grazing interactions are both closely related to phytoplankton responses to biotic and abiotic surrounding conditions and their physiological consequences. Stressors impact phytoplankton fitness and influence physiological and chemical feedbacks (Sheyn et al., 2016; Smriga et al., 2016; Thornton, 2014; Vincent & Neale, 2000). Within the wide diversity of biotic and abiotic stressors, the role of solar radiation has been featured in this thesis. Measuring the effects of sunlight stress and phytoplankton recovery can be confronted from different perspectives. High irradiances

induce direct and indirect damage to aquatic organisms that affect several physiological mechanisms (Vincent & Neale, 2000). Direct detrimental effects can be assessed by targeting either the indirect stressors (e.g., reactive oxygen species, ROS), the damage (e.g., membrane integrity, DNA damage, or cell death) (Brussaard et al., 2001; Sobrino et al., 2014), or the physiological consequences that they trigger. In vivo assays of phytoplankton stress require targeting the indirect stressors or the physiological consequences. The overproduction of ROS can be monitored with biochemical assays using fluorescent probes (Sheyn et al., 2016; Suschek et al., 2001). The obvious candidates for targeting physiological responses in phytoplankton are those related to primary production mechanisms. ^{14}C assimilation and measurements of esterase activity are used to assess carbon acquisition metabolism in photosynthetic cells (Sobrino et al., 2014). Impairment of the photosynthetic machinery by either direct damage to some proteins and enzymes or by downregulation mechanisms has also been examined and documented as a response to high irradiances and UV treatments (Vincent & Neale, 2000). A non-destructive and fast technique with the capability for in-situ measurements is the monitoring of the photosynthetic efficiency by Fluorescent Induction and Relaxation systems (FIRE) and Pulse-Amplitude-Modulation fluorometry (PAM) (Gorbunov et al., 2020; Sobrino et al., 2014). Photosynthetic efficiency is determined by the ability of the photosystem II to process light energy via the photochemical pathway (Butler, 1972; Cullen & MacIntyre, 1998). Excess energy is dissipated by light reemission as fluorescence and non-photochemical quenching (NPQ) as heat (Butler, 1972; Cullen & MacIntyre, 1998; Gorbunov & Falkowski, 2022). FIRE and PAM systems are able to resolve photon energy budgets by determining photosynthetic performance and thus providing insight into light-stress responses of photosynthetic organisms (Gorbunov & Falkowski, 2022).

Finally, both culture-based methods and natural community approaches are required to improve our knowledge about plankton grazing interactions and their drivers. Acknowledging and reducing culturing bias is crucial for establishing adequate laboratory experiments (Weisse et al., 2016). Highly detailed documentation of organisms' behaviour can only be achieved in species-specific experiments performed with cultures in lab-controlled conditions. However, it is still as important to welcome a certain level of unpredictability in experiments with natural assemblages to grasp a portion of the actual dynamics occurring in the environment.

HYPOTHESES AND OBJECTIVES

The general aim of this thesis is to understand the implications of chemotaxis and light-stress events in protist trophic interactions at the microscale.

Trophic interactions are key drivers of any ecosystem, dictating the flow of energy and matter, the connectivity between its inhabitants and thus the ecosystem's ability to respond to environmental perturbations (Pomeroy, 1974; Worden et al., 2015). Environmental stressors are important drivers of community assembly and producers of variability by inducing differential responses within the stressed individuals. Physiological internal responses are often translated into the surrounding environment by the release of metabolites and the generation of chemical plumes. In the heterogeneous microscale, chemical gradients, and thus chemotactic abilities, are key to locating hot spots of resources and inducing organisms' interactions. Hence, chemotaxis and stress responses are two related factors with significant implications in microscale relationships.

Although heterotrophic protists are the major consumers of marine primary production (Schmoker et al., 2013), notable knowledge gaps regarding their feeding behaviour hinder the full comprehension of their trophic interactions. Incomplete knowledge regarding prey selection, trophic strategies, and feeding rates in the dynamic context of the microscale is identified as a limiting gap influencing both the fields of protist ecology and biogeochemical cycles (Worden et al., 2015). Protist selective feeding and trophic strategies have been acknowledged, but not yet fully comprehended. Therefore, this thesis has studied two expected major drivers of selective grazing (namely, chemotaxis and environmental stress) with cultured protists and natural communities. The thesis is organized in three chapters. Chapter 1 documents microcapillary assays to describe the chemotaxis responses of three cultured protists to three marine metabolites: DMSP, DMS, and acrylate. These chemicals are known as important elements of the carbon and sulphur cycles (Hopkins et al., 2023; Moran et al., 2022) but also as putative infochemicals potentially shaping a wide range of interactions within different trophic levels (Seymour et al., 2010; Shemi et al., 2021; Steinke et al., 2002). The three distinct protists examined allowed the description of different chemotactic behaviours linked to their specific trophic strategies. The results obtained are described with an ecological perspective. Chapter 2 details the potential application of an in-situ chemotactic assay (ISCA, Lambert et al., 2017) for chemotaxis experiments targeting heterotrophic protists in natural communities. The methodological caveats are described. Chapter 3 focuses on the role of solar radiation as a stressor of microplankton, characterizing its effects on the phytoplankton assemblage in terms of photochemical efficiency and DMSP exudation. Light-stressed phytoplankton is subsequently evaluated as prey for light-exposed and non-exposed microzooplankton communities and cultures to look for preferential grazing patterns while monitoring photosynthetic efficiency recovery of the prey. This approach allowed to examine whether preferential predation on stressed prey occurs and, if so, whether this enhances the photosynthetic performance of the prey population, in the context of the healthy herds hypothesis (Laundon et al., 2021; Packer et al., 2003).

Specific objectives and hypotheses

The general aim of this thesis was fulfilled by defining four main hypotheses addressed by several objectives.

HYPOTHESIS 1: DMSP and DMS will trigger positive chemotaxis in herbivore protists.

Objective 1. To examine the chemotactic potential of DMSP, DMS and acrylate for herbivore protists.

To this aim, we develop a microcapillary assay to address these specific objectives:

- To observe the space and time resolved chemotactic response of individual cells of cultured dinoflagellates to cue gradients by image analysis tools.
- To quantify dinoflagellate cell aggregation and cell distribution patterns induced by chemical gradients.

- To describe the swimming behaviours of cultured dinoflagellates in response to chemical gradients and relate them to their trophic modes and chemotactic behaviours.
- To relate the dinoflagellates' chemotactic responses to their feeding strategies by testing their osmotrophic uptake of ^{35}S -DMSP.
- To test DMSP, DMS and acylate chemotactic potential in natural communities using a method for in-situ chemotaxis assays.

HYPOTHESIS 2: Light-stress events induce DMSP release in phytoplankton assemblages and cultures.

Objective 2. To document the effects of light-stress events on phytoplankton assemblages.

- To characterize light-stress events by relating irradiance doses to decreases in the photosynthetic efficiency of the phytoplankton assemblage.
- To evaluate potential DMSP release due to light stress by measuring bulk dissolved DMSP concentrations.
- To examine relationships between sunlight exposure, phytoplankton photosynthetic stress and DMSP release.

HYPOTHESIS 3: Light-stressed communities and cultures are grazed more than their healthier counterparts.

Objective 3. To test the effects of phytoplankton light-stress on microzooplankton grazing with cultures of model organisms and natural communities.

- To quantify and compare phytoplankton consumption in control and light-stressed natural communities.
- To investigate if there is differential grazing of microzooplankton on control and light-stressed, natural phytoplankton assemblages, using cultured microzooplankton.
- To compare the results obtained with natural communities with those obtained with a model culture-based system: *G. dominans* grazing on *I. galbana*.

HYPOTHESIS 4: Higher grazing pressures on light-stressed prey will improve phytoplankton recovery from stress.

Objective 4. To investigate the influence of grazing on phytoplankton recovery dynamics from a light-stress event.

- To modify the micrograzing pressure in natural communities by two distinct approaches: the dilution technique and the addition of a cultured grazer.
- To characterize and quantitatively monitor the recovery of phytoplankton photosynthetic efficiency in parallel to monitoring mortality by grazing.
- To compare the results obtained with natural communities with those obtained with a model culture-based system: *G. dominans* grazing on *I. galbana*.

The four hypotheses of this thesis suggest a sequence of events that potentially relate chemotaxis, light stress and selective grazing in protistan communities (Figure 6). Note, however, that each of the hypotheses may hold by itself even if the others are falsified. Hypothesis 1 and related objectives are addressed in chapters 1 and 2, using either culture-based models and natural communities, respectively. Hypothesis 2-4 together with objectives 2-4 are developed through chapter 3 sections: hypothesis 2 is targeted in section 3.1, hypothesis 3 in sections 3.2 and 3.4 and hypothesis 4 in sections 3.3 and 3.4.

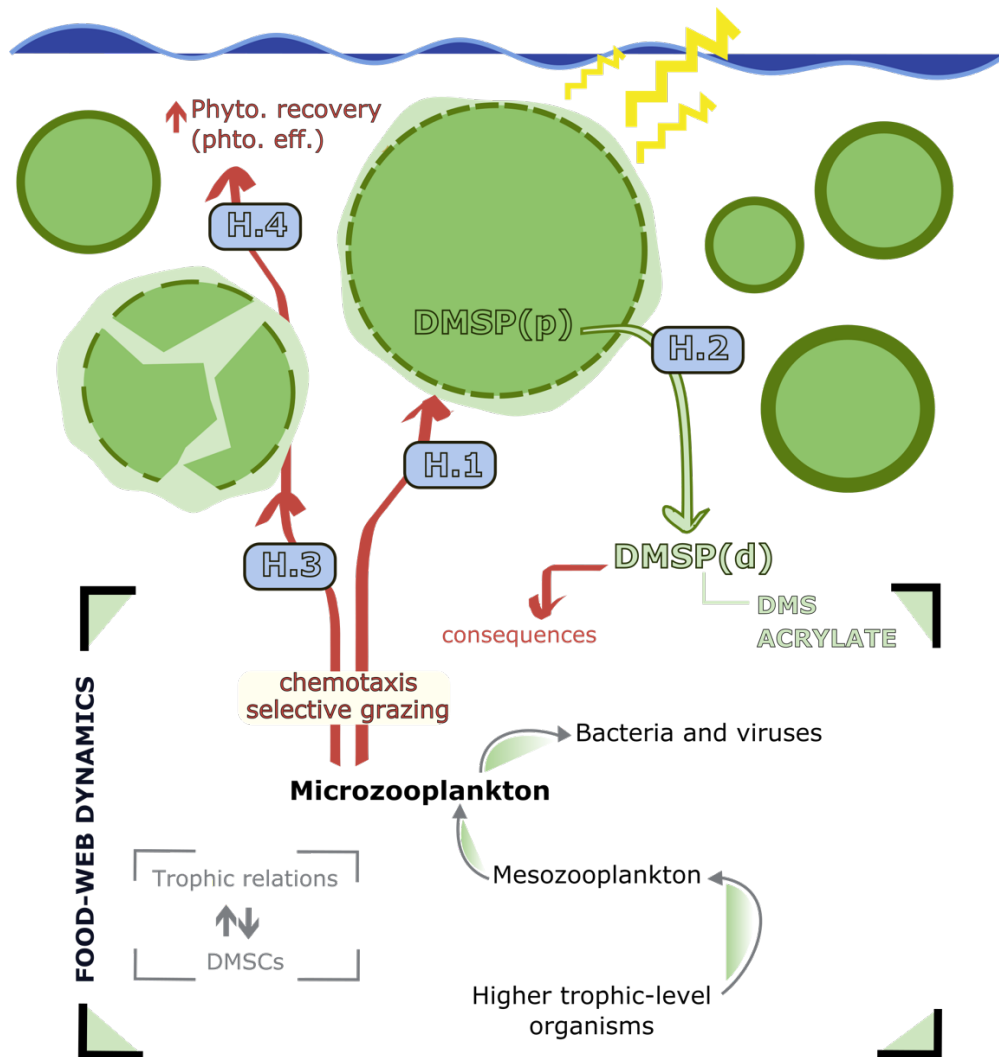


Figure 6. Thesis hypotheses describe a sequence of events that relate chemotaxis, light stress and selective grazing in protistan communities. The schematic diagram represents a phytoplankton assemblage (green circles) under high irradiance conditions (yellow symbols). The light stress may induce the release of DMSP into the dissolved pool (H.2) where it triggers consequences throughout the food web. Microzooplankton selective grazing may be driven by chemotactic responses (H.1), leading to preferential predation on the DMSP-releasing stressed cells (H.3). This would induce an overall benefit for the whole phytoplankton assemblage by removing low-fitness individuals (H.4). (Phyto. Recovery: phytoplankton recovery. Phyto. Eff = photosynthetic efficiency).

■ CHAPTER 1 –

THE CHEMOTACTIC BEHAVIOURAL RESPONSE OF MARINE HERBIVORE PROTISTS TO DMSP AND RELATED COMPOUNDS

Queralt Güell-Bujons, Medea Zanolli, Idan Tuval, Albert Calbet and Rafel Simó

The contents of this chapter have been included in an article submitted in the ISME Journal, currently under revision.

INTRODUCTION

Chemotaxis and microzooplankton grazing

Emerging marine ecosystem properties, like nutrient recycling and carbon and energy fluxes, can be quantified at the meso- and regional scales using biogeochemical tracers and proxies. However, true comprehension lies in delving into the microscale realm, where planktonic microorganisms thrive and interact (Azam & Malfatti, 2007; Fenchel, 2002; Seymour et al., 2017). In this dynamic environment, marine microbial interactions are often driven by chemical cues, which play crucial roles in feeding behaviour (Grünbaum, 2002; Seymour et al., 2017), cooperation and competition strategies (Brown et al., 2019; Garcés et al., 2013) and grazing relationships (Harvey et al., 2013; Roberts et al., 2011). Within this playground of planktonic chemical cross-talking, observed chemotactic responses of motile microorganisms have multiple potential ecological implications still to be discovered. Microzooplankton account for most of the daily grazing on phytoplankton across the oceans (Calbet & Landry, 2004). Grazing constitutes a multifaceted predator-prey interaction in which chemical cues, alongside other factors such as nutritional quality, behaviour, and defensive responses of the prey, play crucial roles (Deuer & Grünbaum, 2006; Hamm et al., 2003; Pohnert et al., 2007). Nevertheless, the extent to which microzooplankton respond to microscale chemical gradients in terms of prey selection and preferential grazing on specific individuals or populations remains largely unresolved. If chemical-based prey selection is confirmed as a widespread behaviour, it would challenge the way grazing is modelled, which currently relies on neutral encounter rates defined by predator and prey densities (Gerritsen & Strickler, 1977), relative speeds (Visser & Kiørboe, 2006) and the use of size-based frameworks (García-Oliva & Wirtz, 2022).

DMSP, DMS and acrylate: Relevance and chemotactic potential

Amongst the myriad compounds that can act as chemical cues for marine micrograzers (Brown et al., 2019; Hay, 2009; Pohnert et al., 2007), dimethylsulfoniopropionate (DMSP) and related compounds hold particular importance due to their pervasive presence in the pelagic ocean (Simó, 2001) and their chemotactic potential (Seymour et al., 2010). DMSP is produced as a cellular solute by most marine algae and many bacteria (Keller et al., 1989; Zheng et al., 2020), where it plays several physiological roles (osmolyte, antioxidant, metabolic overflow), particularly under stress conditions (Simó, 2001; Stefels et al., 2007). Intracellular concentrations span orders of magnitude amongst taxa (undetectable - 100s mM), varying greatly with physiological responses to stressors (Archer et al., 2010, 2018; Stefels et al., 2007; Sunda et al., 2002), and reaching up to 10% of the total cell carbon in highly productive microalgae such as haptophytes and dinoflagellates (Keller et al., 1989; Stefels et al., 2007). Taxonomy and physiology-dependent variability results in a wide range of particulate DMSP concentrations in the ocean (5-4000 nM) (Kiene et al., 2000, 2019). Overall, the global open ocean DMSP production is estimated to be 3.8 Pg C/year (Galí et al., 2015). Within the marine environment, DMSP is partly converted into dimethylsulfide (DMS) and acrylate by DMSP-lyase enzymes hosted by phyto- and bacterioplankton species (Alcolombri et al., 2015; Hopkins et al., 2023). The conversion of DMSP to DMS initiates another cycle that expands beyond the ocean environment into the atmosphere. Global DMS emissions amounts 15-40 Tg S year⁻¹ and accounts for most of the biogenic atmospheric sulphate (Hopkins et al., 2023). The release of DMSP, DMS, and acrylate occurs from various point sources, including phytoplankton cells experiencing oxidative stress (Sunda et al., 2002) or excess of reduced sulphur (Stefels et al., 2007), faecal pellets and other aggregates colonised by bacteria (Steiner et al., 2019; Tang, 2001), as well as algal cells disrupted by viral attack or grazing (Evans et al., 2007; Simó et al., 2018). The low background concentrations of dissolved DMSP typically measured in bulk seawater (1 – 25 nM; Kiene et al., 2000) reflects its fast turnover (1-129 nM·d⁻¹, Kiene et al., 2000). Actually, once released, these compounds may accumulate in the phycosphere or particle-sphere, which is the high viscosity zone surrounding cells or aggregates. This area is enriched with released organic molecules, with concentrations orders of magnitude higher than those found in the background

seawater (Guadayol et al., 2021; Seymour et al., 2017). Although modeled dissolved DMSP-related compound concentrations in the phycosphere may fluctuate from the low nanomolar range to micromolar levels (Breckels et al., 2010; Fredrickson & Strom, 2008), bursting cells, or high viscosity spheres around cells or aggregates, are more likely to generate patches with micromolar concentrations. Within and beyond this sphere, the diffusion of chemicals leads to the formation of submillimetre patches and gradients (Azam & Malfatti, 2007), providing a potential microscale landscape that influences trophic interactions (Edgcomb, 2021; Hopkins et al., 2023; Seymour et al., 2010).

Point-sourced DMSP is a powerful chemoattractant for a diverse range of marine organisms, including bacteria, phototrophic and heterotrophic protists, and fish (DeBose et al., 2008; Miller et al., 2004; Seymour et al., 2010). However, it has also been suggested to act as a grazing deterrent for some herbivorous protists in experiments with bulk additions (Fredrickson & Strom, 2008; Strom et al., 2003) and when DMSP release from microalgae is triggered under light stress (Strom et al., 2020). Thus, the DMSP chemotactic role in grazing is still under examination. Conversely, DMS is well-known for triggering searching behaviour in birds, turtles, and seals (DeBose et al., 2008; Kowalewsky et al., 2006; Nevitt, 2008), yet its chemoattraction for microbial plankton, particularly protists, appears to be weaker compared to DMSP (Breckels et al., 2011; Seymour et al., 2010; Teng et al., 2021). In zooplankton, DMS has shown searching and grazing-enhancing effects (Shemi et al., 2021; Steinke et al., 2006). Regarding acrylate, while it was initially postulated as a predator repellent (Wolfe et al., 1997), actual evidence supporting this notion remains scarce (Teng et al., 2021).

Our aims and approach

In this study, we aimed to explore the chemotactic response of three herbivorous dinoflagellates — *Karlodinium armiger*, *Oxyrrhis marina*, and *Gyrodinium dominans*—to variable microscale gradients of DMSP, DMS, and acrylate to address **hypothesis 1** (*DMSP and DMS will trigger positive chemotaxis in herbivore protists*). To achieve this, we used a modified microcapillary assay (Breckels et al., 2011; Martel, 2006), accompanied by video recording and state-of-the-art image analysis tools. The three microzooplankters were selected for their distinct trophic modes: *K. armiger* is a mixotroph that combines heterotrophy and photosynthesis (Berge et al., 2008), *O. marina* is an efficient phagotroph and osmotroph (Droop & Pennock, 1971), and *G. dominans* is a strict phagotroph (Jeong et al., 2010). All three species are known consumers of DMSP producers (Berge et al., 2008; Deuer & Grünbaum, 2006; Kang et al., 2020; Kim & Jeong, 2004; S. Strom et al., 2020) but vary in habitat preference and feeding behaviours. While *O. marina* preferentially occurs in intertidal pools, salt marshes and embayments (Watts et al., 2011), *G. dominans* and *K. armiger* thrive in coastal and open ocean waters, with *G. dominans* even found in red-tide dinoflagellate blooms (Nakamura et al., 1995). *K. armiger* diet includes a wide range of prey sizes, including large inert particles where DMSP may accumulate (Poulsen et al., 2011; Tang, 2001).

MATERIALS AND METHODS

Experimental cultures. All three dinoflagellate cultures (*O. marina* ICM-ZOO-OM001, *G. dominans* ICM-ZOO-GD001 and *K. armiger* ICM-ZOO-KA001) were originally isolated from the NW Mediterranean by A. Calbet in 1996, 2011, and 2013, respectively. *Rhodomonas salina* strain K-0294, was obtained from the Scandinavian Culture Collection of Algae and Protozoa at the University of Copenhagen and cultured in the Institute of Marine Sciences (ICM-CSIC) since 2018. We maintained the dinoflagellate cultures with autoclaved filtered seawater (FSW) on a 14:10 hour light to dark cycle at 19°C, 50 $\mu\text{E m}^{-2} \text{s}^{-1}$ of light, and with a *R. salina* diet. The prey culture was kept in FSW supplemented with f/2 medium (Guillard, 1975) under the same conditions than the microzooplankton cultures, but with a higher light intensity (100 $\mu\text{E m}^{-2} \text{s}^{-1}$). The cell concentration of both the grazer and prey populations were monitored regularly with a Multisizer™ 3 Coulter Counter (Beckman Coulter). The prey used to feed *O. marina* was previously concentrated by centrifugation at 1000 x g for 10 min. Prior to the experiments, the dinoflagellate cultures were starved until the majority had no prey left in their vacuoles and no prey were present in the culture. Dilutions of the cultures were made as needed to achieve the required microzooplankton concentration (8E+03 for *K. armiger* and 2E+04 for *O. marina* and *G. dominans*). For the experiments we used artificial seawater (ASW) both as control and dilution medium for the substrates (Supplementary Information).

Microcapillary assay. To assess the chemotactic potential of DMSP, DMS and acrylate we employed a microcapillary technique (Adler, 1973) previously modified (Levandowsky et al., 1984) and adapted to *O. marina* cultures (Martel, 2006). The microcapillaries (CM Scientific) were square-shaped and manufactured in borosilicate glass, 0.2 mm wide per 50 mm long, and with a wall thickness of 0.100 mm. The three dinoflagellates were tested against three chemicals: DMSP (TCI America), DMS (Sigma-Aldrich) and sodium acrylate (Sigma-Aldrich), each in 3 concentrations: 2, 20 and 200 μM . Solutions of each substrate were prepared on the day of the experiment by serial dilutions with ASW. The experiment consisted of incubations of microcapillary pairs filled by capillary action with solutions of the substrate of interest, and ASW as the control solution (Supplementary Information). The capillaries were placed on the bottom of a sterile Petri dish (8.5 cm diameter) filled with 15 ml of the culture to be tested (Figure 1.1A). The assays were recorded using a Leica DMil bright field microscope with 25x magnification and the Leica MC170HD camera acquiring images at 30 frames per second. The videos lasted ten minutes except for the 200 μM DMSP assays with *G. dominans* and *O. marina* cultures, where the experiment was stopped after 5 min. Each chemical and concentration combination was tested in triplicates, except for *K. armiger* experiments, which were tested only once. Minor adjustments to the setup were made for *K. armiger* assays, where the capillaries were cut in half and placed in smaller (5 cm) Petri dishes. We handle the capillaries with tweezers to avoid contamination.

Image analysis and trajectory tracking. The video records were individually inspected to obtain 10 min or 5 min long videos of steady image after addition of the capillaries. Each video was pre-processed by subtracting the background from each frame to eliminate any static features, such as the capillaries and debris. The background image was used to extract the coordinates of the capillaries' internal perimeter and of the central point of the capillary entrance, set as the origin of the coordinates system (Figure 1.1B). Individual cells were located in every frame and their trajectories were reconstructed using the Python package Trackpy 0.5 (10.5281/zenodo.4682814) (Figure 1.1C-E).

Cell accumulation and chemotactic index calculations. The average concentration of cells was determined during the total recording period and across all recording area, highlighting the locations most frequently visited by each organism (Figure 1.2A, C, E). The concentration profiles were calculated in two areas of space where cell accumulation was observed: inside the capillary and in the external semi-circular region centred in the origin (Figure 1.1B and Figure 1.2 B, D, F, Supplementary

Information). Reflecting the symmetry of the infochemical gradient, the concentration profiles were calculated along the capillary axis inside and radially outside. The concentrations profiles were fitted to a decaying exponential function [1]:

$$\begin{aligned} C(d) &= a * \exp\left(-\frac{d}{\lambda_{in}}\right) + b && \text{inside the capillary} \\ C(r) &= a * \exp\left(-\frac{r}{\lambda_{out}}\right) + b && \text{outside the capillary} \end{aligned} \quad [1]$$

The exponential decay constants λ_{in} , and λ_{out} quantify respectively the depth of exploration inside the capillary and the extension of the patch at the capillary entrance (Figure 1.2B, D, F). In the case of *K. armiger* with DMSP 20 μ M and 200 μ M, the concentration $C(d)$ was fitted to a piecewise function composed of a constant plateau preceding the exponential decay (Figure 1.2B). For the three organisms, the values of λ_{in} and λ_{out} are averaged between experimental repetitions.

Maximum chemotactic indices $I_{c_{max}}$ were calculated both inside and at the entrance of the capillaries, as [2]:

$$I_{c_{max}} = \frac{\bar{c}_S}{\bar{c}_C} \quad [2]$$

where \bar{c}_S is the average cell concentration in the substrate (cue)-filled capillary during the 2 minutes around the maximum cell accumulation, and \bar{c}_C is the average concentration inside the control capillary over the entire assay (Supplementary Information). Inside the capillaries, the concentrations are calculated in the rectangular area within a distance λ_{in} from the entrance, outside the capillaries on the semi-circular region of radius λ_{out} . Accordingly, two chemotactic indices are finally reported: one inside and one outside the capillary (Supplementary Information). Significant differences in cell concentration between the cue and the control capillary were evaluated with the nonparametric Kruskal-Wallis test prior to computing the $I_{c_{max}}$ (Supplementary Tables S1.4-S1.6). When non-significant differences were found ($p > 0.01$), $I_{c_{max}}$ was considered equal to 1 (neutral, no response). All statistical analyses were conducted in R v4.0.2 (R Development Core Team, 2021).

Swimming behaviour analyses. The swimming behaviour in response to a DMSP patch was characterised in terms of swimming speed and trajectory straightness. The trajectory straightness S was evaluated for trajectories ingoing and outgoing the infochemical source and for trajectories unaffected by the chemical (marked as “neutral zone”). S is calculated as described by Batschelet (1981) [3]:

$$S = D/L \quad [3]$$

where D is the distance in the 2D plane between the initial point and the end point of a trajectory and L is the path length, defined as $\sum_{i=1}^N l_i$ for a trajectory made of N steps of length l_i . Hence, $S = 1$ for a totally straight trajectory, and $S \ll 1$ for a very convoluted path. Incoming, outgoing, and unaffected trajectories are computed within circular coronas with a width of 140 μ m, corresponding to roughly seven times the approximate body length of the cell (20 μ m) (Supplementary Information). For ingoing and outgoing trajectories, S was calculated on a portion of the trajectory fully contained in the diffusing infochemical patch (up to 200 μ m after 60 seconds of recording). S for trajectories unaffected by the chemical was calculated during the first 60 seconds of recording at a distance > 400 μ m. Given the inherent dependence of parameter S on the trajectory length, a robustness test was conducted to evaluate its stability across a diverse range of trajectory lengths (Supplementary Information). The data used for S calculations were derived from assays with 20 μ M and 200 μ M DMSP.

³⁵S-DMSP uptake experiments. Four aliquots of starved cultures of each organism were prepared in tissue culture flasks of 70 ml volume (Becton Dickinson). The aliquots were treated with a combination of 3 antibiotics: kanamycin (1000 µg ml⁻¹), neomycin (250 µg ml⁻¹), and penicillin (1000 µg ml⁻¹) the day before the experiment to reduce bacterial abundance and activity. Each set of aliquots included two experimental replicates, one killed with 10% glutaraldehyde to serve as blank and one kept in a radioactivity-free lab to follow cell concentration and volume with the Multisizer™ 3 Coulter Counter (Beckman Coulter). The first three aliquots were spiked with 20.000 dpm ml⁻¹ of ³⁵S-DMSP (specific activity of 1186 dpm fmol⁻¹; final concentration of 17 pmol l⁻¹) and incubated at 19°C with continuous light (67 µE m⁻² s⁻¹) for a maximum of 48 h. Although dissolved DMSP was not measured in the culture, very low concentrations were expected since neither the prey nor the grazer are known to produce DMSP in high concentrations (Keller et al., 1989). Following a previously described protocol (Saló et al., 2009), sample aliquots were filtered through 3-5 µm (nominal pore) nitrocellulose filters, washed twice with FSW, and immersed in Ultima Gold cocktail for measurement with a Beckman scintillation counter. The filtrate was re-filtered through 0.2 µm (nominal pore) nitrocellulose filters and analysed to detect uptake of the radioisotope by the free-living bacteria that may have survived the antibiotic treatment. Uptake in the bacterial fraction represented <2% of the total radioisotope added. Chemically synthesised and purified ³⁵S-DMSP was provided by Steve Archer (Bigelow, Laboratory for Ocean Sciences, USA).

RESULTS

Use of a microcapillary assay to create microscale diffusion gradients from a point source

We introduced an experimental capillary with cue and a control capillary without cue into a culture of the herbivore protist, and video-recorded cell distributions and swimming tracks (Figure 1.1A). This assay, based on previous works (Martel, 2006), was designed to replicate the formation of a microscale (hundreds of μm spread) gradient of a target compound resulted from diffusion from a point source (Supplementary Information), such as a leaky or bursting cell or aggregate in nature (Azam & Malfatti, 2007; Seymour et al., 2017; Stocker, 2012). We observed the chemotactic response of individual motile cells to this gradient (Figure 1.1B). Unlike the classical capillary assay, where chemotactic cells are identified based on a dual yes/no criterion after entering the capillary, our approach allowed us to study the swimming behaviour and cell distribution both inside the capillary and on the outer side of the entrance (Figure 1.1C, D, E).

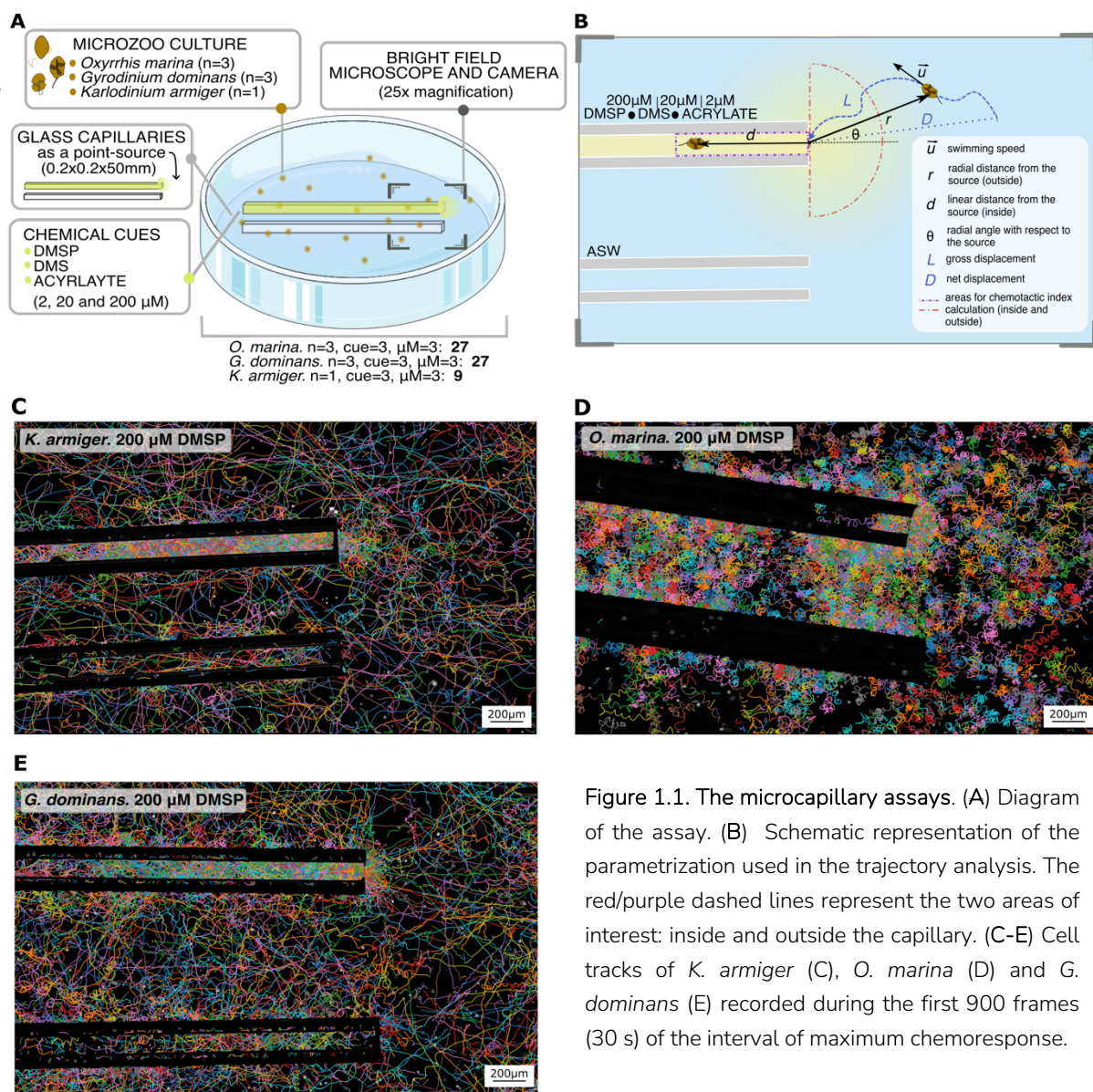


Figure 1.1. The microcapillary assays. (A) Diagram of the assay. (B) Schematic representation of the parametrization used in the trajectory analysis. The red/purple dashed lines represent the two areas of interest: inside and outside the capillary. (C-E) Cell tracks of *K. armiger* (C), *O. marina* (D) and *G. dominans* (E) recorded during the first 900 frames (30 s) of the interval of maximum chemoresponse.

Chemoattracting role of DMSP

Cell tracks around the cue and control capillaries showed accumulation of *K. armiger*, *O. marina* and *G. dominans* in the proximity of the DMSP source and inside the DMSP-filled capillary (Figure 1.1C-E). Each organism exhibited distinct swimming patterns in response to the cue. *K. armiger* and *G. dominans* displayed more straight trajectories and inspected the inside of the DMSP capillary. In contrast, *O. marina* swam in more circular and convoluted tracks and accumulated mainly at the entrance of the capillary. This behaviour is quantitatively depicted by the cell density colormaps (Figure 1.2A, C, E and Supplementary Figure S1.1) and the spatial profiles of cell density inside and outside the capillaries (Figure 1.2B, D, F and Supplementary Figure S1.2). Because the observed accumulation profiles decreased exponentially from the tip in both inwards and outwards of the capillary, the depth of the exploration inside the capillary (λ_{in}) and the size of the cell patch outside of it (λ_{out}) of each organism was quantified by fitting an exponential function to the cell distribution data (Figure 1.2B, D, F and M&M). The three species accumulated above the control at the outer side of the entrance of the DMSP capillary, in patches of similar size ($\lambda_{out} \sim 84\text{--}140\ \mu\text{m}$). The exception was *K. armiger* at 2 μM DMSP, which showed little chemotactic response, indistinguishable from the control, in the preliminary (only one replicate was conducted) results obtained. Different behaviours were observed inside the capillary for each species. *K. armiger* swam deep into the capillary ($\lambda_{in} \sim 700\text{--}2300\ \mu\text{m}$) with higher DMSP concentration leading to larger accumulation. *G. dominans* accumulated both at the outer and inner sides of the capillary entrance, exploring part of the capillary ($\lambda_{in} \sim 330\text{--}600\ \mu\text{m}$); and *O. marina* aggregated preferentially around the outer side of the entrance of the capillary and scarcely explored the inside it ($\lambda_{in} \sim 130\text{--}290\ \mu\text{m}$).

Cell accumulations over time inside the DMSP capillary also differed between organisms: *K. armiger* and *O. marina* showed steady long-term accumulation during the incubation, while *G. dominans* presented a fluctuating, up-and-down pattern in cell concentration (Supplementary Figure S1.3). Consequently, regression-based long-term accumulation rates were positive for *O. marina*, positive but weaker for *K. armiger*, and slightly negative for *G. dominans* (Supplementary Tables S1.1–S1.3).

We further evaluated the chemoattractant potential of DMSP using the maximum chemotactic index ($I_{c_{max}}$) (Figure 1.3), which was considered different than 1 (no response) when mean cell counts inside or outside the cue capillary were significantly different from mean cell counts inside or outside the control capillary (Supplementary Tables S1.4–S1.6). Outside the capillary, the values of $I_{c_{max}}$ were higher than 1 for the three organisms at medium and high DMSP concentrations, with the highest indices (from 4.6 to 8.8) recorded at the intermediate concentration (20 μM). Inside the capillary, the values of $I_{c_{max}}$ for *G. dominans* were higher than outside at all DMSP concentrations, and the highest index of all experiments (12.2) was recorded for this organism at 20 μM . Both *O. marina* and *K. armiger* showed higher indices inside than outside at 2 μM , and similar or slightly lower at 20 and 200 μM . *O. marina* and *G. dominans* showed the strongest inside chemoattraction with the intermediate DMSP concentration, whereas the strongest response of *K. armiger* was with 200 μM and there was no significant response with 2 μM . These results confirm that DMSP elicits positive chemotaxis (i.e., chemoattraction) in *O. marina* (Breckels et al., 2011; Seymour et al., 2010) and *G. dominans* and suggest so for *K. armiger* too.

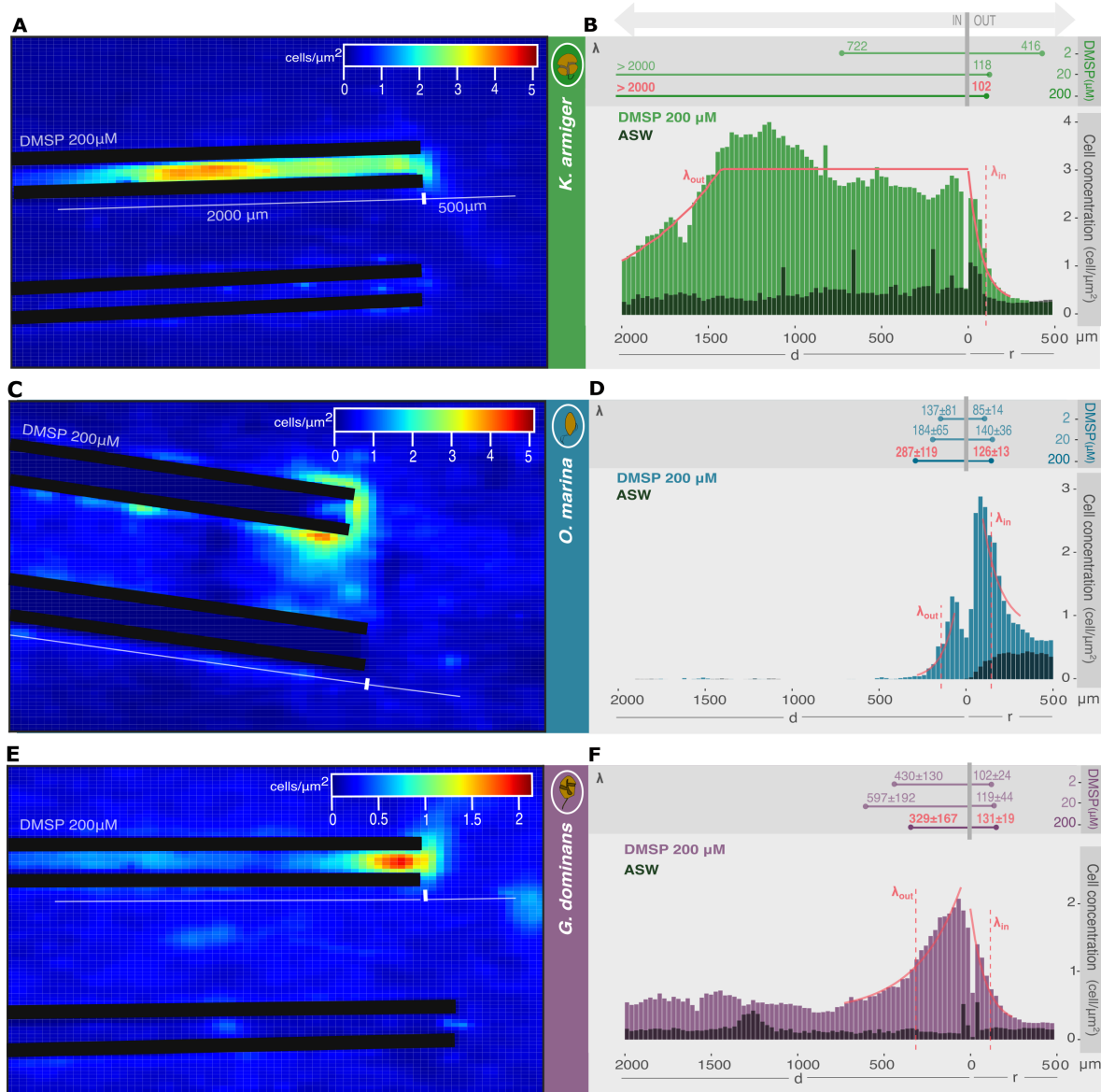


Figure 1.2. Cell density distributions in the microcapillary assays. Cell density distributions of *K. armiger* (A, B), *O. marina* (C, D), and *G. dominans* (E, F) in microcapillary assays with 200 μM DMSP, depicted as colormaps (A, C, E) and histograms (B, D, F). Note that the capillary with the cue is always compared with a control without the cue. The control capillary is always the one at the bottom in the colormaps and is represented in the histograms as black bars. The red lines show the exponential fit on the accumulation profile, and the red dashed ones the depth of exploration inside the capillary (λ_{in}) and the size of the cell patch outside of it (λ_{out}) for that replicate. The upper panels of the histograms illustrate all λ values, specified for each DMSP concentration. Symbols: d = linear distance, inside; r = radial distance, outside.

Chemotactic responses to DMS

Cell density histograms of *K. armiger* showed positive response to 2 and 200 μM DMS, especially on the outer side of the capillary entrance (Supplementary Figure S1.2). Like in the DMSP assays, *K. armiger* exhibited the widest cell dispersion inside the DMS capillary. However, notable positive response was only observed one time at the lowest DMS concentration (2 μM), both inside and outside the capillary (Figure 1.3). Most $I_{c_{max}}$ values significantly higher than 1 were obtained with *O. marina* and *G. dominans* (Figure 1.3). For *O. marina*, positive responses were observed in most experiments, yet with lower cell concentrations than with DMSP (Supplementary Figure S1.3). $I_{c_{max}}$ values were highest at 20

μM outside and 20 and 200 μM inside the capillary (Figure 1.3). *G. dominans* showed $I_{C_{\max}}$ values higher than 1 in most assays both inside and outside the capillary, albeit with lower cell concentrations compared to DMSP (Figure 1.3 and Supplementary Figure S1.3). Overall, DMS triggered a chemoattraction response, but weaker than that to DMSP under the experimental concentrations and conditions tested.

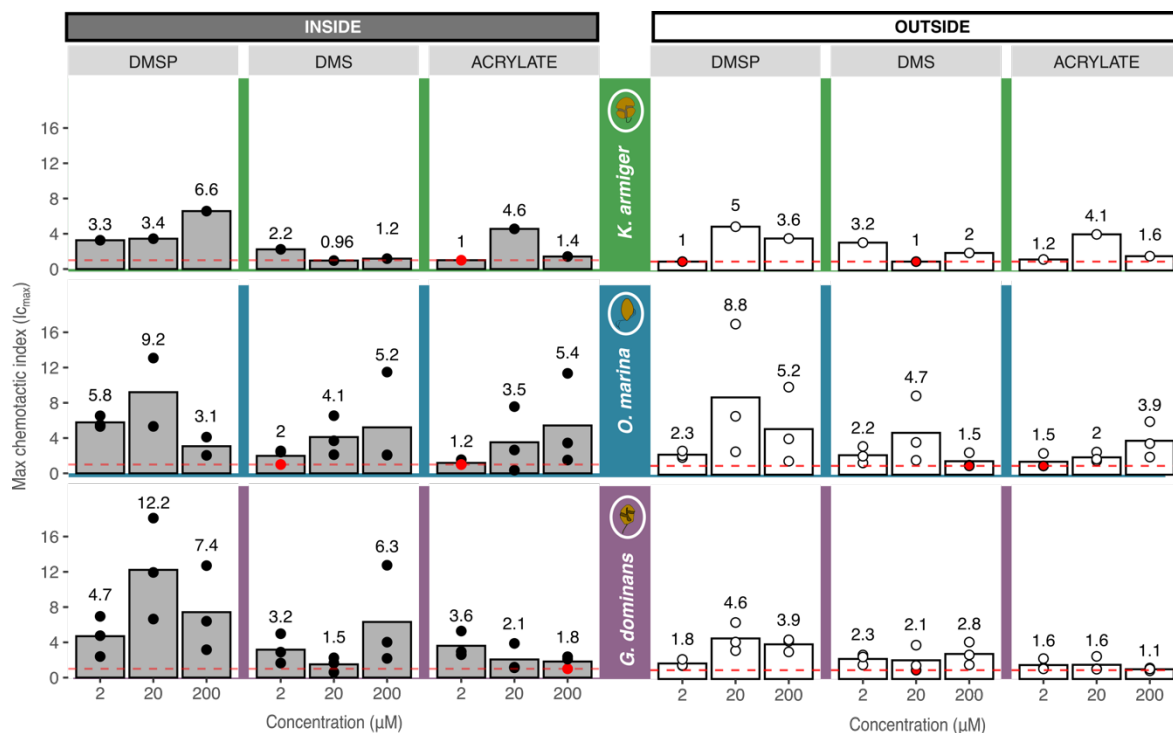


Figure 1.3. Maximum chemotactic indices ($I_{C_{\max}}$) to DMSP, DMS and acrylate. The grey columns indicate the average $I_{C_{\max}}$ (cell concentration in the substrate over cell concentration in the control) inside the capillary. The white columns indicate the average $I_{C_{\max}}$ in the outside area. Average $I_{C_{\max}}$ are given also numerically. Dots refer to the $I_{C_{\max}}$ obtained in each replicate experiment. Non-significant differences ($p > 0.01$) in cell concentration that translated into $I_{C_{\max}} = 1$ are illustrated with red dots. $I_{C_{\max}} > 1$ indicates positive chemoattraction, $I_{C_{\max}}$ around 1 indicates neutral effect, and $I_{C_{\max}} < 1$ indicates chemotactic repulsion. The red dashed line indicates $I_{C_{\max}} = 1$. Three concentrations (2, 20 and 200 μM) were tested per cue. The standard deviations of the averages are reported in Supplementary Tables S1.4-S1.6.

Absence of chemotactic repulsion by acrylate

Like DMS, acrylate elicited scattered positive responses, which were weaker and less consistent than those observed for DMSP. We only observed attraction to acrylate above the control for *K. armiger* in the one test with 20 μM (Supplementary Figure S1.3), which resulted in $I_{C_{\max}} > 4$ both inside and outside (Figure 1.3). *O. marina* showed increased cell concentrations above the control in some replicates with 20 and 200 μM acrylate (inside) and 200 μM acrylate (outside) (Supplementary Figure S1.3 and Figure 1.3). *G. dominans* only showed positive chemotaxis to acrylate inside the capillary with 2 μM (Figure 1.3). While significant differences in cell counts between cue and control capillaries were observed for most incubations (Supplementary Tables S1.4-S1.6), mean $I_{C_{\max}}$ remained close to 1 in most cases, particularly with increasing acrylate concentrations (Figure 1.3). Notably, indices lower than 1 (indicative of negative chemotaxis) were not observed for any of the three dinoflagellates. In conclusion, acrylate elicited a generally neutral, sometimes attraction response, with no evidence of repulsion.

Swimming behaviour of dinoflagellates in response to DMSP gradients

We observed changes in motility in the three organisms in presence of a DMSP gradient. Notably, a chemokinetic response (change in swimming speed) was specifically observed in *G. dominans*, where cells farther away from the DMSP source exhibited typical swimming speeds below 200 $\mu\text{m}/\text{s}$, which increased to 300 $\mu\text{m}/\text{s}$ near the DMSP source (Figure 1.4A, B and Supplementary Figure S1.4). This behaviour was consistently observed in all repetitions at intermediate (20 μM) and high (200 μM) concentrations of DMSP, except for one replicate at 20 μM (Supplementary Figure S1.4). Conversely, no chemokinetic response was observed in either *K. armiger* or *O. marina*.

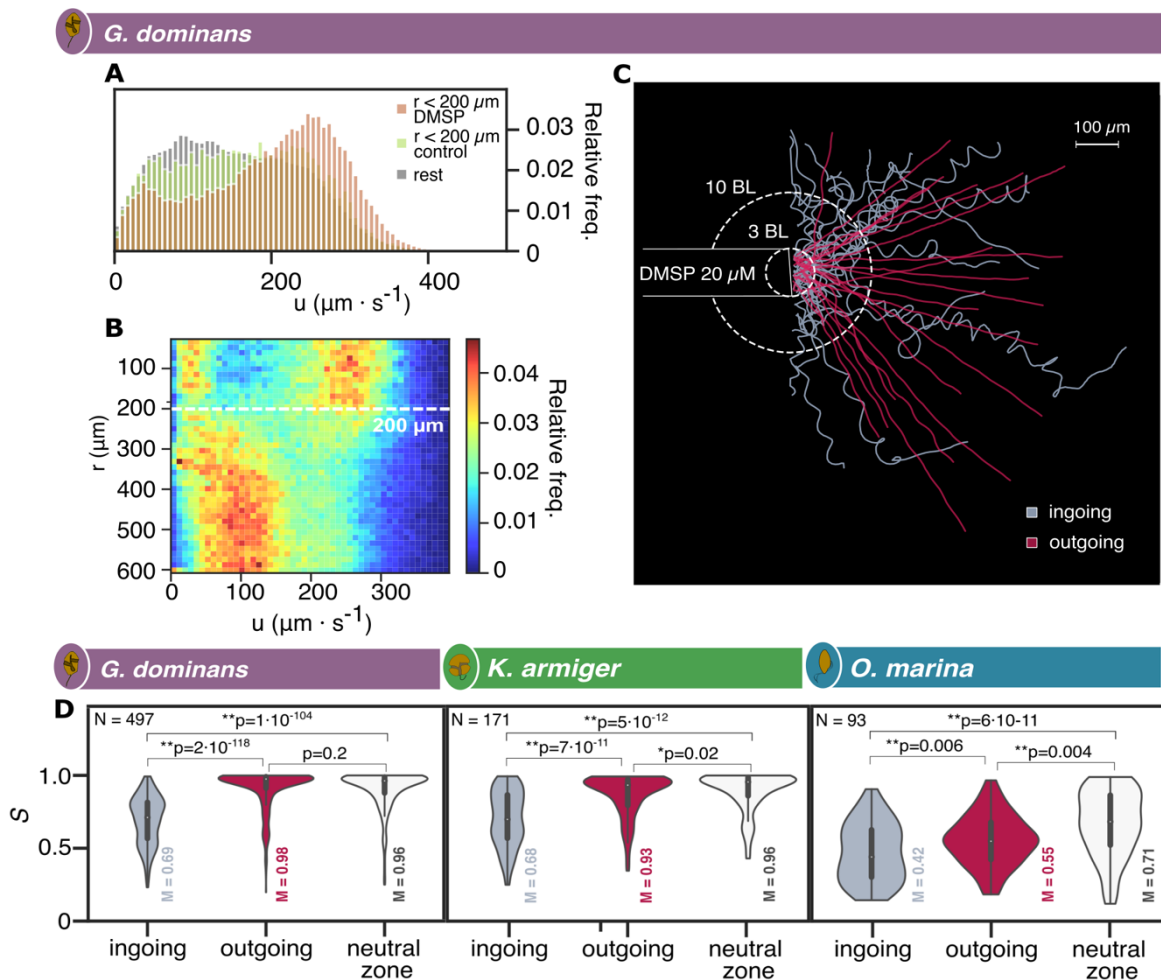


Figure 1.4. Swimming behaviour response to DMSP. (A) Relative frequencies of the instantaneous swimming speed of *G. dominans* tested with DMSP 200 μM in 3 different zones: within a 200 μm radius from the DMSP source (orange), within a 200 μm radius from the control capillary entrance (green) and in the remaining frame area (grey). (B) Heat map of the relative frequencies of swimming speeds values versus radial distance in *G. dominans* cells trajectories tested with DMSP 200 μM . (C). Ingoing (grey) and outgoing (magenta) *G. dominans* trajectories tested with DMSP 20 μM . (D) Violin plots showing the data distribution of S values for ingoing (grey), outgoing (magenta), and background (white) trajectories. M represents the median value of each distribution and N is the number of trajectories analysed for each organism. Significant differences between S-values of the three zones are also displayed in the figure with ** when $p < 0.01$ and * when $p < 0.05$. The section of the tracks employed in the analysis comprised between 3 and 10 BL (7BL=140 μm) and are from 20 μM and 200 μM DMSP assays.

Regarding swimming trajectories, *G. dominans* and *K. armiger* showed a similar behavioural pattern: convoluted trajectories when approaching the DMSP source, and ballistic radial trajectories when exiting the capillary and moving away from it (Figure 1.4C). This behavioural shift is illustrated by the straightness index S (Figure 1.4D and Supplementary Figure S1.8), which quantifies the net to gross displacement ratio of the trajectories (see Figure 1.1B). The index S is thus a measure of the tortuosity of the path. Straight trajectories, where the organism takes the shortest path between two points, have high values of S , while tortuous paths have low S . There was a noteworthy change in the median values of S between ingoing and outgoing trajectories for *G. dominans* (0.69 vs 0.98) and *K. armiger* (0.66 vs 0.98). The outgoing trajectories resembled background trajectories, i.e., those unaffected by the cue (Figure 1.4D). This indicates that both organisms altered their swimming behaviour into a searching pattern (convoluted trajectories) when sensing an increasing gradient of DMSP, and reverted to their background ballistic swimming when leaving the gradient. For *O. marina*, the most notable difference was between the background swimming trajectories in the far (neutral) zone and those within the DMSP patch, regardless the in or out direction (Figure 1.4D). Inside the patch the swimming became more convoluted, with median S of 0.42 (ingoing) and 0.55 (outgoing), compared to outside the patch (0.71).

³⁵S-DMSP uptake by chemosensitive dinoflagellates

To investigate whether the chemoattraction of our model organisms to DMSP was solely due to its role as an infochemical or also to its interest as a source of reduced sulphur, or both, we spiked the cultures with ³⁵S-DMSP and monitored biological uptake over 24-48 h (Figure 1.5). A previous study (Saló et al., 2009) showed the ability of *O. marina* to take up DMSP and assimilate its sulphur into biomass. For the sake of comparison between organisms, radioisotope uptake per cell (dpm cell⁻¹) was normalised by cell volume (dpm μm⁻³), a proxy of biomass. The three dinoflagellates showed distinct uptake patterns. In the initial 5 hours, *K. armiger* and *O. marina* exhibited uptake rates of 1.34E-04 dpm μm⁻³ h⁻¹ and 1.26E-04 dpm μm⁻³ h⁻¹, respectively. Although their uptake rates were comparable, their satiation levels differed significantly ($p = 0.036$): while *K. armiger*'s uptake rate levelled off at 6.81E-04 dpm μm⁻³, *O. marina*'s uptake reached 1.30E-03 dpm μm⁻³. Conversely, *G. dominans* uptake was much slower (5.36E-06 dpm μm⁻³ h⁻¹) and had not yet levelled off after 48 h (Figure 1.5). These results demonstrate that all three dinoflagellates are capable of DMSP uptake but differ largely in their uptake potential and efficiency.

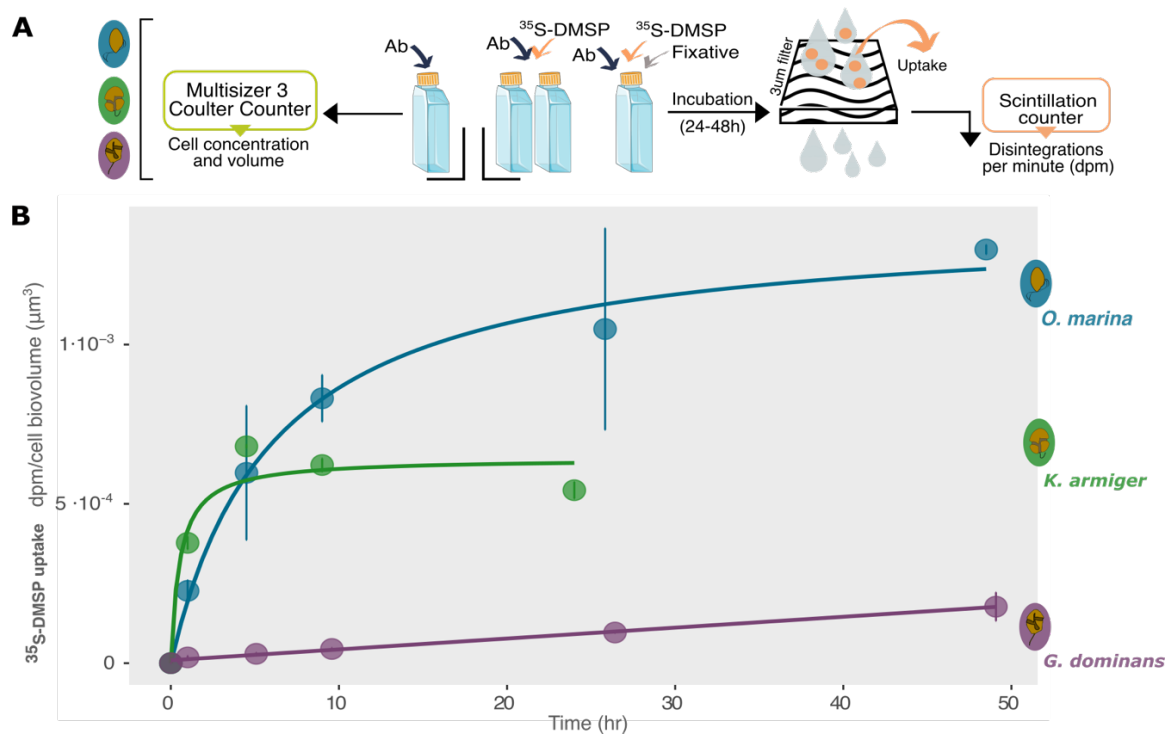


Figure 1.5. Kinetics of DMSP uptake. (A) Diagram of the uptake experiments (Ab= antibiotics). (B) Time course of ^{35}S -DMSP uptake expressed as dpm incorporated per total cell biovolume ($\text{dpm}/\mu\text{m}^3$). Standard deviation of replicate experiments ($n=2$) is depicted by vertical lines.

DISCUSSION

Chemosensory behaviour endows marine microbes with the key ability to detect and respond to targeted chemical information in an environment that is intrinsically heterogeneous (Grünbaum, 2002; Harvey et al., 2013). In this study, we investigated the chemotactic responses of three herbivorous protists to microscale dissolved patches of three marine chemical cues. Our experimental setup aimed to mimic release events in the sea, such as leaky or bursting algal cells, or microbial-rich aggregates (Kjørboe & Jackson, 2001; Simon et al., 2002).

Our results confirmed a weak and variable chemoattractant role of DMS for *O. marina* (Breckels et al., 2011; Seymour et al., 2010), and revealed this role for the first time in *G. dominans*. DMS, produced from algal DMSP due to oxidative stress, grazing, viral infection, and bacterial degradation (Evans et al., 2007; Simó, 2001; Sunda et al., 2002) is expected to attract predators to physiologically compromised or aggregated prey. DMS production is typically accompanied by the production of acrylate. The role of acrylate as a grazing defence mechanism (Teng et al., 2021; Wolfe et al., 1997) is questioned here based on the lack of observed repulsion responses. Since neither repeated attraction to low micromolar acrylate concentrations (Wolfe et al., 1997) nor repulsion by higher concentrations (Breckels et al., 2011) were observed, acrylate cannot be postulated as an infochemical for the three dinoflagellates tested. However, each chemical has its own optimal range of response induction (Breckels et al., 2011) and, although we tested a broad range of concentrations (2, 20 and 200 μM), it is still possible that we missed the range of maximal induction. Previous experiments with *O. marina* showed higher chemotactic indices with DMS concentrations lower than the ones tested here, but repulsion to acrylate was observed within the range we tested (Breckels et al., 2011). Conversely, both the visual inspection and the numerical data confirmed the strong and unquestionable chemoattractant role of DMSP. Chemoattraction to DMSP had been already reported for *O. marina* (Breckels et al., 2011; Deuer & Grünbaum, 2006; Martel, 2006; Seymour et al., 2010) and now it is first described for *G. dominans* and *K. armiger*. DMSP induced strong aggregations within the patch, leading to significantly higher chemotactic indices ($I_{c_{\max}}$), with the highest values observed for *G. dominans*. The lack of experimental replication with *K. armiger* prevented adequate evaluation of the statistical significance of the results for this organism. In the context of the controversy about the role of DMSP as a grazing attractor (Seymour et al., 2010) or deterrent (Fredrickson & Strom, 2008; Strom et al., 2003), our results support the attraction role and the idea that experimental bulk DMSP additions in grazing assays would mask natural microscale gradients and create a confounding landscape that hinders location and ingestion of the prey (Seymour et al., 2010).

DMSP also prompted behavioural changes that reflected how each organism perceives, interprets, and uses DMSP. The observed alteration of the inwards swimming tracks in the three organisms illustrates the role of DMSP as a widespread foraging infochemical for marine protists (Seymour et al., 2010). In all cases, the elicited swimming response was consistent with helical klinotaxis, where helical paths are used to respond to and orientate in chemical gradients (Crenshaw, 1993; Fenchel, 2001; Seymour et al., 2009). The more convoluted paths lead to shorter longitudinal displacements but improve the search by optimizing spatial sampling and orientation in gradients, especially when navigating an environment where the chemical signal is dim and the chemical plumes are stretched and advected by the flow (Ramírez-Gómez et al., 2020). Convoluted displacement patterns in the presence of prey (or prey signals) have been amply documented, from insects, fishes, and birds (DeBose et al., 2008; Nevitt, 2008; Willis, 2005) to a variety of protists (Harvey et al., 2013; Seymour et al., 2009), including marine dinoflagellates (Boakes et al., 2011; Deuer & Grünbaum, 2006; Roberts et al., 2011; Sheng et al., 2007). This interpretation is reinforced by the observation of a return to ballistic swimming in the outgoing trajectories of *G. dominans* and *K. armiger* away from the source, suggesting that the behavioural (exploratory) alteration ceases once the DMSP-releasing target has been successfully located but there

is no addition benefit in staying. Ecologically, we would expect *G. dominans* and *K. armiger* to quickly abandon a DMSP hotspot if they fail to find prey, as such hotspots might attract potential predators. In the case of the osmotrophic *O. marina*, the DMSP-elicited alteration of the swimming behaviour persisted after the localization of the source.

O. marina exhibits high prey versatility with strong osmotrophic capabilities (Droop & Pennock, 1971; Roberts et al., 2011). Because its fast response to DMSP (Seymour et al., 2010), we missed the immediate response in our experimental setup (<30 s), but subsequent behaviour confirmed its appetite for DMSP as a substrate. The low straightness index S , regardless of the displacement direction, indicated the interest of *O. marina* to remain in the patch. Its circular swimming behaviour, minimizing the chances of deviating away (Fenchel, 2001), aligns with its reported tendency of to remain in food patches for extended periods. (Boakes et al., 2011; Deuer & Grünbaum, 2006). Rapid aggregation near the DMSP source and steady long-term accumulation inside the DMSP capillary, yet with limited exploratory extent (low λ_{in}), suggest that *O. marina* uses DMSP as an infochemical. When no prey are found, it remains in the patch to efficiently exploit DMSP as a substrate too, as supported by the high DMSP uptake rates with the highest satiation level observed in radioisotope assays. Thus, the short exploration depth inside the capillary reflects the high affinity of *O. marina* for DMSP uptake, which makes the dinoflagellate to change its swimming behaviour, reduce its exploratory activity and remain within the substrate patch, likely exploiting its osmotrophic capability and avoiding extended energy expenditure.

G. dominans is a typical phago-heterotroph that ingests prey by engulfment, lacking osmotrophic potential (Jeong et al., 2010). It showed a characteristic exploratory behaviour: tortuous trajectories and higher swimming speeds towards increasing DMSP concentrations. Analogous to what has been observed in other heterotrophic dinoflagellates after exposure to prey (Sheng et al., 2007), the increase in velocity reflected *G. dominans* interpretation of DMSP as a prey signal, as the local 50% augment in swimming speed increased its probability to encounter prey (Gerritsen & Strickler, 1977). In the absence of DMSP signal in the background conditions, lower swimming speeds reduced the risk of being encountered by predators (Visser & Kiørboe, 2006). The absence of prey and the inefficient use of DMSP as a substrate (very low uptake rates) resulted in no long-term accumulation in the capillary, leading to abandoning the DMSP patch and returning to regular ballistic swimming. This behaviour suggests that *G. dominans* and organisms alike use DMSP as a foraging infochemical; if the DMSP source cannot be engulfed (e.g., due to its cell size), *G. dominans* will shortly resume exploration elsewhere avoiding lingering in a potential hot spot for higher-trophic level predators.

K. armiger is a plastic mixotroph that can feed on a wide range of prey sizes, including particles much larger than itself, using peduncle feeding (Berge et al., 2008; Jeong et al., 2010). Our ^{35}S -DMSP uptake assays manifested its osmotrophic ability. DMSP sensing triggered a search behaviour with convoluted trajectories. The poorer detectability (higher $I_{C_{max}}$ in the $\geq 20 \mu\text{M}$ DMSP capillaries) and the search behaviour prompted a thorough inspection of the capillary that translated into the largest λ_{in} values. Inside the capillary, accumulation over time indicated fast uptake of DMSP; however, low satiation levels and the absence of prey elicited to leave the patch and return to ballistic trajectories. Overall, the data indicate that *K. armiger* is suited to detect high concentrations of DMSP and aggregate at the DMSP source, facilitating its proximity to DMSP-leaky particles for feeding via its peduncle. Confirmation of *K. armiger* behaviour would require further experimentation with multiple replicates.

Our findings have implications for our understanding and modelling of grazing in marine microbial plankton. Microzooplankton protists graze down ca. 60% of daily primary production in the ocean (Calbet & Landry, 2004). While microzooplankton grazing rates are typically assessed and modelled based on cell sizes, encounter rates and turbulent flow (García-Oliva & Wirtz, 2022; Gerritsen & Strickler, 1977; Visser & Kiørboe, 2006), our work highlights the occurrence of selection based on

chemotaxis, with preference for DMSP- or DMS-leaky prey. This has additional consequences for sulphur biogeochemical cycling. Grazing on DMSP-containing prey exerts a strong control on DMS concentration in the surface of the ocean and in the resulting emission of volatile sulphur to the atmosphere (Simó et al., 2018), with climate implications (Simó, 2001). Yet, the ultimate effects of chemotaxis-driven grazing on plankton ecology and ocean biogeochemistry are far from straightforward. Despite showing that three dinoflagellates with distinct trophic modes are all attracted by algal cues, the diversity of the elicited behaviours complicates the picture. Chemotaxis to DMSP may enhance prey encounter and ingestion, but it also allows the protist to stay next to a feeding resource and change its local chemical environment. If the subsequent production of a secondary cue like DMS in turn attracts higher predators such as copepods or other mesozooplankton species that feed on the protist grazer (Shemi et al., 2021), this may lead to tri-trophic interactions that will help relieve the grazing pressure on the DMSP producing prey (Lewis et al., 2013; Savoca & Nevitt, 2014).

Furthermore, our study also demonstrates that chemotaxis favours protist aggregation on or around a DMSP source. In marine ecology, aggregation brings a trade-off of advantages and risks that is hard to resolve: contradictory results exist on the effects of aggregation on the probability of feeding and being predated (Falgueras-Cano et al., 2022; Folt, 1987). For heterotrophic dinoflagellates, enhanced feeding by aggregation on marine snow has been documented (Shanks & Walters, 1996), and marine snow particles can be DMSP-rich (Steiner et al., 2019); therefore, chemotaxis-driven aggregation on marine snow may be a beneficial collective behaviour for micrograzers.

Natural point-sources cannot be expected to be composed of a single chemical cue. In the case of a chemical plume from a lysed or sloppy eaten cell, or a faecal pellet, it is expected that DMSP will concur with lower concentrations of DMS, and acrylate (Shemi et al., 2021) as well as saccharides and other released metabolites (Clerc et al., 2023). Our experiments were designed to investigate the chemotactic properties of single compounds and the induced responses of in particular strains. Future studies should address the potential synergies or counteraction of concurring cues (Clerc et al., 2023), and more complex biological settings that better reproduce food web interactions (Kuhlish et al., 2024).

REFERENCES

- Adler, J. (1973). A method for measuring chemotaxis and use of the method to determine optimum conditions for chemotaxis by *Escherichia coli*. *Journal of General Microbiology*, 74(1), 77–91. <https://doi.org/10.1099/00221287-74-1-77>
- Alcolombri, U., Ben-Dor, S., Feldmesser, E., Levin, Y., Tawfik, D. S., & Vardi, A. (2015). Identification of the algal dimethyl sulfide-releasing enzyme: A missing link in the marine sulfur cycle. *Science*, 348(6242), 1466–1469. <https://doi.org/10.1126/science.aab1586>
- Archer, S. D., Ragni, M., Webster, R., Airs, R. L., & Geider, R. J. (2010). Dimethyl sulfoniopropionate and dimethyl sulfide production in response to photoinhibition in *Emiliania huxleyi*. *Limnology and Oceanography*, 55(4), 1579–1589. <https://doi.org/10.4319/lo.2010.55.4.1579>
- Archer, S. D., Stefels, J., Airs, R. L., Lawson, T., Smyth, T. J., Rees, A. P., & Geider, R. J. (2018). Limitation of dimethylsulfoniopropionate synthesis at high irradiance in natural phytoplankton communities of the Tropical Atlantic. *Limnology and Oceanography*, 63(1), 227–242. <https://doi.org/10.1002/lno.10625>
- Azam, F., & Malfatti, F. (2007). Microbial structuring of marine ecosystems. *Nature Reviews Microbiology*, 5(10), 782–791. <https://doi.org/10.1038/nrmicro1747>
- Batschelet, Edward. (1981). *Circular statistics in biology*. Academic Press.
- Berge, T., Hansen, P., & Moestrup, Ø. (2008). Feeding mechanism, prey specificity and growth in light and dark of the plastidic dinoflagellate *Karlodinium armiger*. *Aquatic Microbial Ecology*, 50, 279–288. <https://doi.org/10.3354/ame01165>
- Boakes, D. E., Codling, E. A., Thorn, G. J., & Steinke, M. (2011). Analysis and modelling of swimming behaviour in *Oxyrrhis marina*. *Journal of Plankton Research*, 33(4), 641–649. <https://doi.org/10.1093/plankt/fbq136>
- Breckels, M. N., Boakes, D. E., Codling, E. A., Malin, G., Archer, S. D., & Steinke, M. (2010). Modelling the concentration of exuded dimethylsulphoniopropionate (DMSP) in the boundary layer surrounding phytoplankton cells. *Journal of Plankton Research*, 32(2), 253–257. <https://doi.org/10.1093/plankt/fbp116>
- Breckels, M. N., Roberts, E. C., Archer, S. D., Malin, G., & Steinke, M. (2011). The role of dissolved infochemicals in mediating predator-prey interactions in the heterotrophic dinoflagellate *Oxyrrhis marina*. *Journal of Plankton Research*, 33(4), 629–639. <https://doi.org/10.1093/plankt/fbq114>
- Brown, E. R., Cepeda, M. R., Mascuch, S. J., Poulson-Ellestad, K. L., & Kubanek, J. (2019). Chemical ecology of the marine plankton. *Natural Product Reports*, 36(8), 1093–1116. <https://doi.org/10.1039/C8NP00085A>
- Calbet, A., & Landry, M. R. (2004). Phytoplankton growth, microzooplankton grazing, and carbon cycling in marine systems. *Limnology and Oceanography*, 49(1), 51–57. <https://doi.org/10.4319/lo.2004.49.1.0051>
- Clerc, E. E., Raina, J.-B., Keegstra, J. M., Landry, Z., Pontrelli, S., Alcolombri, U., Lambert, B. S., Anelli, V., Vincent, F., Masdeu-Navarro, M., Sichert, A., De Schaetzen, F., Sauer, U., Simó, R., Hehemann, J.-H., Vardi, A., Seymour, J. R., & Stocker, R. (2023). Strong chemotaxis by marine bacteria towards polysaccharides is enhanced by the abundant organosulfur compound DMSP. *Nature Communications*, 14(1), 8080. <https://doi.org/10.1038/s41467-023-43143-z>
- Crenshaw, H. C. (1993). Orientation by helical motion--III. Microorganisms can orient to stimuli by changing the direction of their rotational velocity. *Bulletin of Mathematical Biology*, 55(1), 231–255.
- DeBose, J. L., Lema, S. C., & Nevitt, G. A. (2008). Dimethylsulfoniopropionate as a foraging cue for reef fishes. *Science*, 319(5868), 1356–1356. <https://doi.org/10.1126/science.1151109>
- Deuer, S. M., & Grünbaum, D. (2006). Individual foraging behaviors and population distributions of a planktonic predator aggregating to phytoplankton thin layers. *Limnology and Oceanography*, 51(1), 109–116. <https://doi.org/10.4319/lo.2006.51.1.0109>
- Droop, M. R., & Pennock, J. F. (1971). Terpenoid quinones and steroids in the nutrition of *Oxyrrhis marina*. *Journal of the Marine Biological Association of the United Kingdom*, 51(2), 455–470. <https://doi.org/10.1017/S002531540003191X>
- Edgcomb, V. P. (2021). Eat me, or don't eat me? *Nature Microbiology*, 6(11), 1341–1342. <https://doi.org/10.1038/s41564-021-00992-y>
- Evans, C., Kadner, S. V., Darroch, L. J., Wilson, W. H., Liss, P. S., & Malin, G. (2007). The relative significance of viral lysis and microzooplankton grazing as pathways of dimethylsulfoniopropionate (DMSP) cleavage: An *Emiliania huxleyi* culture study. *Limnology and Oceanography*, 52(3), 1036–1045. <https://doi.org/10.4319/lo.2007.52.3.1036>
- Falgueras-Cano, J., Falgueras-Cano, J. A., & Moya, A. (2022). Aggregated distribution as an explanation for the paradox of plankton and collective animal behavior. *Biology*, 11(10), 1477. <https://doi.org/10.3390/biology11101477>

- Fenchel, T. (2001). How dinoflagellates swim. *Protist*, 152(4), 329–338. <https://doi.org/10.1078/1434-4610-00071>
- Fenchel, T. (2002). Microbial behavior in a heterogeneous world. *Science, New Series*, 296(5570), 1068–1071.
- Folt, C.L. (1987). An experimental analysis of costs and benefits of zooplankton aggregation. In *Predation. Direct and indirect impacts on aquatic communities*. (pp. 300–314). W.C. Kerfoot and A. Sih.
- Fredrickson, K. A., & Strom, S. L. (2008). The algal osmolyte DMSP as a microzooplankton grazing deterrent in laboratory and field studies. *Journal of Plankton Research*, 31(2), 135–152. <https://doi.org/10.1093/plankt/fbn112>
- Galí, M., Devred, E., Levasseur, M., Royer, S.-J., & Babin, M. (2015). A remote sensing algorithm for planktonic dimethylsulfoniopropionate (DMSP) and an analysis of global patterns. *Remote Sensing of Environment*, 171, 171–184. <https://doi.org/10.1016/j.rse.2015.10.012>
- Garcés, E., Alacid, E., Reñé, A., Petrou, K., & Simó, R. (2013). Host-released dimethylsulphide activates the dinoflagellate parasitoid *Parvilucifera sinerae*. *ISME Journal*, 7(5), 1065–1068. <https://doi.org/10.1038/ismej.2012.173>
- García-Oliva, O., & Wirtz, K. (2022). Size-dependent and -independent prey selection of dinoflagellates. *Marine Biology*, 169(9), 122. <https://doi.org/10.1007/s00227-022-04102-2>
- Gerritsen, J., & Strickler, J. R. (1977). Encounter probabilities and community structure in zooplankton: A mathematical model. *Journal of the Fisheries Research Board of Canada*, 34(1), 73–82. <https://doi.org/10.1139/f77-008>
- Grünbaum, D. (2002). Predicting availability to consumers of spatially and temporally variable resources. *Hydrobiologia*, 180, 175–191.
- Guadayol, Ò., Mendonca, T., Segura-Noguera, M., Wright, A. J., Tassieri, M., & Humphries, S. (2021). Microrheology reveals microscale viscosity gradients in planktonic systems. *Proceedings of the National Academy of Sciences*, 118(1), e2011389118. <https://doi.org/10.1073/pnas.2011389118>
- Guillard, R.R.L. (1975). Culture of phytoplankton for feeding marine invertebrates. In *Culture of marine invertebrates animals* (pp. 29–60). Smith, M.L. and Chanley, M.H., Eds. http://dx.doi.org/10.1007/978-1-4615-8714-9_3
- Hamm, C. E., Merkel, R., Springer, O., Jurkojc, P., Maier, C., Prectel, K., & Smetacek, V. (2003). Architecture and material properties of diatom shells provide effective mechanical protection. *Nature*, 421(6925), 841–843. <https://doi.org/10.1038/nature01416>
- Harvey, E. L., Jeong, H. J., & Menden-Deuer, S. (2013). Avoidance and attraction: Chemical cues influence predator-prey interactions of planktonic protists. *Limnology and Oceanography*, 58(4), 1176–1184. <https://doi.org/10.4319/lo.2013.58.4.1176>
- Hay, M. E. (2009). Marine chemical ecology: Chemical signals and cues structure marine populations, communities, and ecosystems. *Annual Review of Marine Science*, 1(1), 193–212. <https://doi.org/10.1146/annurev.marine.010908.163708>
- Hopkins, F. E., Archer, S. D., Bell, T. G., Suntharalingam, P., & Todd, J. D. (2023). The biogeochemistry of marine dimethylsulfide. *Nature Reviews Earth & Environment*, 4(6), 361–376. <https://doi.org/10.1038/s43017-023-00428-7>
- Jeong, H. J., Yoo, Y. D., Kim, J. S., Seong, K. A., Kang, N. S., & Kim, T. H. (2010). Growth, feeding and ecological roles of the mixotrophic and heterotrophic dinoflagellates in marine planktonic food webs. *Ocean Science Journal*, 45(2), 65–91. <https://doi.org/10.1007/s12601-010-0007-2>
- Kang, H. C., Jeong, H. J., Park, S. A., Eom, S. H., Ok, J. H., You, J. H., Jang, S. H., & Lee, S. Y. (2020). Feeding by the newly described heterotrophic dinoflagellate *Gyrodinium jinhaense*: Comparison with *G. dominans* and *G. moestrupii*. *Marine Biology*, 167(10), 156. <https://doi.org/10.1007/s00227-020-03769-9>
- Keller, M. D., Bellows, W. K., & Guillard, R. R. L. (1989). Dimethyl sulfide production in marine phytoplankton. In *Biogenic sulfur in the environment* (pp. 167–182). <https://doi.org/10.1021/bk-1989-0393.ch011>
- Kiene, R. P., Linn, L. J., & Bruton, J. A. (2000). New and important roles for DMSP in marine microbial communities. *Journal of Sea Research*, 43(3–4), 209–224. [https://doi.org/10.1016/S1385-1101\(00\)00023-X](https://doi.org/10.1016/S1385-1101(00)00023-X)
- Kiene, R. P., Nowinski, B., Esson, K., Preston, C., Marin, R., Birch, J., Scholin, C., Ryan, J., & Moran, M. A. (2019). Unprecedented DMSP concentrations in a massive dinoflagellate bloom in Monterey Bay, CA. *Geophysical Research Letters*, 46(21), 12279–12288. <https://doi.org/10.1029/2019GL085496>
- Kim, J., & Jeong, H. (2004). Feeding by the heterotrophic dinoflagellates *Gyrodinium dominans* and *G. spirale* on the red-tide dinoflagellate *Prorocentrum minimum*. *Marine Ecology Progress Series*, 280, 85–94. <https://doi.org/10.3354/meps280085>

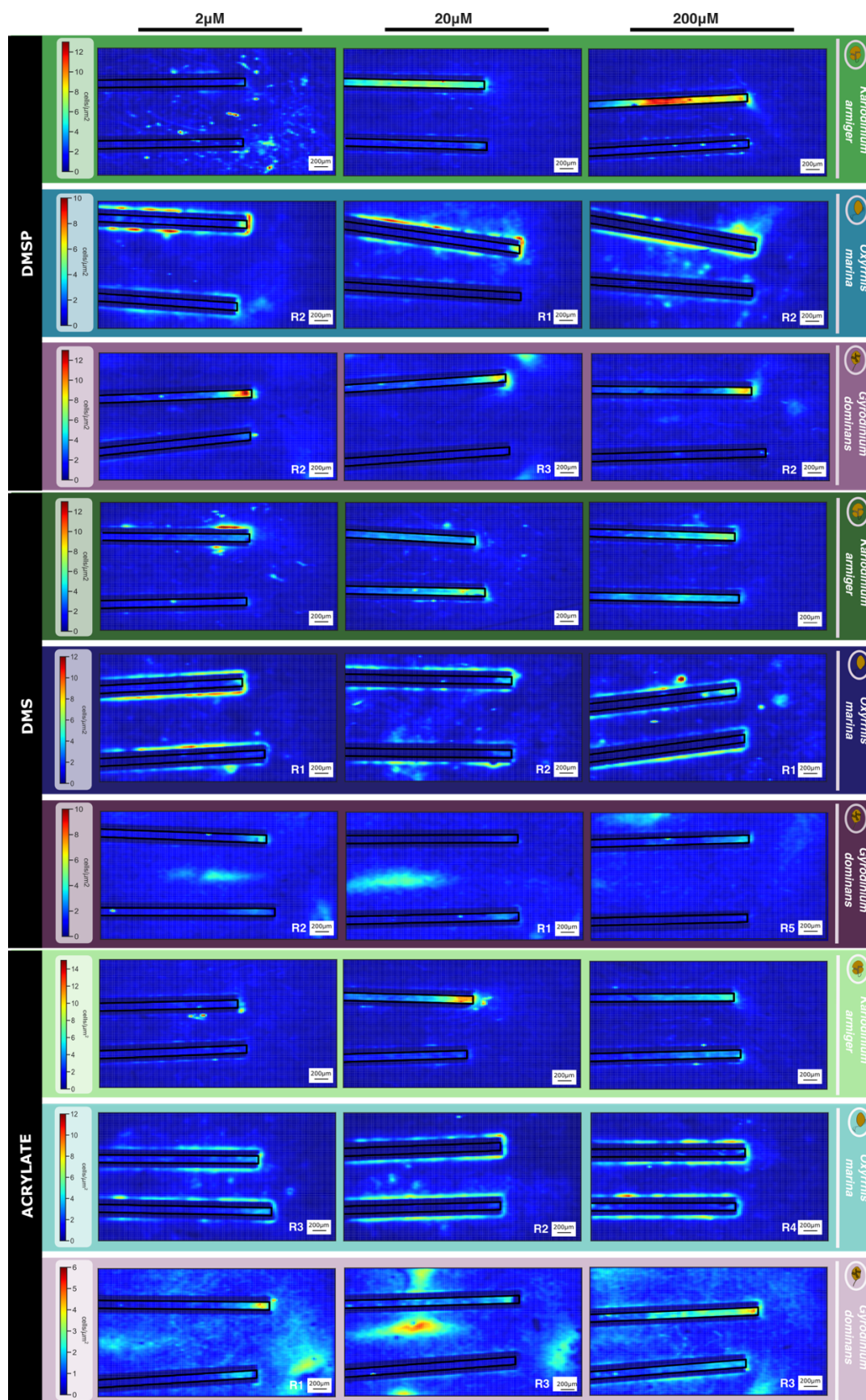
- Kjørboe, T., & Jackson, G. A. (2001). Marine snow, organic solute plumes, and optimal chemosensory behavior of bacteria. *Limnology and Oceanography*, 46(6), 1309–1318. <https://doi.org/10.4319/lo.2001.46.6.1309>
- Kowalewsky, S., Dambach, M., Mauck, B., & Dehnhardt, G. (2006). High olfactory sensitivity for dimethyl sulphide in harbour seals. *Biology Letters*, 2(1), 106–109. <https://doi.org/10.1098/rsbl.2005.0380>
- Kuhlish, C., Shemi, A., Barak-Gavish, N., Schatz, D., & Vardi, A. (2024). Algal blooms in the ocean: Hot spots for chemically mediated microbial interactions. *Nature Reviews Microbiology*, 22(3), 138–154. <https://doi.org/10.1038/s41579-023-00975-2>
- Levandowsky, M., Cheng, T., Kehr, A., Kim, J., Gardner, L., Silvern, L., Tsang, L., Lai, G., Chung, C., & Prakash, E. (1984). Chemosensory responses to amino acids and certain amines by the ciliate *Tetrahymena*: A flat capillary assay. *The Biological Bulletin*, 167(2), 322–330. <https://doi.org/10.2307/1541279>
- Lewis, N. D., Breckels, M. N., Steinke, M., & Codling, E. A. (2013). Role of infochemical mediated zooplankton grazing in a phytoplankton competition model. *Ecological Complexity*, 16, 41–50. <https://doi.org/10.1016/j.ecocom.2012.10.003>
- Martel, C. M. (2006). Prey location, recognition and ingestion by the phagotrophic marine dinoflagellate *Oxyrrhis marina*. *Journal of Experimental Marine Biology and Ecology*, 335(2), 210–220. <https://doi.org/10.1016/j.jembe.2006.03.006>
- Miller, T. R., Hnilicka, K., Dziedzic, A., Desplats, P., & Belas, R. (2004). Chemotaxis of *Silicibacter* sp. strain TM1040 toward dinoflagellate products. *Applied and Environmental Microbiology*, 70(8), 4692–4701. <https://doi.org/10.1128/AEM.70.8.4692-4701.2004>
- Nakamura, Y., Suzuki, S., & Hiromi, J. (1995). Population dynamics of heterotrophic dinoflagellates during a *Gymnodinium mikimotoi* red tide in the Seto Inland Sea. *Marine Ecology Progress Series*, 125, 269–277. <https://doi.org/10.3354/meps125269>
- Nevitt, G. A. (2008). Sensory ecology on the high seas: The odor world of the procellariiform seabirds. *Journal of Experimental Biology*, 211(11), 1706–1713. <https://doi.org/10.1242/jeb.015412>
- Pohnert, G., Steinke, M., & Tollrian, R. (2007). Chemical cues, defence metabolites and the shaping of pelagic interspecific interactions. *Trends in Ecology & Evolution*, 22(4), 198–204. <https://doi.org/10.1016/j.tree.2007.01.005>
- Poulsen, L., Moldrup, M., Berge, T., & Hansen, P. (2011). Feeding on copepod fecal pellets: A new trophic role of dinoflagellates as detritivores. *Marine Ecology Progress Series*, 441, 65–78. <https://doi.org/10.3354/meps09357>
- Ramírez-Gómez, H. V., Jimenez Sabinina, V., Velázquez Pérez, M., Beltran, C., Carneiro, J., Wood, C. D., Tuval, I., Darszon, A., & Guerrero, A. (2020). Sperm chemotaxis is driven by the slope of the chemoattractant concentration field. *eLife*, 9, e50532. <https://doi.org/10.7554/eLife.50532>
- Roberts, E. C., Wootton, E. C., Davidson, K., Jeong, H. J., Lowe, C. D., & Montagnes, D. J. S. (2011). Feeding in the dinoflagellate *Oxyrrhis marina*: Linking behaviour with mechanisms. *Journal of Plankton Research*, 33(4), 603–614. <https://doi.org/10.1093/plankt/fbq118>
- Saló, V., Simó, R., Vila-Costa, M., & Calbet, A. (2009). Sulfur assimilation by *Oxyrrhis marina* feeding on a ³⁵S-DMSP-labelled prey. *Environmental Microbiology*, 11(12), 3063–3072. <https://doi.org/10.1111/j.1462-2920.2009.02011.x>
- Savoca, M. S., & Nevitt, G. A. (2014). Evidence that dimethyl sulfide facilitates a tritrophic mutualism between marine primary producers and top predators. *Proceedings of the National Academy of Sciences*, 111(11), 4157–4161. <https://doi.org/10.1073/pnas.1317120111>
- Seymour, J. R., Amin, S. A., Raina, J.-B., & Stocker, R. (2017). Zooming in on the phycosphere: The ecological interface for phytoplankton–bacteria relationships. *Nature Microbiology*, 2(7), 17065. <https://doi.org/10.1038/nmicrobiol.2017.65>
- Seymour, J. R., Marcos, & Stocker, R. (2009). Resource patch formation and exploitation throughout the marine microbial food web. *The American Naturalist*, 173(1), E15–E29. <https://doi.org/10.1086/593004>
- Seymour, J. R., Simó, R., Ahmed, T., & Stocker, R. (2010). Chemoattraction to dimethylsulfoniopropionate throughout the marine microbial food web. *Science*, 329(5989), 342–345. <https://doi.org/10.1126/science.1188418>
- Shanks, A., & Walters, K. (1996). Feeding by a heterotrophic dinoflagellate (*Noctiluca scintillans*) in marine snow. *Limnology and Oceanography*, 41(1), 177–181. <https://doi.org/10.4319/lo.1996.41.1.0177>
- Shemi, A., Alcolombri, U., Schatz, D., Farstey, V., Vincent, F., Rotkopf, R., Ben-Dor, S., Frada, M. J., Tawfik, D. S., & Vardi, A. (2021). Dimethyl sulfide mediates microbial predator–prey interactions between zooplankton and algae in the ocean. *Nature Microbiology*, 6(11), 1357–1366. <https://doi.org/10.1038/s41564-021-00971-3>

- Sheng, J., Malkiel, E., Katz, J., Adolf, J., Belas, R., & Place, A. R. (2007). Digital holographic microscopy reveals prey-induced changes in swimming behavior of predatory dinoflagellates. *Proceedings of the National Academy of Sciences*, 104(44), 17512–17517. <https://doi.org/10.1073/pnas.0704658104>
- Simó, R. (2001). Production of atmospheric sulfur by oceanic plankton: Biogeochemical, ecological and evolutionary links. *Trends in Ecology & Evolution*, 16(6), 287–294. [https://doi.org/10.1016/S0169-5347\(01\)02152-8](https://doi.org/10.1016/S0169-5347(01)02152-8)
- Simó, R., Saló, V., Almeda, R., Movilla, J., Trepát, I., Saiz, E., & Calbet, A. (2018). The quantitative role of microzooplankton grazing in dimethylsulfide (DMS) production in the NW Mediterranean. *Biogeochemistry*, 141(2), 125–142. <https://doi.org/10.1007/s10533-018-0506-2>
- Simon, M., Grossart, H., Schweitzer, B., & Ploug, H. (2002). Microbial ecology of organic aggregates in aquatic ecosystems. *Aquatic Microbial Ecology*, 28, 175–211. <https://doi.org/10.3354/ame028175>
- Stefels, J., Steinke, M., Turner, S., Malin, G., & Belviso, S. (2007). Environmental constraints on the production and removal of the climatically active gas dimethylsulphide (DMS) and implications for ecosystem modelling. *Biogeochemistry*, 83(1–3), 245–275. <https://doi.org/10.1007/s10533-007-9091-5>
- Steiner, P. A., Sintes, E., Simó, R., De Corte, D., Pfannkuchen, D. M., Ivančić, I., Najdek, M., & Herndl, G. J. (2019). Seasonal dynamics of marine snow-associated and free-living demethylating bacterial communities in the coastal northern Adriatic Sea. *Environmental Microbiology Reports*, 11(5), 699–707. <https://doi.org/10.1111/1758-2229.12783>
- Steinke, M., Stefels, J., & Stamhuis, E. (2006). Dimethyl sulfide triggers search behavior in copepods. *Limnology and Oceanography*, 51(4), 1925–1930. <https://doi.org/10.4319/lo.2006.51.4.1925>
- Stocker, R. (2012). Marine microbes see a sea of gradients. *Science*, 338(6107), 628–633. <https://doi.org/10.1126/science.1208929>
- Strom, S., Barberi, O., Mazur, C., Bright, K. J., & Fredrickson, K. (2020). High light stress reduces dinoflagellate predation on phytoplankton through both direct and indirect responses. *Aquatic Microbial Ecology*, 84, 43–57. <https://doi.org/10.3354/ame01924>
- Strom, S. L., Wolfe, G., Slajer, A., Lambert, S., & Clough, J. (2003). Chemical defense in the microplankton II: Inhibition of protist feeding by β -dimethylsulfoniopropionate (DMSP). *Limnology and Oceanography*, 48(1), 230–237. <https://doi.org/10.4319/lo.2003.48.1.0230>
- Sunda, W., Kieber, D. J., Kiene, R. P., & Huntsman, S. (2002). An antioxidant function for DMSP and DMS in marine algae. *Nature*, 418(6895), 317–320. <https://doi.org/10.1038/nature00851>
- Tang, K. W. (2001). Defecation of dimethylsulfoniopropionate (DMSP) by the copepod *Acartia tonsa* as functions of ambient food concentration and body DMSP content. *Journal of Plankton Research*, 23(5), 549–553. <https://doi.org/10.1093/plankt/23.5.549>
- Teng, Z.-J., Wang, P., Chen, X.-L., Guillonneau, R., Li, C.-Y., Zou, S.-B., Gong, J., Xu, K.-W., Han, L., Wang, C., Scanlan, D. J., Chen, Y., & Zhang, Y.-Z. (2021). Acrylate protects a marine bacterium from grazing by a ciliate predator. *Nature Microbiology*, 6(11), 1351–1356. <https://doi.org/10.1038/s41564-021-00981-1>
- Vila-Costa, M., Simó, R., Harada, H., Gasol, J. M., Slezak, D., & Kiene, R. P. (2006). Dimethylsulfoniopropionate uptake by marine phytoplankton. *Science*, 314(5799), 652–654. <https://doi.org/10.1126/science.1131043>
- Visser, A. W., & Kjørboe, T. (2006). Plankton motility patterns and encounter rates. *Oecologia*, 148(3), 538–546. <https://doi.org/10.1007/s00442-006-0385-4>
- Watts, P. C., Martin, L. E., Kimmance, S. A., Montagnes, D. J. S., & Lowe, C. D. (2011). The distribution of *Oxyrrhis marina*: A global disperser or poorly characterized endemic? *Journal of Plankton Research*, 33(4), 579–589. <https://doi.org/10.1093/plankt/fbq148>
- Willis MA. Odor-modulated navigation in insects and artificial systems. *Chemical Senses*. 2005 Jan 1;30(Supplement 1):i287–8. <https://doi.org/10.1093/chemse/bjh227>
- Wolfe, G. V., Steinke, M., & Kirst, G. O. (1997). Grazing-activated chemical defence in a unicellular marine alga. *Nature*, 387(6636), 894–897. <https://doi.org/10.1038/43168>
- Zheng, Y., Wang, J., Zhou, S., Zhang, Y., Liu, J., Xue, C.-X., Williams, B. T., Zhao, X., Zhao, L., Zhu, X.-Y., Sun, C., Zhang, H.-H., Xiao, T., Yang, G.-P., Todd, J. D., & Zhang, X.-H. (2020). Bacteria are important dimethylsulfoniopropionate producers in marine aphotic and high-pressure environments. *Nature Communications*, 11(1), 4658. <https://doi.org/10.1038/s41467-020-18434-4>

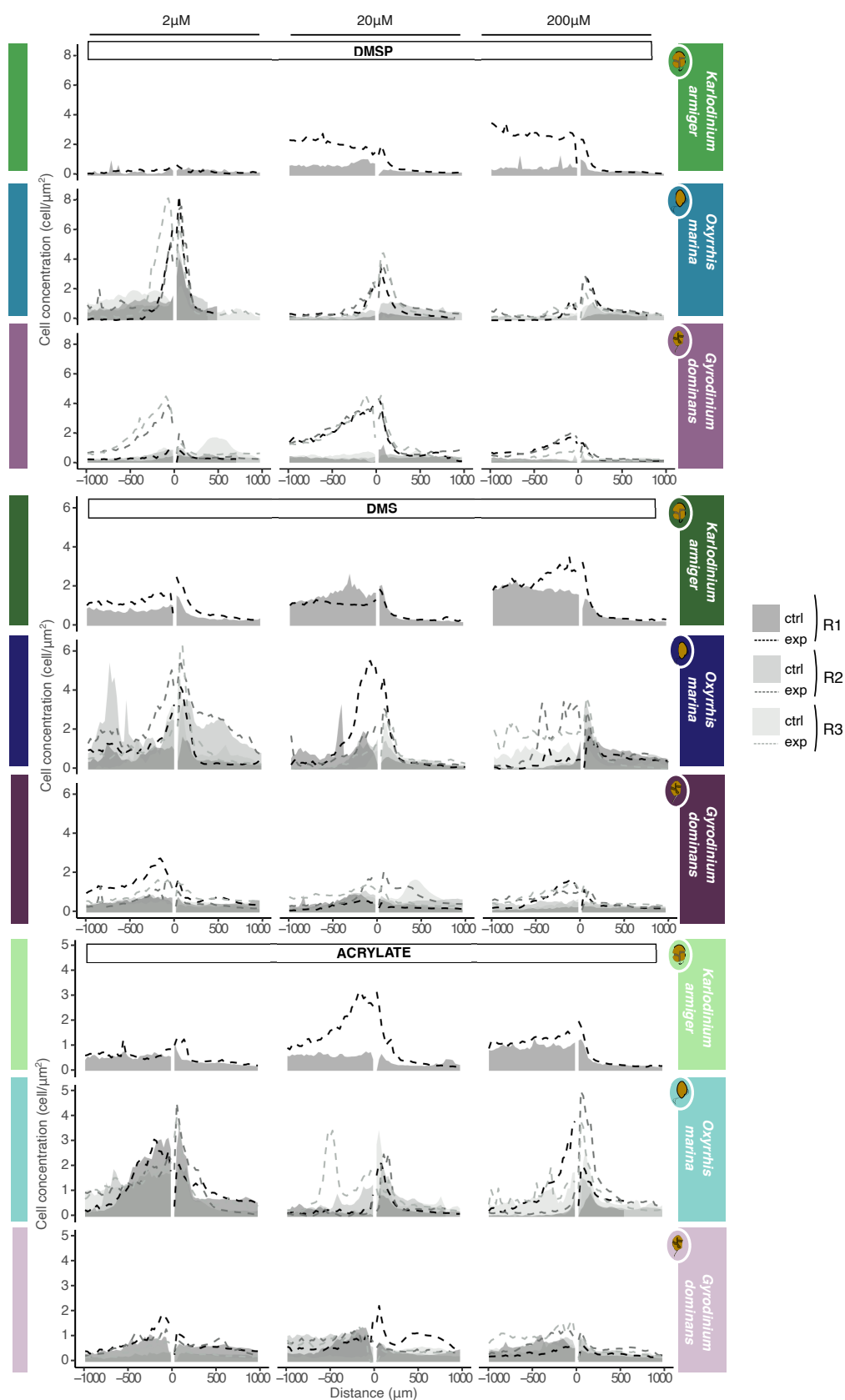
**CHAPTER 1 -
SUPPLEMENTARY INFORMATION**

**THE CHEMOTACTIC BEHAVIOURAL RESPONSE OF MARINE HERBIVORE
PROTISTS TO DMSP AND RELATED COMPOUNDS**

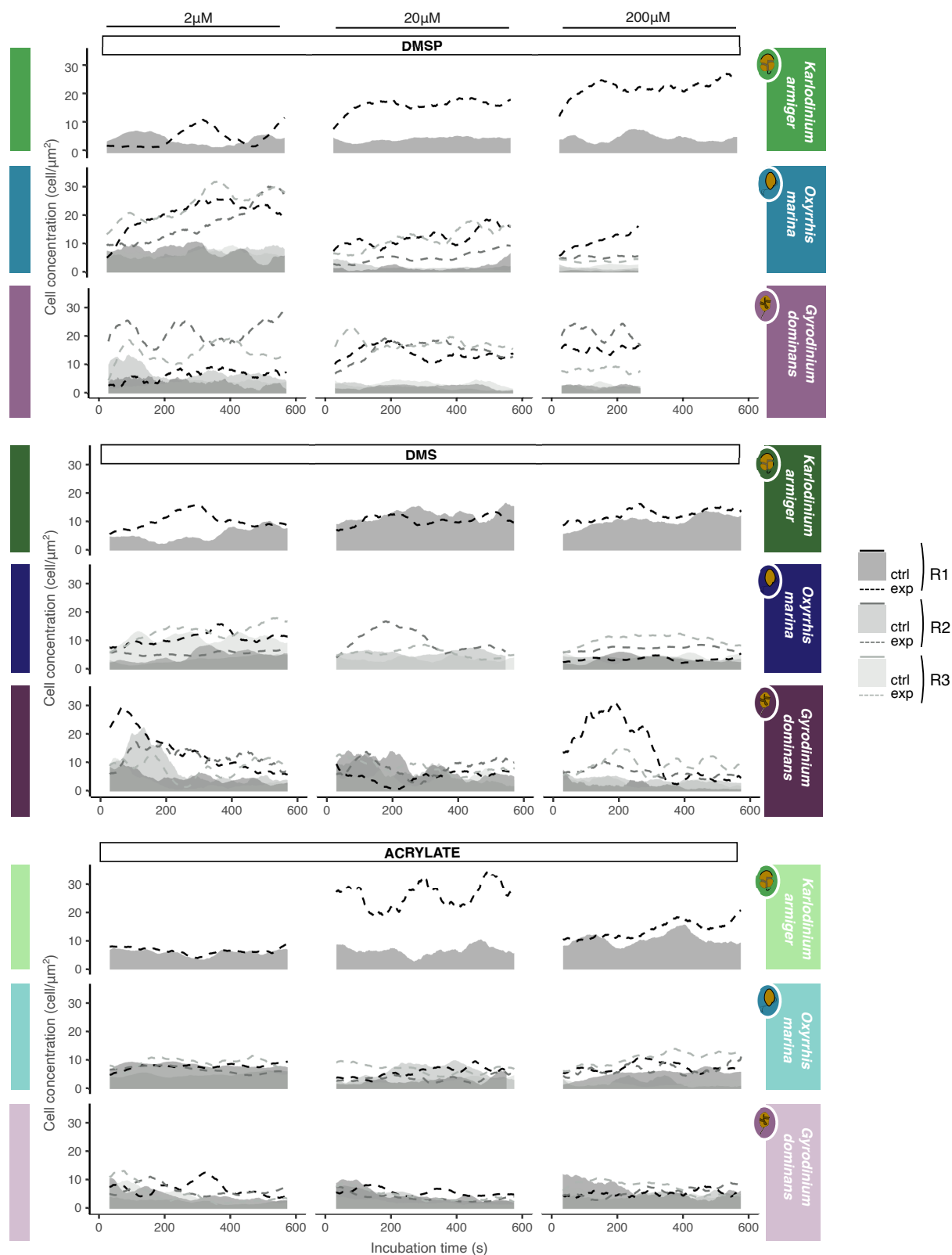
Queralt Güell-Bujons, Medea Zanolli, Idan Tuval, Albert Calbet and Rafel Simó



Supplementary Figure S1.1. Cell density distributions in the microcapillary assays depicted by colormaps. Cell density distributions of *K. armiger*, *O. marina*, and *G. dominans* in microcapillary assays. The figure shows the distributions in one replicate for each substrate and concentration. Cell density (cell μm^{-2}) values were normalised with background cell concentration.



Supplementary Figure S1.2. Cell density distributions in the microcapillary assays depicted by histograms. Cell density distributions of *K. armiger*, *O. marina* and *G. dominans* in microcapillary assays depicted by histograms. The figure shows the distributions in all replicates, substrates, and concentrations. Note that the capillary with substrate (dashed lines) is always compared with a control without substrate (filled area). The 0 on the X axis of the histograms represents the capillary entrance, with the inside area on the left (negative distance) and the outside on the right (positive distance).



Supplementary Figure S1.3. Cell density temporal evolution. Total cell concentration in the two zones of interest was followed through all the incubation. Cell concentration inside and outside was calculated to observe temporal patterns in *K. armiger*, *O. marina*, and *G. dominans* microcapillary assays. The figure shows the total cell concentration in all replicates, substrates, and concentrations. Note that the capillary with substrate (dashed lines) is always compared with a control without substrate (filled area).

Supplementary Table S1.1. Linear regression results of *K. armiger* cell concentrations over time inside the capillaries. Accumulation in the DMSP capillary (cell $\mu\text{m}^2 \text{s}^{-1}$) was assessed by subtracting the slope in the control capillary (C) from the slope in the DMSP capillary (D). Std.err: standard error of the slope; p: probability of slope=0; Rep: replicate; err(D-C): propagated error of the slope subtraction.

<i>K. armiger</i>							
Slope	Std.err	p	adj. R ²	Rep	Capillary	Slope(D-C)	err(D-C)
2 μM							
0.0085	0.0006	1.36E-43	0.13	R1	DMSP	0.0127	0.0007
-0.0042	0.0003	4.80E-32	0.09	R1	CTRL		
20 μM							
0.0019	0.0002	1.46E-23	0.07	R1	DMSP	-0.0018	0.0002
0.0037	8.78E-05	8.21E-250	0.56	R1	CTRL		
200 μM							
0.0051	0.0003	5.43E-59	0.17	R1	DMSP	0.0051	0.0003
-0.0007	0.0003	0.0117	0.004	R1	CTRL		

Supplementary Table S1.2. Linear regression results of *O. marina* cell concentrations over time inside the capillaries. Accumulation in the DMSP capillary (cell $\mu\text{m}^2 \text{s}^{-1}$) was assessed by subtracting the slope in the control capillary (C) from the slope in the DMSP capillary (D). Std.err: standard error of the slope; p: probability of slope=0; Rep: replicate; err(D-C): propagated error of the slope subtraction; err: propagated error of the mean.

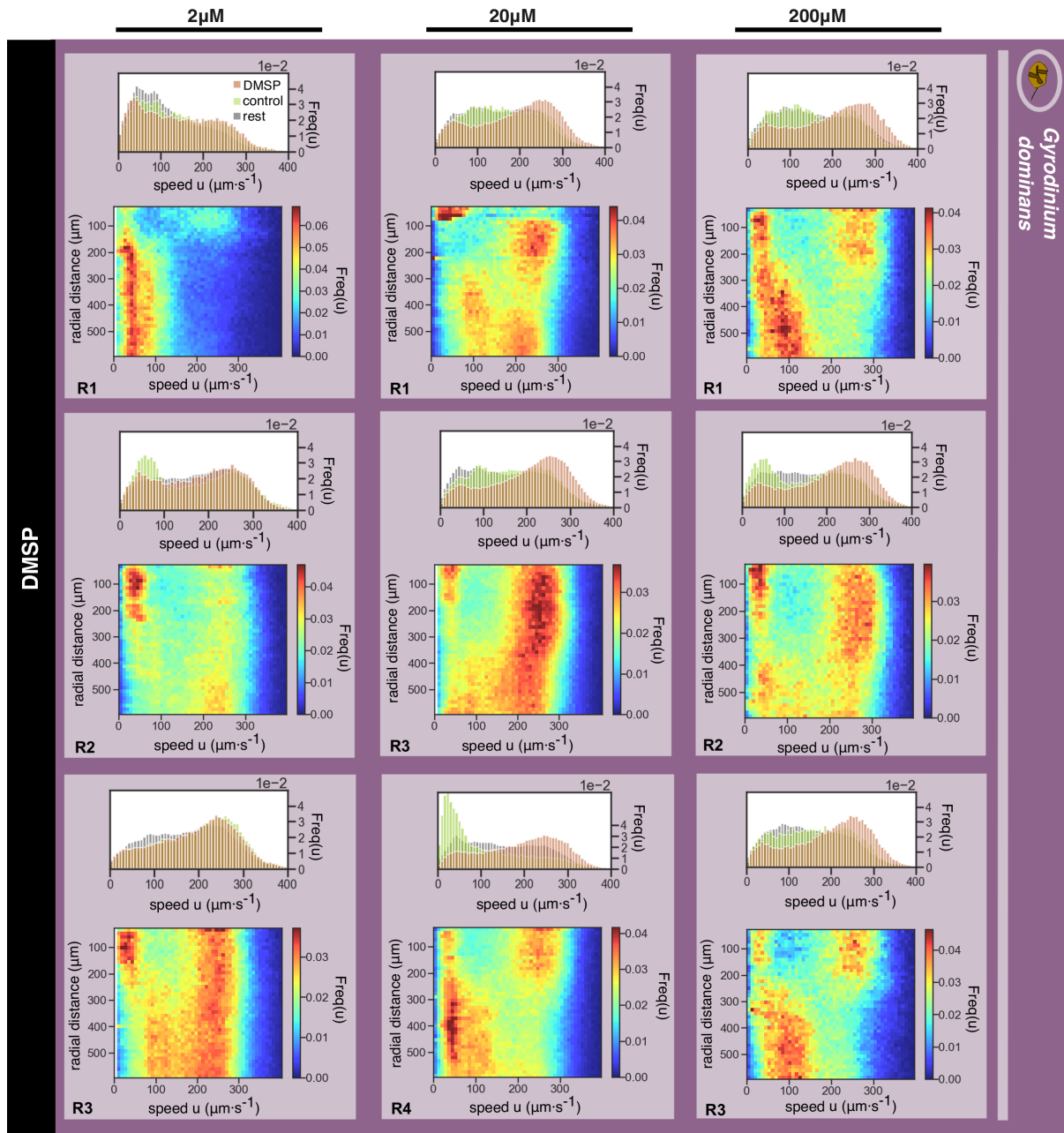
<i>O. marina</i>									
Slope	Std.err.	p	adj. R ²	Rep	Capillary	Slope(D-C)	err(D-C)	mean	err.
2 μM									
0.0109	0.0004	1.02E-120	0.32	R1	DMSP	0.0223	0.0005	0.0280	0.0003
-0.0115	0.0003	3.43E-205	0.48	R1	CTRL				
0.0456	0.0003	0.00E+00	0.93	R2	DMSP	0.0363	0.0004		
0.0092	0.0002	0.00E+00	0.70	R2	CTRL				
0.0266	0.0005	1.02E-310	0.64	R3	DMSP	0.0253	0.0006		
0.0013	0.0002	1.94E-09	0.02	R3	CTRL				
20 μM									
0.0164	0.0004	1.95E-267	0.58	R1	DMSP	0.0116	0.0004	0.0131	0.0002
0.0048	0.0002	4.46E-105	0.29	R1	CTRL				
0.0101	0.0002	0.00E+00	0.67	R2	DMSP	0.0112	0.0002		
-0.0010	0.0001	1.67E-39	0.12	R2	CTRL				
0.0187	0.0003	0.00E+00	0.67	R3	DMSP	0.0164	0.0003		
0.0023	0.0000	0.00E+00	0.76	R3	CTRL				
200 μM									
0.0347	0.0004	9.7E-322	0.95	R1	DMSP	0.0342	0.0004	0.0119	0.0002
0.0005	0.0001	6.33E-06	0.04	R1	CTRL				
0.0018	0.0003	6.51E-10	0.07	R2	DMSP	0.0028	0.0003		
-0.0010	0.0002	4.07E-08	0.06	R2	CTRL				
0.0035	0.0003	5.18E-38	0.28	R3	DMSP	-0.0013	0.0004		

0.0048	0.0003	1.18E-58	0.40	R3	CTRL				
--------	--------	----------	------	----	------	--	--	--	--

Supplementary Table S1.3. Linear regression results of *G. dominans* cell concentrations over time inside the capillaries. Accumulation in the DMSP capillary (cell $\mu\text{m}^2 \text{s}^{-1}$) was assessed by subtracting the slope in the control capillary (C) from the slope in the DMSP capillary (D). Std.err: standard error of the slope; p: probability of slope=0; Rep: replicate; err(D-C): propagated error of the slope subtraction; err: propagated error of the mean.

<i>G. dominans</i>									
Slope	Std.err.	p	adj. R ²	Rep	Capillary	Slope(D-C)	err(D-C)	mean	err.
2 μM									
0.0045	0.0003	4.00E-61	0.18	R1	DMSP	0.0117	0.0003	0.0101	0.0003
-0.0072	0.0001	2.02E-31	0.64	R1	CTRL				
0.0115	0.0006	8.62E-69	0.20	R2	DMSP	0.0168	0.0007		
-0.0053	0.0003	4.07E-56	0.16	R2	CTRL				
0.0037	0.0005	3.45E-12	0.03	R3	DMSP	0.0018	0.0005		
0.0019	0.0001	1.02E-59	0.17	R3	CTRL				
20 μM									
-0.0111	0.0003	1.16E-19	0.46	R1	DMSP	-0.0094	0.0003	-0.0028	0.0002
-0.0017	0.0001	9.78E-35	0.10	R1	CTRL				
-0.0050	0.0004	4.30E-32	0.09	R2	DMSP	-0.0005	0.0004		
-0.0045	5E-05	0	0.83	R2	CTRL				
0.0007	0.0002	0.0032	0.005	R3	DMSP	0.0016	0.0003		
-0.0009	0.0001	4.34E-08	0.02	R3	CTRL				
200 μM									
0.0056	0.0008	5.03E-13	0.10	R1	DMSP	0.0038	0.0008	-0.0054	0.0008
0.0018	0.0004	4.09E-07	0.08	R1	CTRL				
-0.0110	0.0019	1.98E-08	0.06	R2	DMSP	-0.0201	0.0019		
0.0091	0.0003	3.13E-14	0.72	R2	CTRL				
-0.0076	0.0007	4.35E-23	0.17	R3	DMSP	0.0001	0.0009		
-0.0077	0.0006	2.50E-36	0.27	R3	CTRL				

Instantaneous swimming speed. *G. dominans* showed a clear increase in swimming speed when tested with DMSP 20 μM and 200 μM (Supplementary Fig. S1.4). The histograms in the upper part of the panel display the observed relative frequency of swimming speeds in each repetition in 3 different zones: near the entrance of the DMSP filled capillary, near the control capillary and in the remaining frame area. Cells swimming close to the DMSP source ($r < 200 \mu\text{m}$) show a shift towards higher velocities (between 200 $\mu\text{m/s}$ and 300 $\mu\text{m/s}$) in comparison to the rest of the cells. The colormaps in the lower part of each panel show the frequency of the observed swimming speed as a function of the distance from the DMSP source. A patch of cells swimming between 200 $\mu\text{m}\cdot\text{s}^{-1}$ and 300 $\mu\text{m}\cdot\text{s}^{-1}$ is distinguished in the upper part of the colormap corresponding to shorter radial distances. Contrastingly, cells further away from the source swim typically below 150 $\mu\text{m}\cdot\text{s}^{-1}$. The patch of fast swimming cells extends in most repetitions up to 200 μm from the DMSP source, except for R3 at 20 μM and R2 at 200 μM in which the patch extends up to approximately 400 μm . In most repetitions, we observe also a patch of slowly moving cells ($< 70 \mu\text{m}\cdot\text{s}^{-1}$) at the entrance of the capillary. This behaviour is sometimes observed also in the control capillary (R2 at 2 μM , R4 at 20 μM , R2 at 20 μM) and may be caused by cells whose flagella became trapped at the pipette entrance. These cells slowly oscillate around the capillary entrance until they successfully break free and return to the bulk. A less clear chemokinetic behaviour is observed for repetitions at 2 μM . A mild chemokinetic effect is observed in R1, while in repetitions R2 and R3 the cells swim fast (between 200 $\mu\text{m}\cdot\text{s}^{-1}$ and 300 $\mu\text{m}\cdot\text{s}^{-1}$) in the entire frame area and not only near the DMSP source as in the other repetitions.



Supplementary Figure S1.4. Probability distribution of the instantaneous swimming speed of *G. dominans* at each DMSP concentration. Each panel contains two plots. The top chart compares the relative frequencies of the observed swimming speed within 3 different zones, represented in 3 colours: (i) orange: $r < 200\ \mu\text{m}$ from the entrance of the DMSP-filled capillary, (ii) green: $r < 200\ \mu\text{m}$ from the entrance of the control capillary and (iii) grey: the remaining frame area ($r > 200\ \mu\text{m}$ from both capillaries). The bottom chart is a colormap of the relative frequency of the instantaneous swimming speed at different radial distances from the entrance of the DMSP-filled capillary.

Table S1.4. Median values, errors, and significant differences of cellular densities (cell/ μm^2) from both capillaries (Cap. C=control and S=substrate-filled) in *K. armiger* incubations. Significant differences were evaluated with the nonparametric Kruskal-Wallis test. The statistical test was applied to each concentration (2-200 μM), and cue (D=DMSP, M=DMS, A=ACRYLATE, Std.D=standard deviation, N=number of frames, Std.E= standard error).

<i>K. armiger</i> - INSIDE									
Cap.	Mean (cell density)	Std.D	N	Std.E	p.value	lc _{max}	Mean lc _{max}	Std.E lc _{max}	Sample
C	2.37	1.22	1619	0.030	p<2.2E-16	3.26	3.26	0.00	D2_1
S	7.73	1.38	361	0.073					D2_1
C	3.95	0.54	1619	0.013	p<2.2E-16	3.44	3.44	0.00	D20_1
S	13.61	0.86	361	0.045					D20_1
C	2.91	0.81	1619	0.020	p<2.2E-16	6.57	6.57	0.00	D200_1
S	19.11	0.98	361	0.052					D200_1
C	3.33	1.42	1619	0.035	p<2.2E-16	2.23	2.23	0.00	M2_1
S	7.44	0.96	361	0.050					M2_1
C	8.42	1.01	1619	0.025	p=5.31E-06	0.96	0.96	0.00	M20_1
S	8.08	0.41	361	0.021					M20_1
C	7.56	1.39	1620	0.034	p<2.2E-16	1.18	1.18	0.00	M200_1
S	8.92	0.36	361	0.019					M200_1
C	3.86	1.06	1619	0.026	p=0.1568	1.00	1.00	0.00	A2_1
S	4.02	0.73	361	0.038					A2_1
C	4.67	1.15	1619	0.028	p<2.2E-16	4.55	4.55	0.00	A20_1
S	21.25	2.93	361	0.154					A20_1
C	6.49	1.29	1617	0.032	p<2.2E-16	1.42	1.42	0.00	A200_1
S	9.21	1.41	361	0.074					A200_1

<i>K. armiger</i> - OUTSIDE									
Cap.	Mean (cell density)	Std.Dev	N	Std.Err	p.value	lc _{max}	Mean lc _{max}	Std.Err lc _{max}	Sample
C	2.48	0.83	1619	0.021	p=0.9997	1.00	1.00	0.00	D2_1
S	2.27	0.28	181	0.021					D2_1
C	1.00	0.33	1619	0.008	p<2.2E-16	4.96	4.96	0.00	D20_1
S	4.94	0.48	361	0.025					D20_1
C	2.43	0.94	1619	0.023	p<2.2E-16	3.62	3.62	0.00	D200_1
S	8.82	1.04	306	0.059					D200_1
C	2.28	0.87	1619	0.022	p<2.2E-16	3.15	3.15	0.00	M2_1
S	7.18	0.86	361	0.045					M2_1
C	4.04	1.19	1619	0.029	p=0.01899	1.00	1.00	0.00	M20_1
S	3.79	0.97	361	0.051					M20_1
C	2.82	0.69	1620	0.017	p<2.2E-16	1.98	1.98	0.00	M200_1
S	5.59	0.57	361	0.030					M200_1
C	2.10	0.36	1619	0.009	p<2.2E-16	1.24	1.24	0.00	A2_1

S	2.61	0.22	361	0.012					A2_1
C	2.09	0.74	1619	0.018	p<2.2E-16	4.09	4.09	0.00	A20_1
S	8.56	0.78	361	0.041					A20_1
C	4.23	1.55	1617	0.039	p<2.2E-16	1.62	1.62	0.00	A200_1
S	6.83	0.64	361	0.033					A200_1

Table S1.5. Median values, errors, and significant differences of cellular densities (cell/ μm^2) from both capillaries (Cap. C=control and S=substrate-filled) in *O. marina* incubations. Significant differences were evaluated with the nonparametric Kruskal-Wallis test. The statistical test was applied to each replicate (1-3), concentration (2-200 μM), and cue (D=DMS, M=DMS, A=ACRYLATE, Std.D=standard deviation, N=number of frames, Std.E=standard error).

<i>O. marina</i> - INSIDE									
Cap	Mean (cell density)	Std.D	N	Std.E	p.value	lc _{max}	Mean lc _{max}	Std.E lc _{max}	Sample
C	3.14	1.45	1620	0.036	p<2.2E-16	5.49	5.78	0.65	D2_1
S	17.26	1.46	361	0.077					D2_1
C	2.73	0.77	1619	0.019	p<2.2E-16	6.53			D2_2
S	17.83	2.25	361	0.119					D2_2
C	4.16	0.94	1620	0.023	p<2.2E-16	5.31			D2_3
S	22.12	1.61	361	0.085					D2_3
C	0.77	0.65	1619	0.016	p<2.2E-16	13.08	9.20	5.48	D20_1
S	10.07	1.74	361	0.091					D20_1
C	1.01	0.60	1619	0.015	p<2.2E-16	5.33			D20_2
S	5.38	0.84	361	0.044					D20_2
C	0.06	0.09	1619	0.002	p<2.2E-16	172.11			D20_3
S	9.50	0.73	361	0.038					D20_3
C	0.01	0.01	720	0.000	p<2.2E-16	1030.64	3.07	1.46	D200_1
S	7.04	1.42	361	0.075					D200_1
C	0.50	0.26	720	0.010	p<2.2E-16	4.11			D200_2
S	2.06	0.24	361	0.012					D200_2
C	0.96	0.23	720	0.008	p<2.2E-16	2.04			D200_3
S	1.96	0.34	361	0.018					D200_3
C	3.02	1.90	1619	0.047	p<2.2E-16	2.54	1.98	0.83	M2_1
S	7.68	1.17	361	0.062					M2_1
C	1.74	0.90	1620	0.022	p<2.2E-16	2.41			M2_2
S	4.18	0.42	361	0.022					M2_2
C	6.34	1.52	1618	0.038	p=0.01629	1.00			M2_3
S	6.58	1.37	361	0.072					M2_3
C	4.87	2.88	1620	0.072	p<2.2E-16	6.54	4.11	2.24	M20_1
S	31.85	2.10	361	0.110					M20_1
C	4.04	0.92	1541	0.024	p<2.2E-16	2.12			M20_2
S	8.54	0.82	361	0.043					M20_2

C	1.09	0.51	1619	0.013	p<2.2E-16	3.69			M20_3
S	4.03	0.27	361	0.014					M20_3
C	0.90	0.48	1620	0.012	p<2.2E-16	2.10	5.21	5.43	M200_1
S	1.88	0.34	361	0.018					M200_1
C	0.77	0.39	1620	0.010	p<2.2E-16	11.49			M200_2
S	8.88	0.12	361	0.006					M200_2
C	2.72	0.38	1620	0.010	p<2.2E-16	2.06			M200_3
S	5.58	0.12	361	0.006					M200_3
C	5.53	0.52	1620	0.013	p=0.05181	1.00	1.18	0.31	A2_1
S	5.61	0.73	361	0.039					A2_1
C	2.91	0.50	1619	0.013	p<2.2E-16	1.54			A2_2
S	4.49	0.33	361	0.017					A2_2
C	4.83	0.64	1618	0.016	p=0.02255	1.00			A2_3
S	4.94	0.35	361	0.018					A2_3
C	0.76	0.37	1549	0.009	p<2.2E-16	2.64	3.52	3.69	A20_1
S	2.01	0.61	361	0.032					A20_1
C	3.76	1.97	1620	0.049	p<2.2E-16	0.35			A20_2
S	1.33	0.18	361	0.009					A20_2
C	0.62	0.34	1619	0.008	p<2.2E-16	7.57			A20_3
S	4.69	0.30	361	0.016					A20_3
C	1.06	1.08	1620	0.027	p<2.2E-16	3.44	5.43	5.21	A200_1
S	3.63	1.22	361	0.064					A200_1
C	0.61	0.41	1620	0.010	p<2.2E-16	11.34			A200_2
S	6.94	0.98	361	0.051					A200_2
C	2.57	0.68	1620	0.017	p<2.2E-16	1.51			A200_3
S	3.88	0.67	361	0.035					A200_3

O. marina - OUTSIDE									
Cap	Mean (cell density)	Std.D	N	Std.E	p.value	Ic _{max}	Mean Ic _{max}	Std.E Ic _{max}	Sample
C	4.39	0.77	1620	0.019	p<2.2E-16	1.95	2.27	0.38	D2_1
S	8.56	0.62	361	0.033					D2_1
C	4.32	1.00	1619	0.025	p<2.2E-16	2.18			D2_2
S	9.40	0.72	361	0.038					D2_2
C	2.80	0.84	1620	0.021	p<2.2E-16	2.69			D2_3
S	7.53	0.84	187	0.062					D2_3
C	0.99	0.59	1619	0.015	p<2.2E-16	6.63	8.77	7.48	D20_1
S	6.55	0.48	361	0.025					D20_1
C	1.07	0.30	1619	0.007	p<2.2E-16	2.60			D20_2

S	2.79	0.12	361	0.006					D20_2
C	0.37	0.31	1619	0.008	p<2.2E-16	17.09			D20_3
S	6.35	0.85	361	0.045					D20_3
C	0.60	0.14	720	0.005	p<2.2E-16	9.93	5.17	4.31	D200_1
S	5.96	0.54	361	0.028					D200_1
C	0.92	0.20	720	0.008	p<2.2E-16	4.06			D200_2
S	3.72	0.35	361	0.018					D200_2
C	1.38	0.26	720	0.010	p<2.2E-16	1.53			D200_3
S	2.11	0.17	361	0.009					D200_3
C	1.89	0.37	1619	0.009	p<2.2E-16	3.21	2.21	0.94	M2_1
S	6.07	0.43	361	0.023					M2_1
C	1.79	0.41	1620	0.010	p<2.2E-16	1.33			M2_2
S	2.39	0.06	361	0.003					M2_2
C	4.74	0.76	1618	0.019	p<2.2E-16	2.10			M2_3
S	9.94	0.37	361	0.020					M2_3
C	1.19	0.50	1620	0.012	p<2.2E-16	8.95	4.75	3.77	M20_1
S	10.67	0.35	361	0.018					M20_1
C	1.97	0.67	1541	0.017	p<2.2E-16	3.67			M20_2
S	7.23	0.91	361	0.048					M20_2
C	2.57	0.48	1619	0.012	p<2.2E-16	1.63			M20_3
S	4.20	0.13	213	0.009					M20_3
C	2.86	0.99	1620	0.025	p=8.83E-10	1.09	1.53	0.84	M200_1
S	3.10	0.40	187	0.029					M200_1
C	3.44	0.77	1620	0.019	p=0.05444	1.00			M200_2
S	3.55	0.30	361	0.016					M200_2
C	1.34	0.30	1620	0.007	p<2.2E-16	2.50			M200_3
S	3.35	0.28	361	0.015					M200_3
C	2.83	0.31	1620	0.008	p=0.842	1.00	1.47	0.82	A2_1
S	2.80	0.11	361	0.006					A2_1
C	2.17	0.35	1619	0.009	p<2.2E-16	1.00			A2_2
S	4.93	0.09	181	0.007					A2_2
C	2.20	0.51	1618	0.013	p<2.2E-16	2.41			A2_3
S	5.31	0.63	361	0.033					A2_3
C	2.25	0.82	1549	0.021	p<2.2E-16	2.57	1.97	0.53	A20_1
S	5.78	0.83	361	0.044					A20_1
C	2.50	0.84	1620	0.021	p<2.2E-16	1.57			A20_2
S	3.92	0.73	334	0.040					A20_2
C	2.18	0.19	1619	0.005	p<2.2E-16	1.77			A20_3
S	3.85	0.27	331	0.015					A20_3
C	0.99	0.31	1620	0.008	p<2.2E-16	6.02	3.85	2.03	A200_1
S	5.94	1.28	223	0.085					A200_1

C	1.65	0.61	1620	0.015	p<2.2E-16	3.53			A200_2
S	5.84	0.20	361	0.010					A200_2
C	2.81	0.95	1620	0.024	p<2.2E-16	2.00			A200_3
S	5.62	0.65	361	0.034					A200_3

Table S1.6. Median values, errors, and significant differences of cellular densities (cell/ μm^2) from both capillaries (Cap. C=control and S=substrate-filled) in *G. dominans* incubations. Significant differences were evaluated with the nonparametric Kruskal-Wallis test. The statistical test was applied to each replicate (1-3), concentration (2-200 μM), and cue (D=DMS, M=DMS, A=ACRYLATE, Std.D=standard deviation, N=number of frames, Std.E=standard error).

<i>G. dominans</i> - INSIDE									
Cap	Mean (cell density)	Std.D	N	Std.E	p.value	lc _{max}	Mean lc _{max}	Std.E lc _{max}	Sample
C	2.47	0.96	1619	0.024	p<2.2E-16	2.39	4.70	2.28	D2_1
S	5.92	0.69	361	0.036					D2_1
C	4.19	2.28	1621	0.057	p<2.2E-16	4.75			D2_2
S	19.92	1.54	361	0.081					D2_2
C	2.25	0.61	1622	0.015	p<2.2E-16	6.95			D2_3
S	15.61	1.84	361	0.097					D2_3
C	1.12	0.44	1620	0.011	p<2.2E-16	11.93	12.22	5.73	D20_1
S	13.33	1.38	361	0.073					D20_1
C	2.34	0.79	1620	0.020	p<2.2E-16	6.64			D20_2
S	15.52	2.56	361	0.135					D20_2
C	0.69	0.16	1622	0.004	p<2.2E-16	18.10			D20_3
S	12.56	1.34	361	0.070					D20_3
C	1.94	0.36	722	0.013	p<2.2E-16	6.40	7.42	4.85	D200_1
S	12.41	0.76	361	0.040					D200_1
C	1.25	0.57	720	0.021	p<2.2E-16	12.70			D200_2
S	15.85	2.18	361	0.115					D200_2
C	1.86	0.49	721	0.018	p<2.2E-16	3.16			D200_3
S	5.87	0.87	361	0.046					D200_3
C	2.48	0.93	1619	0.023	p<2.2E-16	4.98	3.17	1.69	M2_1
S	12.33	1.63	361	0.086					M2_1
C	4.19	2.94	1619	0.073	p<2.2E-16	1.64			M2_2
S	6.90	1.46	361	0.077					M2_2
C	1.61	1.39	1619	0.035	p<2.2E-16	2.89			M2_3
S	4.65	1.29	361	0.068					M2_3
C	4.30	1.73	1619	0.043	p<2.2E-16	0.62	1.50	0.82	M20_1
S	2.66	0.64	361	0.034					M20_1
C	3.28	1.49	1618	0.037	p<2.2E-16	1.65			M20_2

S	5.42	0.94	361	0.050					M20_2
C	2.51	0.80	1622	0.020	p<2.2E-16	2.24			M20_3
S	5.64	0.51	361	0.027					M20_3
C	1.04	0.62	1619	0.015	p<2.2E-16	12.75	6.31	5.65	M200_1
S	13.28	1.61	361	0.085					M200_1
C	2.07	0.41	1620	0.010	p<2.2E-16	2.18			M200_2
S	4.50	0.48	361	0.025					M200_2
C	1.57	0.59	1619	0.015	p<2.2E-16	4.02			M200_3
S	6.31	1.01	361	0.053					M200_3
C	3.20	1.47	1619	0.036	p<2.2E-16	2.60	3.61	1.46	A2_1
S	8.31	1.37	361	0.072					A2_1
C	1.21	0.51	1619	0.013	p<2.2E-16	5.28			A2_2
S	6.38	0.95	361	0.050					A2_2
C	2.90	2.06	1618	0.051	p<2.2E-16	2.95			A2_3
S	8.56	1.97	361	0.103					A2_3
C	3.61	2.03	1619	0.050	p<2.2E-16	1.18	2.06	1.58	A20_1
S	4.26	0.62	361	0.033					A20_1
C	3.07	1.35	1619	0.034	p=1.81E-13	1.11			A20_2
S	3.42	0.69	361	0.036					A20_2
C	0.82	0.21	1620	0.005	p<2.2E-16	3.88			A20_3
S	3.17	0.24	361	0.013					A20_3
C	5.02	2.35	1620	0.058	p=0.06103	1.00	1.82	0.73	A200_1
S	4.81	1.13	361	0.059					A200_1
C	2.89	0.78	1619	0.019	p<2.2E-16	2.10			A200_2
S	6.07	0.99	361	0.052					A200_2
C	3.26	0.79	1619	0.020	p<2.2E-16	2.37			A200_3
S	7.71	0.53	361	0.028					A200_3

<i>G. dominans</i> - OUTSIDE									
Cap	Mean (cell density)	Std.D	N	Std.E	p.value	lc _{max}	Mean lc _{max}	Std.E lc _{max}	Sample
C	1.53	0.60	1619	0.015	p<2.2E-16	1.51	1.76	0.40	D2_1
S	2.31	0.23	361	0.012					D2_1
C	3.26	1.27	1621	0.031	p<2.2E-16	1.55			D2_2
S	5.07	0.54	361	0.029					D2_2
C	1.46	0.29	1622	0.007	p<2.2E-16	2.22			D2_3

S	3.24	0.49	264	0.030					D2_3
C	1.06	0.49	1620	0.012	p<2.2E-16	6.41	4.60	1.64	D20_1
S	6.77	0.18	361	0.010					D20_1
C	1.20	0.21	1620	0.005	p<2.2E-16	3.22			D20_2
S	3.87	0.36	361	0.019					D20_2
C	1.69	0.72	1622	0.018	p<2.2E-16	4.19			D20_3
S	7.09	0.32	181	0.024					D20_3
C	0.74	0.14	722	0.005	p<2.2E-16	4.28	3.93	0.75	D200_1
S	3.18	0.28	361	0.015					D200_1
C	1.03	0.61	720	0.023	p<2.2E-16	4.45			D200_2
S	4.56	0.50	361	0.027					D200_2
C	1.02	0.20	720	0.008	p<2.2E-16	3.07			D200_3
S	3.12	0.15	204	0.010					D200_3
C	1.27	0.27	1619	0.007	p<2.2E-16	1.60	2.27	0.60	M2_1
S	2.03	0.12	361	0.006					M2_1
C	0.99	0.38	1619	0.009	p<2.2E-16	2.73			M2_2
S	2.70	0.32	361	0.017					M2_2
C	1.01	0.52	1619	0.013	p<2.2E-16	2.50			M2_3
S	2.53	0.23	361	0.012					M2_3
C	1.78	0.68	1619	0.017	p=0.8633	1.00	2.12	1.51	M20_1
S	1.67	0.36	361	0.019					M20_1
C	1.17	0.53	1618	0.013	p<2.2E-16	3.84			M20_2
S	4.49	0.49	361	0.026					M20_2
C	1.40	0.41	1622	0.010	p<2.2E-16	1.53			M20_3
S	2.14	0.27	361	0.014					M20_3
C	0.81	0.42	1619	0.010	p<2.2E-16	4.18	2.84	1.29	M200_1
S	3.40	0.47	361	0.025					M200_1
C	1.12	0.24	1620	0.006	p<2.2E-16	2.73			M200_2
S	3.07	0.41	361	0.022					M200_2
C	1.27	0.19	1619	0.005	p<2.2E-16	1.60			M200_3
S	2.04	0.11	361	0.006					M200_3
C	1.57	0.52	1619	0.013	p<2.2E-16	1.28	1.58	0.64	A2_1
S	2.01	0.32	249	0.021					A2_1
C	1.37	0.35	1619	0.009	p<2.2E-16	2.32			A2_2
S	3.17	0.32	361	0.017					A2_2
C	1.76	0.51	1618	0.013	p=2.72E-14	1.15			A2_3
S	2.02	0.26	361	0.014					A2_3
C	1.32	0.31	1619	0.008	p<2.2E-16	2.57	1.61	0.83	A20_1
S	3.39	0.18	361	0.009					A20_1
C	1.24	0.39	1619	0.010	p<2.2E-16	1.16			A20_2
S	1.44	0.35	361	0.018					A20_2

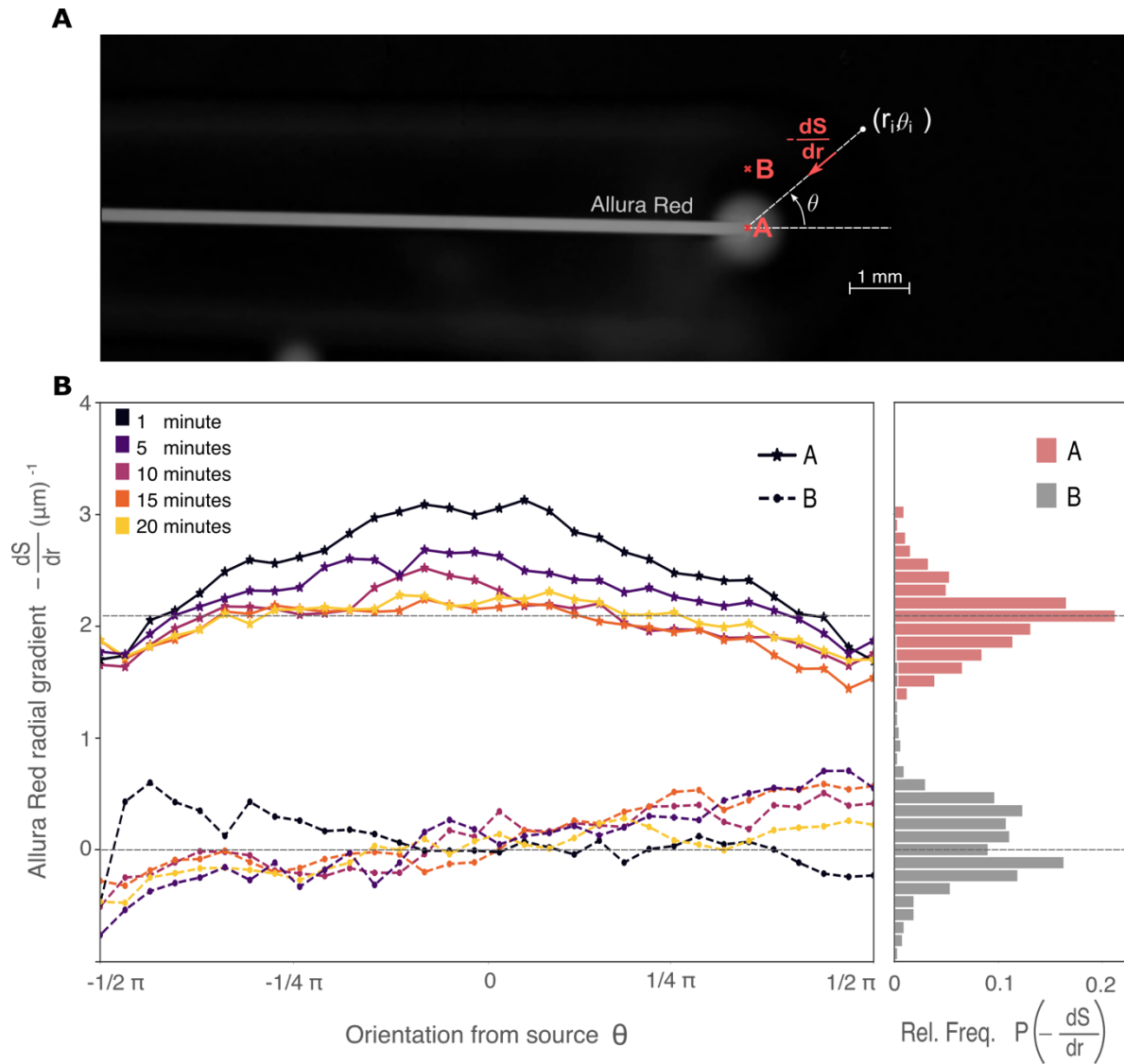
C	1.49	0.40	1620	0.010	$p < 2.2E-16$	1.11			A20_3
S	1.66	0.15	220	0.010					A20_3
C	1.57	0.42	1620	0.011	$p < 2.2E-16$	1.25	1.10	0.16	A200_1
S	1.96	0.19	361	0.010					A200_1
C	1.78	0.26	1619	0.006	$p = 1.87E-09$	0.93			A200_2
S	1.65	0.06	361	0.003					A200_2
C	1.83	0.20	1619	0.005	$p < 2.2E-16$	1.14			A200_3
S	2.08	0.17	361	0.009					A200_3

EXTENDED MATERIALS & METHODS

Diffusion experiment from a capillary of squared cross-section. The experimental design required both capillaries in the same frame and thus they were placed in close proximity. Consequently, after some time the control capillary would be reached by the diffusing substrate plume from the test capillary. The typical timescale needed for the plume to reach the control capillary can be approximated as:

$$\tau \sim \frac{x^2}{4D}$$

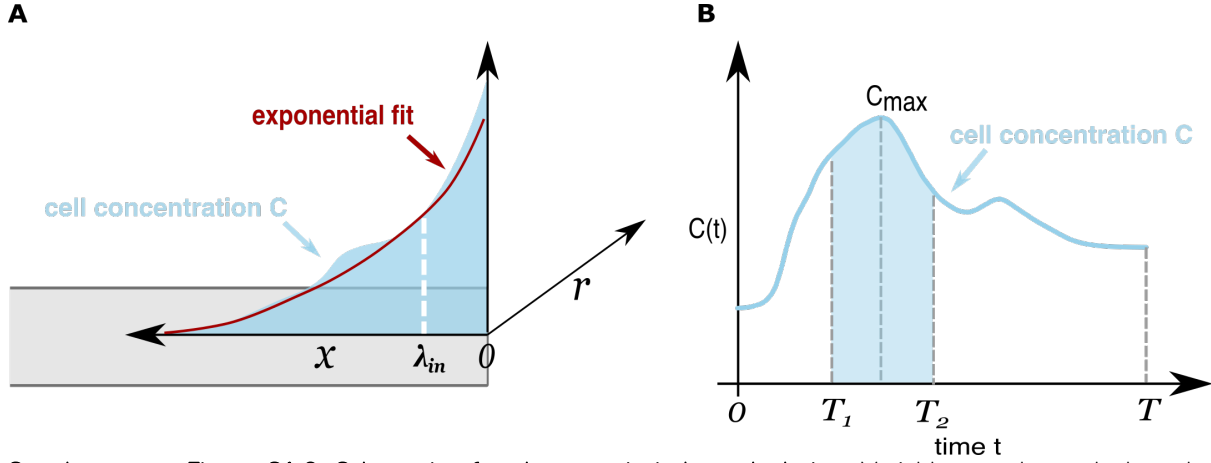
where D is the diffusion coefficient of the solute and x the distance between the two capillaries. In the experiment, the distance between test and control capillaries was typically $x \sim 1$ mm. Knowing the diffusion coefficients of DMSP ($D_{\text{DMSP}} \sim 6 * 10^{-6} \text{ cm}^2/\text{s}$), DMS ($D_{\text{DMS}} \sim 1.1 * 10^{-5} \text{ cm}^2/\text{s}$) and acrylate ($D_{\text{acrylate}} \sim 1.1 * 10^{-5} \text{ cm}^2/\text{s}$), the times after which the plumes would reach the entrance of the control capillary were $\tau_{\text{DMSP}} \sim 8$ min, $\tau_{\text{DMS}} = \tau_{\text{acrylate}} \sim 4$ min, i.e., within the duration of most video recordings. Nevertheless, we expected that the presence of a continuous DMSCs source would maintain a much stronger gradient at the entrance of the test capillary for the whole duration of the experiment. To confirm the expected gradients, we recorded the diffusion process from a square-shaped CM Scientific microcapillary immersed in L1 medium for 20 minutes using Allura Red as solute (Supplementary Figure S1.5). The strength of the Allura Red gradients during the recording time at the source and 1 mm away (points A and B in Supplementary Figure S1.5A) was quantified by image analysis. The diffusion constant of Allura Red ($D_{\text{Allura Red}} \sim 5 * 10^{-6} \text{ cm}^2/\text{s}$) is almost the same as that of DMSP and half those of DMS and acrylate. Accordingly, the Allura Red gradients measured 20 minutes after the start of the diffusion process will thus be comparable with those of DMSP after the same time and those of DMS and acrylate after 10 minutes. Gradients were calculated for a scalar field S ranging between 0 and 1 proportional to a color linear scale (0 = black pixel, no Allura Red, 1= gray pixel, max Allura Red concentration inside the capillary) in units of μm^{-1} . Gradients are calculated radially over a semicircle centered at the entrance of the capillary $\theta \in [-\pi/2, \pi/2]$ (point A), where $\theta = 0$ corresponds to the direction parallel to the capillary. The same was done at point B one millimeter away from A. The temporal evolution of the gradients is shown in the left panel of Supplementary Figure S1.5B. The histograms (right panel Supplementary Figure S1.5B) represent the discrete probability distribution of the gradients dS/dr integrated for all values of $\theta \in [-\pi/2, \pi/2]$ over the total recording time (sampled once every minute). The results confirm that strong gradients were maintained near the chemical source compared to the control capillary for all compounds (DMSP, DMS, acrylate) for the whole duration of a 10-min. experiment.



Supplementary Figure S1.5. Allura Red gradients as a proxy for DMSCs gradients (A) Diffusive plume from a square-shaped CM Scientific microcapillary filled with Allura Red in L1 medium at room temperature. The snapshot was taken 1 minute after the insertion of the Allura Red-filled capillary in the medium. The diffusion process was recorded over 20 minutes with an IDS camera. (B) Gradients of a scalar field S quantifying the Allura Red concentration. S is defined as a scalar number between 0 (black pixel, no Allura Red) and 1 (gray pixel, max Allura Red concentration inside the capillary). The gradients dS/dr are calculated radially in A and B over a semicircle $\theta \in [-\pi/2, \pi/2]$, where $\theta = 0$ corresponds to the direction parallel to the capillary. The left panel shows the radial distribution of the Allura-Red gradients after 1, 5, 10, 15 and 20 minutes from the addition of the capillary to the medium. The right panel reports the probability distribution of the gradients measured in A and B, sampled every minute between 1 and 20 minutes starting from the addition of the capillary to the medium.

Artificial seawater (ASW). The ASW was elaborated by mixing and heating 1 l of distilled water with 43 g of sea salts (Sigma-Aldrich) and 1g of standard NaCl. The solution was filtered through GF/F to get rid of precipitated salts. The final salinity was 37.3 psu and the pH was adjusted to 7.9 by adding HCl. A second sterile filtration was conducted.

Chemotactic index calculation. To determine the maximum chemo-response observed during the experimental time, the chemotactic index Ic_{max} was calculated when cell accumulation in the substrate-filled capillary was at its peak (Supplementary Figure 1.6). To do so, the concentrations $C(x,t)$ (inside the capillary) and $C(r,t)$ (outside the capillary) were evaluated as a function of time and smoothed out with a 1-minute rolling average.



Supplementary Figure S1.6. Schematics for chemotactic index calculation. Variables used to calculate the chemotactic index inside the capillary. (A) The cell concentration profile $C(x)$ is fitted to a decaying exponential with constant λ_{in} . The area of the capillary comprised between 0 and λ_{in} is the one taken into account to calculate the chemotactic index. (B) Temporal evolution of cell concentration $C(t)$ in the area between 0 and λ_{in} . The experiment lasted a total time T (5 or 10 minutes depending on the repetition), and the times T_1 and T_2 embrace the 2-minute window of maximum chemoattraction, highlighted in blue.

The average cell concentration inside the substrate-filled capillary is then calculated as:

$$\bar{C}_S = \frac{1}{\lambda_{in}} \cdot \frac{1}{T_2 - T_1} \cdot \int_{T_1}^{T_2} dt \cdot \int_0^{\lambda_{in}} dx C(x, t)$$

where T_1 and T_2 are the extremes of the two-minute time window centered around the moment of maximum cell concentration, and λ_{in} is the exponential decay constant obtained from the fit of the concentration profile.

For the control, the average concentration is calculated as:

$$\bar{C}_C = \frac{1}{\lambda_{in}} \cdot \frac{1}{T} \cdot \int_0^T dt \cdot \int_0^{\lambda_{in}} dx C(x, t)$$

Where T is the total recording time. The average here is performed over the entire duration of the experiment to get a stable result for all repetitions and avoid null values of cell concentration.

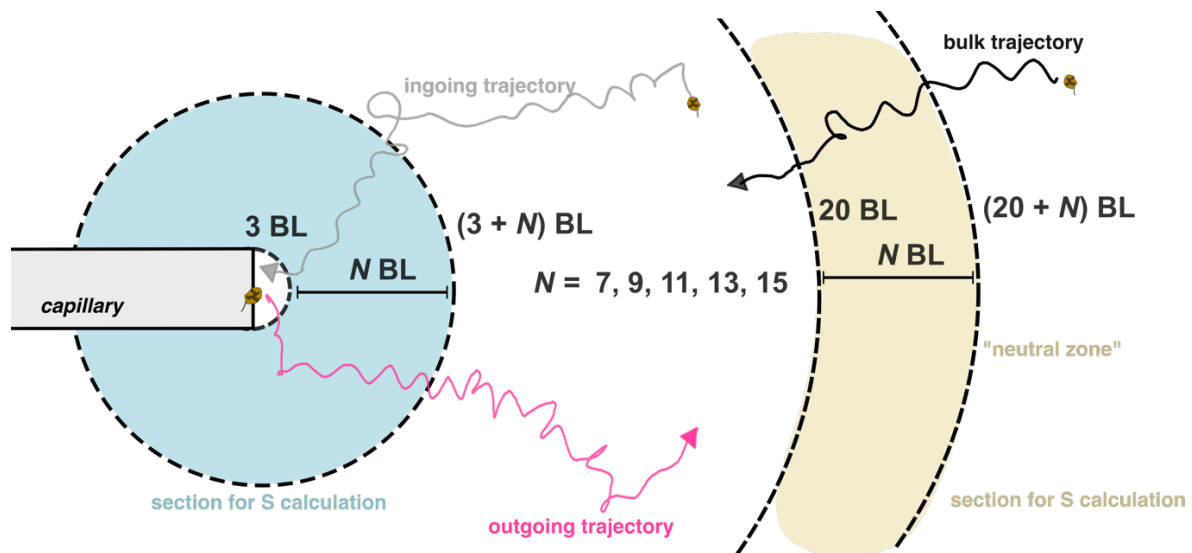
Overall, Ic_{max} is calculated as:

$$Ic_{max} = \frac{\bar{C}_S}{\bar{C}_C}$$

The same calculation is carried out radially outside the capillaries, on a semi-circular region of radius λ_{out} . Accordingly, we get two chemotactic indices: one inside and one outside the capillary.

Definition and robustness of the straightness index S . The straightness of a path is calculated as $S = D/L$, where D is the net 2D displacement and L the path length, has the drawback of being length-dependent. Considering a convoluted path and selecting a section of it, the calculated value of S for that particular section can vary depending on the length of the chosen section. For example, S would tend to 1 for a very short path, independently on how convoluted is the total trajectory.

To overcome the potential effect of the length of the track on S , for all trajectories we only used a fixed section of the path comprised between 3 and 10 body lengths (BL) calculated radially from the DMSP source after the first 1 minute of recording. Considering an average BL of 20 μm and a diffusion coefficient for DMSP of $0.6\text{E-}5\text{ cm}^2\text{ s}^{-1}$, the distance travelled by the diffusing solute in 1 minute is $x \sim \sqrt{(2Dt)} = 270\text{ }\mu\text{m}$. The value of S calculated within 10 BL (200 μm) thus corresponds to a trajectory fully contained within the DMSP patch. Trajectories that did not fully cross the 3 BL and 10 BL lines were discarded from the statistics. Non-continuous trajectories were allowed as long as the track cuts were shorter than 10% of the path length. To test the robustness of the index, S was calculated on trajectories covering a progressively greater distance (Supplementary Fig. S1.7). S was calculated on cells swimming towards or away from the DMSP source, covering a radial distance of 7, 9, 11, 13 and 15 body lengths (BL) with respect to the position of the entrance of the capillary. A cell is considered to be moving away from the DMSP source when its trajectory starts from less than 3 BL (60 μm) with respect to the capillary entrance and moves at least N BL far away from it ($N = 7, 9, 11, 13, 15$). The opposite is assumed for cells approaching the capillary. The straightness index was calculated also on the same range in an area unaffected by the chemoattractant (radial distance between 20 BL and 27 BL from the DMSP source during the first minute of recording), indicated as "neutral zone" (Supplementary Fig. S1.7). This area is located at 20 BL (400 μm) from the capillary. S in the neutral zone is calculated only on trajectories happening in the first minute of recording, to ensure that the area is unaffected by the diffusing DMSP plume. The nonparametric Kruskal-Wallis test, complemented with a post hoc Dunn's test, was employed to detect significant differences in S values amongst the three zones for each organism (Supplementary Table S1.7).

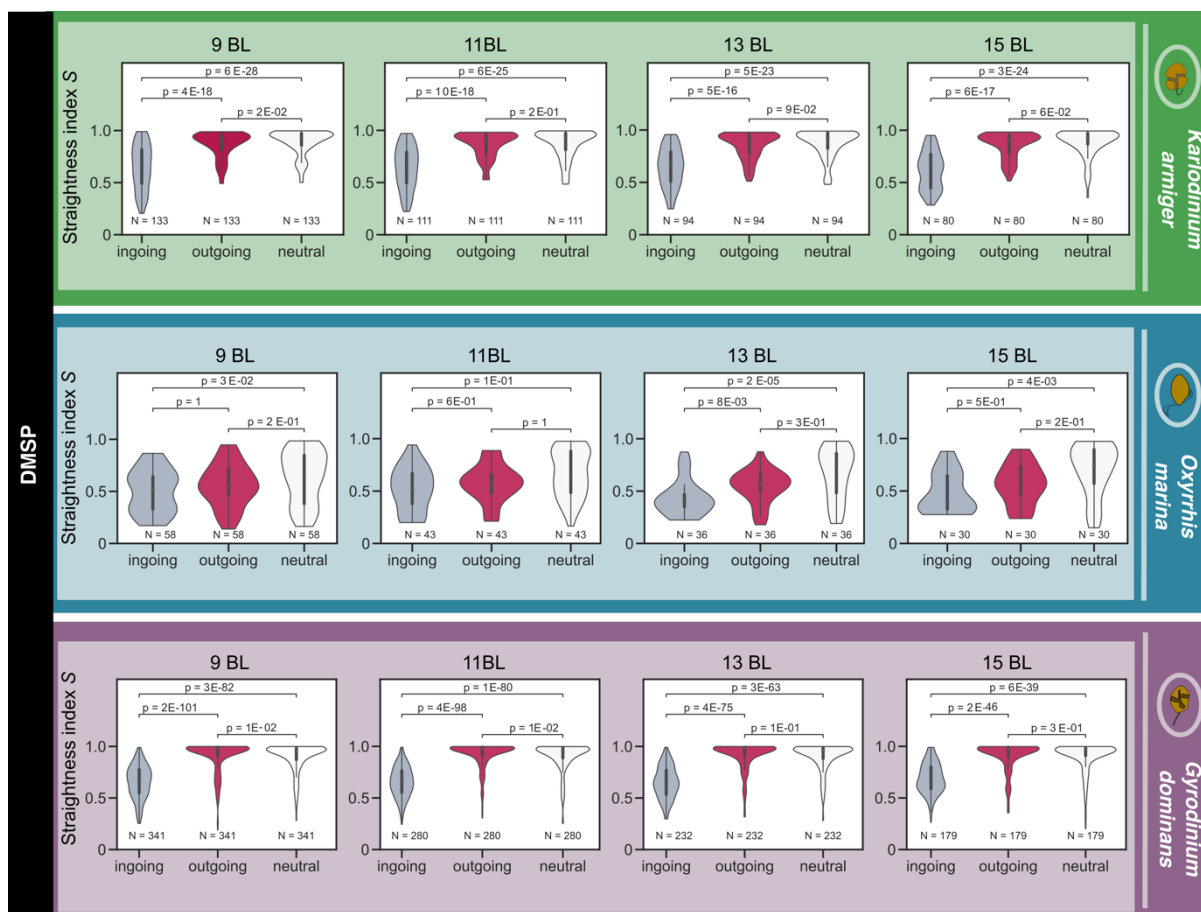


Supplementary Figure S1.7. Scheme of areas used for calculating the straightness index S . Trajectory straightness is calculated for 3 types of trajectories: trajectories going into the capillary from the bulk (gray), trajectories going back to the bulk after visiting the capillary (pink), and trajectories fully contained in the bulk (black). BL stands for "1 body length", corresponding to 20 μm . S is calculated on the trajectory section contained in two areas: the area near the capillary entrance (blue) and the area unaffected by the chemical (brown). The two areas are both circular coronas centered at the entrance of the capillary and whose smaller radius is set to, respectively, 3BL and 20BL from the capillary entrance. S is calculated on progressively larger areas by incrementing the size of the outer radius of each circular corona by N BL ($N = 7, 9, 11, 13, 15$).

For all three dinoflagellates, *S* varied over a few hundredths in all areas, with no clear increasing or decreasing trend, suggesting that *S* is a robust parameter within the range studied (Supplementary Fig. S1.8). For *K. armiger*, the median *S* ranged between 0.65-0.68 for ingoing trajectories, 0.91-0.93 for outgoing trajectories, and 0.93-0.95 in the neutral zone. For *G. dominans*, the median *S* of incoming cells ranged between 0.66-0.70. Constant and close values were obtained for the outgoing trajectories (0.98) and in the neutral zone (0.96). For *O. marina*, the median *S* ranged between 0.45-0.50 for incoming cells, 0.53-0.55 for outgoing cells, and 0.71-0.76 in the neutral zone.

Table S1.7. Median *S* values and statistical results of the Kruskal-Wallis test complemented with the post-hoc Dunn's test for each organism. The statistical tests were applied to detect significant differences in *S* values between the 3 groups of trajectories (ingoing, outgoing and neutral zone). Each test and median is analysed at different travelled distances calculated with a defined number (N) of body lengths (BL) to demonstrate the index (*S*) robustness.

	Kruskal-Wallis test		Post-hoc Dunn's test (p-values)			Median <i>S</i> values		
	H-statistic	p-value	Ingoing vs outgoing	Ingoing vs neutral	Outgoing vs neutral	Ingoing	Outgoing	Neutral zone
<i>K. armiger</i>								
7 BL (140 µm)	136	3E-30	7E-11	5E-12	0.02	0.68	0.93	0.96
9 BL (180 µm)	113	2E-25	4E-18	6E-28	0.02	0.65	0.92	0.94
11 (220 µm)	102	4E-23	1E-18	6E-25	0.2	0.66	0.91	0.94
13 (260 µm)	91	1E-20	5E-16	5E-23	0.09	0.66	0.91	0.93
15 (300 µm)	92	1E-20	6E-17	3E-24	0.06	0.64	0.91	0.93
<i>O. marina</i>								
7 BL (140 µm)	41	1E-9	6E-3	6E-11	4E-3	0.42	0.55	0.71
9 BL (180 µm)	7	0.03	1	0.03	0.2	0.55	0.54	0.66
11 (220 µm)	4	0.1	0.6	0.1	1	0.55	0.62	0.66
13 (260 µm)	19	7E-05	0.008	2E-5	0.3	0.4	0.58	0.75
15 (300 µm)	10	6E-03	0.5	0.004	0.2	0.42	0.6	0.75
<i>G. dominans</i>								
7 BL (140 µm)	540	4E-118	2E-118	1E-104	0.2	0.69	0.98	0.96
9 BL (180 µm)	412	2E-90	2E-101	3E-82	0.01	0.67	0.98	0.95
11 (220 µm)	382	1E-83	4E-98	1E-80	0.01	0.66	0.98	0.96
13 (260 µm)	300	5E-66	4E-75	3E-63	0.1	0.64	0.98	0.96
15 (300 µm)	195	3E-43	2E-46	6E-39	0.3	0.68	0.98	0.96



Supplementary Figure S1.8. Robustness test of the straightness index S for each organism. Each panel contains the violin plots with the S data distribution for trajectories covering a progressively greater distance (9, 11, 13, and 15 BL). Trajectories are divided into 3 types: trajectories approaching the DMSP source (ingoing – grey), trajectories moving away from the DMSP source (outgoing – magenta), and trajectories comprised in a neutral zone unaffected by DMSP (neutral – white). N refers to the number of trajectories analysed in each set. Significant differences between the three zones can be detected by the p -values presented in each individual plot.

■ CHAPTER 2 –

THE IN-SITU CHEMOTAXIS ASSAY (ISCA) AS A TOOL TO EXAMINE MICROPLANKTON CHEMOTAXIS

Queralt Güell-Bujons, Jean-Baptiste Raina, Yaiza Castillo, Justin Seymour, Albert Calbet and Rafel Simó

INTRODUCTION

Heterogeneous microscales

The pelagic marine ecosystem is a complex, dynamic, and heterogeneous environment that is continuously changing at different temporal and spatial scales. In the marine environment, microbial communities and their behaviour are tightly linked to the complex microarchitecture driven by physical, chemical, and biological processes (Stocker & Seymour, 2012). Microscale heterogeneity is usually defined by the occurrence of nutrient hotspots involving organic particles, phytoplankton cells, zooplankton faecal pellets, or other nutritional-rich patches (Azam, 1998; Clerc et al., 2022; Lambert et al., 2017; Stocker, 2012). The high concentration of resources in these microenvironments fosters multifaceted interactions between microorganisms of several trophic levels (Clerc et al., 2022; Kjørboe, 2000; Seymour et al., 2017; Shemi et al., 2021). The unique chemical signatures of these microenvironments makes chemotaxis one of the key traits for exploiting the ocean microscale (Stocker & Seymour, 2012).

Chemotaxis to DMSP and related compounds

Chemical communication encompasses a broad spectrum of compounds involved in reproductive processes, symbiotic and parasitic interactions, allelopathic relationships and feeding behaviours (Brown et al., 2019; Hay, 2009; Pohnert et al., 2007). Among the countless number of chemical cues released by microscale hotspots, DMSP and related compounds stand out because of the multiple (and sometimes opposite) behavioural responses they elicit (Breckels et al., 2011; Seymour et al., 2010; Shemi et al., 2021; Steinke et al., 2002; Strom et al., 2003; Teng et al., 2021) and their pervasive occurrence in the ocean (Hopkins et al., 2023; Simó, 2001). The multiple roles of DMSP and related compounds in biogeochemistry, plankton physiology, marine ecology, and atmospheric chemistry highlight the importance of these molecules in the ocean (Hopkins et al., 2023; Kiene et al., 2000; Simó, 2001; Stefels, 2000). DMSP is synthesised by a wide range of phytoplankton species (Keller et al., 1989) and many bacteria (Zheng et al., 2020) in response to several physiological processes (Simó, 2001; Stefels, 2000). When exudated or released into the dissolved pool, DMSP operates as a key chemical currency exchanged through the marine food web (Simó, 2001). DMSP can be converted into DMS and acrylate by DMSP lyase enzymes, found in many phytoplankton and bacterial species (Hopkins et al., 2023, and references therein). DMS is a volatile compound holding significant scientific interest for its roles in the marine environment, where it mediates food-web interactions (Shemi et al., 2021; Steinke et al., 2002), and in the atmosphere, where it impacts aerosol chemistry and influence cloud formation and brightness (Galí et al., 2013). Acrylate has been postulated as an algal and bacterial defence molecule (Teng et al., 2021; Wolfe et al., 1997), and can also act as a substrate for bacteria (Raina et al., 2009; Tyssebotn et al., 2017; Xue et al., 2022). Overall, the cycle of DMSP and its degradation products play an important role in ecosystem dynamics due to its connection with multiple systemic processes (Hopkins et al., 2023).

The release of DMSP, DMS, and acrylate has been detected from various point sources, including stressed cells suffering oxidative stress or photosynthesis surplus (Stefels et al., 2007; Sunda et al., 2002), faecal pellets, marine snow or other aggregates (Steiner et al., 2019; Tang, 2001), and lysed algal cells due to virus infections or grazing processes (Evans et al., 2007; Simó et al., 2018). These released cues shape chemical microenvironments, providing directional information to chemotactic microorganisms. In addition, the higher viscosity near the surface of microscale hotspots further increases the persistence of these chemical gradients, resulting in concentrations orders of magnitude larger than in the surrounding bulk seawater (Guadayol et al., 2021; Seymour et al., 2017). Although the chemoattractant role of DMS has been extensively characterised for birds, seals, and penguins (Cunningham et al., 2008; Kowalewsky et al., 2006; Nevitt, 2008), weaker responses have been reported for marine protists (Breckels et al., 2011; Seymour et al., 2010). The roles of DMSP and acrylate as chemical cues are still controversial. DMSP is a powerful chemoattractant for bacteria and some protists (Breckels et al., 2011; Seymour et al., 2010), but has also been proposed as a grazing deterrent

(Fredrickson & Strom, 2008; Strom et al., 2003). Scarce support defines acrylate as a repellent at high concentrations (Breckels et al., 2011; Teng et al., 2021) but also as an interesting bacterial resource when present at low levels (Raina et al., 2009; Tyssebotn et al., 2017; Xue et al., 2022). The vast majority of these observations come from culture-based studies, and the role of these compounds in protist natural communities is mostly unknown (Raina et al., 2022).

Chemotaxis assaying methods

The literature on methods for assaying chemotaxis dates back to the capillary assay developed sixty years ago to observe chemotaxis-driven bacterial motility (Adler, 1973). This culture-based method and subsequent modifications facilitated the recognition of the chemosensory capacity of protists in the 1980s and 1990s (Leick & Helle, 1983; Spero, 1984; Verity, 1991). Since then, numerous methods have been invented and optimised (e.g. Ayo et al., 2009; Cancellieri, 2001; Deuer & Grünbaum, 2006; Harvey et al., 2013; Korolik & Ottemann, 2018; Martel, 2006), documenting how chemical cues trigger directional motility towards prey or resources and resulting in aggregation. Current investigations employing novel methods and advanced optimization tools provide thorough examinations of protist chemotactic responses (Chapter 1, Seymour et al., 2010). However, all of the available techniques can only be used in laboratory settings, which often constrains their application to cultures and do not reflect the natural variability and complexity of communities in the environment. The need for in situ assays measuring behaviour under natural conditions prompted the development of an in-situ chemotaxis assay (ISCA) (Lambert et al., 2017). This method is based on microfluidics principles and consists of an inert slab containing an array of 20 wells connected to the outside seawater by a port. The ISCA is easy to use: wells are filled with potential chemoattractants, and once the device is submerged, these chemicals diffuse out from the wells and generate microgradients analogous to those around phytoplankton cells or nutrient patches and aggregates (Lambert et al., 2017; Raina et al., 2022; Smriga et al., 2016). Chemotactic microbes can then respond by swimming inside the well where they are trapped and can subsequently be sampled from. After the incubation, the contents of the well are retrieved and analysed with the most appropriate method. Thorough tests have proved the correct functioning of the device and its optimal setup for laboratory cultures and in situ conditions regarding bacterial communities (Clerc et al., 2023; Lambert et al., 2017; Tout et al., 2015). ISCA applications targeting the protist community are restricted to one study testing the responses of bacterivore nanoflagellates from natural communities (Rodríguez Giner, 2017).

Our aims and approach

Chapter 1 provided detailed documentation of the chemotactic behaviour of three dinoflagellate protists against DMSP, DMS, and acrylate. While a strong DMSP chemoattractant potential was confirmed for the three dinoflagellates, DMS triggered a weaker and more variable response. Acrylate did not induce any repulsion, but attraction could not be confirmed either. In this chapter, we used the ISCA to scale up this analysis to complex natural communities directly from the environment. Hence, hypothesis 1 stating that DMSP and related compounds trigger chemotaxis in protists is tested here with natural communities.

MATERIALS AND METHODS

Experimental cultures. The dinoflagellate cultures (*O. marina* ICM-ZOO-OM001 and *G. dominans* ICM-ZOO-GD001) were originally isolated from the NW Mediterranean by A. Calbet in 1996 and 2011, respectively. The prey, *Rhodomonas salina* strain K-0294, was obtained from the Scandinavian Culture Collection of Algae and Protozoa at the University of Copenhagen and cultured in the Institute of Marine Sciences (ICM-CSIC) since 2018. We maintained the dinoflagellate cultures with autoclaved filtered seawater (FSW) on a 14:10 hour light to dark cycle at 19°C, 50 $\mu\text{E m}^{-2} \text{s}^{-1}$ of light, and with a *R. salina* diet. The prey culture was kept in FSW supplemented with f/2 medium (Guillard, R.R.L, 1975) under the same conditions as the microzooplankton cultures, but with a higher light intensity (100 $\mu\text{E m}^{-2} \text{s}^{-1}$). The cell concentration of both the grazer and prey populations was monitored regularly with a Multisizer 3 Coulter Counter (Beckman Coulter). Before the experiments, the dinoflagellate cultures were starved until the majority were prey-depleted in their vacuoles and cellular size was considerably reduced.

Sampling and enrichments of natural communities. The in-situ chemotaxis assay (ISCA) was conducted with five different communities from two distant oceanic locations (Table 2.1). Three experiments were carried out with Mediterranean waters encompassing both nutrient-poor coastal ocean communities (MED: 41.59°N, 2.86°E) and richer coastal waters sampled from the Barceloneta beach (BB: 41.38° N, 2.19°E) and the Barcelona Olympic Harbour (MEDH: 41.39° N, 2.20°E). The other two incubations were conducted with waters originally obtained from two different coastal waters near Sydney (Australia): Clovelly Beach (CB: 33.91° S, 151.26° E) and Glebe Bay (GB: 33.87° S, 151.18° E). Inverse filtration through 100 μm was rapidly performed after sampling all waters to avoid mesozooplankton interferences (Figure, 2.1B.2). While the ISCA incubations with Mediterranean communities (MED, BB, MEDH) were started immediately after sample collection, 7–9-day long enrichments were carried out with Sydney coastal waters (CB, GB) to increase micrograzer abundances. Waters were incubated under 14:10 hour light to dark cycle conditions and amended with f/2 nutrients. The aim was to foster phytoplankton growth for a few days to increase the resources for the microzooplankton, which would subsequently take over. Live microscopic observations were routinely performed to detect the presence of motile protist cells and assess the enrichments. Chla was measured at the start and end of the enrichment process while total (DMSPt) and dissolved (DMSPd) DMSP samples were taken on the day of the experiment to characterize the experimental community.

Description of the natural communities. To characterize the experimental communities, the following ancillary measurements were taken: Chlorophyll a (chl_a), DMSPt and DMSPd, DAPI-stained samples.

Chla: The total chl_a ($\mu\text{g L}^{-1}$) was measured in 100-200 ml samples of the original community filtered through Whatman GF/C glass fiber filters. Quantification was conducted by a Turner Designs Fluorometer in 90% acetone extracts obtained by 24h dark extraction at 4°C (Duarte Ferreira et al., 2021).

DMSP concentrations: Aliquots for DMSPd were taken from the original community and from the FSW used in ISCA GB incubation, and were gravity filtered through 25-mm Whatmann GF/F filters applying the small-volume drip filtration method (Kiene & Slezak, 2006). The 1-2 ml filtrate was transferred to gas-tight borosilicate serum vials. DMSPt was measured from the original community and in the FSW used in ISCA GB incubation by sampling ~13 ml aliquots of unfiltered water into gas-tight borosilicate serum vials. Volumes of 30 μl of HCl 37% were added to all the vials to remove the DMS present and preserve the DMSP (Kinsey & Kieber, 2016). Acidified samples were stored at room temperature in the dark. The DMSP was later converted to DMS by alkaline hydrolysis with NaOH for at least 24 h. The resulting DMS was quantified with a cryogenic purge-and-trap system coupled to a Shimadzu GC-14A gas chromatograph with flame photometric detection (Masdeu-Navarro et al., 2022).

DAPI-stained samples. The characterization of the original community was complemented by DAPI-stained samples observed under the epifluorescence microscope. Aliquots of 1 ml from the original community were fixed with glutaraldehyde 1% final concentration and kept at 4°C for 24 h. The fixed samples were treated for observation as described in the epifluorescence microscopy section.

Table 2.1. ISCA incubations performed with natural communities.

Experiment	Oceanic location	Sampling site & coordinates	Chemicals (200 μ M) Dilution from MQ-stock solutions
ISCA BB	Mediterranean Sea	Barceloneta beach (BB) Coordinates: 41.38° N, 2.19°E	ISCA 1 - CONTROL ISCA 2 - ACRYLATE (1/100) ISCA 3 - DMS (1/100) ISCA 4 - DMSP (1/10)
ISCA MEDH	Mediterranean Sea	Barcelona Olympic Harbour (MEDH) Coordinates: 41.39° N, 2.20°E	ISCA 1 - CONTROL ISCA 2 - ACRYLATE (1/100) ISCA 3 - DMS (1/100) ISCA 4 - DMSP (1/10)
ISCA MED	Mediterranean Sea	Offshore Mediterranean Sea (MED) Coordinates: 41.59°N, 2.86°E	ISCA 1 - CONTROL ISCA 2 - ACRYLATE (1/100) ISCA 3 - DMS (1/10) ISCA 4 - DMSP (1/10)
ISCA GB	Sydney coastal waters	Glebe Bay (GB) Coordinates: 33.87° S, 151.18° E	ISCA 1 - CONTROL (1/10) ISCA 2 - CONTROL (1/100) ISCA 3 - DMSP (1/10) ISCA 4 - DMSP (1/100) ISCA 5 - DMS (1/100) ISCA 6 - ACRYLATE (1/100)
ISCA CB	Sydney coastal waters	Clovelly Beach (CB) Coordinates: 33.91° S, 151.26° E	ISCA 1 - CONTROL (1/100) ISCA 2 - DMSP (1/100)

ISCA incubations – culture-based experiments. The chemical solutions used in the ISCA consisted of FSW, DMS+acrylate basic solution (used as negative control), and DMSP at several concentrations (1 mM, 200 μ M, and 20 μ M). DMSP was used in the culture-based assays since positive chemoattraction of *O. marina* to DMSP had been already reported (Breckels et al., 2011; Seymour et al., 2010, Chapter 1). The autoclaved FSW used in the ISCA incubations was the same used for the culture maintenance. DMSP (TCI America) was diluted with the same FSW to obtain the final concentrations tested. The negative control was prepared by treating the DMSP solution with alkaline hydrolysis, obtaining DMS and acrylate as degradation products in a basic suspension. On one occasion, *R. salina* exudates were collected to test their chemotactic potential. 20 ml of the *R. salina* culture were centrifuged for 10 min at 1000 g. The supernatant was carefully removed to be used in the ISCA experiments.

The ISCA device consisted of an array of four rows with five wells each (4x5) of 110 μ l volume. The wells were connected to the surrounding seawater by a port of 800 μ m diameter. The device fabrication process is described in detail in (Lambert et al., 2017). Each chemical cue was allocated to an ISCA row, filling all the wells, which were then considered as technical replicates. Hence, each ISCA device contained four chemical compounds. The ISCA incubation process can be consulted in Figure 2.1. The wells were filled with 25-27G needles (BD PrecisionGlide, USA) coupled to 1 ml syringes (112350P-Polnet, PO) and the device was attached to the bottom of the cuvettes with double-sided tape or Velcro. The cuvette was slowly filled with 150 ml of the culture using a serological pipette and left standing on a stable surface for the appropriate time (Figure 2.1B.1). After the incubation, the culture volume was completely retrieved and the contents of each well were recovered into a separate vial. The obtained volume (110 μ l) was fixed with 2% of acetic Lugol's solution and kept at 4°C for subsequent analysis.

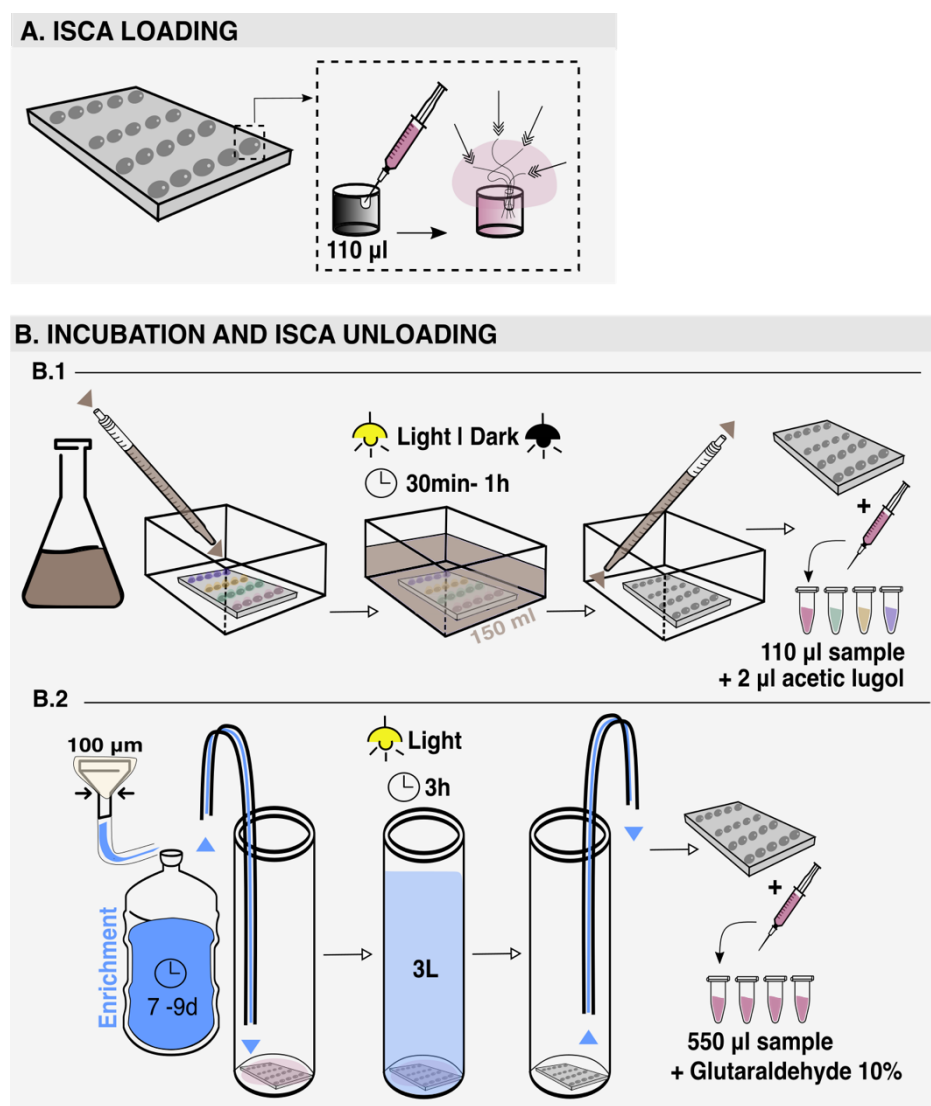


Figure 2.1. Methodological diagram of ISCA incubations. (A) Closeup drawing of the ISCA wells and the chemical microplumes that can induce microbial chemotaxis. (B) ISCA incubation process. (B.1) Culture-based ISCA incubations: the microzooplankton culture is added to the cuvettes where the loaded ISCA is settled. After the incubation the culture is retrieved and the content of each well is fixed with acetic Lugol's solution. (B.2) Natural communities ISCA: pre-filtered communities by inverse filtration are enriched for over a week. Then enriched community is introduced in the cylinders where the ISCA device is placed. After the incubation the water is retrieved and the contents of each ISCA row are pooled together and fixed.

ISCA incubations – Natural communities. The ISCA experiments started with the preparation of the chemical cues to load the ISCA device (Table 2.1). DMSP (TCI America), DMS (Sigma-Aldrich) and sodium acrylate (Sigma-Aldrich) were diluted with filtered seawater (FSW) to obtain a final concentration of 200 μM . Once the method was tested with microzooplankton cultures and DMSP, the complete set of the three chemicals was used in natural communities. The reasoning behind this chemical selection is based on processes occurring at the microscale in the ocean, where exudated DMSP is converted into DMS and acrylate (Simó, 2001). FSW was obtained using the same sampled water for each experiment filtered four times through 0.2 μm sterile syringe filters (Branchia, Labbox, Spain). Aliquots of 1 ml of the obtained FSW were fixed in 1% glutaraldehyde for subsequent DAPI staining and posterior observation in the epifluorescence microscope to confirm the absence of cells. Each ISCA device was completely filled with either a chemical cue or the control water (FSW) using 25-

27G needles (BD PrecisionGlide, USA) coupled to 1 ml syringes (112350P-Polnet, PO) (Figure, 2.1A). Hence, each device solely contained one chemical cue to avoid cross-contamination of the plumes during the incubations. Once the ISCA were loaded the incubation started (Figure 2.1B.2). Each loaded ISCA was carefully attached to the bottom of a cylinder using double-sided tape or Velcro. With the ISCA facing upwards, the cylinders were slowly filled from the bottom to the top with 3 L of natural seawater using a peristaltic pump and malleable silicon tubes. The water stream was directed towards the wall of the cylinder to avoid water splatters. The 3 litters ensured a column of water above the ISCA to soften and dilute any potential turbulence occurring with the incubation that would disrupt the chemical plumes. The devices were incubated for 3 h, to ensure enough time for the community to respond while avoiding microzooplankton duplications. After the incubation, the experimental water was slowly retrieved following the inverse process, from top to bottom, until no more water was left on top of the device. After carefully detaching the ISCA from the bottom, the contents of the wells were retrieved using 25-27G needles (BD PrecisionGlide, USA) and 1 ml syringes (112350P-Polnet, PO). The contents of each row were pooled together to increase the collected volume for posterior analysis (550 μ l, $n=5$). Therefore, from each ISCA device, we obtained 4 replicates fixed with glutaraldehyde 1% final concentration for a period between 30min-48h at 4°C.

Microscopy techniques for cell enumeration

Inverse microscopy. Before the analysis, the Lugol-fixed samples were stabilised at room temperature (21°C). Afterwards, the entire volume was transferred to a Sedgewick-Rafter chamber to count the total number of cells on an inverted microscope (XSB-1A) using a 25x objective and a 250x total magnification.

Epifluorescence microscopy. The fixed samples were stained with 5 μ l of DAPI at 0.5 mg/l concentration and kept in the dark for 5 minutes. The stained samples were filtered on black polycarbonate 0.2 μ m filters and mounted on microscope slides to be kept at -20°C until subsequent analysis. Cell enumeration was performed manually on images automatically acquired using a Zeiss Axio Imager Z2m epifluorescence microscope (Carl Zeiss, Germany) connected to a Zeiss camera (AxioCamHR, Carl Zeiss MicroImaging, S.L., Barcelona, Spain) through the AxioVision 4.8 software. The software was programmed to take a defined number of images randomly allocated throughout the filter area where cells were located (Table 2.2). DAPI-stained cells were observed with the specific UV filter set (370/40 nm excitation, 425/46 emission, and FT 395 beam splitter) and chl *a* content was identified under blue light (475/30 nm excitation, 527/54 BP emission, and FT 495 beam splitter). All pictures from each experiment were taken using the same intensities and exposure times (Table 2.2).

Table 2.2. Epifluorescence microscope parameters. (program. = programmed, mag. = magnification, insp. =inspected). *Different number of images were programmed depending on the filters analysed.

Experiment	Images program.	Microscope mag.	Area insp. (mm ²)	Intensities and exposure times
ISCA BB	249/124/109*	100x	1.5/0.8/0.7	UV: 300ms / Chla: 200ms
ISCA MEDH	249	63x	3.7	UV: 5ms / Chla: 5ms
ISCA MED	249	100x	1.5	UV: 150ms / Chla: 150ms
ISCA GB	703	63x	10.5	UV: 10ms / Chla: 5ms
ISCA CB	703	63x	10.5	UV: 10ms / Chla: 5ms

Chemotactic response quantification

Cell density and chemotactic index (Ic). The contents of the wells were quantified using the two microscopy techniques described. In the culture tests, the total number of cells inside the wells was documented by inspecting all the retrieved volume from the wells. Chemotactic indices (Ic) were evaluated to inform about potential chemoattraction responses by dividing the total number of cells accumulated in the chemical wells by the total number in the control ones (Seymour et al., 2010). The analyses in natural communities reported the accumulation of microplankton inside the wells as cell density by dividing the total number of cells counted by the inspected area (cell/mm²).

The Welch's statistical test was used to evaluate significant differences in DMSP concentration when two samples were compared. One-tail Welch's test was applied in the experiment evaluating the density-driven flow since higher cell density was expected in the 1/10 dilution. In multi-comparison experiments, data was tested first for homogeneity of variances with the Levene's test. Since similar variances were obtained in all cases, the data was log-transformed ($\log(x+1)$) and differences were tested with one-way ANOVA. Dunnett's test was applied as a post-hoc test to compare controls vs treatments. Significant differences in cell densities were translated in chemotactic indices. $Ic > 1$ indicates positive chemoattraction while $Ic < 1$ indicates repulsion. Neutral effects are suggested when Ic is around 1.

Community characterization. The percentage of cells with chl a signal was also determined in the communities to detect any possible changes in community composition. The analysis allowed the detection of any enrichment or depletion of phytoplankton cells within the microplankton community in each of the chemical tests. When possible, the size of the cells higher than 5 μm was also registered. The average size was then computed to detect potential differences in size-based community composition between the different treatments.

RESULTS

Culture-based ISCA incubations

To optimize the ISCA method for targeting chemotaxis in microzooplankton organisms we first conducted culture-based incubations with *O. marina*, an heterotrophic dinoflagellate used as a model organism and easy to culture in high concentrations (Roberts et al., 2011). Additionally, the already confirmed *O. marina* chemoattraction towards DMSP (Breckels et al., 2011; Seymour et al., 2010, Chapter 1) indicated that this organism was an excellent candidate for the test incubations. These tests assessed several parameters (O_1 – O_4): directed swimming towards the inside of the wells, the applicability of neutral and negative controls, the proper light conditions, and the optimal timing for sampling. Additional tests were performed incorporating additional chemical solutions and *Gyrodinium dominans* as another cultured microzooplankton (O_5, G_1).

Initially, three solutions were tested. Autoclaved FSW was used as a neutral control since it was the dilution media applied to maintain the microzooplankton culture. A solution of DMS and acrylate was obtained by alkaline hydrolysis of a DMSP solution. Its strong basic profile acted as a repellent and was used in the incubations as a negative control. DMSP was tested at 3 different concentrations (1 mM, 200 μ M, and 20 μ M) to determine which one induced the strongest chemotaxis. The phototaxis capabilities of *O. marina* (Roberts et al., 2011) induce aggregation and thus heterogeneous cell distribution in the culture. Therefore, light and dark conditions were tested in the incubations. The temporal scale of the experiments was revised to obtain strong chemotactic responses while also avoiding cell replication inside the wells.

As expected, light conditions induced the formation of visible clumps of cells in *O. marina* cultures. Hence, to avoid heterogeneity in cell distribution, the rest of the tests were performed in the dark. The incubation time also affected the response observed. The shortest incubation (O_3) triggered higher cell accumulation in the neutral control (FSW) than in the DMSP wells (Figure 2). Longer incubation times improved the response by attracting more cells to the two DMSP concentrations than to the neutral control (Figure 2.2). The highest total number of cells inside the wells was achieved with the longest incubation time tested (1 hour, O_2). The extremely low number of cells in the DMS+acrylate wells translated into significant differences with the FSW control cell content, confirming the repellent action of this alkaline solution (Table S2.1, Supplementary Information). Significant differences between the DMSP-filled wells and the control ones were only detected in O_3, illustrating a lower DMSP-induced cell accumulation due to the short incubation time, and in O_4 with the wells with DMSP 20 μ M (Supplementary information, Table S2.1).

The second round of tests (O_5 and G_1) incorporated two extra chemical solutions and another microzooplankton species, *Gyrodinium dominans*, besides *O. marina* (Figure 2.2). The O_5 incubation incorporated the supernatant of a *R. salina* culture as a chemical signal. This solution was compared to FSW and also used to resolubilise the other tested chemicals. The other chemicals were DMSP 200 μ M and Marine Broth (MB: 2216 BD Difco) at 10% (which has often been used as a positive control for chemotaxis in previous studies) (Lambert et al. 2017, Clerc et al. 2023). *R. salina* supernatant gathered more cells than the controls but lower than the two other chemicals tested. DMSP and MB diluted with the *R. salina* supernatant induced a high accumulation of cells inside its wells. Yet, the only significant differences were detected between DMSP 200 μ M and the FSW control (Supplementary information, Table S2.1). Incubations with *G. dominans*, a strictly heterotrophic dinoflagellate commonly found in the ocean, showed a slight repellent role of the supernatant of *R. salina* and supported a significant chemoattractant role of 20 μ M DMSP (Supplementary information, Table S2.1).

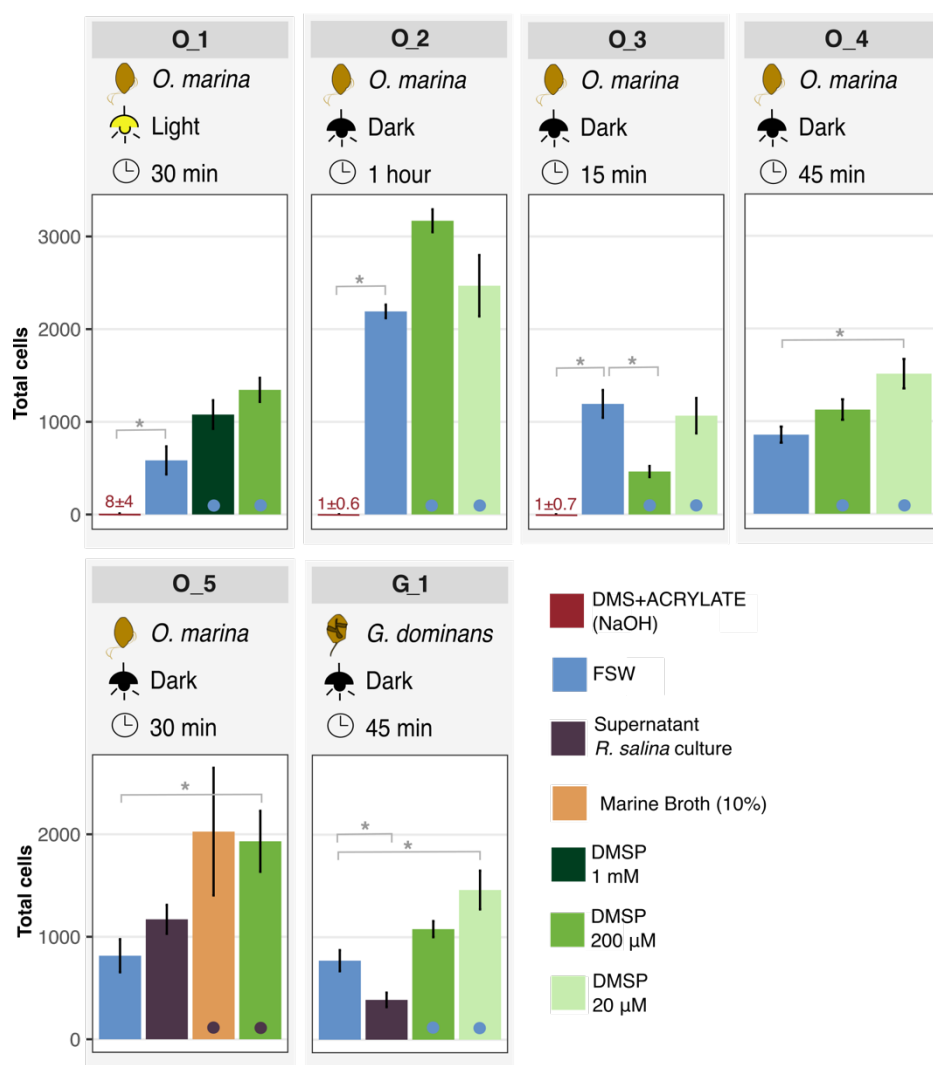


Figure 2.2. Experimental setup and cell count. Each panel summarizes the experimental conditions used in each incubation on top of the plots. The total cells represent the average amount of cells counted in each well (110 μ l) with the error bars representing the standard error. The counts in DMS+ACRYLATE wells are indicated as numbers since the bar was too small to be visualised. The colour of the small dots within each bar indicates the solution used to resuspend the chemicals. Significant differences ($p < 0.05$) are marked in the plot with an asterisk (*). (O= *O. marina*, G= *G. dominans*).

The tests allowed the examination of the chemoattractant potential of DMSP at different concentrations. The chemotactic index (Ic) was used to quantify the strength of the response. The Ic obtained with *O. marina* and *G. dominans* incubations were compared between DMSP concentrations (Figure 2.3). Although ten out of twelve indices were higher than 1, suggesting a positive chemoattractant role for DMSP, only four were calculated based on significant differences between cell numbers in control and DMSP wells. Among the indices based on significant differences, 3 out of the 4 confirmed the chemoattractant role of DMSP, with $Ic > 1$. The highest indices were obtained in *O. marina* test O_5, where DMSP was diluted with *R. salina* supernatant. When considering only DMSP diluted with FSW, the two highest indices were obtained with the lowest concentration tested (20 μ M) and 45 min as the incubation time. The vast majority of the indices were between 1.5 and 2, encompassing all three tested concentrations and both organisms. The *O. marina* shortest incubations (O_3: 15 min) induced significantly higher cell numbers in the control than in the DMSP wells, illustrated by the 0.39 Ic detected with 200 μ M DMSP. The results suggest 20 μ M as the optimal DMSP concentration to trigger stronger significant chemotactic responses in both organisms.

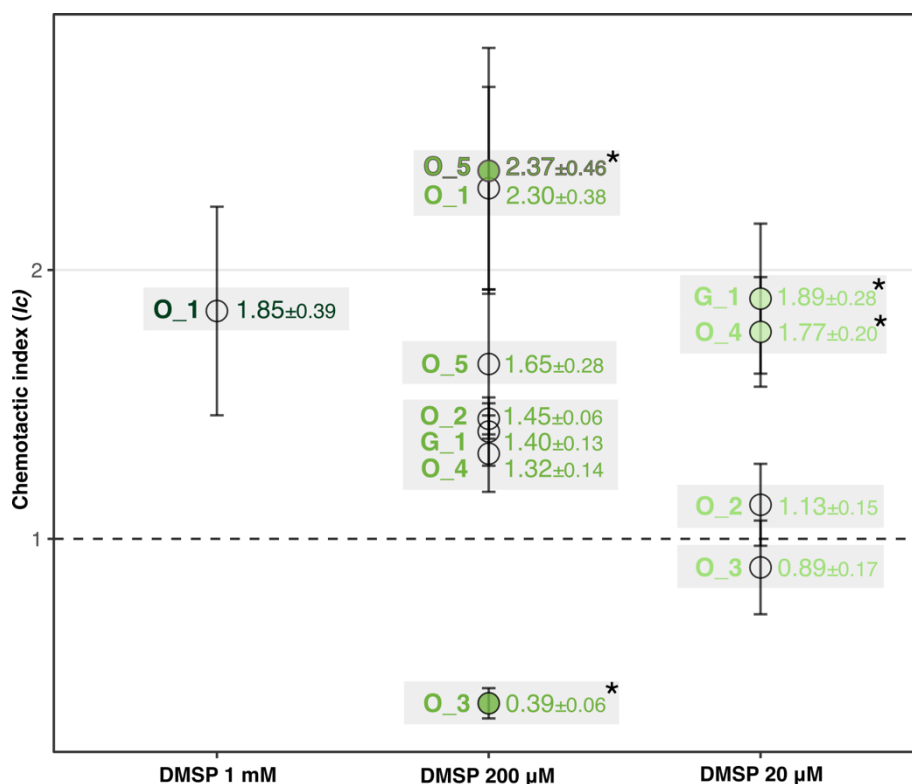


Figure 2.3. Chemotactic indices (Ic). The dots represent the chemotactic index calculated by dividing the cell counts in the DMSP wells divided by the cell counts in the control wells. Chemotactic indices based on cell concentrations significantly different from the controls are identified with full dots, empty dots indicate no significant differences with the controls. The indices based on significant differences were tested with the one sample t-test (Supplementary information, Table S2.2) to confirm that all were significantly different than 1 (*). The indices are grouped by DMSP concentration used as chemical cue (x-axis). Error bars represent the standard error. Grey rectangles specify the exact Ic with the associated propagated error. O_5 data with a purple outline identifies the wells with DMSP diluted with *R. salina* supernatant.

Overall, the chemoattractant role of DMSP was observed in both organisms but further tests would be required to establish the optimal concentration. Dark incubation and time scales longer than 15 min are recommended to observe consistent chemotactic-driven responses. The basic solution of DMS and acrylate was a great option as a negative control.

ISCA incubations – Natural communities (Mediterranean Sea)

The positive outcomes of the test performed with cultures encouraged the application of ISCA with natural communities. We conducted three experiments in Mediterranean waters with contrasting nutrient conditions. Two of the incubations were carried out in the laboratory with communities sampled from the Barceloneta Beach (BB) and the Barcelona Olympic Harbour (MEDH). The third one (MED) was carried out during the SUMMIT-MED cruise, with offshore communities, which contain lower nutrient and phytoplankton concentrations than the previous ones.

ISCA experiments with natural communities were used to test three different chemical cues (DMSP, DMS, and acrylate) all of them at 200 µM concentration. The control and solvent for the chemicals was FSW from the environment sampled, as described in the methodology section. Incubation results were analysed by counting the cells accumulated inside the wells. The metric used, cell density (cell/mm²), was compared between treatments within each experiment (Figure 2.4).

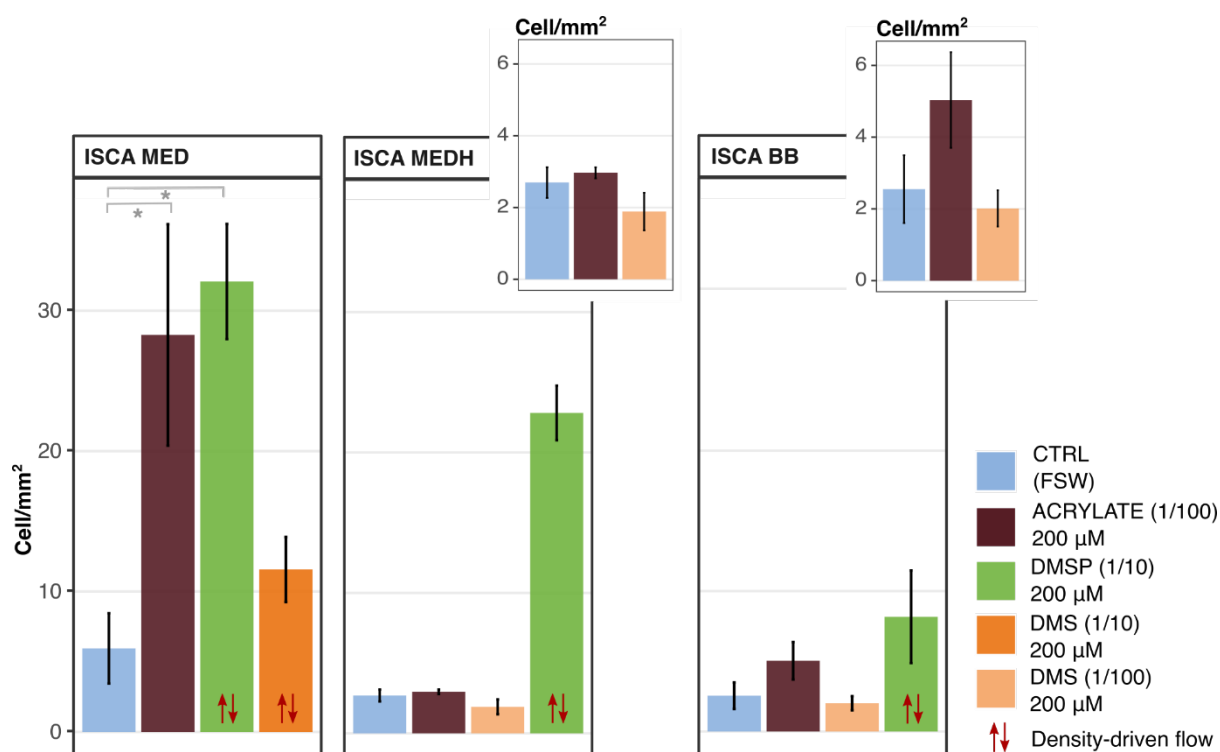


Figure 2.4. Cell density accumulated in the ISCA wells. The large panels display the cell densities (cell/mm²) obtained in the ISCA wells (550 µl) with the error bars representing the standard error. The two arrows symbol is used to identify the wells where density-driven flow was expected. The smaller top right panels show a zoom in the results from the wells with lower cell densities to identify potential differences masked in the big panels due to the y-axis scale. Significant differences ($p < 0.05$) are marked in the plot with an asterisk (*).

The two communities from coastal seawater near Barcelona (MEDH and BB) displayed similar trends: higher cell density in the well with DMSP compared to the rest of the treatments (Figure 2.4). The cell concentrations in DMSP wells were one order of magnitude higher than the other treatments in the MEDH incubation, whereas they were only three times higher than the control wells in the BB incubation. However, these high cell densities are likely an artefact caused by a methodological error. Indeed, the DMSP solution was prepared from a 2 mM stock made with MQ water and was then diluted 10 times to reach 200 µM. The DMSP solution used in the ISCA was therefore 10% less saline (and therefore lighter) than the bulk seawater surrounding the ISCA. This difference can cause a density-driven flow by which a fraction of the more buoyant well content is replaced by the bulk seawater, which carry cells into the wells and cause an artefact. The rest of chemical solutions (DMS and acrylate), prepared with a 1/100 dilution from stock, allowed for comparisons with the control wells since no density-driven flow was expected. However, no significant differences in cell density were detected between any of these wells (Supplementary information, Table S2.3). The results obtained in the MED incubation differed from the ones achieved with coastal Barcelona waters. The methodological error prevented the use of the dilutions of DMSP and DMS, prepared with a 1/10 dilution from a 2mM stock with MQ as diluent. However, the results did not reflect a higher number of cells in the DMS wells (Figure 2.4) as happened in the other two incubations. The wells with DMS prepared with 1/10 dilution contained higher cells than the control, but lower than acrylate and DMSP treatments. Non-significant differences between cell density in the DMS and the control (Supplementary information, Table S2.3) wells suggested a low-to-insignificant effect of the density-driven flow. The highest cell densities were recorded in the wells with DMSP and acrylate, about one order of magnitude larger than in the control wells. The significant differences in cell density (Supplementary information, Table S2.3) allowed the calculating of α and I_c for acrylate (4.75 ± 2.40). If we neglect the methodological error, a significant

difference in cell density was also confirmed between the DMSP wells and the control ones (Supplementary information, Table S2.3), leading to an Ic index of 5.39 ± 2.37 .

The percentage of cells with chl *a* (% chl *a*) was assessed in the samples from the different wells to detect the influence of chemical gradients in the composition of the communities. Hence, the % chl *a* was calculated for each sample of the three ISCA incubations (Figure 2.5). Due to the methodological error explained above, only the non-compromised wells (i.e. the wells with chemical diluted 1/100 from the stock) were considered. The percentage of chl *a*-containing cells was only analysed in control and acrylate wells in ISCA MED, where no differences were observed (Figure 2.5). In the ISCA MEDH incubation, differences in community composition could only be detected in the DMS wells which suggested a lower percentage of photosynthetic organisms. In contrast, a higher percentage of heterotrophic organisms were detected in the control and acrylate wells of ISCA BB compared to the percentage assessed in the natural seawater (SW). The DMS-driven community had a similar % of chl *a*-containing cells to that of the natural community. Yet, only one sample could be examined and no error was assessed.

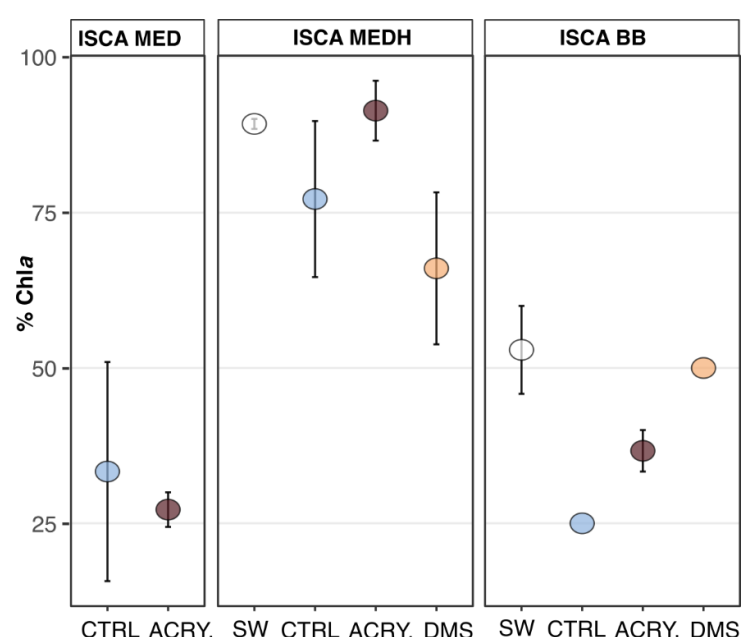


Figure 2.5. Percentage of chl *a*-containing cells (%). The percentage of photosynthetic organisms was calculated in the original seawater (SW) and in each of the communities from the wells (CTRL=control, ACRY= acrylate). Only the wells with chemical solutions prepared with 1/100 dilution were considered.

ISCA incubations with natural communities (Sydney coastal waters)

As a response to the dilution artefact detected in the ISCA incubations in the Mediterranean experiments, we designed a test to examine the magnitude of the methodological error. The test was performed with one enriched community from Sydney coastal waters (GB). Chemotaxis experiments were also conducted with this same community and in a second community enriched from water from a coastal beach sample (CB). First, the communities were characterised with a set of ancillary measurements: Chl *a*, DMSPd and DMSPt. Chl *a* was measured at the start and end of the enrichment process (Figure 2.6). DMSPd and DMSPt were evaluated on the day of the experiment (Figure 2.7). The DMSP content of the FSW used as control and diluent for the chemical cues was also examined in the ISCA GB experiment (Figure 2.7C).

Successful enrichments of the phytoplankton community were achieved with the protocol explained in the methodology section. Chl *a* content tripled in the CB community and increased one order of magnitude in the GB enrichment (Figure 2.6). The enrichment in photosynthetic organisms happened along with an increase in motile cells observed under a bright-field microscope (personal observation), suggesting an increment of small flagellates and bigger dinoflagellates.

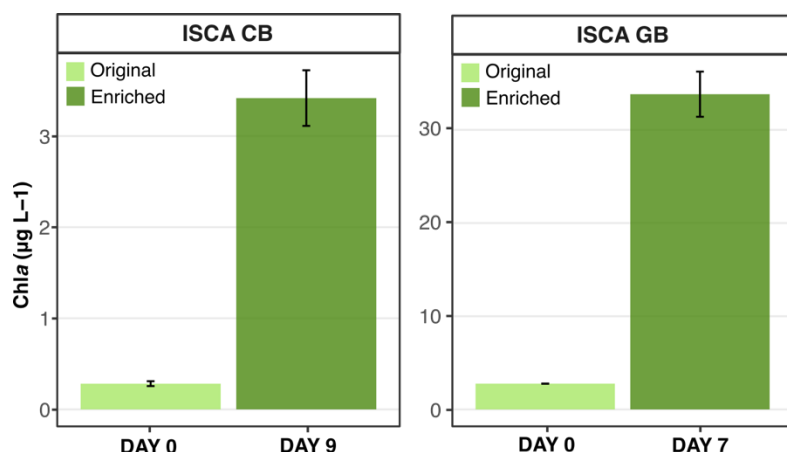


Figure 2.6. Chla concentrations during the enrichment process. Chla content of the communities is represented as columns (y-axis) in the start and end of the enrichments process (x-axis). The two communities (CB and GB) used for the ISCA experiments are represented in individual subplots. Please note the change of the scale in the y-axis. Standard error is represented in the error bars.

Dissolved and particulate DMSP content (measured altogether as DMSPt) differed significantly between the communities used for each ISCA incubation (Figure 2.7A, Supplementary information, Table S2.4). The DMSPt of the ISCA GB community doubled the one present in the ISCA CB sample. However, when the results were normalised to chla values the outcome reversed, with much more DMSPt per chla detected in the CB community (Figure 2.7A). Despite the different content in total DMSP, bulk DMSPd reached similar concentrations in both ISCA incubations (Figure 2.7B). High content of dissolved DMSP was confirmed with values between 10 and 15 nM. Surprisingly high DMSP concentrations were also measured in the FSW used in the ISCA GB experiment (Figure 2.7C). The results were consistent between the two techniques applied (measuring DMSPd and DMSPt), displaying DMSP concentrations of ~60 nM significantly different than DMSPd concentrations from the original seawater (Supplementary information, Table S2.4). Strong replicate variability was detected in all measured DMSPd and in the FSW total DMSP.

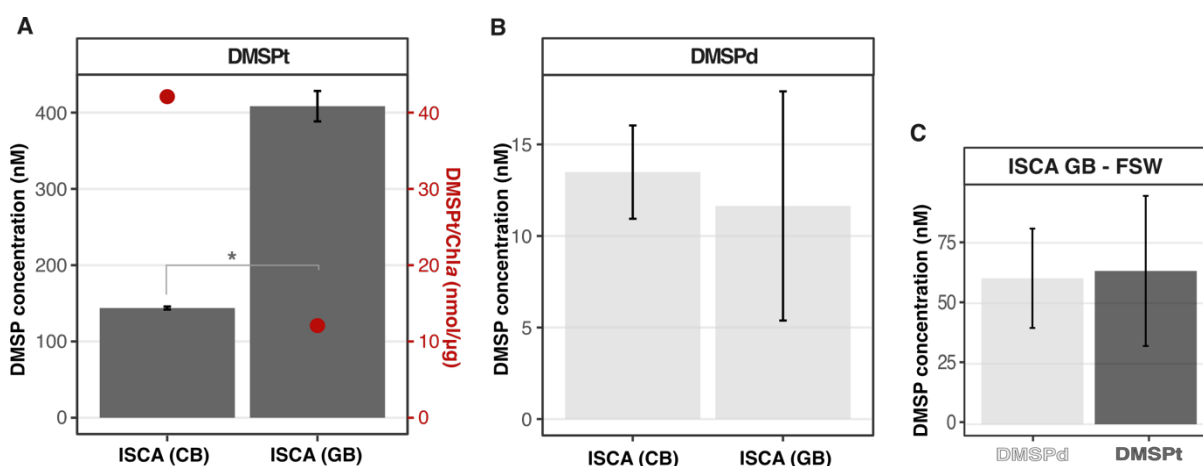


Figure 2.7. DMSP concentrations in the natural communities. (A). Total DMSP (left axis) was represented as grey bars and the DMSPt normalised by chla concentration with red dots (right red axis). (B). Dissolved DMSP (DMSPd) concentration (nM) in the two ISCA incubations (CB and GB). Error bars represent the standard error in DMSPt and the standard deviation in DMSPd. Significant differences ($p < 0.05$) evaluated with a Welch's test are illustrated with *. (C). DMSPd and DMSPt measured in the FSW used as diluent and control in the ISCA GB incubation.

To assess the influence of the density-driven flow, DMSP 200 µM and CTRL solutions prepared from stock batches using MQ were used. To examine the extension of the effect, both solutions were adjusted using either 1/10 or 1/100 dilution from the stock. Cell content was compared between the two distinct dilutions of the same chemical (1/10 vs 1/100) or between the different chemicals prepared with the same dilution (CTRL vs DMSP) (Figure 2.8). The cells > 5 µm were manually counted on images

automatically acquired. The results disclosed a notably higher accumulation of cells in the wells with solutions diluted 1/10, doubling the ones present in the wells with 1/100 dilutions. The Welch's one-tail test confirmed the significantly larger cell accumulation inferred from the cell counts (Supplementary information, Table S2.5, Figure 2.8). Therefore, the dilution with MilliQ significantly altered the cell count results with this community. No difference in cell counts was observed between the two chemicals in either of the two dilutions used, hindering the observation of chemotactic responses.

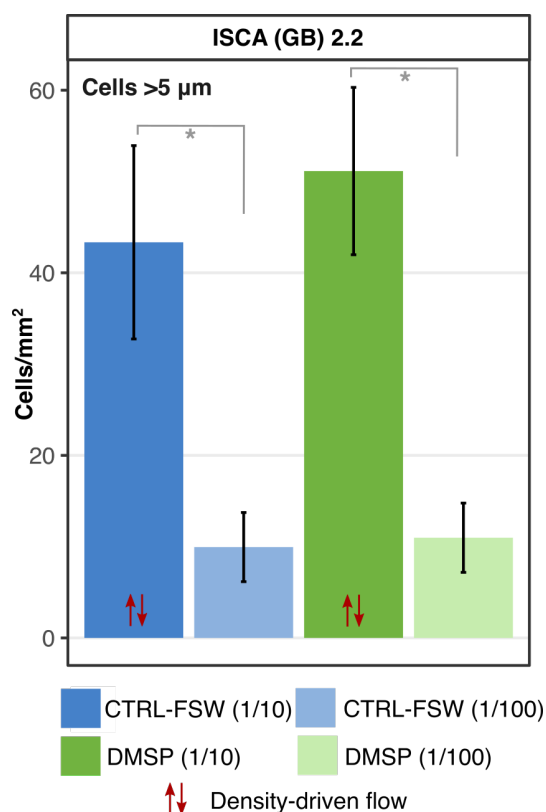


Figure 2.8. Cell density. The bar plot represents the cell density calculated from cells (>5 μm) counts. Technical replicates (wells of each row) were pooled together before preparing the filters for the microscope (550 μl). Biological replicates were used to obtain the average cell density for each chemical and dilution. Error bars illustrate the standard error calculated. Significant differences ($p < 0.05$) assessed using a one-tail Welch's test are illustrated with * between the two dilutions used in both chemicals.

Chemotaxis experiments were performed with both communities diluting all chemicals in a 1/100 proportion from stock solutions to reach 200 μM concentration. While only CTRL and DMSP solutions were tested in ISCA CB, DMS and acrylate were also included in the ISCA GB incubation (Figure 2.9). No significant differences in cell densities were detected between the wells with distinct chemicals in both ISCA incubations (Supplementary information, Table S2.6).

To examine if the distinct chemical plumes induced the assembly of different communities, two parameters were measured: % Chla-containing cells and cell-size distribution (Figure 2.10). The percentage of cells with chla signal was quantified and compared between chemical treatments and the original community (SW) (Figure 2.10A). While no differences were detected in ISCA CB, the percentages differed in the communities of ISCA GB. The chla signal was detected in 60% of the cells of the original community and decreased in all communities from the wells. Similar percentages between 45-50% were obtained with the communities from the wells with control, DMSP and acrylate solutions. The community assembled in the well diffusing DMS, contained a much lower percentage (<40%) of chla-containing cells.

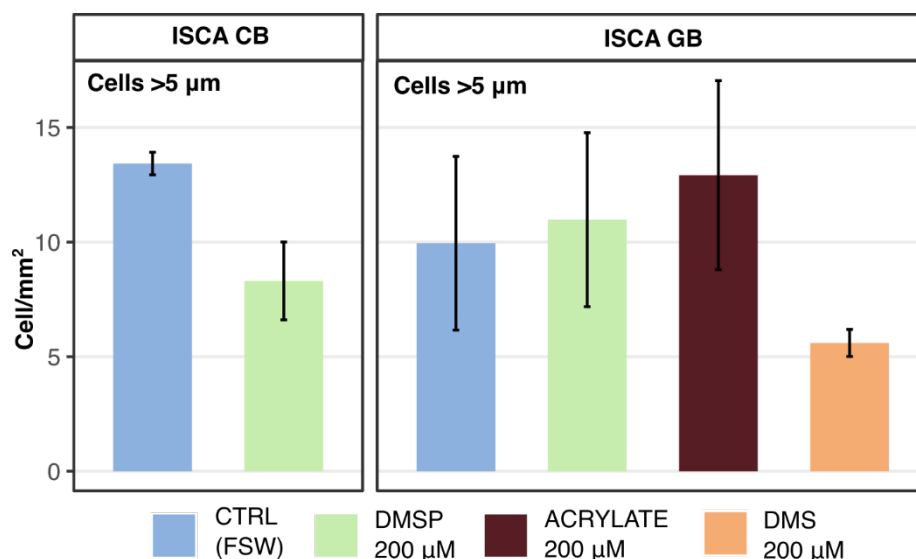


Figure 2.9. Cell density. The bar plot represents the cell density calculated from cells (>5 µm) counts. Technical replicates (wells of each row) were pooled together before preparing the filters for the microscope (1000 µl in ISCA CB and 550 µl in ISCA GB). Biological replicates were used to obtain cell density for each chemical and dilution. Error bars illustrate the standard error of the mean.

The size distribution of the community was assessed by calculating the average size of cells >5 µm. The results were compared again between wells with different chemicals and the outside community (Figure 2.10B). The communities analysed in the ISCA CB notably differed in size distribution. The average size of the cells was bigger in the control wells and even more in the DMSP ones compared to the size distribution of the original community (SW). The size pattern oscillated in the communities found in the different wells of the ISCA GB incubation. No distinctive size was observed in the communities responding to DMSP or DMS when contrasted with the original community (SW). Control and acrylate wells contained communities with slightly larger cells, represented by higher average sizes.

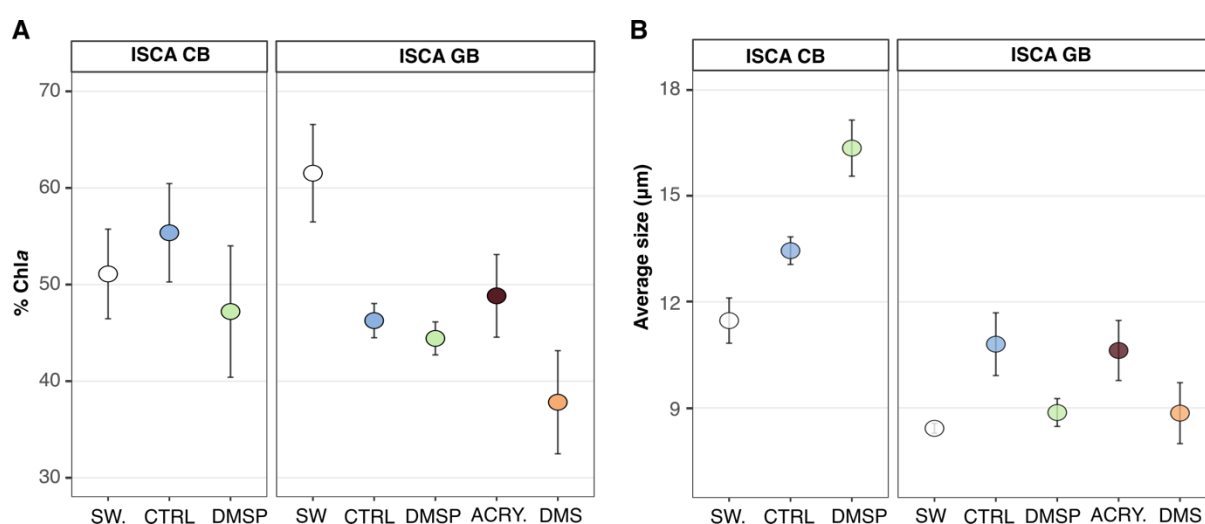


Figure 2.10. Characterization of the communities assembled. (A). Percentage of cells with chl a signal and (B) average size of the cells >5µm in the communities of the original seawater and the ones assembled in the ISCA wells. (SW= original seawater, CTRL= control, ACRY. = acrylate).

DISCUSSION

Culture-based ISCA incubations

The incubations with cultures provided valuable information about the ISCA suitability for microzooplankton and informed about the optimal conditions. The main objective was to test for controls, proper light conditions, temporal regimes, and the organisms' behaviour with the ISCA device. The most important outcome was the confirmation that microzooplankton organisms were able to use chemotaxis and accumulate inside the ISCA wells. The inclusion of a negative control (DMS+acrylate basic solution) inducing high repulsion confirmed the entrance of the cells due to selective biological-chemical interactions in the other wells. The neutral control, FSW, contained fewer cells than the chemoattractants in all experiments except for the O_3 test, where the incubation lasted only 15 minutes. The different incubation periods disclose the minimum time required to see a stable, consistent response. Since the concentration of *O. marina* was consistent within the experiments, the number of cells accumulated could be compared between incubation times. The results from the 15-minute incubation (O_3) illustrate a lower cell accumulation in the DMSP-filled wells due to insufficient time for inducing a chemotactic response in the *O. marina* population. The test displaying the highest number of accumulated cells was the one incubated longer (O_2: 1 hour). Thus, these results confirm as appropriate the same time (1 hour) used in ISCA protocols targeting bacteria chemotaxis (Clerc et al., 2023; Lambert et al., 2017). Regarding light conditions, darkness provided more reliable results. The known *O. marina* positive phototaxis (Roberts et al., 2011) caused cell aggregations that could be visually observed in the cultures. The cell clumps induced heterogeneous cell distribution, directly impairing the ISCA results by potentially presenting different effective cell concentrations outside the different wells. Although the light-induced cell aggregation was prevented by using dark conditions, the occurrence of other factors inducing cell clumps in the cultures was feasible. The high cell concentrations reached in the cultures together with the starved conditions ensured before the experiments, can trigger the protist aggregation around probable patches of organic matter, dissolved nutrients, or bacterial congregations (personal observation, Figure 2.11).

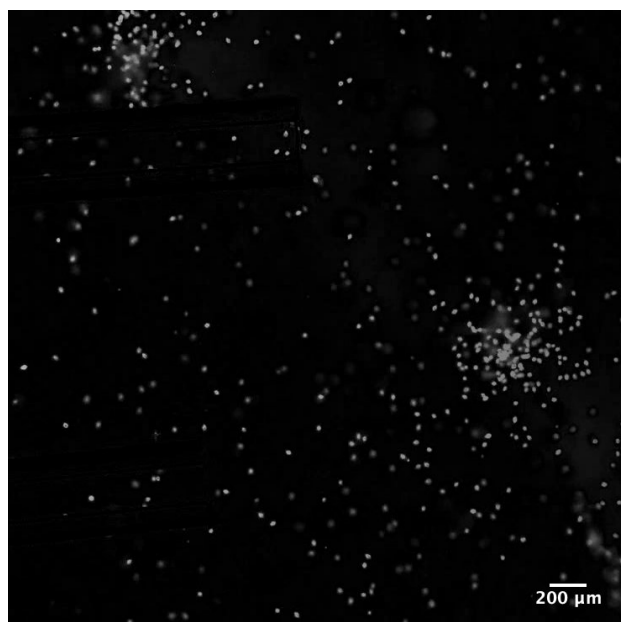


Figure 2.11. Bright field microscopic observation (25x) of a *G. dominans* culture. The image presents the cells as bright grey dots to illustrate the cell clumps developed in starved cultures.

The O_5 and G_1 tests informed about other potential chemoattractants and the application of the method with another cultured microzooplankton (G_1: *G. dominans*). *R. salina* supernatant triggered a slightly higher but not significant cell accumulation than FSW in *O. marina* but not in *G. dominans*. Although both organisms were fed with a *R. salina* diet, the differences observed might respond to

distinct sensing abilities and trophic preferences of the two dinoflagellates (Chapter 1). Additionally, the known osmotrophic capacity of *O. marina* and its larger trophic versatility (Droop & Pennock, 1971; Jeong et al., 2010; Roberts et al., 2011), not currently demonstrated for *G. dominans*, might induce the former to respond to some dissolved nutrients present in the *R. salina* supernatant. Consistently, in the O_5 experiment, we could also observe the potential synergistic role of *R. salina* supernatant. Marine broth and DMSP induced a stronger chemotactic response when diluted with *R. salina* supernatant than when dissolved in FSW. *G. dominans* single test displayed a stronger positive chemotactic response to DMSP 20 μM compared to 200 μM . Although most of the DMSP-induced chemotactic indices were higher than 1, DMSP positive chemotactic role can only be suggested based on the 4 indices calculated from significantly different cell contents. The only indices <1 were obtained in the O_3 incubations where the incubations lasted only 15 minutes.

ISCA incubations with natural communities: Mediterranean Sea

The main outcome of the incubations with Mediterranean natural communities was the observation of a significant methodological error. The preparation of some chemical solutions with 1/10 dilutions from a MilliQ-based stock, caused notable changes in salinity between the wells and the natural sample where the ISCA was submerged. This salinity difference induced a density-driven flow, with some of the well content being replaced by water from the bulk seawater. This flow carried cells from the bulk seawater into the wells. Thus, cell accumulation was not induced by chemotaxis and was not selective to the chemical diffusing from the well. This error had important implications in the results of the ISCA incubations BB and MEDH, where the wells with DMSP diluted 1/10 contained much more cells than the rest of the wells. Because of the methodological error, we cannot know if the higher cell density was due to biological-chemical reasons or if it was just the result of a physical artefact. The magnitude of the interference induced by the density-driven flow will be dependent on cell concentration in the outside community, defining the number of cells pulled inside. Comparing the wells where the density-driven flow was expected, the highest difference in cell density was detected in the MEDH incubation, followed by the BB experiment. Chla concentration, used as a proxy for community richness, followed the same pattern and pointed to the MEDH natural community as the richest one. Surprisingly, the results of the MED incubation do not reflect any potential density-driven flow since no significant differences were detected between the contents of the DMS wells (diluted 1/10) and the control ones. Consistently, this community was also characterised by the lowest chla values typical for offshore oceanic waters.

The results of the wells unaffected by the osmotic effect displayed no significant differences between the control, DMS, and acrylate treatments in the MEDH and BB incubations. The only significant increase in cell density was detected in the DMSP and acrylate wells of the ISCA MED experiment. Unexpected acrylate-induced cell aggregation questions the proposed repellent role for heterotrophic protists (Teng et al., 2021; Wolfe et al., 1997) and advocates for its use as a substrate already proven for bacteria (Raina et al., 2009; Tyssebotn et al., 2017; Xue et al., 2022). Although no significant density-driven flow was observed in that incubation, the accumulation of cells due to physic effects cannot be totally ruled out. Thus, the significant increase in cell density detected in the DMSP wells cannot be strongly stated and no chemotactic response to the three chemicals examined is conclusive in Mediterranean communities. The analysis of the community composition in terms of the percentage of chla-containing cells also did not contribute to conclusive patterns. The detection of lower percentage of phytoplankton in the control wells of ISCA BB could inform about the predominance of motile organisms in the non-photosynthetic community. Hence, it is difficult to discern the chemotaxis role in the assembly of the communities responding to DMS and acrylate. The ISCA MEDH incubation only showed a different percentage of chla-containing organisms in the DMS treatment, but high data variability was also observed. Although it would be expected that heterotrophic organisms respond more to DMS plumes due to the chemotaxis role of the compound in trophic interactions (Pohnert et al., 2007; Shemi et al., 2021), the results do not support a strong statement. Finally, no information on this topic was provided

by the ISCA MED incubation. In all experiments conducted with natural communities, low cell density was obtained. The small volume analysed (550 μ l) and the low number of counted cells under the microscope hindered the obtention of reliable results.

ISCA incubations with natural communities: Sydney coastal waters

The experiments conducted with Sydney coastal waters had two main objectives: investigate the magnitude of the methodological error and perform incubations with enriched communities responding to the same chemicals tested before.

The ISCA CB was used to test the effect of density-driven flow in the results. Clear and significant differences were observed between the two dilutions used in both control and DMSP treatments. Cell density was four and five times higher in the wells where the 1/10 dilution was applied to the chemicals. These results corroborate the observations in the Mediterranean experiments and confirm fluid flow as the reason behind high cell density in 1/10 dilutions. Still, we should take into account that the high cell concentration of the enriched communities might have fostered even more the observed effects.

The ancillary measurements characterised the communities used and delivered interesting information regarding DMSP concentrations in the natural samples. The preceding incubation of the communities succeeded in increasing the concentration of photosynthetic organisms as illustrated by *chl*a contents. Even though the observation of live samples under the microscope also confirmed the increase in concentration of motile cells resembling flagellates and dinoflagellates, we could not confirm an increase of heterotrophic protists.

DMSP was measured as total DMSP (including both dissolved and particulate fractions) and also as dissolved DMSP using the small-volume drip filtration. Total DMSP is mainly contributed by the particulate fraction and thus highly dependent on phytoplankton biomass and species composition (McParland & Levine, 2019). Therefore, although higher DMSPt values were detected in the GB community, the data normalised by *chl*a-content informed about richer DMSP communities in the ISCA CB. Dissolved DMSP was notably concentrated in both communities (ISCA CB and ISCA GB), falling at the high-end of the typical ranges found in background seawater (Kiene et al., 2000). Similar DMSPd concentrations, despite different DMSPt contents, suggests distinct phytoplankton exudation rates related to community composition or environmental stressful conditions (Archer et al., 2010; Breckels et al., 2010; Fredrickson & Strom, 2008; Simó, 2001; Stefels, 2000; Stefels et al., 2007). High dissolved DMSP might interfere with chemotactic relationships, weakening the response to plumes of DMSP from the ISCA (Seymour et al., 2010) and potentially boosting other bacterial responses (Clerc et al., 2023). The additional problem of working with communities that are rich in particulate DMSP appears when generating the FSW used as control and diluent. The method applied to obtain FSW from the communities involved four filtration steps using syringe filters. The amount of pressure exerted through this filtration can disrupt cells and expel their contents (Kiene & Slezak, 2006). Along with other potential chemical cues, DMSP is transferred to the dissolved phase generating a FSW highly enriched with this infochemical. Although the DMSP concentration was still lower than the ones used in the DMSP wells, the high DMSP content indicate that the FSW was a bad neutral control and diluent. The obtention of similar concentrations for DMSPt and DMSPd confirmed that a considerable proportion of the enrichment in DMSP ended up in the dissolved phase.

Chemotactic responses were assessed in both ISCA incubations using 1/100 dilutions in all chemicals. No significant response was detected since cell density was similar in all the wells diffusing distinct potential infochemicals. The results can be related to three main causes: (i) the community was not chemotactic to the tested chemicals with the concentrations and conditions used, (ii) the concentrations used did induce chemoattraction but cell aggregation occurred outside of the well within the diffusing plume, and (iii) the high dissolved DMSP concentration found in the seawater and in the FSW interfered with chemotactic responses. Factor (i) needs to be considered since each infochemical acts in a distinct

optimal range (Breckels et al., 2011) that can differ between organisms (Chapter 1, Seymour et al., 2010). The high DMSP concentration tested was chosen based on previous chemotactic results with the microcapillary method (chapter 1) and on the idea to mimic high concentration release events from bursting algal cells or other aggregates (Kjørboe & Jackson, 2001; Stocker & Seymour, 2012). Additionally, chemotactic responses are strongly context-dependent, influenced by the in situ biotic and abiotic parameters (Kuhlisch et al., 2024). The use of dimmed ambient light could have also impaired the responses if phototaxis eclipsed chemotaxis. Factor (ii) can be related to the ability of some organisms to stay within a chemical patch (Fenchel, 2001) in order to take up and use the chemical as a substrate to build macromolecules and biomass (Chapter 1 – *O. marina* response, Boakes et al., 2011; Deuer & Grünbaum, 2006). If the organisms from the natural communities were attracted to lower concentrations of DMSP and had this capability, they would rather remain within the chemical plume outside of the well. Factor (iii) can be explained by the observed consequences of bulk additions of DMSP (Fredrickson & Strom, 2008; Strom et al., 2003) able to interfere with chemical gradients, generating confusion and hindering the location of a prey or a patch (Chapter 1, Seymour et al., 2010).

The percentage of photosynthetic organisms and the average size were recorded to observe if different assemblage compositions responded to each chemical. These data were compared with the natural community (SW) and between the different chemical cues. Differences in chl *a* percentage were only detected in the ISCA GB, with a lower percentage of phytoplankton in the wells filled with chemicals and control solution. Although we cannot decipher the main reason behind these results, they suggest that the heterotrophic assemblages had a higher number of motile cells, which would explain why all chemicals had similar chl *a* percentages. One way of tackling this question could have been to count the number of cells within the phytoplankton and the heterotrophic assemblages that presented flagella or motile structures. Unfortunately, the quality of our images did not allow the detection of these structures. The average cell size estimated for each treatment suggests differences in the community compositions. However, we lack taxonomic and morphological information to further discuss this topic.

This chapter was an attempt to address hypothesis 1 (*DMSP and DMS will trigger positive chemotaxis in herbivore protists*) through the objective of testing chemotaxis with natural communities. The potential of the ISCA device for targeting microzooplankton behaviour was tested first with protist cultures, where promising results were obtained and experimental conditions were optimised. However, we did not obtain the expected outcomes when natural communities were tested. Besides the methodological artefact disqualifying the Mediterranean incubations, the ISCA application in the enrichments from Sydney coastal waters did not present reliable chemotaxis responses. Therefore, the role of DMSP, DMS and acylate as infochemicals for natural microzooplankton assemblages could not be described. Additionally, two main messages arise from this chapter: (i) The usage of enrichments is advisable when working with low concentration of organisms, to avoid too few cell numbers and therefore unreliable counts. Using a method alternative to microscopy for the enumeration and characterisation of the communities inside the wells, such as microscale metagenomic analysis (Raina et al., 2022), would improve the reliability of the results. (ii) The preparation of the FSW to be used as control and diluent of the chemicals should be revised when working with rich or enriched natural communities. Applying consecutive filtrations by syringe filters induce the release of particulate content into the dissolved phase, including the potential release of infochemicals.

REFERENCES

- Adler, J. (1973). A method for measuring chemotaxis and use of the method to determine optimum conditions for chemotaxis by *Escherichia coli*. *Journal of General Microbiology*, 74(1), 77–91. <https://doi.org/10.1099/00221287-74-1-77>
- Archer, S. D., Ragni, M., Webster, R., Airs, R. L., & Geider, R. J. (2010). Dimethyl sulfoniopropionate and dimethyl sulfide production in response to photoinhibition in *Emiliana huxleyi*. *Limnology and Oceanography*, 55(4), 1579–1589. <https://doi.org/10.4319/lo.2010.55.4.1579>
- Ayo, B., Latatu, A., Artolozaga, I., Jürgens, K., & Iriberry, J. (2009). Factors affecting preference responses of the freshwater ciliate *Uronema nigricans* to bacterial prey. *Journal of Eukaryotic Microbiology*, 56(2), 188–193. <https://doi.org/10.1111/j.1550-7408.2008.00387.x>
- Azam, F. (1998). Microbial control of oceanic carbon flux: The plot thickens. *Science, New Series*, 280(5364), 694–696.
- Boakes, D. E., Codling, E. A., Thorn, G. J., & Steinke, M. (2011). Analysis and modelling of swimming behaviour in *Oxyrrhis marina*. *Journal of Plankton Research*, 33(4), 641–649. <https://doi.org/10.1093/plankt/fbq136>
- Breckels, M. N., Boakes, D. E., Codling, E. A., Malin, G., Archer, S. D., & Steinke, M. (2010). Modelling the concentration of exuded dimethylsulphoniopropionate (DMSP) in the boundary layer surrounding phytoplankton cells. *Journal of Plankton Research*, 32(2), 253–257. <https://doi.org/10.1093/plankt/fbp116>
- Breckels, M. N., Roberts, E. C., Archer, S. D., Malin, G., & Steinke, M. (2011). The role of dissolved infochemicals in mediating predator-prey interactions in the heterotrophic dinoflagellate *Oxyrrhis marina*. *Journal of Plankton Research*, 33(4), 629–639. <https://doi.org/10.1093/plankt/fbq114>
- Brown, E. R., Cepeda, M. R., Mascuch, S. J., Poulson-Ellestad, K. L., & Kubanek, J. (2019). Chemical ecology of the marine plankton. *Natural Product Reports*, 36(8), 1093–1116. <https://doi.org/10.1039/C8NP00085A>
- Cancellieri, P. J. (2001). Chemosensory attraction of *Pfiesteria* spp. to fish secret. North Carolina State University.
- Clerc, E. E., Raina, J.-B., Keegstra, J. M., Landry, Z., Pontrelli, S., Alcolombri, U., Lambert, B. S., Anelli, V., Vincent, F., Masdeu-Navarro, M., Sichert, A., De Schaetzen, F., Sauer, U., Simó, R., Hehemann, J.-H., Vardi, A., Seymour, J. R., & Stocker, R. (2023). Strong chemotaxis by marine bacteria towards polysaccharides is enhanced by the abundant organosulfur compound DMSP. *Nature Communications*, 14(1), 8080. <https://doi.org/10.1038/s41467-023-43143-z>
- Clerc, E. E., Raina, J.-B., Peaudecerf, F. J., Seymour, J. R., & Stocker, R. (2022). Survival in a sea of gradients: Bacterial and archaeal foraging in a heterogeneous ocean. In L. J. Stal & M. S. Cretoiu (Eds.), *The Marine Microbiome* (Vol. 3, pp. 47–102). Springer International Publishing. https://doi.org/10.1007/978-3-030-90383-1_2
- Cunningham, G. B., Strauss, V., & Ryan, P. G. (2008). African penguins (*Spheniscus demersus*) can detect dimethyl sulphide, a prey-related odour. *Journal of Experimental Biology*, 211(19), 3123–3127. <https://doi.org/10.1242/jeb.018325>
- Deuer, S. M., & Grünbaum, D. (2006). Individual foraging behaviors and population distributions of a planktonic predator aggregating to phytoplankton thin layers. *Limnology and Oceanography*, 51(1), 109–116. <https://doi.org/10.4319/lo.2006.51.1.0109>
- Droop, M. R., & Pennock, J. F. (1971). Terpenoid quinones and steroids in the nutrition of *Oxyrrhis marina*. *Journal of the Marine Biological Association of the United Kingdom*, 51(2), 455–470. <https://doi.org/10.1017/S002531540003191X>
- Duarte Ferreira, G., Romano, F., Medić, N., Pitta, P., Hansen, P. J., Flynn, K. J., Mitra, A., & Calbet, A. (2021). Mixoplankton interferences in dilution grazing experiments. *Scientific Reports*, 11(1), 23849. <https://doi.org/10.1038/s41598-021-03176-0>
- Evans, C., Kadner, S. V., Darroch, L. J., Wilson, W. H., Liss, P. S., & Malin, G. (2007). The relative significance of viral lysis and microzooplankton grazing as pathways of dimethylsulphoniopropionate (DMSP) cleavage: An *Emiliana huxleyi* culture study. *Limnology and Oceanography*, 52(3), 1036–1045. <https://doi.org/10.4319/lo.2007.52.3.1036>
- Fenchel, T. (2001). How dinoflagellates swim. *Protist*, 152(4), 329–338. <https://doi.org/10.1078/1434-4610-00071>
- Fredrickson, K. A., & Strom, S. L. (2008). The algal osmolyte DMSP as a microzooplankton grazing deterrent in laboratory and field studies. *Journal of Plankton Research*, 31(2), 135–152. <https://doi.org/10.1093/plankt/fbn112>
- Galí, M., Ruiz-González, C., Lefort, T., Gasol, J. M., Cardelús, C., Romera-Castillo, C., & Simó, R. (2013). Spectral irradiance dependence of sunlight effects on plankton dimethylsulfide production. *Limnology and Oceanography*, 58(2), 489–504. <https://doi.org/10.4319/lo.2013.58.2.0489>

- Guadayol, Ò., Mendonca, T., Segura-Noguera, M., Wright, A. J., Tassieri, M., & Humphries, S. (2021). Microrheology reveals microscale viscosity gradients in planktonic systems. *Proceedings of the National Academy of Sciences*, 118(1), e2011389118. <https://doi.org/10.1073/pnas.2011389118>
- Guillard, R.R.L. (1975). Culture of phytoplankton for feeding marine invertebrates. In *Culture of marine invertebrates animals* (pp. 29–60). Smith, M.L. and Chanley, M.H., Eds. http://dx.doi.org/10.1007/978-1-4615-8714-9_3
- Harvey, E. L., Jeong, H. J., & Menden-Deuer, S. (2013). Avoidance and attraction: Chemical cues influence predator-prey interactions of planktonic protists. *Limnology and Oceanography*, 58(4), 1176–1184. <https://doi.org/10.4319/lo.2013.58.4.1176>
- Hay, M. E. (2009). Marine chemical ecology: Chemical signals and cues structure marine populations, communities, and ecosystems. *Annual Review of Marine Science*, 1(1), 193–212. <https://doi.org/10.1146/annurev.marine.010908.163708>
- Hopkins, F. E., Archer, S. D., Bell, T. G., Suntharalingam, P., & Todd, J. D. (2023). The biogeochemistry of marine dimethylsulfide. *Nature Reviews Earth & Environment*, 4(6), 361–376. <https://doi.org/10.1038/s43017-023-00428-7>
- Jeong, H. J., Yoo, Y. D., Kim, J. S., Seong, K. A., Kang, N. S., & Kim, T. H. (2010). Growth, feeding and ecological roles of the mixotrophic and heterotrophic dinoflagellates in marine planktonic food webs. *Ocean Science Journal*, 45(2), 65–91. <https://doi.org/10.1007/s12601-010-0007-2>
- Keller, M. D., Bellows, W. K., & Guillard, R. R. L. (1989). Dimethyl sulfide production in marine phytoplankton. In *Biogenic Sulfur in the Environment* (pp. 167–182). <https://doi.org/10.1021/bk-1989-0393.ch011>
- Kiene, R. P., Linn, L. J., & Bruton, J. A. (2000). New and important roles for DMSP in marine microbial communities. *Journal of Sea Research*, 43(3–4), 209–224. [https://doi.org/10.1016/S1385-1101\(00\)00023-X](https://doi.org/10.1016/S1385-1101(00)00023-X)
- Kiene, R. P., & Slezak, D. (2006). Low dissolved DMSP concentrations in seawater revealed by small-volume gravity filtration and dialysis sampling. *Limnology and Oceanography: Methods*, 4(4), 80–95. <https://doi.org/10.4319/lom.2006.4.80>
- Kinsey, J. D., & Kieber, D. J. (2016). Microwave preservation method for DMSP, DMSO, and acrylate in unfiltered seawater and phytoplankton culture samples. *Limnology and Oceanography: Methods*, 14(3), 196–209. <https://doi.org/10.1002/lom3.10081>
- Kjørboe, T. (2000). Colonization of marine snow aggregates by invertebrate zooplankton: Abundance, scaling, and possible role. *Limnology and Oceanography*, 45(2), 479–484. <https://doi.org/10.4319/lo.2000.45.2.0479>
- Kjørboe, T., & Jackson, G. A. (2001). Marine snow, organic solute plumes, and optimal chemosensory behavior of bacteria. *Limnology and Oceanography*, 46(6), 1309–1318. <https://doi.org/10.4319/lo.2001.46.6.1309>
- Korolik, V., & Ottemann, K. M. (2018). Two spatial chemotaxis assays: The nutrient-depleted chemotaxis assay and the agarose-plug-bridge assay. In M. Manson (Ed.), *Bacterial Chemosensing. Methods in Molecular Biology* (Vol. 1729, pp. 23–31). Humana Press. https://doi.org/10.1007/978-1-4939-7577-8_3
- Kowalewsky, S., Dambach, M., Mauck, B., & Dehnhardt, G. (2006). High olfactory sensitivity for dimethyl sulphide in harbour seals. *Biology Letters*, 2(1), 106–109. <https://doi.org/10.1098/rsbl.2005.0380>
- Kuhlish, C., Shemi, A., Barak-Gavish, N., Schatz, D., & Vardi, A. (2024). Algal blooms in the ocean: Hot spots for chemically mediated microbial interactions. *Nature Reviews Microbiology*, 22(3), 138–154. <https://doi.org/10.1038/s41579-023-00975-2>
- Lambert, B. S., Raina, J.-B., Fernandez, V. I., Rinke, C., Siboni, N., Rubino, F., Hugenholtz, P., Tyson, G. W., Seymour, J. R., & Stocker, R. (2017). A microfluidics-based in situ chemotaxis assay to study the behaviour of aquatic microbial communities. *Nature Microbiology*, 2(10), 1344–1349. <https://doi.org/10.1038/s41564-017-0010-9>
- Leick, V., & Helle, J. (1983). A quantitative assay for ciliate chemotaxis. *Analytical Biochemistry*, 135(2), 466–469. [https://doi.org/10.1016/0003-2697\(83\)90713-3](https://doi.org/10.1016/0003-2697(83)90713-3)
- Martel, C. M. (2006). Prey location, recognition and ingestion by the phagotrophic marine dinoflagellate *Oxyrrhis marina*. *Journal of Experimental Marine Biology and Ecology*, 335(2), 210–220. <https://doi.org/10.1016/j.jembe.2006.03.006>
- Masdeu-Navarro, M., Mangot, J.-F., Xue, L., Cabrera-Brufau, M., Gardner, S. G., Kieber, D. J., González, J. M., & Simó, R. (2022). Spatial and diel patterns of volatile organic compounds, DMSP-derived compounds, and planktonic microorganisms around a tropical scleractinian coral colony. *Frontiers in Marine Science*, 9, 944141. <https://doi.org/10.3389/fmars.2022.944141>
- McParland, E. L., & Levine, N. M. (2019). The role of differential DMSP production and community composition in predicting variability of global surface DMSP concentrations. *Limnology and Oceanography*, 64(2), 757–773. <https://doi.org/10.1002/lno.11076>

- Nevitt, G. A. (2008). Sensory ecology on the high seas: The odor world of the procellariiform seabirds. *Journal of Experimental Biology*, 211(11), 1706–1713. <https://doi.org/10.1242/jeb.015412>
- Pohnert, G., Steinke, M., & Tollrian, R. (2007). Chemical cues, defence metabolites and the shaping of pelagic interspecific interactions. *Trends in Ecology & Evolution*, 22(4), 198–204. <https://doi.org/10.1016/j.tree.2007.01.005>
- Raina, J.-B., Lambert, B. S., Parks, D. H., Rinke, C., Siboni, N., Bramucci, A., Ostrowski, M., Signal, B., Lutz, A., Mendis, H., Rubino, F., Fernandez, V. I., Stocker, R., Hugenholtz, P., Tyson, G. W., & Seymour, J. R. (2022). Chemotaxis shapes the microscale organization of the ocean's microbiome. *Nature*, 605(7908), 132–138. <https://doi.org/10.1038/s41586-022-04614-3>
- Raina, J.-B., Tapiolas, D., Willis, B. L., & Bourne, D. G. (2009). Coral-associated bacteria and their role in the biogeochemical cycling of sulfur. *Applied and Environmental Microbiology*, 75(11), 3492–3501. <https://doi.org/10.1128/AEM.02567-08>
- Roberts, E. C., Wootton, E. C., Davidson, K., Jeong, H. J., Lowe, C. D., & Montagnes, D. J. S. (2011). Feeding in the dinoflagellate *Oxyrrhis marina*: Linking behaviour with mechanisms. *Journal of Plankton Research*, 33(4), 603–614. <https://doi.org/10.1093/plankt/fbq118>
- Rodríguez Giner, C. (2017). Spatial, temporal and behavioral patterns of marine protists. Universitat Politècnica de Catalunya. <https://doi.org/10.5821/dissertation-2117-134621>
- Seymour, J. R., Amin, S. A., Raina, J.-B., & Stocker, R. (2017). Zooming in on the phycosphere: The ecological interface for phytoplankton–bacteria relationships. *Nature Microbiology*, 2(7), 17065. <https://doi.org/10.1038/nmicrobiol.2017.65>
- Seymour, J. R., Simó, R., Ahmed, T., & Stocker, R. (2010). Chemoattraction to dimethylsulfoniopropionate throughout the marine microbial food web. *Science*, 329(5989), 342–345. <https://doi.org/10.1126/science.1188418>
- Shemi, A., Alcolombri, U., Schatz, D., Farstey, V., Vincent, F., Rotkopf, R., Ben-Dor, S., Frada, M. J., Tawfik, D. S., & Vardi, A. (2021). Dimethyl sulfide mediates microbial predator–prey interactions between zooplankton and algae in the ocean. *Nature Microbiology*, 6(11), 1357–1366. <https://doi.org/10.1038/s41564-021-00971-3>
- Simó, R. (2001). Production of atmospheric sulfur by oceanic plankton: Biogeochemical, ecological and evolutionary links. *Trends in Ecology & Evolution*, 16(6), 287–294. [https://doi.org/10.1016/S0169-5347\(01\)02152-8](https://doi.org/10.1016/S0169-5347(01)02152-8)
- Simó, R., Saló, V., Almeda, R., Movilla, J., Trepát, I., Saiz, E., & Calbet, A. (2018). The quantitative role of microzooplankton grazing in dimethylsulfide (DMS) production in the NW Mediterranean. *Biogeochemistry*, 141(2), 125–142. <https://doi.org/10.1007/s10533-018-0506-2>
- Smriga, S., Fernandez, V. I., Mitchell, J. G., & Stocker, R. (2016). Chemotaxis toward phytoplankton drives organic matter partitioning among marine bacteria. *Proceedings of the National Academy of Sciences*, 113(6), 1576–1581. <https://doi.org/10.1073/pnas.1512307113>
- Spero, H. J. (1984). Chemosensory capabilities in the phagotrophic dinoflagellate *Gymnodinium fungiforme*. *Journal of Phycology*, 21(2), 181–184. <https://doi.org/10.1111/j.0022-3646.1985.00181.x>
- Stefels, J. (2000). Physiological aspects of the production and conversion of DMSP in marine algae and higher plants. *Journal of Sea Research*, 43(3–4), 183–197. [https://doi.org/10.1016/S1385-1101\(00\)00030-7](https://doi.org/10.1016/S1385-1101(00)00030-7)
- Stefels, J., Steinke, M., Turner, S., Malin, G., & Belviso, S. (2007). Environmental constraints on the production and removal of the climatically active gas dimethylsulphide (DMS) and implications for ecosystem modelling. *Biogeochemistry*, 83(1–3), 245–275. <https://doi.org/10.1007/s10533-007-9091-5>
- Steiner, P. A., Sintes, E., Simó, R., De Corte, D., Pfannkuchen, D. M., Ivančić, I., Najdek, M., & Herndl, G. J. (2019). Seasonal dynamics of marine snow-associated and free-living demethylating bacterial communities in the coastal northern Adriatic Sea. *Environmental Microbiology Reports*, 11(5), 699–707. <https://doi.org/10.1111/1758-2229.12783>
- Steinke, M., Malin, G., & Liss, P. S. (2002). Trophic interactions in the sea: An ecological role for climate relevant volatiles? *Journal of Phycology*, 38(4), 630–638. <https://doi.org/10.1046/j.1529-8817.2002.02057.x>
- Stocker, R. (2012). Marine microbes see a sea of gradients. *Science*, 338(6107), 628–633. <https://doi.org/10.1126/science.1208929>
- Stocker, R., & Seymour, J. R. (2012). Ecology and physics of bacterial chemotaxis in the ocean. *Microbiology and Molecular Biology Reviews*, 76(4), 792–812. <https://doi.org/10.1128/MMBR.00029-12>
- Strom, S. L., Wolfe, G., Slajer, A., Lambert, S., & Clough, J. (2003). Chemical defense in the microplankton II: Inhibition of protist feeding by β -dimethylsulfoniopropionate (DMSP). *Limnology and Oceanography*, 48(1), 230–237. <https://doi.org/10.4319/lo.2003.48.1.0230>
- Sunda, W., Kieber, D. J., Kiene, R. P., & Huntsman, S. (2002). An antioxidant function for DMSP and DMS in marine algae. *Nature*, 418(6895), 317–320. <https://doi.org/10.1038/nature00851>

- Tang, K. W. (2001). Defecation of dimethylsulfoniopropionate (DMSP) by the copepod *Acartia tonsa* as functions of ambient food concentration and body DMSP content. *Journal of Plankton Research*, 23(5), 549–553. <https://doi.org/10.1093/plankt/23.5.549>
- Teng, Z.-J., Wang, P., Chen, X.-L., Guillonneau, R., Li, C.-Y., Zou, S.-B., Gong, J., Xu, K.-W., Han, L., Wang, C., Scanlan, D. J., Chen, Y., & Zhang, Y.-Z. (2021). Acrylate protects a marine bacterium from grazing by a ciliate predator. *Nature Microbiology*, 6(11), 1351–1356. <https://doi.org/10.1038/s41564-021-00981-1>
- Tout, J., Jeffries, T. C., Petrou, K., Tyson, G. W., Webster, N. S., Garren, M., Stocker, R., Ralph, P. J., & Seymour, J. R. (2015). Chemotaxis by natural populations of coral reef bacteria. *The ISME Journal*, 9(8), 1764–1777. <https://doi.org/10.1038/ismej.2014.261>
- Tyssebotn, I. M. B., Kinsey, J. D., Kieber, D. J., Kiene, R. P., Rellinger, A. N., & Motard-Côté, J. (2017). Concentrations, biological uptake, and respiration of dissolved acrylate and dimethylsulfoxide in the northern Gulf of Mexico. *Limnology and Oceanography*, 62(3), 1198–1218. <https://doi.org/10.1002/lno.10495>
- Verity, P. G. (1991). Feeding in planktonic protozoans: Evidence for non-random acquisition of prey. *The Journal of Protozoology*, 38(1), 69–76. <https://doi.org/10.1111/j.1550-7408.1991.tb04804.x>
- Wolfe, G. V., Steinke, M., & Kirst, G. O. (1997). Grazing-activated chemical defence in a unicellular marine alga. *Nature*, 387(6636), 894–897. <https://doi.org/10.1038/43168>
- Xue, L., Kieber, D. J., Masdeu-Navarro, M., Cabrera-Brufau, M., Rodríguez-Ros, P., Gardner, S. G., Marrasé, C., & Simó, R. (2022). Concentrations, sources, and biological consumption of acrylate and DMSP in the tropical Pacific and coral reef ecosystem in Mo'orea, French Polynesia. *Frontiers in Marine Science*, 9, 911522. <https://doi.org/10.3389/fmars.2022.911522>
- Zheng, Y., Wang, J., Zhou, S., Zhang, Y., Liu, J., Xue, C.-X., Williams, B. T., Zhao, X., Zhao, L., Zhu, X.-Y., Sun, C., Zhang, H.-H., Xiao, T., Yang, G.-P., Todd, J. D., & Zhang, X.-H. (2020). Bacteria are important dimethylsulfoniopropionate producers in marine aphotic and high-pressure environments. *Nature Communications*, 11(1), 4658. <https://doi.org/10.1038/s41467-020-18434-4>

**CHAPTER 2 -
SUPPLEMENTARY INFORMATION**

**THE IN-SITU CHEMOTAXIS ASSAY (ISCA) AS A TOOL TO EXAMINE
MICROPLANKTON CHEMOTAXIS**

Queralt Güell-Bujons, Jean-Baptiste Raina, Yaiza Castillo, Justin Seymour, Albert Calbet and Rafel Simó

Table S2.1. One-way ANOVA - Dunnett's test results. Multiple comparisons of means: Dunnett contrasts. Significant differences in cell numbers tested between the different treatments and the control wells of the laboratory-based ISCA incubations with cultures. (Exp. = Experiment).

Exp.	Chemicals vs control (FSW)	Estimate	Std.Error	t.value	p.value
O_1	DMS+ACRYLATE - FSW	-4.47	0.562	-7.953	<0.001*
	DMSP 1 mM - FSW	0.89	0.562	1.587	0.295
	DMSP 200 μ M - FSW	1.14	0.562	2.027	0.143
O_2	DMS+ACRYLATE - FSW	7.09	0.205	-34.669	<0.001*
	DMSP 20 μ M - FSW	0.10	0.205	0.492	0.929
	DMSP 200 μ M - FSW	0.37	0.180	2.045	0.156
O_3	DMS+ACRYLATE - FSW	-6.70	0.323	-20.762	<0.001*
	DMSP 20 μ M - FSW	-0.13	0.323	-0.409	0.954
	DMSP 200 μ M - FSW	-0.94	0.323	-2.926	0.046*
O_4	DMSP 20 μ M - FSW	0.57	0.139	4.101	0.0113*
	DMSP 200 μ M - FSW	0.28	0.139	1.983	0.1590
O_5	DMSP 200 μ M - FSW	0.87	0.327	2.672	0.0478*
	MB - FSW	0.78	0.310	2.512	0.0641
	R. salina supern. - FSW	0.39	0.327	1.203	0.5031
G_1	DMSP 20 μ M - FSW	0.65	0.190	3.394	0.0117*
	DMSP 200 μ M - FSW	0.37	0.190	1.955	0.1706
	R. salina supern. - FSW	-0.67	0.220	-3.045	0.0232*

Table S2.2. One sample t-test results. The indices obtained in laboratory-based ISCA (based on significant differences in the cell numbers) were evaluated to prove it they were significantly different than 1. (Exp. = Experiment).

Exp.	Hypothetical mean	Mean	Std.Error	t.value	df	p.value
O_3	1.00	0.39	0.024	24.90	5	<0.0001*
O_4	1.00	1.77	0.082	9.43	5	<0.002*
O_5	1.00	2.37	0.163	8.42	7	<0.0001*
G_1	1.00	1.89	0.089	10.05	9	<0.0001*

Table S2.3. One-way ANOVA - Dunnett's test results. Multiple comparisons of means: Dunnett contrasts. Significant differences in cell numbers tested between the different treatments and the control wells of the ISCA incubations with natural communities (Mediterranean Sea). (Exp. = Experiment).

Exp.	Chemicals vs control (FSW)	Estimate	Std.Error	t.value	p.value
ISCA MED	ACRYLATE (1/100) - FSW	1.48	0.431	3.438	0.019*
	DMS (1/10) - FSW	0.76	0.515	1.474	0.367
	DMSP (1/10) - FSW	1.72	0.431	3.989	0.008*
ISCA MEDH	ACRYLATE (1/100) - FSW	0.09	0.204	0.434	0.877
	DMS (1/100) - FSW	-0.28	0.189	-1.472	0.297

ISCA BB	ACRYLATE (1/100) - FSW	0.09	0.204	0.434	0.877
	DMS (1/100) - FSW	-0.28	0.189	-1.472	0.297

Table S2.4. Welch's test. Significant differences in DMSP concentrations tested between the two communities (CB vs GB) and between the dissolved content in GB community and the FSW used as control and diluent. Both communities were used in the ISCA incubations natural communities (Sydney coastal waters). (Exp. = Experiment).

Exp.	Group1	Group2	n1	n2	Statistic	df	p.value
ISCA CB & GB	DMSPt CB	DMSPt GB	3	2	-13.21	1.02	0.046*
	DMSPd GB	DMSPd GB (FSW)	2	4	3.05	3.78	0.041*

Table S2.5. One-tail Welch's test. Significant differences in cell numbers tested between the two dilutions employed in control (FSW) and DMSP wells (1/10 vs 1/100) of the ISCA GB with natural communities (Sydney coastal waters). (Exp. = Experiment).

Exp.	Group1	Group2	n1	n2	Statistic	df	p.value
ISCA GB	CTRL (1/10)	CTRL (1/100)	4	4	4.77	5.11	0.002*
	DMSP (1/10)	DMSP (1/100)	4	4	3.85	4.69	0.007*

Table S2.6. One-way ANOVA - Dunnett's test results. Multiple comparisons of means: Dunnett contrasts. Significant differences in cell numbers tested between the different treatments and the control wells of the ISCA incubations with natural communities (Sydney coastal waters). (Exp. = Experiment).

Exp.	Chemicals vs control (FSW)	Estimate	Std.Error	t.value	p.value
ISCA CB	DMSP (1/100) - FSW	-0.4764	0.2076	-2.295	0.0834
ISCA GB	ACRYLATE (1/100) - FSW	0.3594	0.4395	0.818	0.765
	DMS (1/100) - FSW	-0.3067	0.4395	-0.698	0.834
	DMSP (1/100) - FSW	0.1634	0.4069	0.401	0.959

■ CHAPTER 3 –

EXPLORING THE DYNAMICS OF LIGHT STRESS AND GRAZING INTERACTIONS IN NATURAL COMMUNITIES AND MODEL SYSTEMS

Queralt Güell-Bujons, Yaiza Castillo, Albert Calbet and Rafel Simó

INTRODUCTION

Light as an environmental driver of microzooplankton grazing?

Protist herbivore grazing is the main circulation route of primary production through marine planktonic food webs (Calbet & Landry, 2004; Schmoker et al., 2013) and a cornerstone for nutrient recycling and biogeochemical cycles in the surface ocean (Landry et al., 1997; Worden et al., 2015). Microzooplankton bulk grazing rates have been evaluated and modelled based on predator and prey abundances, sizes, encounter rates and turbulent flow (García-Oliva & Wirtz, 2022; Holling CS, 1965; Visser & Kiørboe, 2006; Weisse et al., 2016). Despite mounting evidence that individual protists have varying affinities for distinct prey cells or particles, and show distinct predatory behaviour accordingly (Jeong et al., 2010; Montagnes et al., 2008; Tillmann, 2004), the mechanisms underlying the coupling/uncoupling of phytoplankton prey and microzooplankton grazing, and their environmental drivers, are poorly understood (Lawrence & Menden-Deuer, 2012).

As the main source of external energy, solar radiation is crucial for surface ecosystems and many of the organisms that constitute them. Phototrophs rely on sunlight for primary production, and heterotrophic protists of the microzooplankton have been reported to follow diel feeding cycles and undergo light-aided digestion of ingested prey (Arias et al., 2020; H. H. Jakobsen & Strom, 2004; Strom, 2001; Tarangkoon & Hansen, 2011). On the other hand, excess light or high ultraviolet radiation (UV) doses cause physiological stress, photosynthesis inhibition, and damage of the cell machinery in aquatic organisms (Vincent & Neale, 2000). In the surface ocean, quick transitions from low to high irradiance conditions due to vertical mixing are common (Strom et al., 2020) and can generate short-term stress events on both the prey and the predators (Hessen et al., 1997; Strom et al., 2020; Vincent & Neale, 2000; Vincent & Roy, 1993; Zagarese & Helbling, 2003). Whether light stress events change predatory behaviour and induce prey selection, and what are the consequences for microzooplankton grazing rates remains mostly unknown.

Light stress on phytoplankton: effects on DMSP and photosynthetic efficiency

Responses of phytoplankton cells to short-term light stress include reduced swimming speed (Hessen et al., 1997), increased cell size and volume (Cooney et al., 2019), augmented production of intracellular ROS (Strom et al., 2020; Sunda et al., 2002), accumulation of photosynthetic products (Moran et al., 2022; Thornton, 2014), changes in morphology and biochemical composition (Hessen et al., 1997; Rijstenbil, 2002; Stefels & van Leeuwe, 1998) and changes in palatability (Strom et al., 2020). Another interesting phytoplankton response to high-light conditions is the increased release of organic matter through leakage processes and active exudation (Cherrier et al., 2015; Fuentes-Lema et al., 2015; Livanou et al., 2017; Moran et al., 2022; Thornton, 2014). The overflow model describes the active exudation of high molecular weight compounds due to a decoupling of photosynthesis and growth caused by suboptimal/stressing conditions such as high light irradiance (Livanou et al., 2017). The released DOM accumulates in the phycosphere (Seymour et al., 2017) and changes its properties (Guadayol et al., 2021). DOM release and accumulation depends largely on the organism taxon and physiological state (Smriga et al., 2016). Noteworthy signalling compounds derived from light-stressed cells that are expected in phycospheres are the demethylated sulphur compounds DMSP and DMS (Thornton, 2014). Large cellular DMSP release may occur due to the overflow mechanism triggered when high light meets nutrient deficiency (Stefels, 2000; Stefels et al., 2007). Increased DMS release may occur as a leakage from a cellular mechanism to scavenge UV-induced, harmful ROS levels (Sunda et al., 2002). The connection between dimethylated sulphur release and high sunlight has been repeatedly illustrated in natural environments (Galí et al., 2013; Toole et al., 2006) and constitutes the basis for the observed correlations between DMS concentration and the solar radiation dose in the upper mixed layer over large regions of the global surface ocean (Lana et al., 2012; Vallina & Simó, 2007).

Light stress has also effects on the photosynthetic machinery of phytoplankton. In situations of high irradiance, light energy is dissipated through various pathways (Butler, 1972; Cullen & MacIntyre, 1998). The primary route involves photosynthetic reactions, capable of converting light energy into chemical energy. However, when this pathway becomes saturated due to excessive light, dynamic photoinhibition processes initiate downregulation mechanisms (Tyystjärvi, 2013). Excess energy can be dissipated in the form of light emission (fluorescence) or heat via non-photochemical quenching (NPQ) (Butler, 1972; Cullen & MacIntyre, 1998; M. Y. Gorbunov & Falkowski, 2022). Otherwise, undissipated energy can result in direct damage through photochemical degradation of biomolecules or in the production of the afore mentioned ROS, which can cause widespread oxidative damage (Vincent & Neale, 2000). All these processes have an impact on the chlorophyll fluorescence yield (i.e., the ratio of photons reradiated to those absorbed) and therefore on photosynthetic efficiency (Gorbunov & Falkowski, 2022).

Potential implications of light-stress for grazing interactions: preferential grazing on stressed prey and the 'healthy herds' hypothesis

Light-stress events can impact the fitness and behaviour of prey organisms, leading to potential alterations in grazing interactions by direct or indirect effects (De Lange & Lüring, 2003; Strom et al., 2020). Preferential grazing may result from multiple contributing elements such as chemical communication (Harvey et al., 2013; Roberts et al., 2011; Tillmann, 2004; Verity, 1991), physiological-biochemical state (Meunier et al., 2012; Wootton et al., 2007), mechanical attributes of the prey (Hamm et al., 2003) and the feeding history of the predator (Boenigk et al., 2001; Meunier et al., 2012). Sensitivity to stress generates low-fitness or under-performing individuals, remarkably distinct from their healthy counterparts (Brussaard et al., 2001; Evans et al., 2006; Strom et al., 2020), therefore introducing variability in prey populations. If this physiological or chemical variability can be sensed by phagotrophic protists with the ability to rapidly respond to short-term alterations of the prey, then a new driver of grazing behaviour emerges. Chemical alterations of the prey microenvironment are a great candidate for connecting prey stress to preferential grazing. DMSP, DMS, and related compounds have been postulated as important shapers of trophic interactions (Edgcomb, 2021; Saló et al., 2009; Seymour et al., 2010; Shemi et al., 2021; Steinke et al., 2002; K. Tang & Simó, 2003). The increased concentrations of these compounds in phyco- and particle-spheres (Seymour et al., 2017; Steiner et al., 2019; K. W. Tang, 2001; Thornton, 2014) might trigger chemotaxis (Chapter 1) and thereby favour selective grazing or avoidance (Strom et al., 2020).

While several instances of preferential grazing or top-down mortality on individuals weakened by biological stressors have been documented (Duffy et al., 2005; Evans & Wilson, 2008; Lopez et al., 2023), greater uncertainty arises when dealing with environmentally stressed prey. Parasitic infections have been recorded to select for either stressed (Laundon et al., 2021) or healthy (Garcés, personal communication, Gutierrez et al., 2022; Williams, 2008) phytoplankton. Similarly, contradictory evidence has been reported for microzooplankton predation where diverse, multi-faceted responses have been observed when combining light stress and herbivore grazing (De Lange & Lüring, 2003; Strom et al., 2020). Culture-based studies have shown reduced grazing of nanoflagellates on picoplankton (Ochs, 1997; Ochs & Eddy, 1998) but also mixed responses of two dinoflagellates feeding on distinct phytoplankton prey (Strom et al., 2020). The copepod *Calanus finmarchicus* showed higher grazing rates on diatom cultures treated with increased UV radiation levels (Fields et al., 2011). No experiments with natural communities have explored this further. Since the consequences of light stress for preferential grazing will depend on multiple features, from the magnitude of the stress to the stressed prey and the micrograzer assemblages, the extrapolation of culture-derived results to natural communities should be taken with caution. Preferential grazing on weakened/stressed individuals would benefit prey populations by decreasing the number of cells with lower fitness and thus improving overall community health and persistence. This phenomenon, formulated as the healthy herds

hypothesis (Packer et al., 2003), has been quite explored in terrestrial animal ecology (Genovart et al., 2010; Slobodkin, 1974; Temple, 1987), but is largely overlooked when discussing microbial grazing interactions. In the microbial ecology field, selective predation towards weaker organisms has been investigated in protists only regarding parasitic and viral infective processes (Duffy et al., 2005; Evans & Wilson, 2008; Gutierrez et al., 2022; Packer et al., 2003; Park et al., 2021; Williams, 2008). To our knowledge, the only study that has addressed selective targeting of stressed prey as a process that improves the overall prey assemblage health focused on the infection of a diatom by a thraustochytrid parasite (Laundon et al., 2021).

Our aims and approach

The combination of laboratory and fieldwork is the best approach to understand ecological processes such as selective feeding behaviour (Weisse et al., 2016). The choice of ecologically relevant species and conditions, including adequate incubation times, are key issues when performing grazing studies (Montagnes et al., 2008). We took this into consideration when designing our work with the aim to examine the impact of light stress on short-term predatory interactions. We combined culture and fieldwork to test hypotheses 2-4 of this PhD thesis:

Hypothesis 2 (*light stress events induce DMSP exudation in phytoplankton assemblages and cultures*) is addressed in section 3.1. DMSP exudation was examined after exposure of phytoplankton assemblages to high irradiances, including UV. The induced photophysiological stress was assessed by monitoring the immediate photosynthetic efficiency (F_v'/F_m'). Having in mind the three routes that a photon can follow in a phytoplankton cell (photochemical, reemission as fluorescence, and NPQ), the measure of the quantum yield of two of the three processes can allow the calculation of the third (Gorbunov & Falkowski, 2022). The Fluorescence Induction and Relaxation (FIRE) systems allow the assessment of fluctuations in photosynthetic efficiency by measuring photochemistry and fluorescence processes to resolve photon energy budgets (Gorbunov & Falkowski, 2022). Reversible fluctuations are closely associated with the closure of photosystem II (PSII) reaction centers and the downregulation of PSII via non-photochemical quenching of excitation energy (Cullen & MacIntyre, 1998; Tyystjärvi, 2013). FIRE systems apply a short strong pulse of light to saturate the PSII and measure fluorescence induction to calculate the minimal and maximal fluorescence quantum yields that will define the photosynthetic efficiency (Gorbunov & Falkowski, 2022). The measurements of the FIRE can be conducted following two distinct approaches, depending on the question behind: (a) After dark acclimation of the sample (typically 10-30 min). Dark-acclimated cells release all electrons from the reaction centres, resulting in a maximal number of open reaction centres. The FIRE pulse excitation and fluorescence recording offers insights into the maximum photosynthetic capacity of the phytoplankton assemblage. This capacity is influenced by the taxonomy and the light history of the community as well as by nutrient limitations or the concurrence of other stressors (Gorbunov & Falkowski, 2022 and references therein). Photosynthetic efficiency after dark acclimation is quantified with the F_v/F_m ratio. (b) Immediately, without dark acclimation. Some reaction centres of the cell are already occupied and not available during the FIRE excitation pulse, so that we measure the effective or relative photosynthetic capacity. The capacity of PSII to accept electrons under these conditions depends on its ability to acquire new electrons and release those already present, contingent upon various physiological traits related to the photosynthetic system (Harrison et al., 2015). The immediate photosynthetic efficiency (with no dark acclimation) is expressed by the F_v'/F_m' ratio, is more ephemeral, and indicates the photophysiological state of the phytoplankton assemblage in response to a short-term stressor. This is the approach we used in our study to monitor phytoplankton photosynthetic performance both at the phase of stress (exposure to high light) and at the phase of recovery (relieve from exposure). Note that, when dealing with dynamic photoinhibition, the photosynthetic recovery will be influenced by the capacity to liberate the occupied reaction centres and the presence of quenching processes to avoid serious oxidative damage. Intrinsic properties of the phytoplankton cells, and their physiological state, will both determine recovery

dynamics. In natural communities, environmental drivers play an additional, indirect role by influencing phytoplankton fitness. Interestingly, having some light is an important factor for recovery because partial dependence on light energy for PSII recovery has been suggested (L. Wu et al., 2017).

Hypothesis 3 (*light-stressed communities are grazed more than their healthier counterparts*) and **4** (*higher grazing pressures towards light-stressed communities improve phytoplankton recovery in terms of photosynthetic efficiency*) are addressed in sections 3.2, 3.3 and 3.4. We investigated the effects of light stress of the prey on prey-predator interactions by short-term exposing prey assemblages to high light (including UV), relieving the high light exposure and hence the stress, and monitoring the recovery of the immediate photosynthetic efficiency while measuring predation. Both natural communities and cultured model organisms were used. The cultured microalga chosen was *Isochrysis galbana*, a motile prymnesiophyte containing high cellular DMSP concentrations (Keller et al., 1989) and already used in selective grazing studies (Strom et al., 2020). It was also a convenient prey for our cultured herbivore predator *Gyrodinium dominans*, a heterotrophic dinoflagellate typically encountered in natural assemblages of the coastal and open ocean (Calbet et al., 2013). Moreover, grazing experiments were conducted in the field using the dilution technique to modify prey-predator encounter rates (Landry & Hassett, 1982). The method quantifies microzooplankton grazing by gradually diluting natural communities with filtered seawater, overcoming the inherent impossibility of separating prey and predators by size (Weisse et al., 2016). Despite the method is based on some unrealistic assumptions (Calbet & Saiz, 2013; Dolan, & McKeon, 2005; Stoecker et al., 2015) and has limitations (Duarte Ferreira et al., 2021; Schmoker et al., 2013), it is still the prevailing approach to estimate microzooplankton grazing in aquatic systems. Additionally, coupled lab-field experiments were performed by adding cultured *G. dominans* to natural assemblages, with the aim to test the grazing response to stressed prey by a predator grown in non-stressing conditions and modify the grazing pressure without the need to apply serial dilutions.

MATERIALS & METHODS

Phytoplankton and zooplankton cultures. The heterotrophic dinoflagellate *Gyrodinium dominans* ICM-ZOO-GD001 was originally isolated from the NW Mediterranean by A. Calbet in 2011. The microzooplankton was cultivated and maintained with a *Rhodomonas salina* K-0294 diet. The alga, obtained from the Scandinavian Culture Collection of Algae and Protozoa at the University of Copenhagen, has been cultured at the Institute of Marine Sciences (ICM-CSIC) since 2018. The prey used for the grazing experiments was *Isochrysis galbana* CCMP 1323, originally isolated from the Irish Sea (North Atlantic) and maintained at the Institute of Marine Sciences (ICM-CSIC). We conserved the dinoflagellate and the prey (*I. galbana*) culture (ISO) with autoclaved filtered seawater (FSW), supplemented with f/2 medium (Guillard, 1975) for the algae culture, on a 14:10 hour light to dark cycle at 19°C, with a light intensity of $50 \mu\text{E} \cdot \text{m}^{-2} \cdot \text{s}^{-1}$. The *R. salina* culture was kept under the same conditions as the ISO culture but with a higher light intensity ($100 \mu\text{E} \cdot \text{m}^{-2} \cdot \text{s}^{-1}$). The *I. galbana* culture was treated with a combination of three antibiotics: kanamycin ($1000 \mu\text{g ml}^{-1}$), neomycin ($250 \mu\text{g ml}^{-1}$), and penicillin ($1000 \mu\text{g ml}^{-1}$) at the start of the batch and the day before the experiment to reduce bacterial abundance and activity. Cell concentration of all cultures was monitored regularly with a Multisizer™ 3 Coulter Counter (Beckman Coulter). Before the experiments, the dinoflagellates were starved until the majority of the individuals were depleted in prey in their vacuoles and no *R. salina* was present in the culture. Dilutions of the cultures were made as needed to achieve the required concentrations (Table 3.1).

Field sampling. Three distinct experimental sets from two oceanic locations were used in this chapter (Table 3.1). Open-ocean communities, with low phytoplankton abundance, were sampled from the Mediterranean Sea (MED) and the Southern Ocean near the Antarctic continent (ANT) (Figure 3.1) during the cruises SUMMIT-MED and POLAR CHANGE, respectively. Additionally, phytoplankton-rich communities were sampled from the Barcelona Olympic Harbour (MEDH). Coordinates and characteristics of each experiment are shown in Table 3.1. Natural community samples from MEDH and ANT experiments were collected from surface waters during low-light intensity hours (early morning or evening) to avoid sampling already sunlight-stressed phytoplankton. MED samples were collected from below the mixed layer (14–30 m) to have phytoplankton assemblages adapted to low sunlight levels.

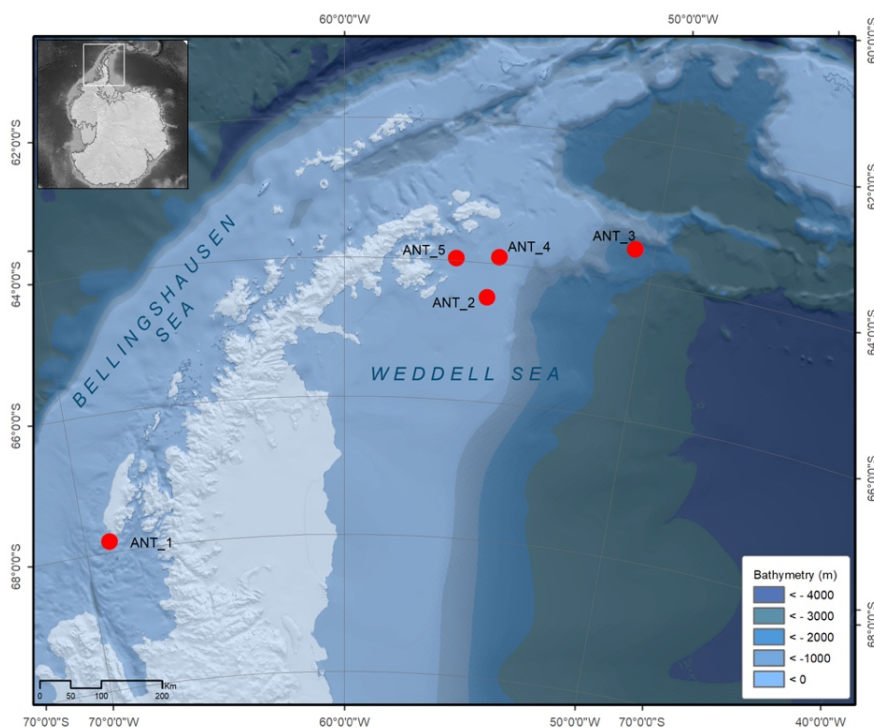



















Figure 3.1. Sampling stations of the POLAR CHANGE cruise around the Southern Ocean close to the Antarctic continent. The experiments conducted in each of the stations (ANT_1-ANT_5) conform the ANT set of experiments.

Table 3.1. Ancillary data and experimental setup of each experiment of sections 3.1-3.4.

SET & EXP CODE	Location (coordinates)	Water mass	Water T (°C)	Chl.a (µg Chla/L)	Initial Fv'/Fm'	Phytoplankton concentration (cell/ml)	DMSPt/cell (nmol/cell) DMSPt/chla (nmol/µg)	Experimental setup
ISO_1	-	<i>I. galbana</i> culture	19°	-	0.521	3.81E+05	4.37E-06	(I) Stress  (II) Grazing. Setup 3
ISO_2	-	<i>I. galbana</i> culture	19°	-	0.534	3.29E+05		(I) Stress  (II) Grazing. Setup 3
ISO_3	-	<i>I. galbana</i> culture	19°	-	0.435	4.30E+04	1.06E-05	(I) Stress  (II) Grazing. Setup 3
MED_1	Open MED Ocean 40° 42' 139" N 2° 55' 270" E	Open ocean BML (25m)	18°	0.05	0.350	NP: 4.72E+02 PP: 1.65E+03 AP: 2.12E+03	Cell: 1.35E-05 Chla: 573.76	(I) Stress 
MED_2	Open MED Ocean 40° 42' 139" N 2° 55' 270" E	Open ocean BML (30m)	17.5°	0.11	0.387	NP: 8.48E+02 PP: 1.52E+03 AP: 2.37E+03	Cell: 1.55E-05 Chla: 334.54	(I) Stress 
MED_3	Open MED Ocean 40° 42' 21.6" N 2° 55' 19.2" E	Open ocean BML (15m)	17.5°	0.16	0.345	NP: 1.20E+03 PP: 1.92E+03 AP: 3.12E+03	Cell: 1.10E-05 Chla: 214.32	(I) Stress 
MED_4	Open MED Ocean 40° 42' 21.6" N 2° 55' 19.2" E	Open ocean BML (18m)	17.5°	0.10	0.404	NP: 7.40E+02 PP: 1.96E+03 AP: 2.70E+03	Cell: 1.36E-05 Chla: 366.37	(I) Stress 
MED_5	Offshore MED Ocean 40° 35' 24" N 2° 51' 39.6" E	Open ocean BML (14m)	-	0.14	0.425	NP: 1.33E+03 PP: 1.65E+03 AP: 2.98E+03	Cell: 1.49E-05 Chla: 318.02	(I) Stress 
MEDH_1	BCN Olympic harbour 41° 23' 7.19" N 2° 12' 0.60" E	Coastal (harbour) Surface water	27°	3.28	0.497	NP: 7.1 · 10 ³ PP: 8.3 · 10 ³ AP: 1.6 · 10 ⁴	Cell: 9.94E-06 Chla: 48.51	(I) Stress  (II) Grazing. Setup 1 Dilution sets 1 0.75 0.5 0.25
MEDH_2	BCN Olympic harbour 41° 23' 7.19" N 2° 12' 0.60" E	Coastal (harbour) Surface water	25°	3.35	0.494	NP: 4.9 · 10 ³ PP: 1.0 · 10 ⁴ AP: 1.5 · 10 ⁴	Cell: 8.73E-06 Chla: 39.09	(I) Stress  (II) Grazing. Setup 1 Dilution sets 1 0.75 0.5 0.25

MEDH_3	BCN Olympic harbour 41° 23' 7.19" N 2° 12' 0.60" E	Coastal (harbour) Surface water	26°	n.d	0.520	NP: $5.8 \cdot 10^3$ PP: $1.4 \cdot 10^4$ AP: $2.0 \cdot 10^4$	Cell: $7.42E-06$	(I) Stress 
								(II) Grazing. Setup 2 NC & <i>G. dominans</i> C+G S+G S
MEDH_4	BCN Olympic harbour 41° 23' 7.19" N 2° 12' 0.60" E	Coastal (harbour) Surface water	25°	3.96	0.528	NP: $4.8 \cdot 10^3$ PP: $1.1 \cdot 10^4$ AP: $1.7 \cdot 10^4$	Cell: $4.99E-06$ Chla: 21.43	(I) Stress 
								(II) Grazing. Setup 2 NC & <i>G. dominans</i> C+G S+G S
ANT_1	Southern Ocean Bellingshausen Sea 67° 50' 24" S 69° 3' 44" W	Surface water	1.17°	0.59	0.433	NP: $6.3E+02$ PP: $2.7E+03$ AP: $3.6E+03$	Cell: $1.58E-05$ Chla: 96.91	(I) Stress 
								(II) Grazing. Setup 1 Dilution sets 1 0.75 0.5 0.25
ANT_2	Southern Ocean Weddell Sea 64° 29' 36" S 55° 14' 39" W	Surface water	0.016°	0.72	0.523	NP: $3.4E+03$ PP: $1.4E+03$ AP: $5.0E+03$	Cell: $7.34E-06$ Chla: 50.94	(I) Stress 
								(II) Grazing. Setup 1 Dilution sets 1 0.75 0.5 0.25
ANT_3	Southern Ocean Weddell Sea 63° 33' 2.5" S 50° 37' 33" W	Surface water	0.220°	0.27	0.289	NP: $2.1E+03$ PP: $5.4E+02$ AP: $2.9E+03$	Cell: $1.77E-05$ Chla: 189.74	(I) Stress 
								(II) Grazing. Setup 1 Dilution sets 1 0.75 0.5 0.25
ANT_4	Southern Ocean Weddell Sea 63° 54' 28" S 54° 56' 50" W	Surface water	-0.075°	0.80	0.370	NP: $4.1E+03$ PP: $1.6E+03$ AP: $5.9E+03$	Cell: $5.68E-06$ Chla: 41.88	(I) Stress 
								(II) Grazing. Setup 1 Dilution sets 1 0.75 0.5 0.25
ANT_5	Southern Ocean Weddell Sea 63° 57' 52" S 56° 20' 42" W	Surface water	-0.016°	0.97	0.498	NP: $5.2E+03$ PP: $7.5E+02$ AP: $6.0E+03$	Cell: $3.70E-06$ Chla: 22.86	(I) Stress 
								(II) Grazing. Setup 1 Chemical addition MQ D M A

Experimental settings. Two main blocks of experiments (I and II, Figure 3.2) were designed to address the thesis objectives and hypotheses. First, stress experiments (I) examined the effects of light-stress events on phytoplankton assemblages to test hypothesis 2 (*light-stress events induce DMSP release in phytoplankton assemblages and cultures*). These experiments were performed with three distinct natural communities (MED, MEDH, ANT) and one phytoplankton culture (ISO). Secondly, experiments targeting grazing and phytoplankton recovery from light-stress events (II), tested hypotheses 3 and 4 with analyses A and B, respectively. Hypothesis 3 is tested with the set of analyses A, asking whether faster grazing occurs on light-stressed phytoplankton assemblages, to the detriment of their healthier counterparts. The results of analyses A are complemented with testing hypothesis 4 with the set of analyses B, where grazing pressures are modified to observe if higher grazing improves photosynthetic efficiency recovery of the assemblage. This second group of experiments (II) used three setups (1-3), natural communities (1), the addition of a cultivated grazer (*G. dominans*) to natural communities (2) and a model system based on two cultured strains: *G. dominans* feeding on *I. galbana*. (3). These setups were applied in two distinct natural communities (MEDH and ANT) and one culture-based approach (ISO).

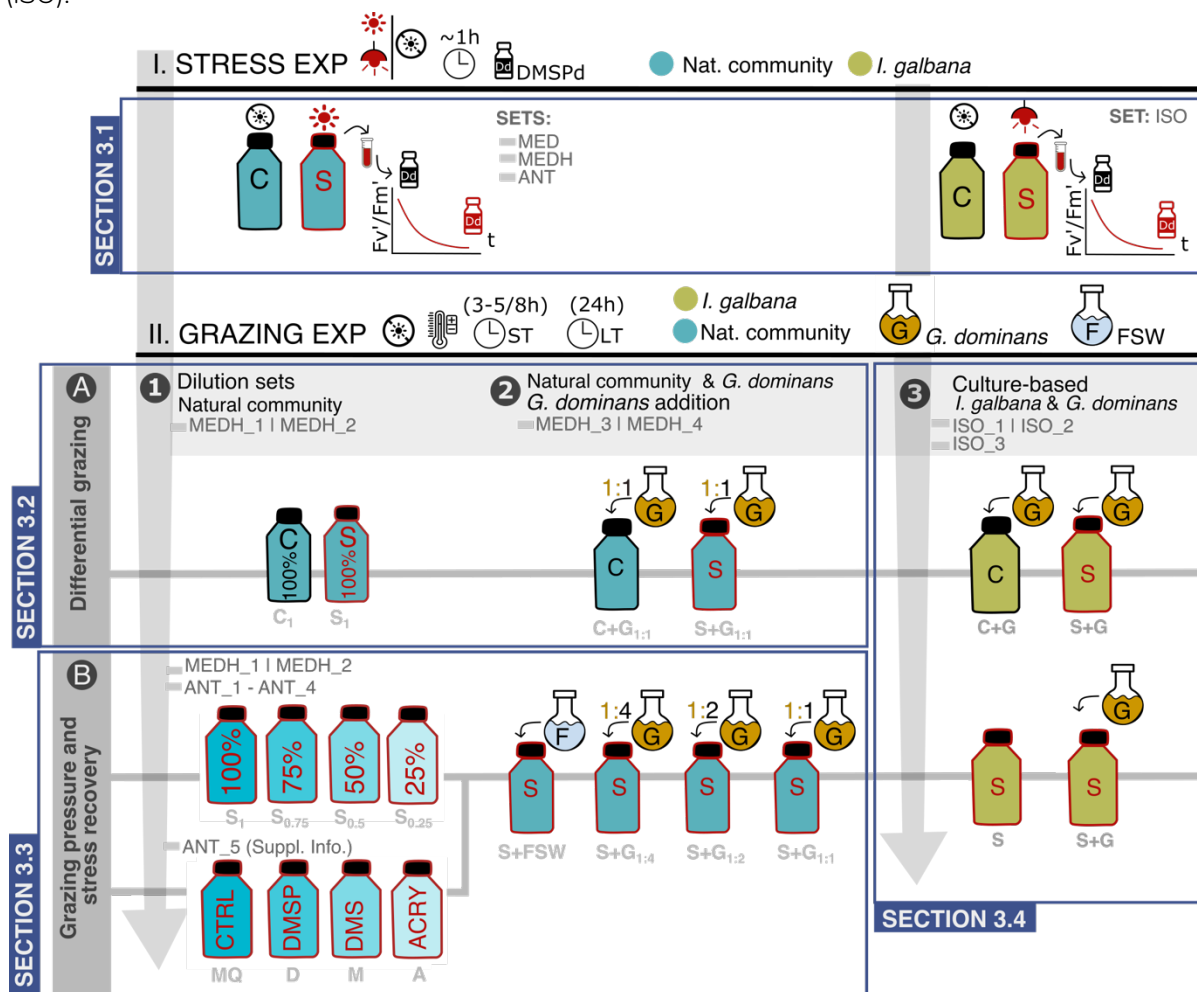


Figure 3.2. General methodological diagram. The different setups used in each experiment are detailed in the diagram. Two main blocks are distinguished: block I (stress experiments) developed in section 3.1, and block II (grazing experiments) expound within three sections (3.2, 3.3, and 3.4). **Block I** consists only of two setups (natural communities and a culture-based system) carried out with four experimental sets: MED, ANT, MEDH and ISO. **Block II** is implemented in three setups (1: Dilution sets, 2: *G. dominans* additions, and 3: culture-based experiments). Two distinct analyses are detailed: **A**, targeting differential grazing versus control and stressed communities) and **B**, focusing on the influence of grazing pressure in stress recovery in bottles with different proportions of grazers. **Symbols:** ☀ natural sunlight, ☂ artificial solar simulator, ☼ non-stress conditions, DMSPd= dissolved DMSP, time (ST= short-term, LT=long-term), 🌡 temperature-controlled, C=control, S=stressed, G= *G. dominans*, F=FSW.

(I) Stress experiments. The aim was the characterization of different light-stress treatments while monitoring the response of the phytoplankton assemblage. The methodology is sketched in Figure 3.2, block I.

Natural communities were prefiltered through 100-200 μm and incubated at the in-situ temperature (Table 3.1), either in an indoor temperature-controlled incubator (MEDH experiments) or in an outdoor incubator with open-circuit surface water running (ANT and MED experiments). Light intensity was maintained low using neutral mesh layers. At the start of the experiments, sunlight-based stress was applied by sequentially exposing the communities to increased natural sunlight intensity, modulated with multiple layers of neutral nylon mesh for around 1h while measuring global solar irradiance intensities (see below). Aliquots of 1 liter were incubated in polytetrafluoroethylene bottles (TeflonH, Nalgene), which transmit the whole solar spectrum, including UV. Stress experiments involving *I. galbana* were conducted in a Suntest CPS+ solar simulator (Atlas Material Testing Technology, Chicago, IL). Aliquots of 250 ml of the *I. galbana* exponentially growing culture were sampled into UV-transparent polytetrafluoroethylene bottles (TeflonH, Nalgene) and incubated at maximum irradiances of $250 \text{ W}\cdot\text{m}^{-2}$ modulated with 3 to 1 layers of neutral plastic mesh. The incubation time ranged from 20 to 40 min depending on the *I. galbana* stress levels detected. The stress levels applied in all the experiments were assessed by monitoring the immediate photosynthetic efficiency (F_v'/F_m') using a miniFIRE (M. Gorbunov) system (see below). Stress conditions were terminated when the photosynthetic efficiency was not decreasing further or when values of photosynthetic efficiency reached 0. One replicate bottle was kept in parallel under control conditions where no stress was applied. Total DMSP (DMSPt) was sampled from the initial community. Dissolved DMSP (DMSPd) samples were taken before and after the stress treatment (see below).

(II) Grazing experiments. These experiments were performed using two analyses to test hypothesis 3 and 4. The aim of the analytical set A was to compare grazing rates on light-stressed versus non-exposed phytoplankton assemblages. Analyses B aimed at exploring the relationship between grazing pressure and the photosynthetic efficiency recovery of the phytoplankton assemblage. Both analyses correspond to block II of Figure 3.2.

The total set of 12 experiments can be categorised as follows: Two dilution experiments (setup 1) and two *G. dominans* addition experiments (setup 2) were conducted in the ICM premises with water from the Barcelona Olympic Harbor (MEDH). Four dilution series (setup 1) and one chemical-addition setup (Supplementary material) were conducted during the POLAR CHANGE cruise (ANT). Additionally, three culture-based experiments (setup 3) were carried out with *G. dominans* feeding on *I. galbana* in laboratory conditions (ISO). All the experiments started with a stress treatment phase, executed as described in the stress experiments section. After conclusion of the stress phase, the communities were incubated in a temperature-stable bath with low light conditions to facilitate photosynthetic recovery. The three distinct setups are detailed below:

❶ **Dilution series:** The dilution technique (Landry & Hassett, 1982) involved dilution series of 100, 75, 50, and 25% prepared with filtered seawater (FSW) in 1 liter bottles. In the MEDH sets, the series were diluted with the autoclaved FSW used normally to grow microzooplankton cultures and supplemented with nutrients to reach a f/20 medium. ANT series were diluted with 0.8 μm FSW generated from the original natural sample and no nutrients were added since nutrient limitation (f/20 nutrients) was not expected (Wu et al., 2019). On one occasion (ANT_5), we amended the four bottles with additions of 1 ml of either DMSP, DMS, or acrylate, reaching a final concentration of 20 μM (Supplementary Information). The control bottle was treated with the chemicals' dilution media, MQ water.

❷ ***G. dominans* additions:** Natural communities were altered to enhance grazing by adding a non-stressed predator, cultured in optimal conditions and starved prior to the experiments. The heterotrophic dinoflagellate *G. dominans* was added at different proportions to the nanophytoplankton abundance

(1:1, 1:2, 1:4, respectively). All 300 ml bottles were diluted equally either with *G. dominans* culture with different grazer concentrations or sterile FSW (S+FSW) for the control without added grazers. Nutrients were supplemented to all bottles to reach a f/20 medium with 5 μM NH_4^+ to avoid differences due to nutrient fertilization when adding the culture.

③ **Culture-based:** The experiments were conducted with *G. dominans* as predator and *I. galbana* as prey. Grazing experiments were run with two different culture batches using two different prey concentrations. ISO_1 and 2 used the same *I. galbana* and *G. dominans* batches and tested saturating and non-saturating prey concentrations (1:10 and 1:6, respectively). Nutrients were supplemented to all bottles to reach a f/20 medium with 5 μM NH_4^+ to avoid differences due to nutrient fertilization when adding the culture. Experiments were run with a final volume of 200 ml. The ISO_3 was run with a different batch of both cultures, using saturating prey conditions (1:10 proportions), and a final volume of 110 ml. Additionally, the stress-treated bottle had a distinct composition in each of the three experiments, by varying the proportion of control and stressed prey cells: 100% stressed cells (ISO_1), 1:6 control:stressed cells (ISO_2), 1:1 control:stressed cells (ISO_3).

Block II consisted of two distinct analyses: (A) Differential grazing on stressed versus control phytoplankton assemblages, and (B) influence of the grazing pressure on light-stress recovery. **Analysis A** focused only on comparing flow cytometry data of the control and the stress-treated bottles. Grazing rates were estimated from the decline of phytoplankton abundance over time. In all setups, photosynthetic efficiency recovery and prey concentration were evaluated simultaneously by sampling at spaced intervals until the end of the recovery phase, considered the end of short-term (ST) experiments. The recovery phase concluded when the photosynthetic efficiency reached saturation. In the dilution series, an extra predation timepoint was sampled 24 hours after the start of the recovery phase to check for differences in longer-term (LT) dynamics in analysis A. This analysis only required the comparison of some bottles of each setup: C_1 vs S_1 (non-diluted bottles in setup 1), $C+G_{1:1}$ vs $S+G_{1:1}$ (bottles with the largest *G. dominans* additions in setup 2) and $C+G$ vs $S+G$ (setup 3). **Analysis B** compared the grazing rates with the recovery potential of stressed bottles with different grazing pressures. Thus, the whole set of stressed bottles with distinct grazing pressures was compared in each setup. This second analysis was conducted in short time scales only. Predation was evaluated by measuring phytoplankton concentration with flow cytometry (FCM) and immediate photosynthetic efficiency was measured with a Fluorescence Induction and Relaxation instrument (miniFIRE, M. Gorbunov).

DMSP measurements. DMSPd was sampled before and after the stress treatment by small-volume drip filtration on 25-mm Whatmann GF/F filters (Kiene & Slezak, 2006). The 2-3 ml filtrate was transferred to gas-tight borosilicate serum vials. Total DMSP (DMSPt) was measured from the original community by sampling ~30 ml aliquots of unfiltered seawater. Additions of 30 μl of HCl 37% were made to both the DMSPd and DMSPt vials to fix the samples while oxidising the DMS present and keeping only the DMSP (Kinsey & Kieber, 2016). Treated samples were stored at room temperature in the dark. The DMSP was later converted to DMS by alkaline hydrolysis with NaOH for at least 24. The evolved DMS was quantified with a cryogenic purge-and-trap system coupled to a Shimadzu GC-14A gas chromatograph with flame photometric detection (Masdeu-Navarro et al., 2022). The Welch's one-tail method was applied to test if significantly higher DMSPd concentrations were found after the stress treatments. DMSPt results were used to characterize the communities and normalize the DMSPd data by calculating the DMSPd/DMSPt ratio before and after the stress. Finally, the difference between the ratios obtained before and after the stress ($\Delta\text{DMSPd/DMSPt}$) was quantified to measure the increase in DMSPd.

FCM analyses. Phytoplankton concentration was quantified by flow cytometry by sampling 5ml of each bottle. Samples were preserved with paraformaldehyde + glutaraldehyde (1% + 0.05% final concentration, respectively) or formaldehyde (3.7% final concentration) and stored at - 80 °C. Posterior

analyses were conducted in a CyFlow Cube 8 (Sysmex Partec) flow cytometer based on side scatter (SSC) and chl_a autofluorescence with the laser emitting at 488nm. Cytograms were analysed with the FlowJo 10.10.0 software (Becton Dickinson & Company) to define the populations and count the corresponding cell concentrations.

Photosynthetic efficiency. The stress metric used was the relative efficiency of excitation energy captured by the photosystem II (PSII) calculated as F_v'/F_m' and known as the immediate photosynthetic efficiency. The metric represents the effective photosynthetic capacity under light treatments related to alterations in the quantum yield of photosynthesis due to the irradiance conditions (Gorbunov & Falkowski, 2022). The FRe system measures the quantum yield of photochemical and fluorescence emission pathways to provide information on the chl_a fluorescence yield. Alterations of the ratio of photons reradiated to those absorbed define fluctuations in photosynthetic efficiency and provide information about the physiological state and the photosynthetic capacity (Gorbunov & Falkowski, 2022 and references therein). To calculate the photosynthetic efficiency, the FRe system emits a strong pulse of light (the single turnover flash) to saturate all reaction centres of the PSII (Gorbunov & Falkowski, 2022). The instrument records two parameters: F_0' as the minimal yield of fluorescence before the flash, and F_m' , the maximum yield of fluorescence due to the reradiation of the maximum number of photons. The difference between F_m' and F_0' is called variable fluorescence (F_v'). The quotient of F_v'/F_m' represents the effective photosynthetic efficiency of the community measured under light conditions (Gorbunov & Falkowski, 2022). The metric has arbitrary units, so that it is independent of the phytoplankton abundance and allows comparisons between environments. Aliquots of 10 ml for ANT and 2 ml for MEDH and ISO were sampled from the bottles at consecutive time intervals to follow both the stress and the recovery dynamics. The aliquots were placed in the chamber of the mini-FRe to apply the induction and relaxation protocol for dilute samples. A hundred acquisitions were averaged for each sample using the *fview* software and the resulting data was processed with the *fprope* software to obtain all the desired parameters.

Environmental and phytoplankton assemblage descriptions. Solar radiation was used as environmental stressor. The use of temperature-stable incubators allowed the conservation of in situ temperatures reducing the probabilities of exerting thermal stress to the communities. Global solar radiation was monitored either by the radiometer of the oceanographic vessel (ANT, MED) or by the data obtained from the closest meteorological station (Barcelona – Raval, Catalonia official Meteorological Service) in MEDH incubations (see below). Phytoplankton assemblages were described in terms of total abundance with chl_a measurements and of size distribution and composition by flow cytometry. The total chlorophyll *a* (chl_a, µg L⁻¹) was measured from 100-200 ml samples of the original community filtered through Whatman GF/C glass fibre filters. Samples were extracted with 90% acetone for 24 h at 4°C and in the dark, and quantification was performed on a calibrated Turner Designs Fluorometer (Duarte Ferreira et al., 2021). FCM based on size and chl_a autofluorescence permitted the identification and quantification of the nano- and picophytoplankton. The biomasses of these two populations of interest were calculated assuming a carbon content of 1319 pgC/cell and 25.87 pgC/cell, respectively.

Light treatments and stress metrics (section 3.1). The stress treatments and phytoplankton responses were characterised by several metrics. Global solar irradiance intensity ($W \cdot m^{-2}$) was obtained either from the vessel radiometer or the closest meteorological station. Intensities (E'_i) in $W \cdot m^{-2}$ were corrected with the number of mesh layers added (m) with equation [1] (one neutral mesh transmits 60% of total irradiance) and used together with the incubation time (Δt_i) for calculating the doses (D) in $Kj \cdot m^{-2}$ applied to the communities (equation [2]).

$$E'_i = E_i \cdot 0.6^m \quad [1]$$

$$D = \sum_{i=1}^n (E'_i \cdot \Delta t_i) / 1000 \quad [2]$$

The light history of the communities was estimated in each environment to contextualize light-stress responses. Similar maximum irradiance to the one of the experimental day was assumed for the previous day. Chla concentration was used to calculate the PAR attenuation coefficient (K_{PAR}) for oceanic case I waters with equation [3] from Morel (1988):

$$K_{PAR} = 0.121 \cdot [chla]^{0.428} \quad [3]$$

In MEDH waters the K_{PAR} was considered 1, since the harbour conditions were considered case II (strong light extinction). With the K_{PAR} we quantified the mean irradiance received in the sampled depth applying the light extinction equation [4], where z is the sampled depth or the depth of the upper mixed layer (MLD). While MED samples were retrieved from a depth below the mixed layer (25 m), ANT and MEDH surface samples were obtained from the upper 5m, i.e., within the mixed layer. Thus, the average of the irradiance between 0 and 5 m (MED) and between 0-20 m (ANT) was used for calculating the mean irradiance with equation [5].

$$I_z = I_0 \cdot e^{(-K_{PAR} \cdot z)} \quad [4]$$

$$\bar{I}_{MLD} = \left(\frac{I_0}{K_{PAR} \cdot MLD} \right) \cdot (1 - e^{(-K_{PAR} \cdot MLD)}) \quad [5]$$

The stress response of the phytoplankton community was assessed with the temporal decrease in photosynthetic efficiency (Fv'/Fm') enabling the calculation of the percentage similarity (% Fv'/Fm') to the initial value of unstressed communities (equation [6]). Low percentages identified high dissimilarity from the initial value and thus a severe decrease in photosynthetic efficiency.

$$\frac{Fv'/Fm'_{tf} \cdot 100}{Fv'/Fm'_{t0}} \quad [6]$$

Quantification and statistics of grazing

Section 3.2

Net growth rates (h^{-1}): To compute and compare net growth rates between control and stressed bottles of MEDH experiments, cell concentration data was log-transformed to apply individual linear regressions and an analysis of covariance (ANCOVA). The significance threshold was set at $p < 0.05$. Non-significant regressions indicating negligible grazing rates were not considered in the ANCOVA test. The net rate of change equation [7] was applied to quantify the net growth rates between the ST and LT temporal intervals that comprised only two sampling points. The rates were computed using phytoplankton concentrations at the initial (C_{t0}) and end (C_{tf}) of the considered interval (Δt) assuming an exponential model. Error propagation was implemented in all metrics.

$$r = \frac{\ln(C_{tf} - C_{t0})}{\Delta t} \quad [7]$$

Section 3.3

Net growth rates (h^{-1}): To assess net growth rates (h^{-1}), phytoplankton concentration was plotted against time, and a log-linear regression analysis was applied. The slope of the fitted line from the regression models provided the net growth rates. Non-significant regressions indicated negligible grazing rates. In *G. dominans* addition experiments (MEDH_3 and MEDH_4), grazing was analysed from 1h after the addition of *G. dominans*, as delayed predation could be inferred from the flow cytometry data. The net rate of change equation [7] was applied to quantify the net growth rates in the ANT sets encompassing only two sampling points.

Section 3.4

Grazing rates (h^{-1}). Linear regressions of log-transformed phytoplankton concentration vs time quantified the grazing rates and allowed their comparison between control and stressed bottles with the analysis of covariance (ANCOVA). The significance threshold was set at $p < 0.05$. Since non-significant regressions were detected in S and C bottles, growth or death processes were considered irrelevant and the decline in phytoplankton concentration was taken as the indicator for grazing processes.

Consumption (%). To follow the decrease in prey concentration, the percentage consumed (%) from the initial population was calculated at each time point.

Regressions and statistical tests were performed in R v4.0.2 (R Development Core Team, 2021) supported by the broom package (Robinson et al., 2023).

Quantification and statistics of recovery (section 3.3-3.4)

Photosynthetic efficiency recovery. The recovery of the photosynthetic efficiency was assessed by measuring F_v'/F_m' over time after alleviation of the stress. The data was analysed with the method described in Montero et al. (2002) for the same kind of data. The temporal series of F_v'/F_m' values was fitted to the following exponential sigmoidal function [8]:

$$f(t) = p - q \cdot \exp^{-st} \quad [8]$$

Where p , q and s are specific constants to be determined for each recovery series and t is time (h). The time constant (s) obtained described the slope of the curve, which indicates how rapidly the upper asymptote was reached; it is reported from now on as the recovery rate constant (r). The upper asymptote value (p) will be referred to as the F_v'/F_m' saturation level. The fits were performed in R v4.0.2 (R Development Core Team, 2021) with the *nls* function based on Bates & Chambers (1992) and Bates & Watts (1988).

The p values was used to compute the percentage recovered from the original F_v'/F_m' value (pre-exposure to light) to normalize all values to their initial levels with equation [6]. High percentages will indicate low dissimilarity from the original value, and thus a high recovery in photosynthetic efficiency. Values exceeding 100% reveal the communities that were able to recover to higher efficiencies than the ones presented originally.

Recovery rate constants (h^{-1}) were plotted against net growth rate constants (h^{-1}) to explore potential relationships between grazing and recovery. Model I regression analyses were applied again to evaluate the significance and the goodness of fit of the model quantifying the relationship of the two processes. The population-specific grazing rates represented depended on the population dominance (cell and biomass), the significance of the regressions in each experimental set and the occurrence of differential grazing patterns between control and stressed bottles. The saturation level reached at the end of the recovery phase was also plotted against the net growth rates to explore potential relationships in section 3.4.

RESULTS

Chapter 3 develops and examines objectives and hypotheses 2-4 with the aim to study the impact of light-stress on short-term predatory interactions. In order to organize the data and information obtained accordingly, results are presented in four sections. First, the role of solar radiation as a stressor of phytoplankton is described in section 3.1, targeting hypothesis 2 (*light stress events induce DMSP exudation in phytoplankton assemblages and cultures*). Then, grazing patterns on light-exposed and non-exposed phytoplankton assemblages are evaluated in section 3.2 to test hypothesis 3 (*light-stressed communities are grazed more than their healthier counterparts*). In section 3.3, the influence of grazing pressure on the photosynthetic efficiency recovery of the prey assemblage is assessed in natural communities to answer hypothesis 4 (*higher grazing pressures on light-stressed communities improve phytoplankton recovery in terms of photosynthetic efficiency*). Finally, section 3.4 evaluates hypotheses 3 and 4 in a model system (*G. dominans* grazing on *I. galbana*).

3.1 Light-stress treatments and responses of four phytoplankton assemblages

Recap of aims and methodology

Sunlight availability is a key driver influencing multiple interrelated processes in aquatic ecosystems with high importance for organisms rhythms (Mittag, 2001). While some effects of UV light on phytoplankton assemblages have been extensively explored (Darroch et al., 2015; Harada et al., 2009; Hessen et al., 1997; Pausz & Herndl, 1999; Slezak & Herndl, 2003; Strom et al., 2020; van Rijssel & Buma, 2002), consequences of short-term sunlight stress with community implications are still understudied (De Lange & Lüring, 2003; Strom et al., 2020; Thornton, 2014). Chapter 3 focuses on how light stress events can introduce physiologically- and chemically-related variability in phytoplankton assemblages, thereby influencing grazing relationships. The consequences of light-stress events are multiple and diverse, contingent upon the type of light stress and the characteristics inherent to the community affected. The suggested release of organic matter under stressful conditions (Cherrier et al., 2015; Thornton, 2014) highlights the importance of phycosphere compounds in stress-derived community interactions. Although DMSP has been identified as one interesting actor in these interactions (Archer et al., 2010, 2018; Stefels, 2000; Strom et al., 2020; Thornton, 2014), understanding of its role and exudation into the phycosphere is still limited. Hence, this first section aims to investigate how distinct phytoplankton assemblages responded to different light-stress events. Additionally, DMSP exudation was assessed after the light-stress treatment. The experimental series comprised three natural communities (MED, MEDH, and ANT) and one single-strain phytoplankton culture (*Isochrysis galbana*: ISO). While natural sunlight served as the stressor for natural communities, an artificial solar simulator was used for the ISO culture (Figure 3.3).

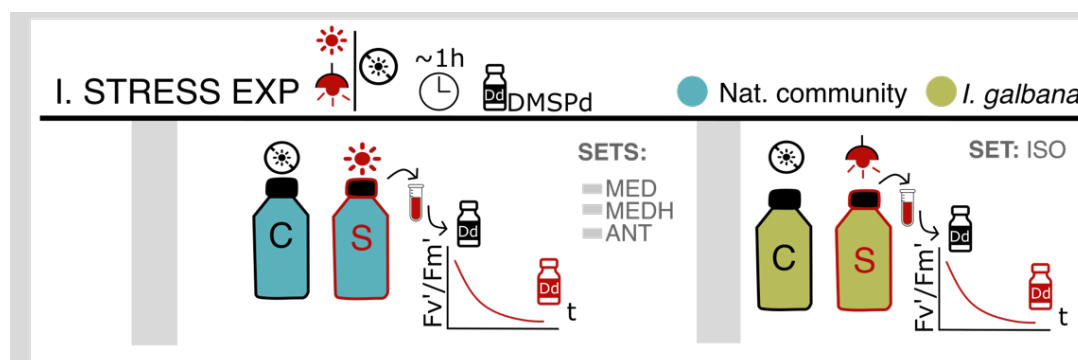


Figure 3.3. Stress experiments diagram. Schematic representation of the experiments conducted with either natural communities: MED, MEDH, ANT, (left) or *Isochrysis galbana* cultures: ISO, (right). Detailed description of the symbols can be found in the methodology section.

Phytoplankton cultures and assemblages

ISO experimental set was composed of three trials performed with two distinct culture batches (Batch May 2022: ISO_3, Batch June 2023: ISO_1 and ISO_2). The two different *I. galbana* cell concentrations tested differed by one order of magnitude (Table 3.1, M&M section). DMSPt/cell was calculated for each batch, being the ISO_3 batch the one with the highest cellular DMSP (Table 3.1, M&M section). As expected, the cultured phytoplankton had high initial F_v'/F_m' values due to optimal growth conditions (Table 3.1, M&M section). The three natural communities were sampled from contrasting field locations differing in most of the features recorded (Figure 3.4, Table 3.1 M&M). The two Mediterranean sets (MED and MEDH) exhibited dissimilarities in terms of chl *a* content and the associated cell biomass. Open-ocean communities (MED) were collected from below the mixed layer (BML) to sample the highest possible concentration of phytoplankton suffering from low sunlight exposition. Yet, their chl *a* contents were the lowest of the three sets (Table 3.1 M&M). MED experiments were performed during summer, with water temperatures around 18°C at the BML water mass located between 14- and 30-meters depth. On the contrary, phytoplankton-rich communities were sampled from a Mediterranean coastal harbour site (MEDH), distinguished by the highest chl *a* content with balanced cell concentrations of nano- and picophytoplankton, being nanophytoplankton the dominant population in terms of cell biomass (Figure 3.4). These samples recorded the highest water temperatures as the experiments were conducted with surface waters collected in summer. The other oceanic locations were around the Antarctica Peninsula (ANT) in the Bellingshausen Sea and the Weddell Sea, with temperatures close to the freezing point (Table 3.1 M&M). Although chl *a* contents were low in these samples, they were higher than in MED sets. ANT phytoplankton assemblages were dominated by nanophytoplankton in terms of cell concentration and biomass.

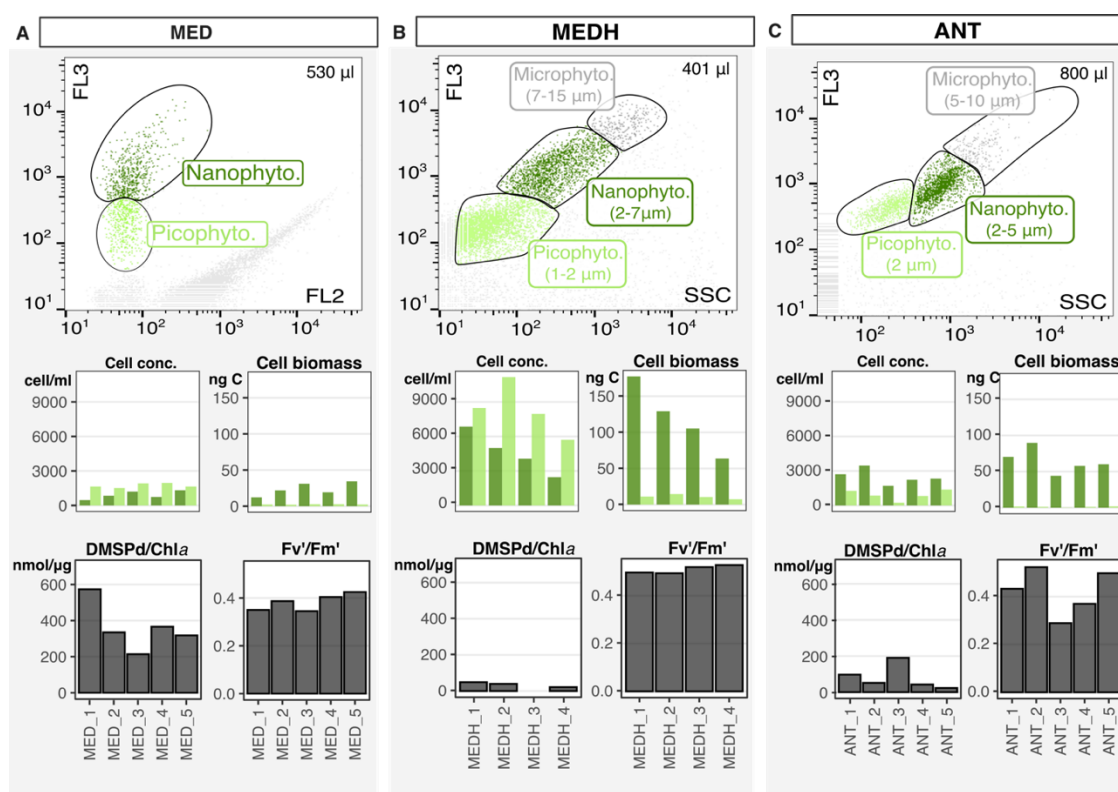


Figure 3.4. Ancillary data of the three distinct sets (MED, MEDH, and ANT) of natural communities used in the experiments. Each plot section (A: MED, B: MEDH, C: ANT) contains the cytograms with the different populations highlighted and the approximated size range represented, cell concentration and cell biomass of nanophytoplankton (dark green) and picophytoplankton (light green), the DMSPd/chl *a* ratio and the initial immediate photosynthetic efficiency (F_v'/F_m') of the community. Picophyto.= picophytoplankton, Nanophyto. = Nanophytoplankton, Microphyto.= microphytoplankton.

The DMSPt/chla ratios were substantially different between each set of samples, following an inverse pattern to cell concentrations (Figure 3.4): the MED communities presented the highest ratios, followed by the ANT samples, with MEDH communities exhibiting the lowest total DMSPt/chla load. Phytoplankton fitness/stress was assessed by measuring the immediate photosynthetic efficiency (F_v'/F_m') of the original community before the experiments. (Figure 3.4). High initial F_v'/F_m' values of the MEDH phytoplankton contrasted with generally lower values observed in MED, suggesting a poorer fitness and the potential presence of some stressors. Initial F_v'/F_m' values of the ANT set were not uniform along the different experiments depicting the influence of stressors over some communities.

Light treatments and phytoplankton stress response and dynamics

Stress treatments were characterised on the basis of the solar radiation dose received, calculated as the product of the monitored irradiance intensity and the incubation time (Table S3.1, Supplementary Information). Phytoplankton response was assessed by following the immediate photosynthetic efficiency (F_v'/F_m') throughout the stress treatment. The value at the end of the treatment was used to calculate the percentage of similarity ($\%F_v'/F_m'$) to the value of the unstressed communities before the exposure, meaning that the lowest percentages corresponded to the most stressed communities. Dose and percentage of similarity characterised the treatments and the response, and allowed comparisons between stress experiments (Figure 3.5).

Although ISO cultures received the mildest stress, they displayed the lowest $\%F_v'/F_m'$ (Figure 3.5). The different responses observed with experiments ISO_1 and ISO_2 versus ISO_3 highlighted the importance of the culture batch used. ISO_3 experienced a milder stress, i.e., higher $\%F_v'/F_m'$ at the end of the treatment although lower cell concentrations were used. The high irradiance doses to which the MED communities were exposed did not translate into important stress levels as evidenced by the highest final values of $\%F_v'/F_m'$ (Figure 3.5). MEDH and ANT samples experienced comparable solar doses but the ANT series stood out with the largest variability between experiments (Figure 3.5). When comparing the different stress responses obtained within each set of experiments, a clear congruence between dose and stress response could be observed in MEDH and ANT experiments. Within each set, the lower $\%F_v'/F_m'$ were obtained with the most severe doses and the other way around.

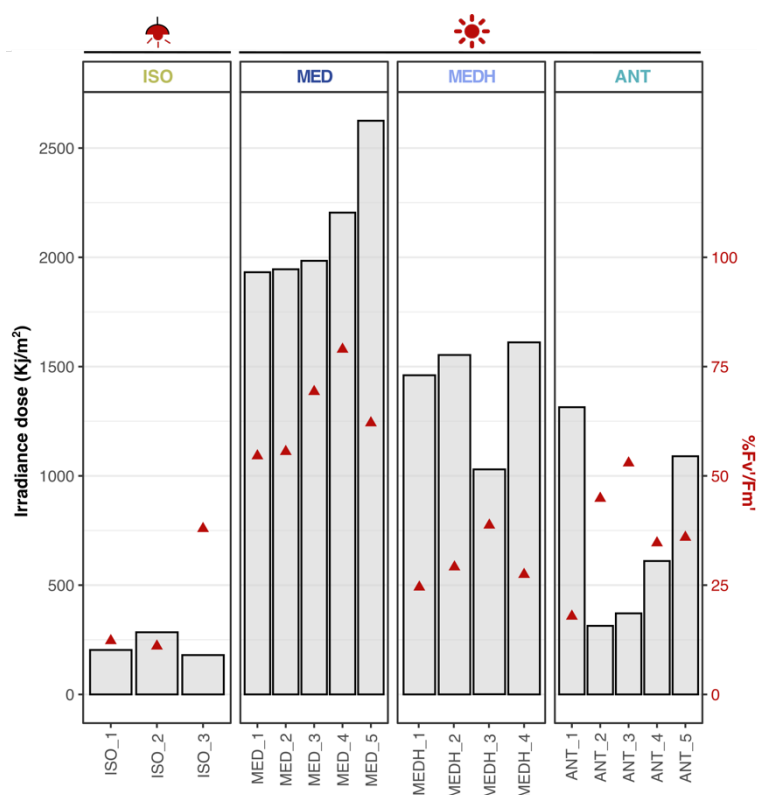


Figure 3.5. Light-stress treatments and phytoplankton response. The grey columns indicate the irradiance dose (Kj/m^2) at the left axis. Red triangles represent the percentage similarity ($\%F_v'/F_m'$) at the end of the treatment (right red axis). Results are detailed for each experiment in the x-axis and grouped by set. The lamp (💡) symbolizes the SUNTEST artificial simulator and the sun (☀️) the natural sunlight irradiance.

The stress dynamics of each phytoplankton community was monitored with the F_v'/F_m' data over the treatment period. Close examination of the $\%F_v'/F_m'$ temporal series revealed distinct dynamics for each community, while also uncovering common patterns (Figure 3.6). The common pattern was an exponential decay, with values decreasing notably within the first half an hour and then stabilizing, since incubation time did not induce higher stress levels. Cultures of ISO exhibited a rapid decline in F_v'/F_m' levels, necessitating shorter stress incubations to avoid reaching negative values (Figure 3.6). Consequently, ISO exhibited the lowest $\%F_v'/F_m'$ values among the populations studied. In most field experiments, the stress incubation could be extended in time by progressively removing neutral mesh layers to obtain gradual stress responses. The MEDH set showed more variability between experiments, with some intervals exhibiting increasing trends after the initial decay. Nevertheless, the final $\%F_v'/F_m'$ values reached were within the same range as the ANT experiments. The MED stress treatments presented the lowest decrease in $\%F_v'/F_m'$, illustrated by a plateau phase at higher $\%F_v'/F_m'$. Although this pattern might suggest a less severe stress response, it is noteworthy that the MED communities were the ones with generally lower initial F_v'/F_m' values. Thus, the dynamics of decay in the F_v'/F_m' and their implications will be influenced by the original conditions and fitness of each community.

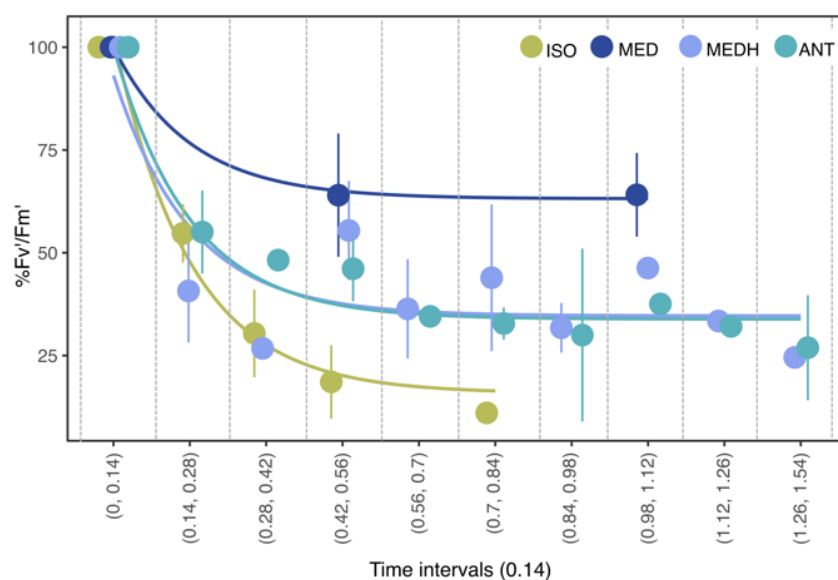


Figure 3.6. Phytoplankton stress response dynamics. Temporal series of $\%F_v'/F_m'$ values obtained throughout the stress treatment. The dots represent the average $\%F_v'/F_m'$ at each specific time interval of 0.14 hours. The average was obtained by gathering at each interval the values of the experiments from each set. The four sets are distinguished by the colour code.

Alterations in ISO cell volume. Culture experiments allowed the monitoring of *I. galbana* cell volume in control and stress treatments. Coulter Counter measurements revealed no meaningful differences in volume between the control and stressed cells in ISO_1 and ISO_2 (Figure 3.7). A slight significant decrease in cellular volume was found in ISO_3 stressed cells (Welch Two Sample t-test, $t=7.91$, $df=5.7$, $p.value=0.0003$).

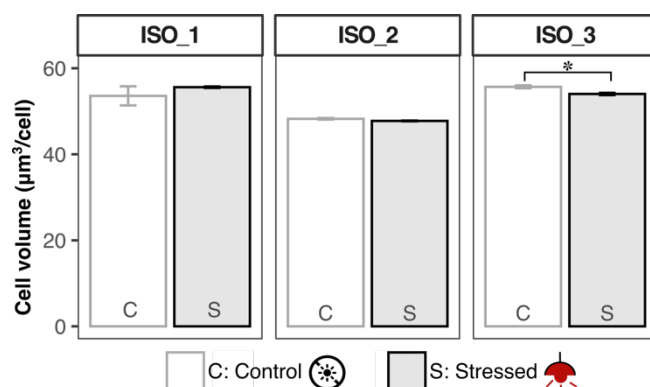


Figure 3.7. *I. galbana* cell volume after control and stressed incubations. Cellular volume (y-axis) of control and stressed *I. galbana* is represented for each experiment. Significant differences are illustrated in the figure with * when $p < 0.05$.

DMSP concentrations. DMSP exudation as a response to light stress was measured as changes in dissolved DMSP concentrations (DMSPd) before (Before_{ST}) and after (After_{ST}) the light-stress treatment (Figure 3.8A). We detected significant differences within each experiment only in the open ocean samples from both the MED and ANT sets (Table S3.2, Supplementary Information), being the DMSPd levels of all MED experiments significantly higher after the stress treatment. While the same pattern was observed in ANT experiments, significant differences were only confirmed in ANT_3 and 4. These two communities were the ones with lower chl_a and phytoplankton abundance. The high data variability in MEDH experiments masked any possible difference induced by the stress treatment. The lowest DMSPd concentrations were obtained in the *I. galbana* cultures, where the stress treatment did not induce any significant DMSP release (Figure 3.8A).

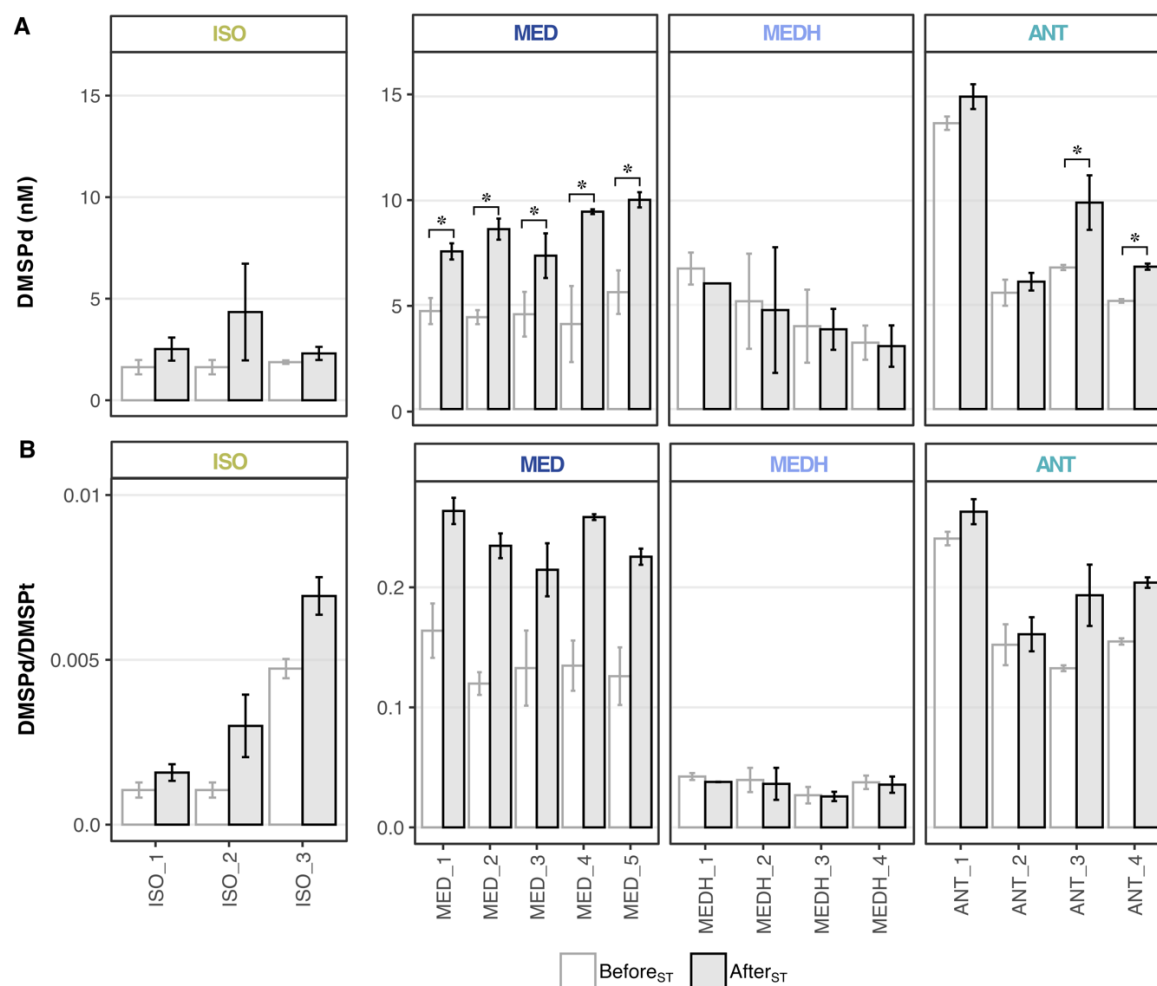


Figure 3.8. DMSP concentrations before and after the stress treatment. (A). DMSPd (nM) data before and after the treatment for each experiment (x-axis) grouped by set. Significant differences are illustrated in the figure with * when $p < 0.05$. **(B).** DMSPd/DMSPt ratio calculated again before and after the treatment for each experiment (x-axis). Notice the different y-axis scale in the ISO set.

Total DMSP (DMSPt) was quantified to provide context and information about the actual DMSP cellular contents of the communities. The DMSPd/DMSPt ratio was applied to normalize the dissolved data across communities. Important dissimilarities were presented among sets with ANT and MED experiments standing out with the highest ratios (Figure 3.8B). Higher ratios than the MEDH and ISO sets were already noticeable before the stress treatment. The ISO culture exhibited the lowest ratios, attributed to a high cellular content that did not correspond with an increased DMSPd. In field communities, the open ocean sets (MED and ANT) presented high ratios, whereas MEDH stood out with

lower ratios (Figure 3.8B). Despite all three sets having comparable concentrations of DMSPd before the treatments (Figure 3.8A), the high DMSPt contents in MEDH probably responding to the high cell concentration, ultimately accounted for the difference in ratios. The quantification of the ratios provided insights into the dynamics of DMSP release. The high ratios in MED and ANT experiments before the stress treatments were detected in the communities with poorer fitness represented by the lower initial F_v'/F_m' values (Figure 3.4A and C).

In Figure 3.9 we integrated various metrics of stress response. Firstly, we elucidate sensitivity and resistance to light stress by relating irradiance dose and the final $\%F_v'/F_m'$ attained. Secondly, we examined the difference in the quotient ($\Delta\text{DMSPd}/\text{DMSPt}$) before and after the stress treatments across experiments, offering insights into dose-response and stress sensitivity within communities, particularly regarding DMSPd release. This analysis reveals diverse levels of resistance among communities, spanning a wide spectrum of responses. At one extreme, the ISO culture displayed high sensitivity, with even low doses inducing a considerable decrease in F_v'/F_m' . Conversely, the MED communities demonstrated improved resistance, representing the other end of the spectrum. The MEDH and ANT sets fell within the mid-range, where moderate doses elicited mild to severe stress responses (20-50% of the initial F_v'/F_m' value).

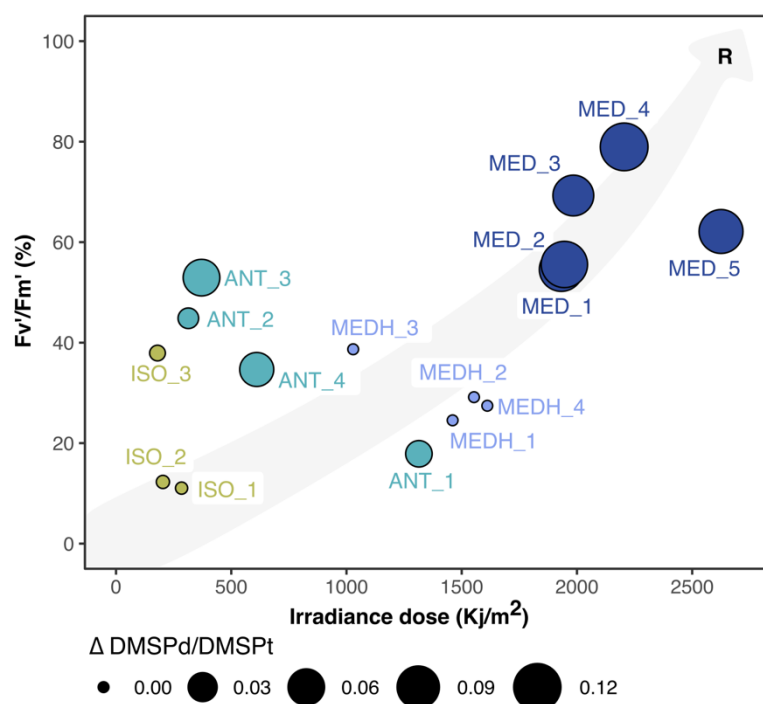


Figure 3.9. Communities' resistance and DMSPd release. Dose (x-axis) is contrasted with the final $\%F_v'/F_m'$ reached (y-axis). The size of the dots illustrates the difference in the DMSPd/DMSPt ratios before and after the stress treatment. Experiments are identified by labels and coloured by set. The background arrow represents the resistance (R) pattern devised.

The light history of the communities was examined in each environment to contextualize their responses to light-stress. We assumed that similar maximum irradiances to those received in the experiment were present on the preceding days to apply the PAR attenuation coefficient (based on chl *a* concentrations) as described by Morel (1988). The high resistance of MED communities aligned with intense solar radiation conditions at 25 m in the BML during summer ($\sim 248 \text{ W/m}^2$). The similar light histories inferred for the mixed layer in the Antarctica water masses ($\sim 143 \text{ W/m}^2$) and the MEDH superficial waters ($\sim 165 \text{ W/m}^2$) translated in akin intermediate resistance. In contrast, the culturing conditions of ISO accustomed the microalgae to much lower irradiances ($\sim 10 \text{ W/m}^2$) without any UV radiation and prompted high light sensitivity. No consistent pattern was observed between sensitivity and the DMSPd/DMSPt ratios. The largest differences in the ratio, induced by an increase in the DMSPd content were observed in the most resistant communities (MED) and in the medium-range ANT set. Despite differing in resistance levels, ISO and MEDH communities did not exhibited differences in the ratios before and after the stress

treatment. Consequently, divergent $\Delta\text{DMSPd}/\text{DMSPt}$ values were observed despite similar doses and sensitivities within these groups. The consistency of $\text{DMSPd}/\text{DMSPt}$ ratios within experimental sets, highlighted the importance of the community composition for observing DMSP exudation as a response to light-stress events.

This section characterised the stress treatments applied and the consequent phytoplankton response in terms of photosynthetic efficiency and DMSP exudation. We successfully induced differential stress treatments and recorded a various range of responses of communities with different light sensitivity. Two main outcomes were accomplished: (i) The confirmation of light history as the main parameter defining light-stress responses and (ii) the dependence on community composition for observing DMSP exudation after irradiance treatments.

3.2 Microzooplankton grazing on light-stressed and non-stressed phytoplankton

Recap of aims and methodology

The mechanisms underlying selective grazing relate to various elements contributing to the variability within prey assemblages (Hamm et al., 2003; Meunier et al., 2012; Montagnes et al., 2008; Verity, 1991; Weisse et al., 2016). While some biological stressors that result in “weaker” individuals have been investigated for their impact on grazing dynamics (Duffy et al., 2005; Evans & Wilson, 2008), the effects of environmental-derived stress like that caused by solar radiation have received limited attention. Contradictory outcomes compound the uncertainty surrounding the influence of light stress on grazing (De Lange & Lüring, 2003; Strom et al., 2020). This section aims to ascertain whether differential grazing occurs on light-stressed phytoplankton assemblages with respect to non-exposed (control) prey. We designed a set of experiments (named as analyses A; Figure 3.10) to test the third hypothesis of the thesis, which proposed that light-stressed cells would undergo more grazing losses than their healthier counterparts. Two distinct setups were used to examine this inquiry: (1) Natural communities with and without light-induced stress, and (2) manipulated communities where a non-stressed cultured predator (*G. dominans*) was added (Figure 3.10). Experiments were conducted with water collected from the Barcelona Olympic Harbour (MEDH).

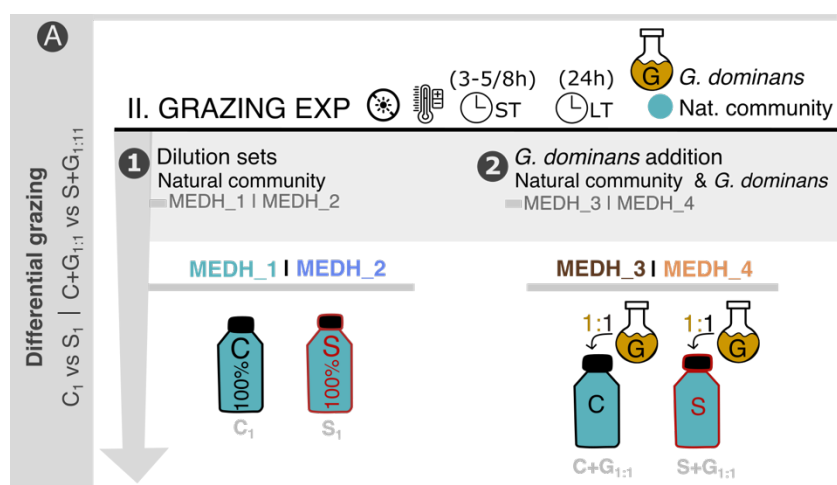


Figure 3.10. Diagram of the set of experiments A. Schematic representation of the two setups (1 and 2) used to test differential grazing between control (C₁ or C+G_{1:1}) and light-stressed (S₁ or S+G_{1:1}) communities. A detailed description of the symbols can be found in the methodology section.

A. DIFFERENTIAL GRAZING (control vs light-stressed communities)

The first analysis compared net growth rates between control and stressed natural communities after the stress treatment. Apart from testing differential grazing with two distinct approaches (dilution sets and *G. dominans* additions), the use of a cultured predator could disclose different patterns between light-exposed (natural predators) and non-exposed (*G. dominans*) grazers. For this analysis, only non-diluted communities (C₁ and S₁) in setup 1 and the bottles with the highest concentration of *G. dominans* (C+G_{1:1} and S+G_{1:1}) in setup 2 (Figure 3.10) were utilised. Additionally, the study examined two temporal scales (short-term, ST, and long-term, LT) to identify the optimal time frame for observing differential grazing on stressed prey.

Short-term (ST) analyses

Photosynthetic efficiency was monitored (data in section 3.3) alongside prey concentration until the end of the recovery phase, which marked the end of the ST study period. Regression analysis of log-transformed cell concentration against time (hours) presented different temporal dynamics of control and stressed phytoplankton in most communities (Figure 3.11).

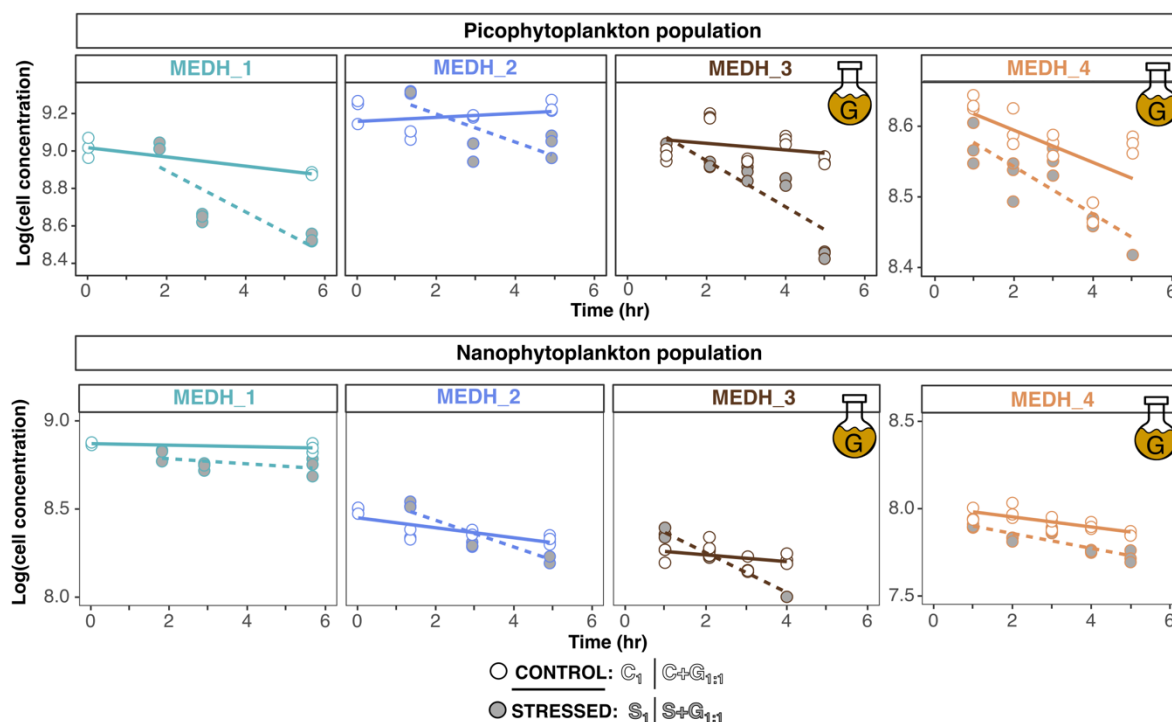


Figure 3.11. Regression analysis of log-transformed cell concentration. Individual linear regressions of control and stressed phytoplankton over time in each experiment. Picophytoplankton and nanophytoplankton populations (as defined by flow cytometry) were analysed separately. MEDH_3 and 4 are the experiments where *G. dominans* (G) was added.

Differences were discernible regarding picophytoplankton concentrations in the regressions of all four communities at late time points. At the end of the incubation, picophytoplankton concentrations in the stressed communities were much lower than in the control ones. The ANCOVA test applied confirmed a significant decrease in concentration in all communities and treatments and significant differences between the net growth rates of control and stressed communities (Figure 3.12, Table S3.3, Supplementary Information). Thus, higher grazing was suggested for light-stressed picophytoplankton assemblages. Differently, nanophytoplankton experienced noticeable concentration diminishment in three (MEDH_2, MEDH_3 and MEDH_4) of the four communities tested, as inferred from the regression dynamics (Figure 3.11) and confirmed by the ANCOVA results (Figure 3.12, Table S3.3, Supplementary Information). No significant consumption was detected in MEDH_1 community regardless of the light exposition. In the rest of nanophytoplankton assemblages, significantly different net growth rates between light-stressed and control treatments were detected in MEDH_2 and MEDH_3 but not in MEDH_4. In the two cases where a difference was detected, light-stressed communities showed a stronger decrease in concentration.

No apparent differences between the patterns of the two approaches (dilution set and *G. dominans* additions) were observed. Surprisingly, the loss rates obtained after the *G. dominans* additions were only higher in the light-stressed community of MEDH_3 (Figure 3.12). Hence, no consistent increase in consumption was detected due to the addition of *G. dominans* by comparison with the natural communities where no extra predator was added.

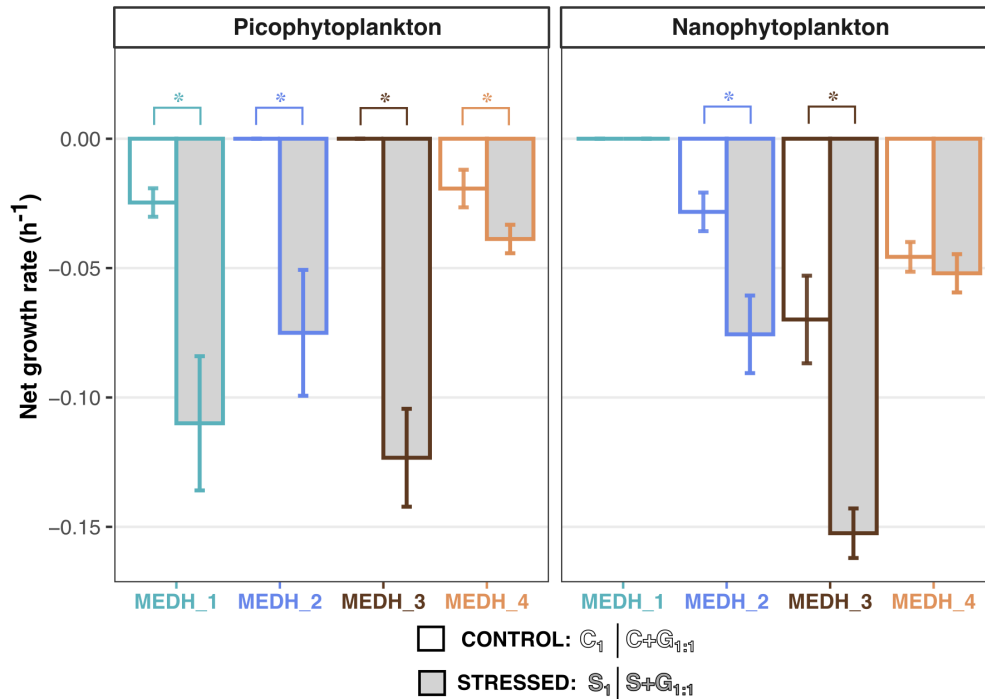


Figure 3.12. Regression slopes and ANCOVA statistical results. The bars represent the slopes of individual linear regressions of phytoplankton loss in the control (white) and light-stressed (grey) communities of each experiment. Non-significant regressions, indicating negligible grazing rates, were not considered and no bar was plotted. ANCOVA-derived significant differences ($p < 0.05$) in the regressions are identified with *. Error bars represent the error of the regressions slope. Pico- and nanophytoplankton loss rates were analysed separately.

Long-term (LT) vs short-term (ST) grazing dynamics

Natural communities (MEDH_1 and 2) were incubated for a total of 24 hours, as done in standard dilution experiments (Landry & Hassett, 1982), to assess the suitability of longer time scales (LT) for capturing differential grazing events (Figure 3.13A).

ST and LT analyses were compared for picophytoplankton because this size range of prey was the one showing significant consumption rates in both communities (MEDH_1 and MEDH_2) (Figure 3.12). In the case of MEDH_2, we also compared total phytoplankton (pico+nano) loss rates. Net growth rates of control and stressed phytoplankton differed notably after 5-6h of incubation but were much more similar after 24 hours experiments in both experiments (Figure 3.13B). Thus, the enhancement of the grazing rate on light-stressed prey observed in ST was notably reduced in LT. These results indicated that the appropriate time scale to look for differential grazing after short-term light-stress is also the short term, within a matter of hours.

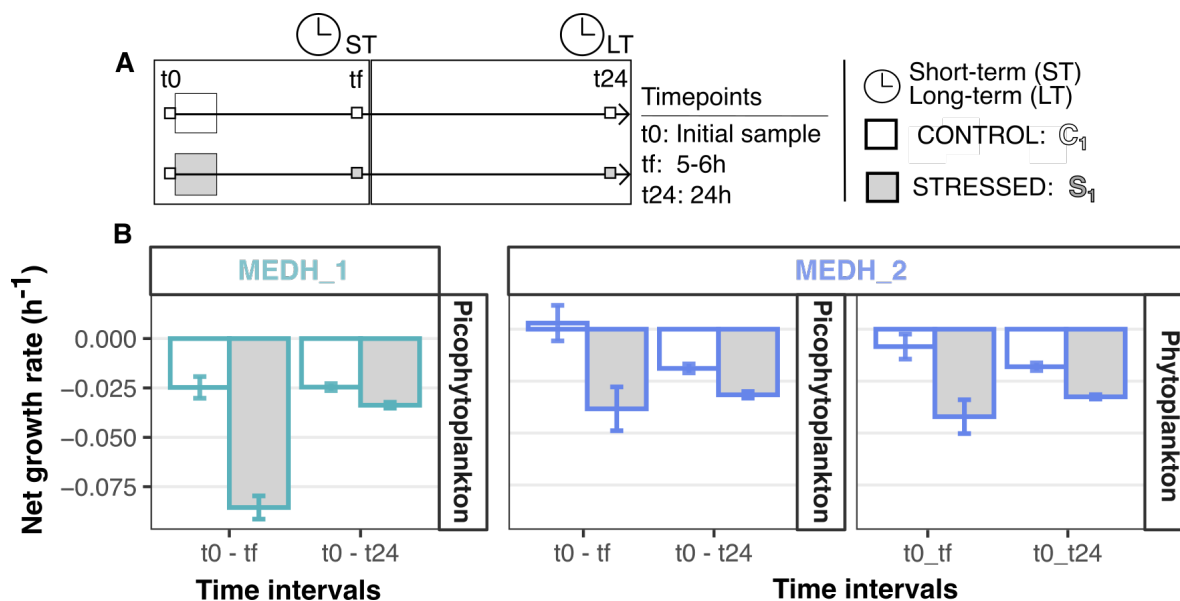


Figure 3.13. Short-term vs long-term net growth rates. (A) Diagram of the temporal incubations and sampling time points in experiments MEDH-1 and 2. (B) Net growth rates at each temporal scale for control (white) and stressed (grey) communities. Error bars represent the propagated error of the measurements.

The main finding of this section was the increased grazing on light-stressed phytoplankton. The consideration of short time frames proved essential for detecting differential grazing after a light-stress event. The day-long incubations used in standard dilution grazing experiments are not adequate to discern this enhanced grazing behaviour. Essentially, the results support the third hypothesis formulated and suggest preferential grazing of microzooplankton on light-stressed phytoplankton.

3.3 Influence of grazing on phytoplankton recovery from light-stress

Recap of aims and methodology

In the previous section we showed that grazing rates are higher on light-stressed phytoplankton assemblages compared to their healthier counterparts. This preferential removal of lower-fitness cells could contribute to the overall increase in population health. This section aimed to evaluate how grazing pressure can influence the phytoplankton photosynthetic recovery from a light-stress event. Specifically, the experiments of analyses B (Figure 3.14) addresses hypothesis 4: *higher grazing pressures would improve phytoplankton recovery from a light-stress event*. Higher grazing rates on stressed cells may speed up the recovery or induce higher fitness levels within a defined timeframe. In line with the temporal patterns observed in the preceding section (3.2), grazing experiments were conducted on short timescales (ST) defined by the duration of the recovery phase. Two experimental sets (MEDH and ANT) from two contrasting oceanic locations were compared in setup 1, and only the MEDH samples were used in setup 2.

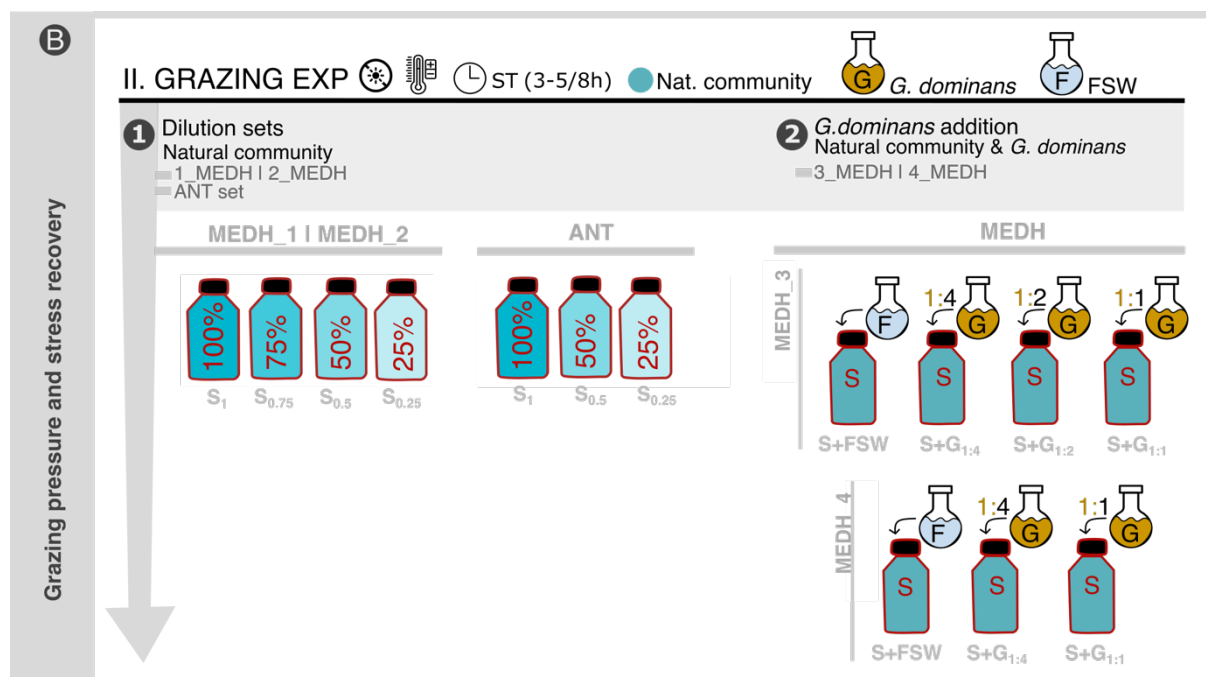


Figure 3.14. Diagram of the grazing experiments of analysis B. Schematic representation of the two setups (1 and 2) used to test the influence of grazing pressure on light-stress recovery. Dilution series were applied to natural communities of the MEDH and ANT sets (setup 1). *G. dominans* (G) addition experiments were only used in MEDH_3 and 4 communities (setup 2). A detailed description of the symbols can be found in the methodology section.

B. EFFECTS OF GRAZING ON RECOVERY FROM STRESS

Grazing pressure

The two setups (dilution experiments and *G. dominans* additions) employed different methods to manipulate grazing pressure. Setup 1 utilised the dilution technique described by Landry & Hassett (1982) in natural communities. This technique reduces grazing pressure by decreasing encounter rates between prey and predators. Setup 2, on the other hand, modulated grazing pressure by adding *G. dominans* as an extra grazer at different concentrations. This second approach isolated the effects of grazing pressure from potential influences of the dilution manipulation on phytoplankton stress and recovery, as dilution itself can impact these processes.

SETUP 1 - Dilution sets. Dilution experiments were used for modulating grazing pressure in natural communities previously stressed by natural sunlight. The setup was optimised to induce different grazing in short time scales; thus, these experiments were not intended to assess daily grazing or growth rates.

In the MEDH_1 and MEDH_2 dilution experiments, log-linear regression fits of the phytoplankton concentrations with time provided net growth rates, inverse of net loss rates (Figure 3.15A). These were calculated separately for nano- and picophytoplankton populations. The results (Table S3.4 Supplementary Information) confirmed a significant decrease in picophytoplankton concentration in both MEDH dilution series. However, no significant net growth rates were detected for nanophytoplankton in MEDH_1 and in the most diluted bottle ($S_{0.25}$) of MEDH_2. The decreasing cell losses with increasing dilution typically observed in dilution experiments after 24h, were not always apparent after only ~5h, which was the end of the recovery phase. The main unexpected results were the notably low loss rates in the 75% dilution ($S_{0.75}$) observed in both experiments.

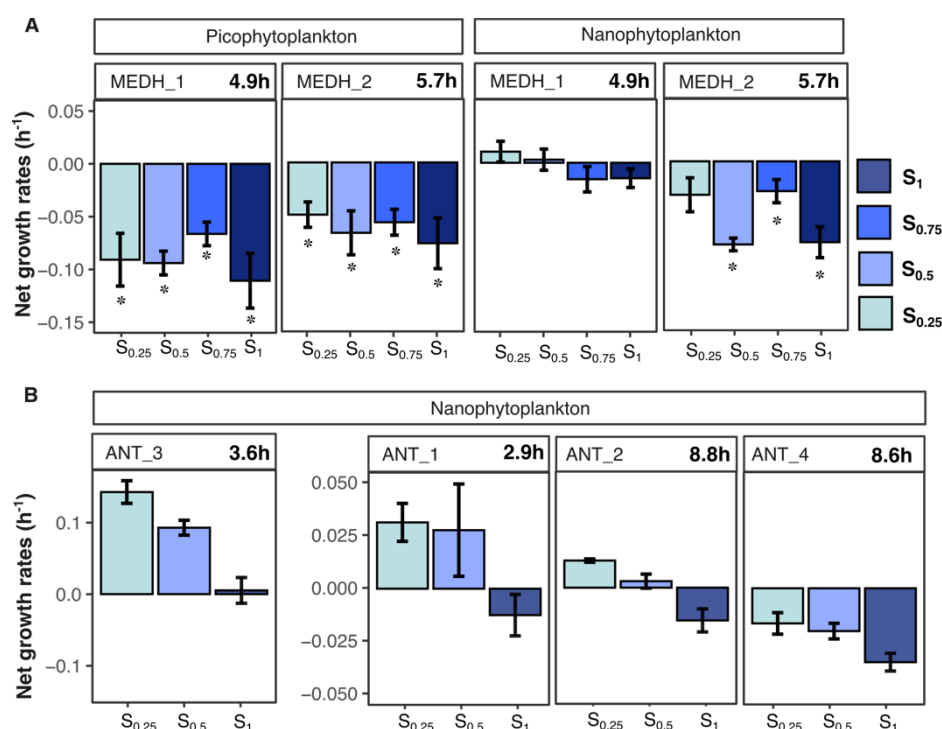


Figure 3.15. Net growth rates of each bottle from dilution series experiments. Net growth rates of each experimental bottle (x-axis) calculated by logarithmic models. The top panel of each plot displays the name and the duration of the experiment. Error bars show the error of the regression. (A). MEDH dilution series. Significant regression slopes ($p < 0.05$) of MEDH_1 and 2 are marked with *. (B). ANT dilution series. No significance could be tested since only two time points were sampled.

The ANT set consisted of four dilution experiments (ANT_1 – ANT_4), each containing only two samples: the initial community and the final point of the recovery phase. Net growth rates were also determined with a logarithmic model with phytoplankton concentrations at the start and end of the recovery period (Figure 3.15B, Table S3.4 Supplementary Information). Due to the different recovery dynamics and the sampling times, the time-frames examined varied between experiments, from 3 to 8h. We focused on the nanophytoplankton assemblage because they clearly dominated in cell concentrations and biomass in all ANT samples. The net growth rates obtained displayed the expected patterns of a dilution series. All four experiments showed higher net loss in the undiluted bottle (S_1) and progressively less loss (or more net growth) in the more diluted treatments ($S_{0.5}$, $S_{0.25}$). Exceptionally high rates were detected in experiment ANT_3, where sampling might have coincided with a phytoplankton duplication event.

Since the dilutions results in the MEDH experiments deviated from the standard patterns, attempts to correlate dilution factors with net growth rates yielded non-significant regressions with inaccurate intercepts. Consequently, the intercept value could not be used in MEDH experiments for correcting net growth rates for the gross growth rate and estimate the grazing rates. Hence, to ensure consistency across all results, growth correction was not applied to the experiments, and differences in net growth rates across dilution factors were taken as indicators of the varying grazing pressures. Hence, the calculated rates (hr^{-1}) are negative when grazing exceeded growth and positive when growth exceeded grazing.

SETUP 2 - *G. dominans* addition experiments. Setup 2 manipulated grazing pressure by adding the cultured predator *G. dominans* to light-exposed and non-exposed natural communities in experiments MEDH_3 and 4. Phytoplankton consumption evaluation began after 1h due to initial inconsistencies. Therefore, short-term grazing rates (net growth rates) were calculated from 1h after the dinoflagellate addition until 4h, when saturation in the recovery phase was assured, by log-linear regression fits of the phytoplankton concentration vs time (Figure 3.16, Table S3.5, Supplementary Information). The rates were calculated separately for the nano- and picophytoplankton populations. Significant decrease of both populations was observed (Table S2.5 Supplementary Information).

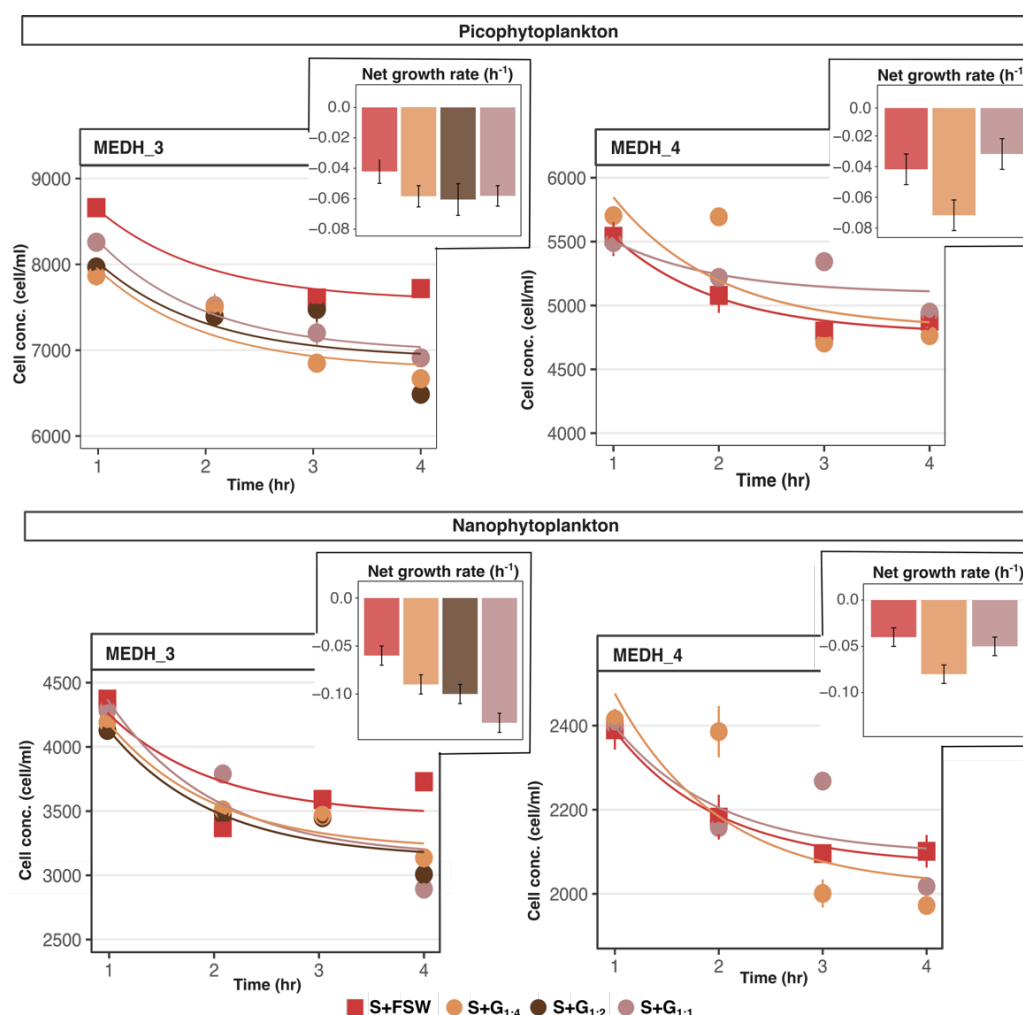
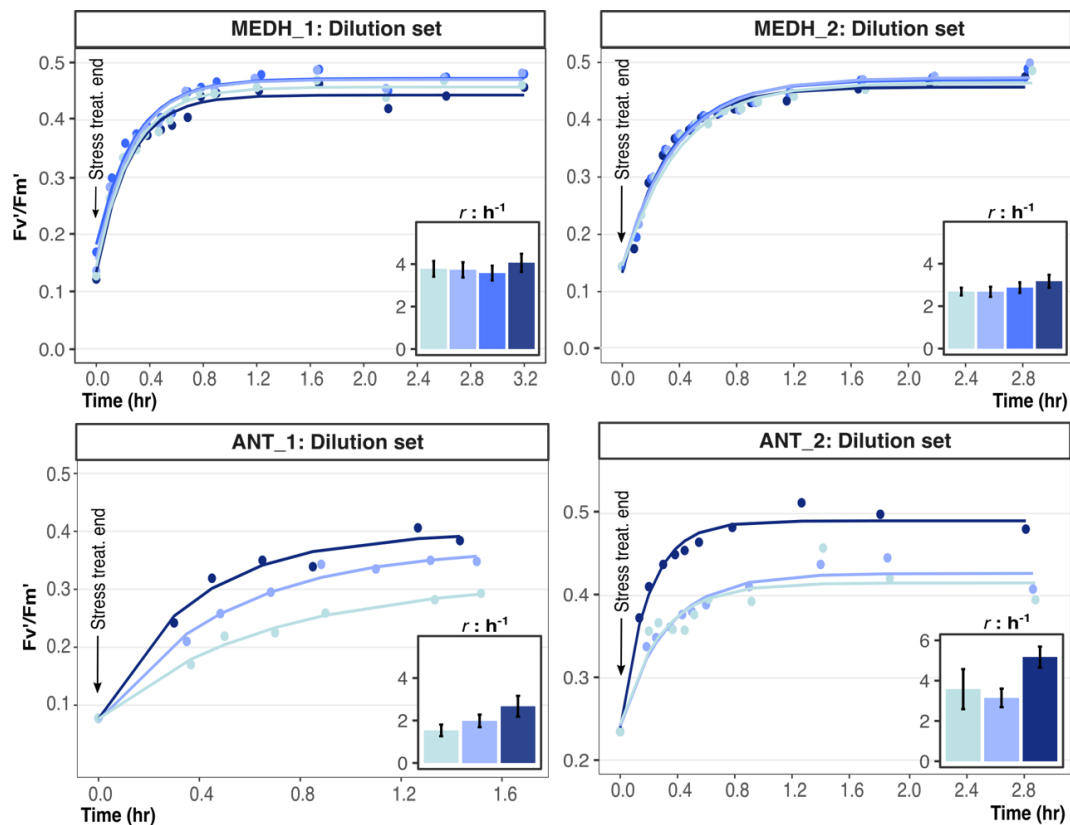


Figure 3.16. Regression analysis of phytoplankton consumption. Log-linear regressions were applied to each bottle for *G. dominans* addition experiments (MEDH_3 and MEDH_4). Picophytoplankton and nanophytoplankton populations were analysed separately. The slopes of the regressions representing the net growth rates of each experimental bottle are illustrated as bars in the small subplots. Errors bars represent the error of the regression slope. All the regressions were significant ($p < 0.05$).

The addition of *G. dominans* to MEDH_3 resulted in a significant decrease of both picophytoplankton and nanophytoplankton compared to controls with only natural predators (S+FSW), where grazing occurred at lower rates (Table S3.5 Supplementary Information). While progressive consumption throughout the experiment was observed in the bottles with *G. dominans*, natural grazers caused a quick decrease in cell concentration within 2 hours followed by an increase towards the end. As expected, for nanophytoplankton, decreasing *G. dominans* proportions resulted in decreasing net loss rates. In contrast, picophytoplankton rates were similar across boosted bottles. Experiment MEDH_4 rendered surprising results (Figure 3.16). The highest consumption for both prey size classes occurred with the lowest *G. dominans* addition (S+G_{1:4}). This treatment showed a delayed but sharp decline in picophytoplankton concentration at 3 hours, followed by stabilization. The highest *G. dominans* proportion (S+G_{1:1}) displayed minimal overall consumption throughout the experiment, leading to net growth rates undistinguishable from those with only natural grazers. Nanophytoplankton mirrored the picophytoplankton dynamics, with the highest consumption occurring with the lower *G. dominans* addition (Figure 3.16, Table S3.5 Supplementary Information).

Photosynthetic efficiency recovery

In both setups, grazing was monitored along with photosynthetic efficiency recovery after the light-stress treatment. The recovery phase concluded when the photosynthetic efficiency reached saturation. The temporal series of F_v'/F_m' values were fitted an exponential sigmoidal function (Montero et al., 2002) and two parameters were obtained: the value of the upper asymptote, referred to as the saturation level (p), and the time constant reported as the recovery rate constant r (h^{-1}). The fits were applied to each bottle and compared within experiments (Figure 3.17). Significant fits in all bottles and experiments confirmed the suitability of the method to represent the data (Table S3.6, Supplementary Information). The analysis of the recovery dynamics in *G. dominans* addition experiments (MEDH_3 and 4) started 10 minutes later than in the dilution experiments to set the initial point after the grazer addition (Figure 3.17).



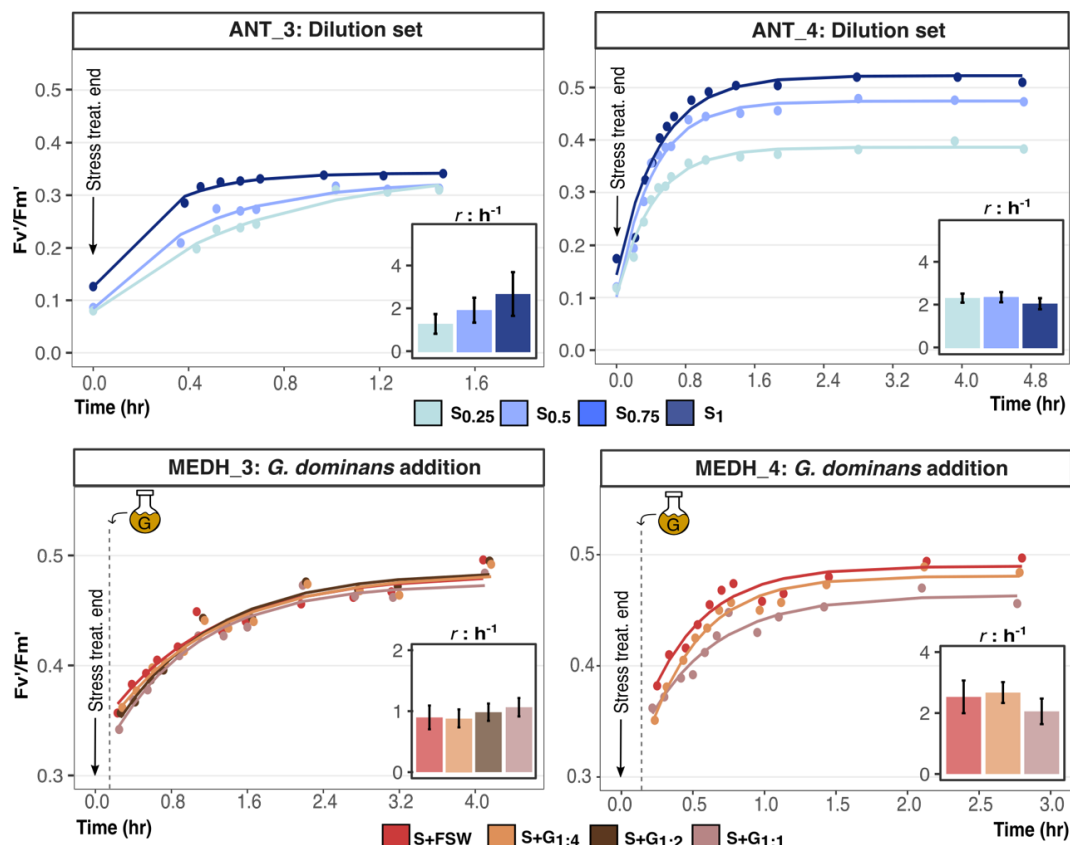


Figure 3.17. Immediate photosynthetic efficiency (F_v/F_m') recovery. Temporal series of F_v/F_m' values illustrating the recovery dynamics. The fitted sigmoidal curve is represented over the monitored data. The specific recovery rate constants (r) of each bottle are presented as bars within the small subplots and identified with the colour code.

Dynamics differed between experimental setups and environments. Comparison within experiments revealed the ANT dilution series and the *G. dominans* additions as the setups with greater differences between treatments. MEDH dilutions did not show a clear influence on recovery dynamics, and patterns could not be inferred from the temporal series. However, subtle variations between the recovery rate constants of the undiluted bottle and the diluted ones were observed in both experiments (Figure 3.17).

Recovery rate constants (r) and saturation values (p) were contrasted between experiments using bottles S_1 and S+FSW. These bottles represent the intrinsic recovery properties of the phytoplankton assemblages with neither dilution (S_1) nor additional grazing pressure (S+FSW) (Figure 3.18). The recovery rates were similar among untreated bottles of different communities, with slightly faster recovery observed in MEDH communities compared to the ANT ones. However, two outliers stood out from the general pattern due to particularly high (ANT_2) and low (MEDH_3) recovery rate constants (Figure 3.18A). Saturation values were normalised by calculating the percentage of similarity to the value of the unstressed communities before light exposure (% F_v/F_m'). Whereas similar percentages were obtained in the MEDH, the ANT communities showed again greater variability with values spanning from 92 to 141% (Figure 3.18B). Values exceeding 100% indicate communities that were able to recover to higher efficiencies than the ones presented originally. Overall, high percentages (>89%) confirmed the observation of substantial recoveries that enabled phytoplankton assemblages to overcome the light stress applied. The highest percentages, observed with the ANT assemblages, might arise from the lower initial values of F_v/F_m' before exposure to high light.

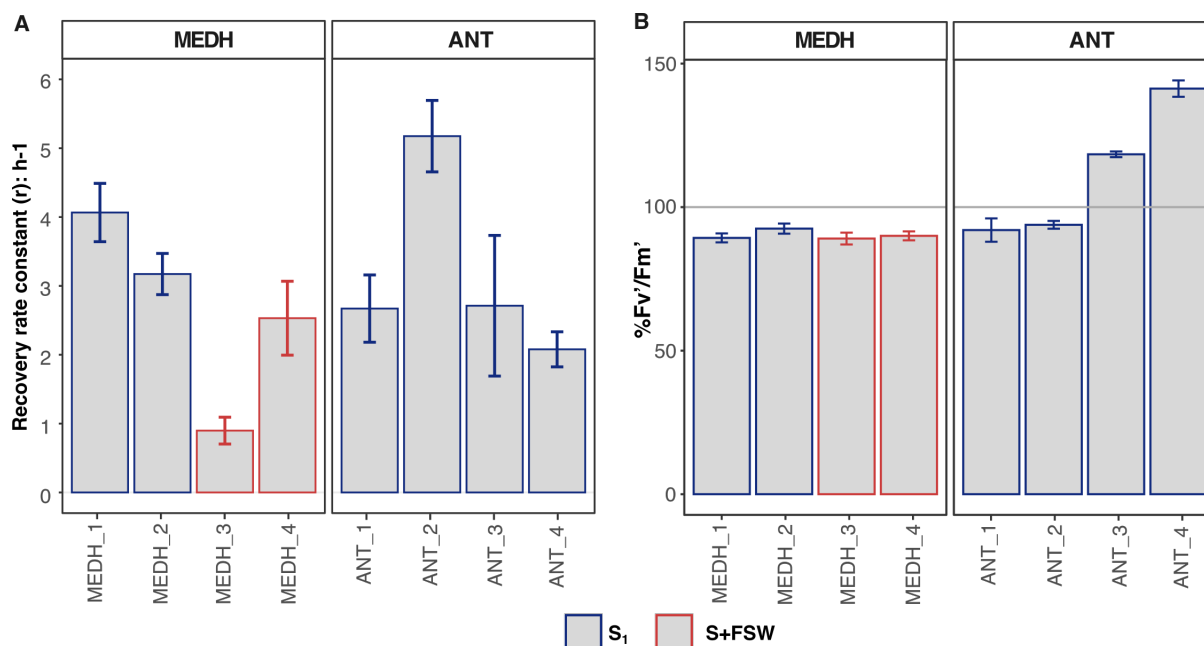


Figure 3.18. Recovery rate constants and saturation values of the immediate photosynthetic efficiency (F_v'/F_m'). (A). Recovery rate constants (r) in h^{-1} . (B) Saturation levels reached at the end of the recovery, as percentage of the initial values before exposure to high light. Non-treated bottles of each experiment are illustrated in blue (S_1) and in red (S+FSW) if FSW was added (to mimic *G. dominans* addition experiments). Error bars represent the standard error of the sigmoidal equation function fit.

Grazing pressure vs photosynthetic efficiency recovery

The relationship between grazing pressure and photosynthetic recovery was investigated by plotting recovery rate constants against net growth rates. Initially, relationship patterns were examined within each experiment using separate figures (Figure 3.19). Recovery rate constants were negatively related to net growth rates (so, positively related to grazing) of picophytoplankton in MEDH dilution experiments (MEDH_1 and MEDH_2). This faster recovery with faster grazing was also observed with nanophytoplankton in MEDH_2. Conversely, nanophytoplankton in MEDH_1 did not show significant recovery; note, however, that this was the experiment where grazing on nanophytoplankton was not significant either (Fig. 3.13). For the ANT dilution experiments, only nanophytoplankton was considered due to their dominance in cell concentration and biomass. Three of the experiments (ANT_1 to ANT_3) showed higher recovery rate constants with lower net growth rates (i.e., higher grazing), while the opposite was observed in ANT_4.

Similar to the dilution series, most of the *G. dominans* addition bottles in experiments MEDH_3 and 4 displayed a positive correlation between grazing pressure and photosynthetic efficiency recovery (Figure 3.19). However, some specific observations were noteworthy. In MEDH_3, picophytoplankton net growth rates with *G. dominans* additions grouped together and positioned apart from the S+FSW bottle regardless of their recovery rates. In contrast, nanophytoplankton net growth rates aligned well with recovery rates, indicating higher grazing and recovery with higher *G. dominans* additions. In MEDH_4, recovery rates presented a positive relationship to grazing rates for picophytoplankton. The highest rates were obtained in the bottle with the lowest *G. dominans* concentration followed by the one with only natural grazers. Also, with nanophytoplankton, the highest grazing and recovery rates were observed with the lowest *G. dominans* addition, while the other two bottles did not show clear differences in any of the two metrics.

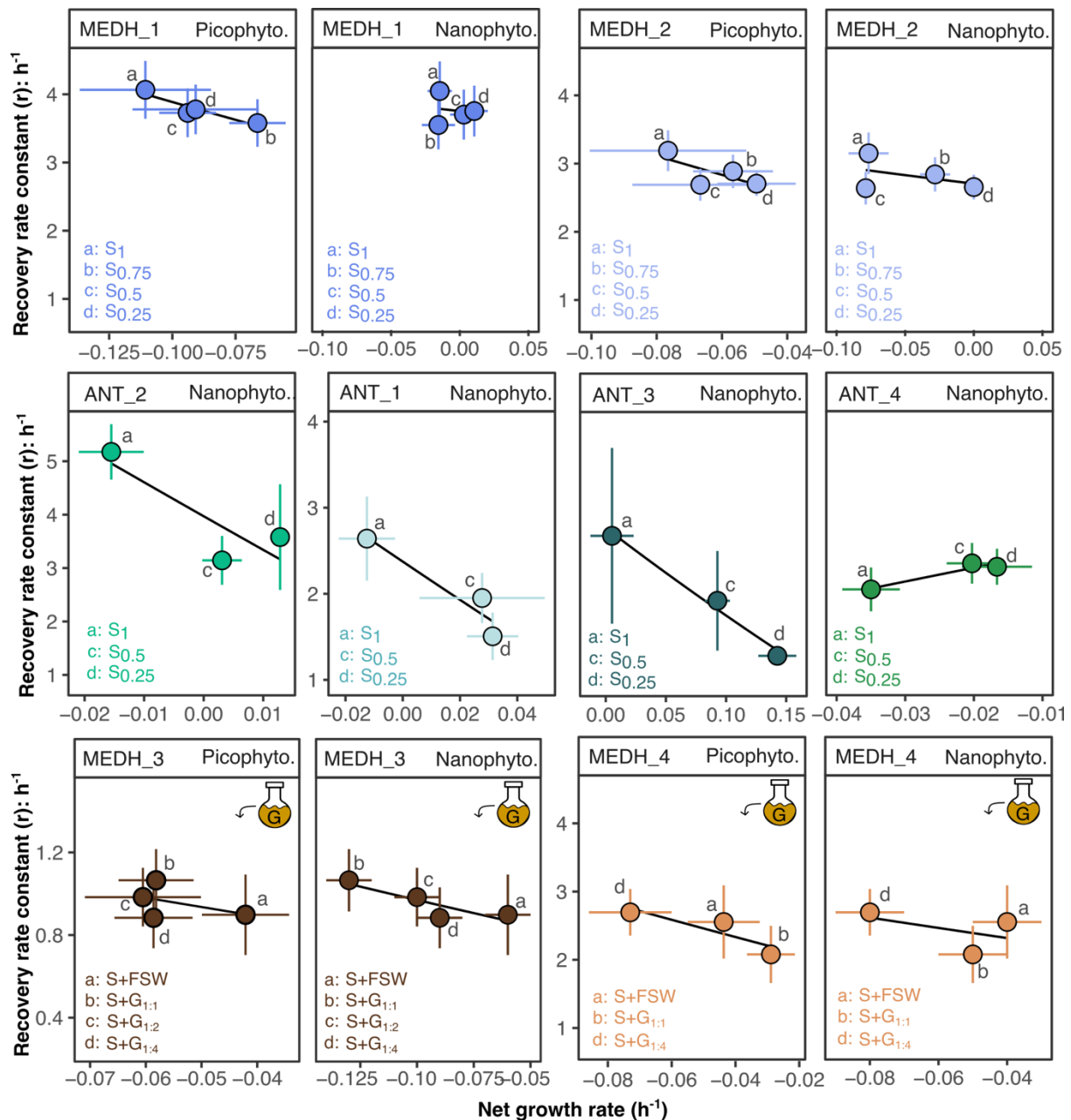


Figure 3.19. Grazing pressure vs photosynthetic recovery. Dot plots relating recovery rate constants (y-axis) with net growth rates (x-axis). The bottles of each experiment are plotted together and represented with individual dots. Model I regression analysis was fit into the data and represented by a straight line. Notice the change in the y-axis in the MEDH_3 and ANT_2 experiments. The top panel of each plot displays the name of the experiment and the phytoplankton population considered in the net growth rates. (Picophyto. = Picophytoplankton, Nanophyto. = Nanophytoplankton).

We then combined all experiments into a single plot exploring the relationship between grazing pressure and photosynthetic efficiency recovery. Since the F_v'/F_m' measurements correspond to the total phytoplankton assemblage, and cannot be told apart for pico- and nanophytoplankton, the net growth rate of only one of the two size-based populations could be represented from each experiment. The decision was made based on three criteria: (i) dominance in terms of estimated biomass, (ii) significant consumption, and (iii) differential grazing between control and stressed cells. Since nanophytoplankton was the clear dominating size population in terms of biomass in all environments it was the default option if the other two conditions were met. Therefore, picophytoplankton was chosen only for two experiments (MEDH_1 and MEDH_4). No significant consumption of nanophytoplankton

was observed in the bottles of MEDH_1 (Figure 3.15) and differential grazing between control and stressed cells was only detected for picophytoplankton (Figure 3.12). In MEDH_4, nanophytoplankton were significantly grazed, but higher grazing on stressed cells was only detected with picophytoplankton (Figure 3.12).

The combined analysis showed a bulk common pattern with two outliers. (Figure 3.20A). Notably, ANT_2 and MEDH_3 emerged from the general pattern due to very high and very low recovery rates, respectively, already evident in Figure 3.18A. MEDH dilutions (1 and 2) showed the highest grazing and recovery rates, and the ANT dilutions 1, 3 and 4 showed the lowest rates. When all experiments were put together, excluding the two outliers, a remarkable 66% of the recovery of the photosynthetic efficiency of phytoplankton was explained by grazing (Figure 3.20B).

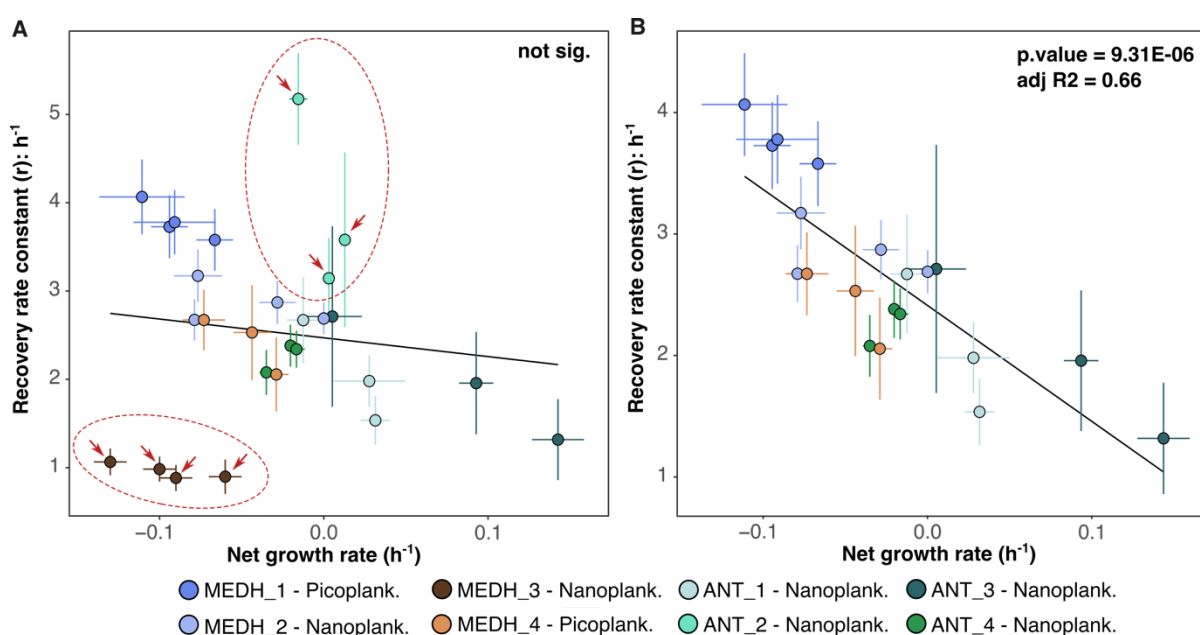


Figure 3.20. Grazing pressure vs photosynthetic recovery. Recovery rate constants of F_v/F_m' (y-axis) related to net growth rates of the chosen phytoplankton population (x-axis). The bottles of all experiments are represented in the left plot with the two outliers marked with a dashed red circle and arrows pointing to each of the bottles. The same plot without the two outlier experiments is on the right. Model I regression analysis was fit to the data and represented by a straight line. The goodness of fit (adj. R2) and the significance of the regression (p.value) are stated within each plot.

To explore potential confounding factors that might lead to the relationship between recovery rate constants and net growth rates, the recovery rates were plotted against all available variables. None of the ancillary measurements of the samples (T, chl_a, initial cell concentration, and initial photosynthetic efficiency F_v/F_m') showed a significant relationship with recovery rates. Similarly, no significant regressions were obtained between recovery rates and the other photosynthetic efficiency metrics registered: F_v/F_m' at the end of the stress treatment and at the end of the recovery phase, the duration of the recovery phase.

As final remarks of this section, the exponential sigmoidal equation effectively analysed the recovery dynamics, providing two key metrics: the recovery rate constant and the saturation level reached. The use of cultured predators alongside natural communities offers a promising approach to modify grazing pressure without relying only on dilution methods. The comparison of the recovery rate constants with parallel net growth rates obtained through two different methods (dilution series and *G. dominans* additions) suggests a positive association between grazing pressure and phytoplankton recovery dynamics. Together, these results provided the first evidence that preferential grazing could help improve the health of a stressed phytoplankton assemblage. Overall, the results confirm microzooplankton grazing as a worthy candidate to be explored within the context of the healthy-herds dynamics hypothesis.

3.4 The relationship of light stress and grazing in a model system: *G. dominans* grazing on *I. galbana*

Aims and methodology recap

Laboratory experiments based on mono-specific cultures are widely used to evaluate grazing interactions and their connection to environmental drivers (Weisse et al., 2016). In this study, we used a simplified food web system comprising a heterotrophic dinoflagellate commonly found in natural assemblages (*G. dominans*), feeding on a prymnesiophyte microalga with high intracellular content of DMSP (*I. galbana*). We conducted three experiments to complement our studies with natural communities, thereby, testing both the third and fourth hypotheses through experimental sets of analyses A and B (Figure 3.21). The stress treatment applied to the prey culture is described in section 3.1. Grazing differences were assessed by feeding the dinoflagellate with either non-exposed (control) or light-stressed *I. galbana* (C+G vs S+G) (A). Simultaneously, photosynthetic efficiency recovery was measured in the stressed treatments with grazing and the ones where only the prey was present (S vs S+G) (B). The experiments were conducted on short time scales (ST).

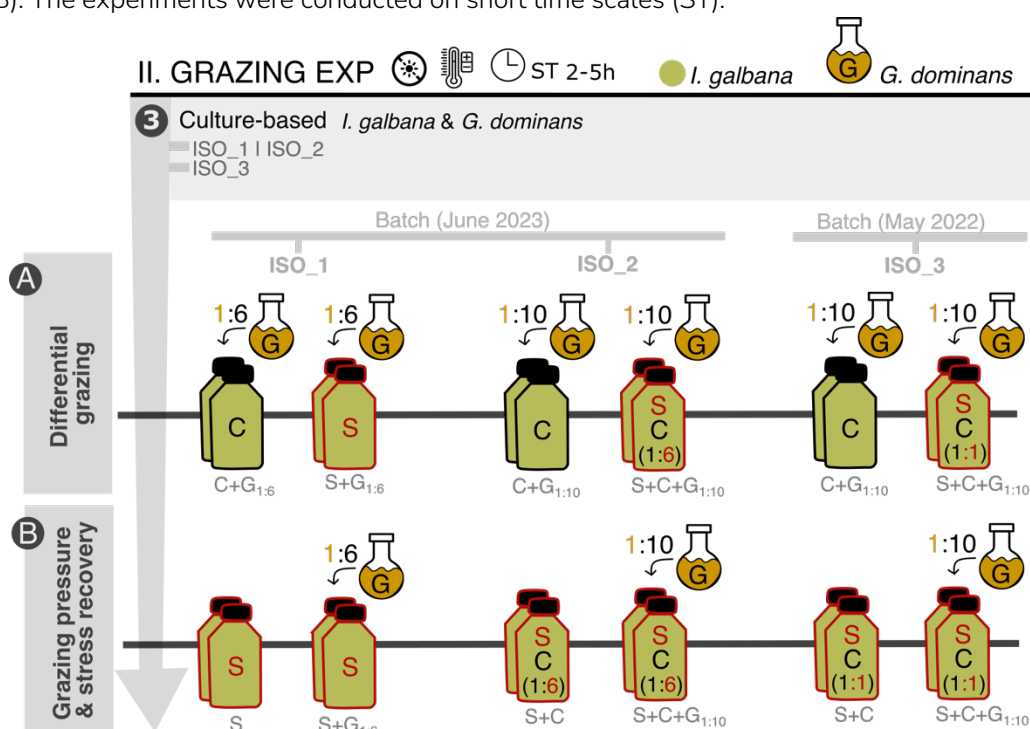


Figure 3.21. Section 3.4 diagram. Schematic representation of setup 3 used in experimental sets A and B. The experiments were performed with two distinct culture batches grown one year apart. Grazing tests were applied with either non-saturating (1:6) or saturating (1:10) prey concentrations. The composition of the stressed bottle varied between the three experiments with different proportions of control and stressed prey cells: ISO_1 contained only stressed *I. galbana*, ISO_2 had a 1:6 proportion of control and stressed prey cells, and ISO_3 contained equal proportions (1:1). A detailed description of the symbols can be found in the methodology section.

A. DIFFERENTIAL GRAZING (control vs light-stressed communities)

Regressions of log-transformed cell concentrations of prey vs time were used to calculate the net loss rates in each bottle (Figure 3.22). The bottles without grazer (S, S+C or C in Figure 3.21) showed no significant growth or death of *I. galbana*; therefore, the net loss rate of prey was considered the grazing rate. Additionally, the percentage of the initial population consumed by *G. dominans* at different incubation time points was quantified (Figure 3.22 and 3.23). *G. dominans* exhibited higher feeding

rates on control bottles (C+G) than on stressed *I. galbana* (S+G or S+C+G), resulting in higher consumption percentages within 5h in the control bottles of two (ISO_1 and 2) of the three experiments (Figure 3.22). Although all the experiments assessed the grazing impact of *G. dominans* on either control or stressed *I. galbana*, they differed in the proportion of stressed prey in the stressed bottle and in the prey concentrations used. The influence of these setup parameters was noticeable in the regression results.

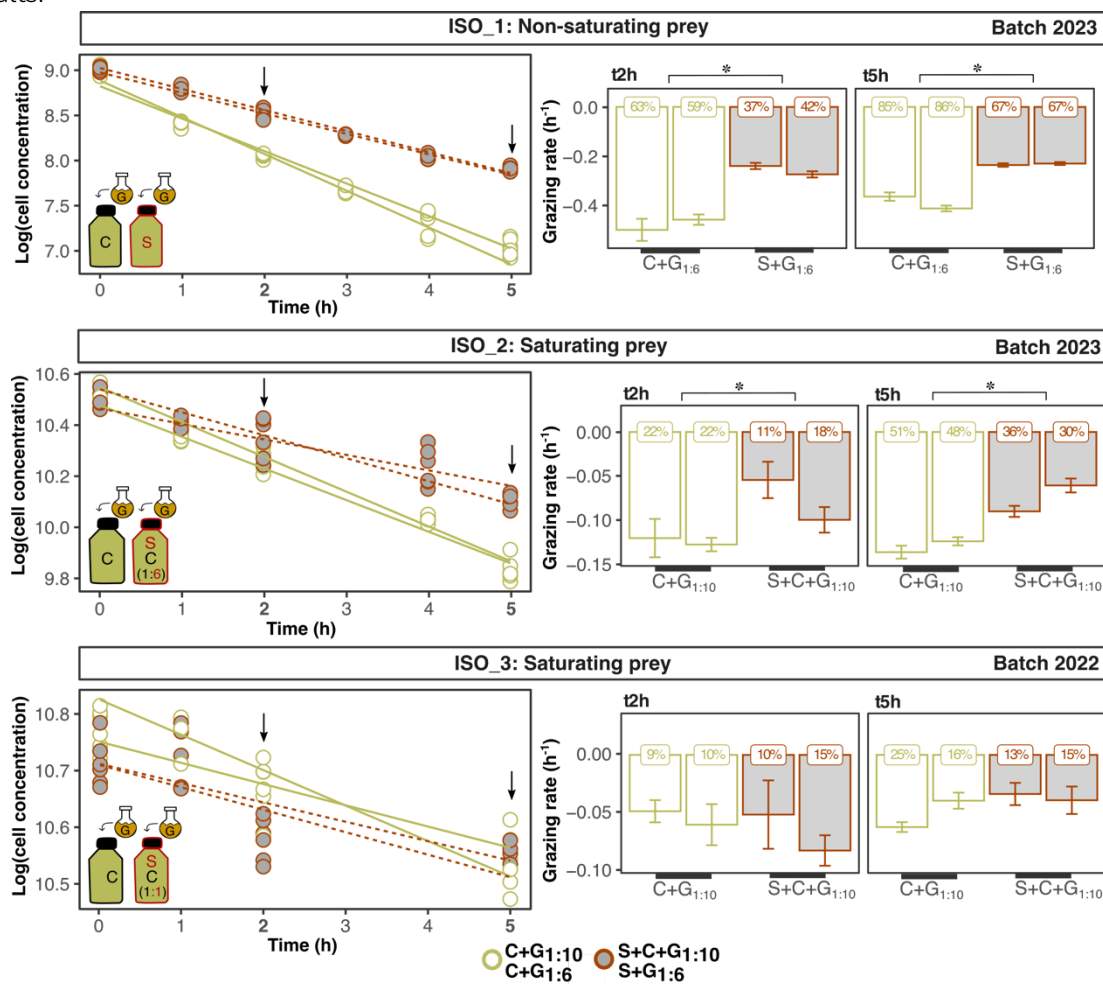


Figure 3.22. Regression analysis of *I. galbana* consumption by *G. dominans*. Left panels display the individual linear regressions applied to log-transformed cell concentration data (y-axis) over time for each replicate. Black arrows localize the time points analysed in detail in the right panels. Bars on the right panels represent the regression slopes of each replicate and bottle between t0 and the indicated time point (t2h and t5h). The percentage of the initial prey that has been consumed is reported as labels within each bar. Significant differences ($p < 0.05$) between the slopes of control (C+G) and stressed bottles (S+G or S+C+G) evaluated with the ANCOVA test are marked with *. C=control prey, S=stressed prey, G= grazer (*G. dominans*).

In ISO_1, the stressed bottle contained 100% of sunlight-treated *I. galbana* and differences in the grazing rates were apparent from the first hour. After 5 hours, the percentage of consumed prey clearly differed between control and stressed prey (86% in C+G and 67% in S+G, respectively) (Figure 3.22 Table S3.9 Supplementary Information). The mix of control and stressed prey (1:6, respectively) used in experiment ISO_2 could have delayed the observation of different rates between C+G and S+C+G bottles. Differences were minor after 2h (22% in C+G vs 11-18% in S+C+G). After 4h, the pattern mirrored that of the ISO_1 experiment, with preferential consumption of the control population. By the end of the incubation, significant differences between grazing rates were evident, with a 51-48% consumption of control *I. galbana* compared to a 36-30% consumption of the stressed variant (Figure 3.22, Table S3.9 Supplementary Information). Equal proportions of control and stressed prey were

added to the stressed bottle in ISO_3. This experiment showed much lower total consumption (20-14%) in both bottles at the end of the incubation (Figure 3.22). Higher variability between replicates was also observed. Although a slightly higher rate was obtained in control *I. galbana* at 5h, differences were not significant (Table S3.9 Supplementary Information).

Unexpectedly, grazing rates were higher at non-saturating prey concentrations (ISO_1); than at saturating prey concentrations (ISO_2 and 3) (Figure 3.22). Although both experiments ISO_2 and 3 were prepared with saturating prey conditions, the lower consumption rates observed in ISO_3 might respond to the different cultures batches of *G. dominans* and *I. galbana* used.

B. EFFECTS OF GRAZING ON RECOVERY FROM STRESS

Grazing pressure

According to the results of the analyses A (Fig. 3.22), grazing rates varied among experiments in the order ISO_1 > ISO_2 > ISO_3, and showed immediate (ISO_1), delayed (ISO_2) and no grazing preference (ISO_3) on the control prey. The temporal evolution of the percentages consumed in the stressed bottles (Figure 3.23) allowed inferences about the grazing on the stressed prey. In ISO_1, the high consumption of prey (67%) occurred entirely on stressed *I. galbana*, as this was the only available prey. In ISO_2, which contained 86% of stressed and 14% of control *I. galbana*, the consumption of 33% of the total prey indicates that, despite the preference for control prey, a minimum of 19% of the stressed cells were consumed in the longer term. In ISO_3, which contained 50% of stressed and control cells, the low consumption (14%) of total prey and the preference for control cells suggests low grazing on stressed *I. galbana*.

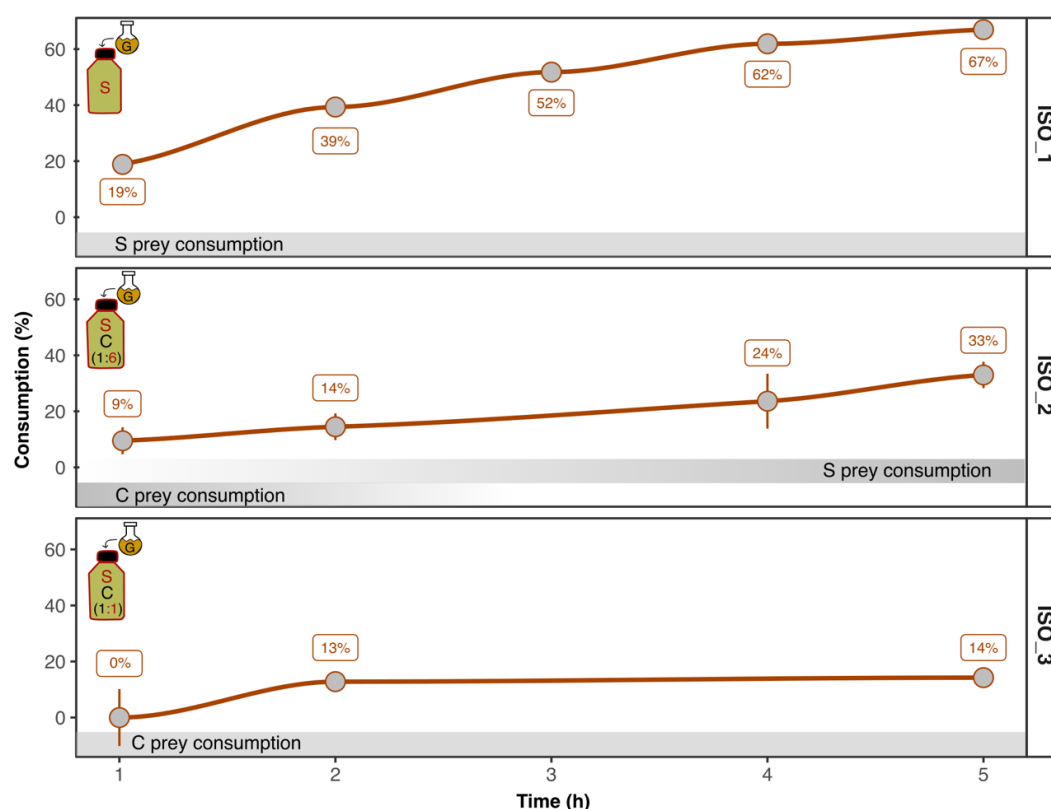


Figure 3.23. Temporal evolution of the percentage consumed from the initial prey population in the bottles containing stressed *I. galbana* and the grazer *G. dominans*. The percentages consumed are illustrated as grey dots and specified with the labels on top of them. The grey bands describe the assumed consumption of the control and stressed prey throughout the incubation, considering preference for control prey. Initial proportions of control and stressed prey in each bottle are displayed in the bottle diagram within each plot. C=control prey, S=stressed prey, G= *G. dominans*.

Photosynthetic efficiency recovery

After the sunlight-stress treatment and the addition of the *G. dominans*, grazing and photosynthetic efficiency recovery were measured simultaneously. The fit of the exponential sigmoidal function (Montero et al., 2002) on the F_v'/F_m' temporal series (Figure 3.24) provided two parameters describing the recovery dynamics: the upper asymptote value referred to as the saturation level (p), and the recovery rate constant r (h^{-1}) (Table S3.10, Supplementary Information). For comparison purposes, the saturation level was expressed as the percentage similarity ($\%F_v'/F_m'$) to the F_v'/F_m' of *I. galbana* before the stress treatment. The results indicated that recovery occurred in all experiments to $>64\%$ of the initial photosynthetic efficiency (Figure 3.24). The highest percentages of recovery were observed in ISO_3, the experiment with the lowest grazing rates, with no notable differences between the saturation level of *I. galbana* alone (S) and that in the presence of *G. dominans* (S+G) (Figure 3.24C). The recovery rate constants were slightly higher in the bottles with *G. dominans* (S+G). In ISO_1 and ISO_2 (Figure 3.24A,B), the percentages of recovery were higher without grazer (S). Conversely, the recovery rate constants were higher with the presence of *G. dominans* (S+G) (Figure 3.24A,B insets).

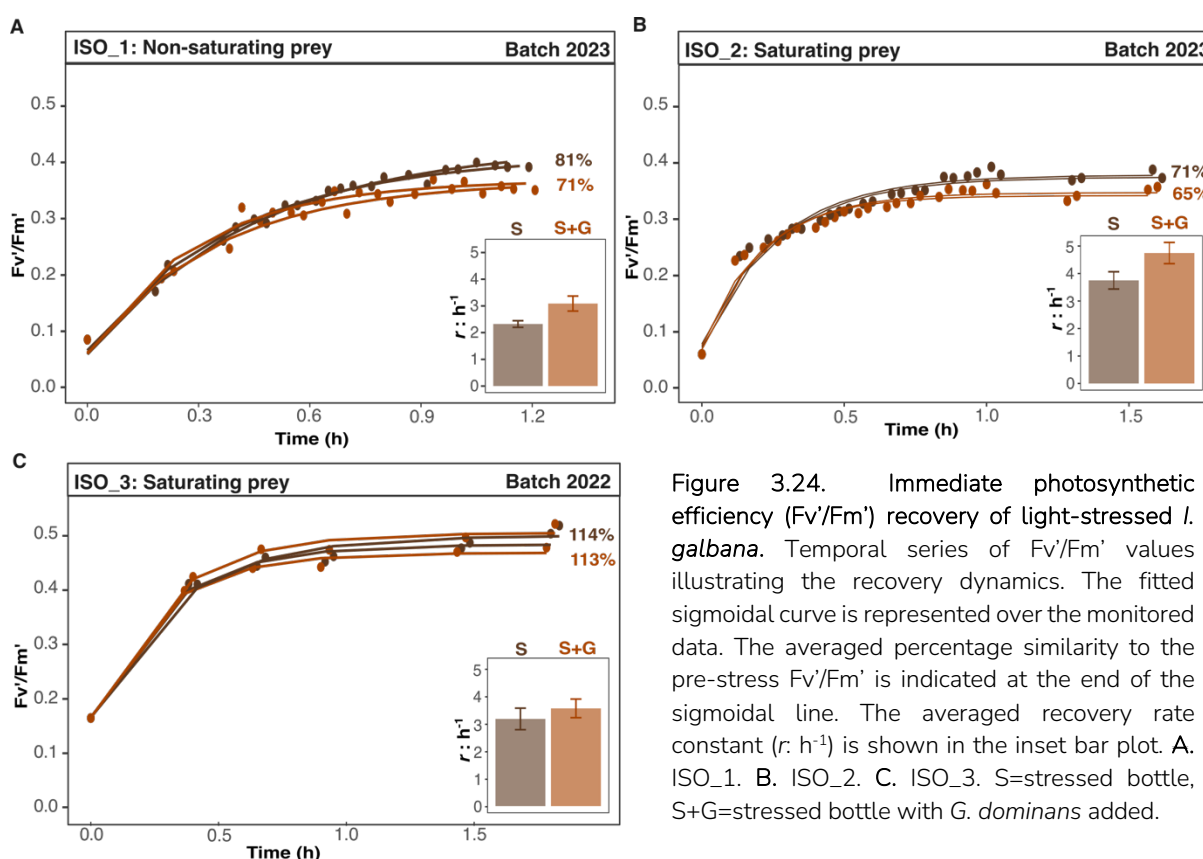


Figure 3.24. Immediate photosynthetic efficiency (F_v'/F_m') recovery of light-stressed *I. galbana*. Temporal series of F_v'/F_m' values illustrating the recovery dynamics. The fitted sigmoidal curve is represented over the monitored data. The averaged percentage similarity to the pre-stress F_v'/F_m' is indicated at the end of the sigmoidal line. The averaged recovery rate constant (r : h^{-1}) is shown in the inset bar plot. A. ISO_1. B. ISO_2. C. ISO_3. S=stressed bottle, S+G=stressed bottle with *G. dominans* added.

Photosynthetic efficiency recovery vs grazing rate

In all experiments, the presence of grazing (S+G bottles) coincided with higher rate constants of recovery from stress than those in grazing-devoid bottles (S) (Figure 3.25A). In contrast, the saturation level of the photosynthetic efficiency decreased in the presence of grazing in experiments ISO_1 and 2 (Figure 3.25B).

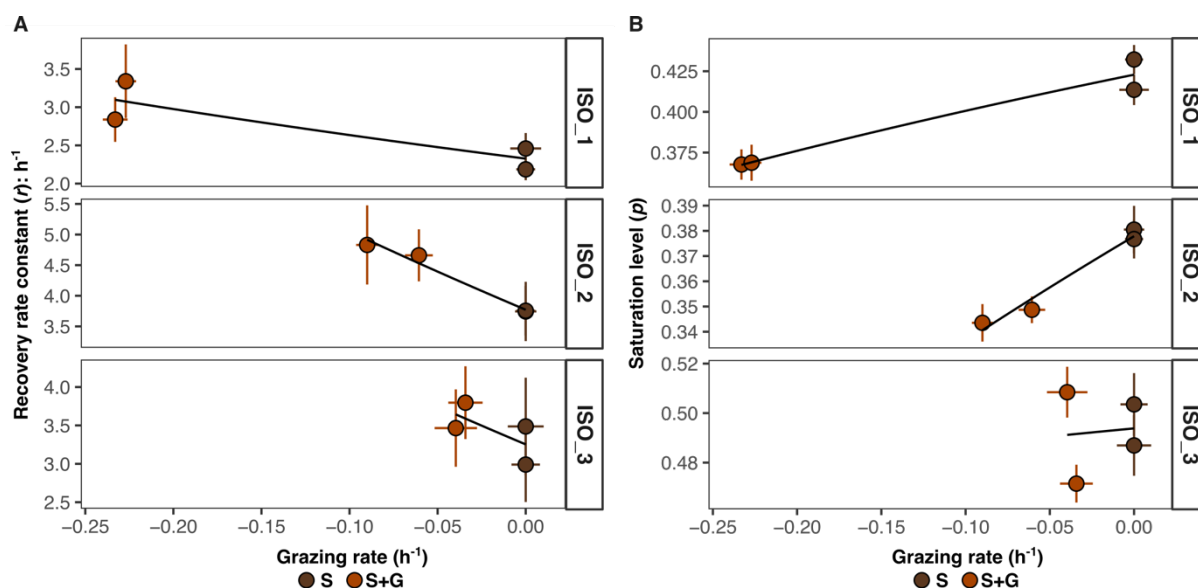


Figure 3.25. Photosynthetic efficiency recovery vs grazing rates of *G. dominans* on *I. galbana*. (A) Recovery rate constants (y-axis) related to grazing rates (x-axis). (B) Saturation levels reached at the end of the recovery phase (y-axis) related to grazing rates (x-axis). Model I regression analysis was fit into the data and represented by a straight line. Replicate bottles are presented individually with the same colour code. S=stressed bottle, S+G=stressed bottle with *G. dominans* added.

Given that the experimental setup included bottles with (S+G) and without (S) predator, isolation of the grazing-induced recovery from the intrinsic phytoplankton recovery from stress was possible by subtracting rate constants in S from those in S+G bottles. The resulting grazing-induced recovery was higher in ISO_2 (0.99 h^{-1}) followed by ISO_1 (0.77 h^{-1}) and much lower in ISO_3 (0.39 h^{-1}). Thus, the higher induced recoveries were observed in the two experiments with larger consumption rates of stressed prey.

This section documents *G. dominans* preference for control (not exposed to high-light) *I. galbana* cells over its light-stressed variant. Higher grazing rates on control prey populations were observed in two out of three experiments. However, stressed *I. galbana* was still consumed at significant rates. Grazing rates were also affected by prey concentration and the batch of the cultures used. Although lower grazing rates were observed on stressed prey, grazing still enhanced recovery rates when compared to incubations with only *I. galbana* (Figure 3.25A). Nonetheless, *I. galbana* reached higher F_v'/F_m' values at the end of the recovery when no grazers were present (Figure 3.25B).

DISCUSSION

In this chapter we delve into the impact of high solar irradiances on inducing light-stress in phytoplankton assemblages and how this stress influences microzooplankton grazing. Firstly, we evaluated the phytoplankton response to light-stress by assessing photosynthetic efficiency and DMSP exudation. Secondly, we examine preferential grazing on high-light exposed and non-exposed assemblages in both natural communities and a model system based on cultured species. The observation of differential grazing patterns between stressed and non-exposed phytoplankton allowed the simultaneous examination of how grazing pressure can influence the recovery of the photosynthetic efficiency of the entire community.

Light-stress events: phytoplankton responses and DMSP exudation

Upwelling events, cloud clearing, or vertical mixing in the water column can generate short periods of intense light exposure (light-stress) for oceanic microbial communities (Strom et al., 2020). Phytoplankton responses to light stress depend on two main factors: the intensity of light they receive and the composition of the community. The light-stress phase of our experiments revealed a spectrum of resistance and sensitivity among different communities in response to light-stress events (Figure 3.9). These responses were primarily driven by the previous light exposure of the community or population, because the stress levels reached (in terms of photosynthetic efficiency) were more consistent with the approximated light history of the assemblages rather than with the solar radiation dose received during the treatment. The metrics utilised (F_v'/F_m') describe the immediate photophysiological state of the cells, which is known to be shaped by both the light history of the community and the current exposure (Harrison et al., 2015). Photoacclimation and adaptation are key population traits that optimize the photochemistry pathway and regulate phytoplankton photophysiology. Acclimation traits include diverse mechanisms related to the photosynthetic units and the xanthophyll cycle (Demmig-Adams, 1990; Suggett et al., 2007). Hence, community responses will be closely related to the dominant phytoplankton species and their traits (Harrison et al., 2015). Generally, while robust photophysiology (lower sensitivity to light stress) is anticipated in communities from environments with high irradiances, poor acclimation and thus higher sensitivity to light stress is inferred for lower light habitats (Harrison et al., 2015).

In our experiments, the highest sensitivity to high light was observed in the cultured microalga *I. galbana*, which was grown in low light without UV radiation. This reflects the importance of the previous light history (Harrison et al., 2015) and the limitations of using lab-adapted species (Anderson et al., 2011; Li et al., 2013; Meunier et al., 2012; Weisse et al., 2016 and references therein). Moreover, the methodology used to measure light-stress dynamics may have also influenced the contrasting responses of natural phytoplankton assemblages and *I. galbana*. We assessed the impairment in the fitness of phytoplankton by monitoring the immediate photosynthetic efficiency (F_v'/F_m'), acknowledging that other photophysiological traits may respond differently (Archer et al., 2018; Cooney et al., 2019; Hessen et al., 1997; Sobrino et al., 2014). In natural communities, F_v'/F_m' reflects the combined photosynthetic efficiency of all members. Hence, the diverse sensitivities of the assemblage components result in a gradual F_v'/F_m' decline under high light exposure. Conversely, the *I. galbana* monoculture exhibited a sharp drop in photosynthetic efficiency that reflects its high sensitivity consistent with findings from other studies on prymnesiophyte cultures (Strom et al., 2020).

We also investigated the hypothesised increase in DMSP release under light-stress. Previous studies suggested the release of dissolved organic matter (DOM) as a response to various stressors such as high irradiance conditions and unbalanced growth (Cherrier et al., 2015; Fuentes-Lema et al., 2015; Livanou et al., 2017; Thornton, 2014). However, inconclusive results have been reported on the up-regulation of DMSP synthesis and exudation across microalgal species and assemblages in response to

high irradiances (Archer et al., 2010, 2018; Darroch et al., 2015). The variety of responses have been seen dependent on cells' previous light-history and the duration and intensity of the exposure (Archer et al., 2010, 2018; Darroch et al., 2015; Galindo et al., 2016; Slezak & Herndl, 2003; Stefels et al., 2007; Thornton, 2014). The accumulation of DOM (and DMSP) in the phycosphere translates the stress response from the individual cell to the surrounding microenvironment, where the chemo-attractor role of DMSP for herbivore protists (Seymour et al., 2010) can affect trophic interactions. Our results, illustrated in Figure 3.8, confirmed higher bulk (in filtered seawater, not in the phycosphere) dissolved DMSP (DMSPd) concentrations after the light-stress treatments in the two open-ocean communities sampled (ANT, MED). In the experiments with MEDH samples and ISO cultures, conversely, the high variability in the data hindered the observation of significant differences. The proportion of dissolved to total DMSP (DMSPd/DMSPt), which is a proxy of DMSP exudation, did not correlate with the irradiance doses or the decrease in photosynthetic efficiency across experimental settings (Figure 3.9), suggesting that phytoplankton assemblage composition was the likely major driver of DMSP exudation patterns (McParland & Levine, 2019). The consistency between DMSPd/DMSPt ratios within each set of experiments reinforces the previous suggestion. Additionally, the small-volume drip filtration method for the measurement of DMSPd is really sensitive to any perturbation, and excess clogging of the filter due to high cell concentration in ISO and MEDH samples could have contributed to data variability. Interestingly, despite similar initial DMSPd concentrations, different communities exhibited distinct DMSPd/DMSPt ratios. The highest ratios were found in the two open-ocean communities (ANT and MED). This finding might be related to the fitness of the photosynthetic community. The photosynthetic efficiency of these two communities was generally lower than the efficiencies recorded in the MEDH communities and in the ISO cultures (Figure 3.4, Table 3.1). The reduced fitness (inferred from the lower photosynthetic efficiencies) may suggest the presence of stressors, such as nutrient limitations (Gorbunov et al., 2020; Gorbunov & Falkowski, 2022) in the oligotrophic MED environments, or environmental factors like temperatures close to the freezing point (Kennedy et al., 2012) and continuous high irradiances (Gorbunov & Falkowski, 2022) in ANT locations (Table 3.1). These stressors might have induced the larger DMSPd/DMSPt ratios observed by enhancing DMSP release. Although the increased DMSPd concentrations measured after a light-stress event in MED and ANT communities would confirm hypothesis 1, the absence of significant differences in MEDH and ISO assemblages hinders the confirmation of a generalised pattern.

Light stress and grazing interactions

The characterization of solar radiation doses and phytoplankton responses to light-stress events was taken one step further by assessing their implications in grazing interactions. Light stress can trigger various changes in phytoplankton, including alterations in chemical composition, physiology, and morphology (Archer et al., 2010; Cooney et al., 2019; Hessen et al., 1997; Rijstenbil, 2002; Stefels & van Leeuwe, 1998; Strom et al., 2020; Thornton, 2014). These changes can be detected by herbivorous protists and make them modify their predation behaviour, potentially influencing food web dynamics. Current literature, mainly based on laboratory cultures, presents conflicting evidence for light-stress as a promoter or inhibitor of grazing (De Lange & Lüring, 2003; Fields et al., 2011; Ochs, 1997; Strom et al., 2020). Studies using natural assemblages are required to gain a more comprehensive understanding of food web responses (Abrams, 2022; Sommaruga, 2003; Weisse et al., 2016). Here, we investigated the hypothesis that light-stressed phytoplankton experience higher grazing pressure using three experimental setups:

- Model system with cultured strains (single prey, single predator)
- Natural communities
- Natural communities supplemented with a cultured grazer

Our results endorsed the hypothesis in natural communities but not in the *I. galbana* culture, where healthy cells experienced higher consumption by *G. dominans*. This highlights the limitations of single-

species model systems for capturing the diversity of behaviours present in natural communities (De Lange & Lüring, 2003; Strom et al., 2020). A previous study with light-stressed *I. galbana* did not find any differential grazing with the dinoflagellate *Amphidinium longum* as a predator (Strom et al., 2020). In our hands, significant differences in *I. galbana* consumption were detected in two of the three experiments (Figure 3.22). ISO_3, conducted with a different batch and an equal proportion of healthy and stressed cells in the stress treatment, did not show any differential grazing. Notably, although *G. dominans* preferred the ingestion of healthier prey, consumption of stressed *I. galbana* also occurred in ISO_1 and ISO_2 as consumption of total prey exceeded the percentage of healthy cells present (Figure 3.23).

With natural communities, where a large variety of individual responses are expected, we observed a repetitive behaviour of higher grazing on light-stressed phytoplankton assemblages (Figure 3.12). Selective predation against individuals with poor fitness is a long-held established phenomenon in terrestrial ecology and predation systems of vertebrate populations (Genovart et al., 2010; Slobodkin, 1974; Temple, 1987). In aquatic systems, preferential grazing over diseased prey is supported with theoretical and experimental-based studies on predator-host-parasite systems (Duffy et al., 2005; Fields et al., 2011; Hall et al., 2005; Lopez et al., 2023; Ostfeld & Holt, 2004; Packer et al., 2003; Park et al., 2021). However, some studies challenge this model by emphasizing host heterogeneity (Gutierrez et al., 2022; Williams, 2008). In light of the ongoing debate and the limited research on natural communities, our study significantly provides data on potential mechanisms of preferential grazing on stressed individuals. The connection of our hypotheses 2 and 3, postulate DMSP exudation as a candidate for linking light stress and increased grazing. Chemical attraction has been already implicated in selective predation by dinoflagellates on parasite-infected (Park et al., 2021) and virus-infected phytoplankton (Evans et al., 2007; Evans & Wilson, 2008). DMSP-containing phycospheres would increase prey-predator encounter rates, due to the expanded range of detection of the prey and reduced searching times triggered by the DMSP chemoattractant role (Breckels et al., 2011; Seymour et al., 2010). Additionally, DMSP presence could also induce a faster selection by increasing prey palatability and reducing the handling time. However, our approach was based on measuring bulk net growth rates to estimate prey consumption. This methodology has important limitations since it only captures the final stages of predation and integrate selection behaviours (Montagnes et al., 2008) as well as trophic cascading effects across the community (Calbet & Saiz, 2013). Thus, we can only propose potential mechanisms to explain the preference for stressed or healthy prey. While increased DMSPd was confirmed in ANT samples, neither MEDH nor ISO experiments showed significant light-induced DMSP exudation. The lower grazing towards stressed *I. galbana* might respond to the low increase in DMSPd that failed to outweigh other less-appealing traits induced by the stress. Physiological changes in phytoplankton prey induced by stressful conditions can impair chemosensory behaviour and species-specific grazing relationships (Strom et al., 2020). The preferential accumulation of ciliates towards physiologically healthy populations of *I. galbana* (and other phytoplankton species) was not maintained when aged and non-growing cultures were used (Verity, 1988). Additionally, dense *O. marina* cultures were only obtained when feeding on fresh, healthy *I. galbana* assemblages (Martel, 2006). These results suggest that stressed/senescent *I. galbana* might not be an ideal prey. The high data variability of DMSPd in MEDH experiments masked any potential exudation process and prevents establishing a relationship between DMSP exudation and increased grazing on stressed communities.

While light stress triggering DMSP exudation might induce increased grazing pressure, the complexity of the surrounding chemical environment needs to be considered (Kuhlisch et al., 2024). Other compounds, released due to the stress or generated outside the cell within the phycosphere, could also play a role in enhancing grazing. DMS stands out as a worthy candidate as it is released by phytoplankton exposure to high irradiances (Galí et al., 2013). Additionally, its involvement in a wide range of chemotactic-driven grazing interactions (Cunningham et al., 2008; Kowalewsky et al., 2006; Nevitt, 2008; Pohnert et al., 2007; Seymour et al., 2010), parasite activation processes (Garcés et al.,

2013), and its role as a trigger of general grazing (Shemi et al., 2021) suggest it as an additional potential link between stress and grazing interactions. The confirmation of microzooplankton preference for stressed cells, also when cultured *G. dominans* was added to natural communities, aligned with the high chemotactic attraction of dinoflagellates, and particularly *G. dominans*, to DMSP and to a lesser extent to DMS (Chapter 1: Güell-Bujons et al., submitted).

The timeframe for observing differential grazing is crucial (Montagnes et al., 2008; Weisse et al., 2016). Our short time (<9h) experiments, limited by the end of the photosynthetic efficiency recovery, efficiently captured chemotaxis-related responses. Standard 24-hour dilution experiments can overlook these effects due to their duration. As light stress triggers the fast exudation of DMSP and other potential chemical cues, and diffusion subsequently blurs the created gradients, short-term observations are essential to capture differential grazing effects. Indeed, consumption observations after 24 h rendered similar grazing rates on control and light-stressed phytoplankton assemblages, while differential grazing was only observed in the short term (Figure 3.13).

Besides the chemical alteration of the phycosphere, other phytoplankton responses to UV and high-light stress events can shape grazing interactions. Increased cell volume (Fields et al., 2011; Hessen et al., 1997), changes in morphology and palatability (Strom et al., 2020; van Donk & Hessen, 1995), and modification of the swimming behaviour (Hessen et al., 1997) are all documented consequences of exposure to high irradiance, and are potentially connected to selective grazing patterns (Strom et al., 2020). In our culture experiments, we assessed the cell volume and swimming behaviour of *I. galbana* in control and stressed populations. Coulter Counter measurements revealed only a 3% decrease in cell volume in ISO_3 after the stress treatment. No differences were observed in the other two experiments. Visual microscopic inspection revealed no apparent change in the swimming of stressed cells. Minimizing or monitoring the aforementioned factors that might be involved in selective grazing is quite more complex in natural communities. Thus, a detailed characterization of the stressed assemblage (e.g., biochemical composition, membrane permeability, metatranscriptomics or metabolomic signatures) would be extremely helpful in future experiments of this kind.

When the grazers were part of the initial community (no grazer addition), they were exposed to high light the same way as the phytoplankton prey; therefore, potential light-stress could also alter the behaviour of the grazers and induce changes in the ingestion and growth of both heterotrophic and mixotrophic protists (Duarte Ferreira et al., 2021; Jakobsen et al., 2000; Li et al., 2000; Moeller et al., 2019; Strom et al., 2020). To overcome this, we did not only examine the grazing effects on light-exposed whole communities but also added a cultured grazer that was not subjected to the light-stress event. Both approaches gave similar results of preferential grazing on light-stressed phytoplankton (Figure 3.12).

The setup used in all grazing experiments with natural communities targeted microzooplankton predation and excluded higher trophic levels by using a prefiltration through 100-200 μm . In marine microbial communities, mesozooplankton predate on micro-herbivores, having an indirect but substantial role in the microzooplankton grazing budget (Calbet, 2008; Calbet & Landry, 1999; Calbet & Saiz, 2013). Also, alternative prey of other trophic levels (e.g., bacteria), which we did not consider with our measurements, could have impacted the grazing dynamics we observed (Abrams, 2022). Therefore, cascade effects triggered by manipulations of microzooplankton grazing, and the effects of light stress across the entire microbial food web require consideration and further investigation (Sommaruga, 2003).

Finally, decreases in phytoplankton concentration due to direct lethal effects of high (UV-including) irradiances could have contributed to the lower net growth rates (higher net loss rates) in the stressed treatments. However, we were as cautious as possible in designing the light exposure events to not cause massive death. The fast and close to complete recovery observed in all our experiments suggest that direct prey loss from stress was not a major confounding factor.

Grazing influence on phytoplankton recovery from light-stress

Increased grazing pressure on light-stressed phytoplankton suggests a hitherto overlooked factor influencing herbivore feeding strategies. Preferential removal of weaker individuals would enhance the recovery of the prey community from stress, thereby improving the overall health of the communities (Laundon et al., 2021). In ecology, this phenomenon is described in the healthy herds hypothesis (Genovart et al., 2010; Packer et al., 2003). We applied high irradiance treatments to exert photophysiological stress in phytoplankton, and induced different grazing pressures to observe how grazing influenced photosynthetic efficiency recovery. Our goal was to isolate the effect of grazing by minimizing any other potential factors that may influence photosynthetic recovery, such as nutrient availability or light intensity. We altered the grazing pressure using three methods: dilution series, addition of *G. dominans* into natural communities, and culture-based prey-predator experiments. Nutrients were added to all bottles with nutrient-limited communities (MEDH), and light was dimmed during the recovery phase. In both sets of dilution experiments (MEDH and ANT), we observed variations in grazing pressures (Figure 3.15). However, unexpected results arose in the MEDH experiments, where net growth rates did not align with dilution factors. Shorter than recommended incubation times (5h), trophic cascades (Calbet & Saiz, 2013), mixotrophy (Duarte Ferreira et al., 2021), low grazing rates due to saturation conditions (Schmoker et al., 2013), non-proportional changes in grazers concentrations (Dolan, & McKeon, 2005), and potential nonlinear grazing interactions (Sandhu et al., 2019) could have caused the irregular results. For instance, the high phytoplankton abundances found in the MEDH experiments and the occurrence of nanoplankton blooms in previous days might have set saturating conditions that interfered with the grazing patterns. No discussion about daily grazing or growth rates was intended due to the short-time incubations and the absence of replicates. Consequently, the focus was centred only on modifying grazing pressure within experiments, no matter if they resulted in the expected quantitative order.

G. dominans addition experiments were an alternative to dilution series to successfully modify the grazing pressure. We started the consumption time series one hour after the addition of the grazer to overcome potential interferences of *G. dominans* with the trophic interactions existing in the community and to allow for *G. dominans* to become accustomed to the new conditions and start grazing (Abrams, 2022). After a time lag, progressive prey consumption led to higher grazing rates in bottles with *G. dominans* additions of the two experiments (Figure 3.16). The different proportions of added grazer served also to test the optimal conditions for boosting grazing in the communities (Supplementary Information). While in the MEDH_3 experiment higher grazing rates were observed in all boosted bottles compared to the unamended ones, in MEDH_4 this only happened with the lower proportion of *G. dominans*; larger grazer additions resulted in lower grazing, indistinguishable from that in the unamended bottles. Allelopathic interactions among *G. dominans* individuals or between the added dinoflagellates and the natural predators could have been the reasons behind reduced predation with high grazer addition (Weisse et al., 2016).

The different grazing rates observed in the three experiments with *I. galbana* and *G. dominans* likely resulted from differences in the experimental setup, either the proportion between predator and prey or the use of a different culture batch. Non-saturating prey concentrations in ISO_1 induced the highest grazing rates in both treatments (Figure 3.22). Lower grazing rates were unexpectedly reported with saturation prey concentrations in ISO_2 (Figure 3.22). *G. dominans* feeding behaviour was anticipated as a type II Holling functional response, characterised by an initial rise in ingestion rates with increasing

prey density, followed by a deceleration as it approaches the saturation point (Calbet et al., 2013). However, the lower grazing rates with high prey density ($4E+04$ cells/ml) resembled the occurrence of predator confusion due to swarming effects (Jeschke & Tollrian, 2005), resulting in non-monotonic responses (Abrams, 2022). Consumption of stressed *I. galbana* was estimated in ISO_1 and ISO_2 as the consumption of total prey exceeded the percentage of healthy cells present (Figure 3.23). The remarkably low prey consumption in ISO_3 could be related to the culture batches used. This highlights the importance of intraspecific responses, strain variability, past growth conditions, or physiological state, for this type of experiments (Weisse et al., 2016 and references therein). The low prey consumption and the high proportion of control prey in the stress bottle point out to minimal grazing pressure over the stressed prey. As a result, non-significant differences in grazing between the two treatments were observed.

Upon relieve of the stress force by light dimming, the observed recovery confirmed the ability of the communities to overcome the stress treatment (Figure 3.17). This recovery refers only to the immediate photosynthetic efficiency, acknowledging that the response of other photophysiological traits may differ. The comparison between the undiluted bottles of dilution series and the S+FSW incubations in *G. dominans* addition experiments, provided information on the intrinsic recovery capacity of each community (Figure 3.18). Unexpected similarities between the intrinsic recovery of communities from contrasting environments were observed. MEDH_3 and ANT_2 stood out with notably low and high recovery rate constants. The different recovery dynamics observed in these two experiments probably reflected the intrinsic recovery capacities of the phytoplankton assemblages, in turn related to the dominant photophysiology mechanisms and strategies to respond to high irradiances (Demmig-Adams, 1990; Suggett et al., 2007). The largest recovery percentages (>100%) of photosynthetic efficiency accomplished in the ANT samples could be related to the high irradiances already present in the natural environment (results section 3.1). The intense solar radiations characterizing the light-history of ANT communities might contribute to the low photosynthetic efficiency measured in the original seawater. Therefore, the sunlight dimming we applied in the recovery phase allowed the recovery of the photosynthetic efficiency to levels higher than those in the natural conditions.

Results from the three experimental setups (dilutions, grazer additions, and model systems) revealed a relationship between grazing rate and stress recovery rate, with more grazing leading to faster photosynthetic efficiency recovery as proposed in hypothesis 4 (Figure 3.19). Obviously, the photosynthetic efficiency of a phytoplankton assemblage, as measured by the F_v/F_m' , is mostly dependent on the population with the predominant biomass. Therefore, to examine how improved recovery is connected to higher grazing rate, the target population should also experience significant consumption, particularly of its stressed cells. Thus, for each experiment, the target phytoplankton population to sensibly compare grazing and recovery must be the one for which most of the conditions concur: dominant biomass, significant grazing regressions, and differential grazing between control and stressed cells. Choosing the right cytometric populations, positive correlations between grazing and recovery were repeatedly observed within most experiments individually (Figure 3.19). Notably, the pattern persisted and even strengthened when most experiments with natural phytoplankton assemblages were analysed together (Figure 3.20).

The general pattern is maintained if we add also the experiments with the model system (Figure 3.26). As it comes to the X axis, we should keep in mind that while actual grazing rates were reported for *G. dominans* feeding on *I. galbana*, in natural communities grazing is reported as net growth rates. Since the actual grazing rates in natural communities must be higher than net growth rates, the observed correlation can only improve. Even though correlation does not mean causation, the observation of this pattern across most experiments conducted with three different setups and communities provides strong support to the suggested positive influence of grazing in phytoplankton recovery from stress.

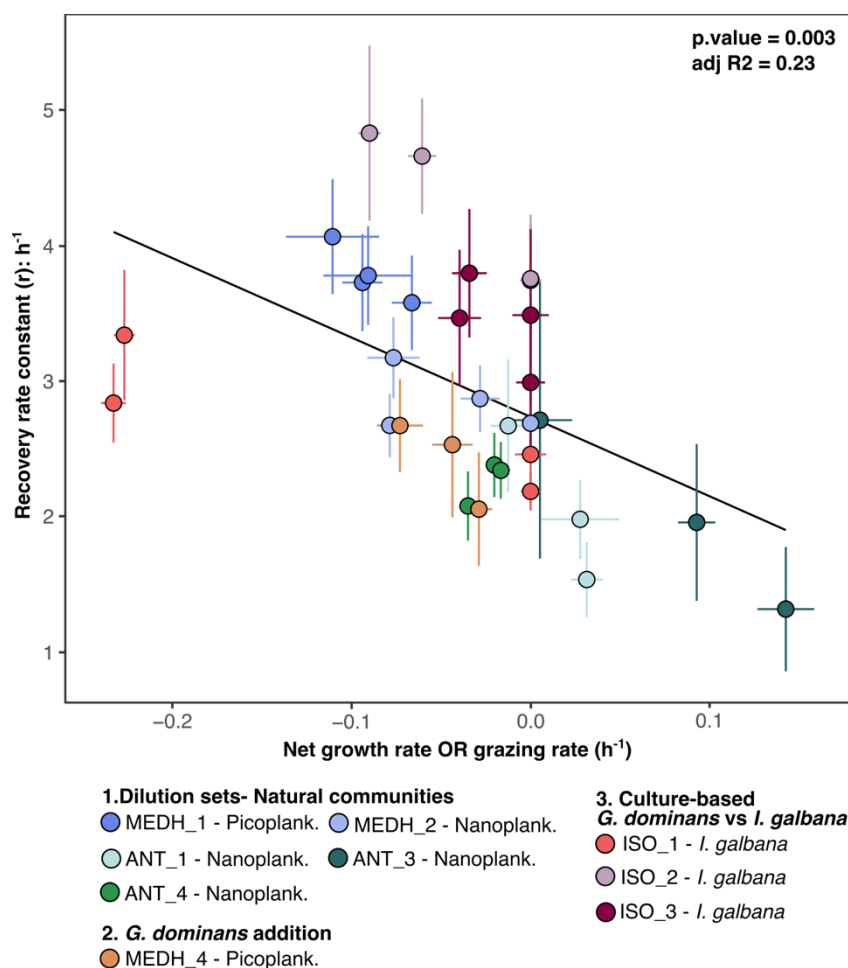


Figure 3.26. Grazing pressure vs photosynthetic recovery. Recovery rate constants (y-axis) related to net growth rates (net loss rates) for natural communities and *G. dominans* additions and grazing rates for *I. galbana* experiments (x-axis). The plot represents the bottles of all experiments except ANT_2 and MEDH_3. Therefore, it includes the three experimental setups used (dilution series of natural communities, *G. dominans* additions to natural communities, and culture-based model system of *G. dominans* grazing on *I. galbana*). Model I regression analysis was fit into the data and represented by the straight line. The goodness of fit (adj. R²) and the significance of the regression (p.value) are indicated.

Finding the reasons behind this relationship is far more complex. According to our results, the best explanation is the occurrence of preferential grazing on the most stressed individuals. Removing preferentially the individuals that have the lowest F_v/F_m' results would increase faster the overall F_v/F_m' values, which we assimilate to recovery. This preference for the stressed cells could be mediated by chemoattraction of the grazer to DMSP-exuding cells. However, preferential grazing on stressed phytoplankton was observed with natural assemblages but not with *I. galbana*, whose grazing by *G. dominans* was faster on the healthy cells. Therefore, there must be something else behind the relationship between grazing and recovery, at least in the specific case of *I. galbana*. Clearly, the model system chosen turned out not being the best, as it behaved differently from the studied natural communities.

Our experimental setup did not allow the observation of selection or capture processes. Thus, bulk net growth rates cannot inform about specific grazing on specific prey (Montagnes et al., 2008). The possibility remains that the influence of grazing in phytoplankton recovery can also be related to other

untargeted grazing outcomes, such as the release of nutrients or other compounds beneficial for the recovery of the photosynthetic efficiency. Although nutrient amendments aimed at neutralising this effect, the release of other favourable chemical factors could not be controlled. With the data we had at hand, we investigated potential confounding factors that might influence recovery rate constants besides the grazing pressure. While no significant correlations were found with any of the other community or stress metrics, the dilution technique itself merited exploration. In this sense, highly diluted treatments can negatively impact phytoplankton growth (Stoecker et al., 2014, 2015). Therefore, lower recovery rates in dilution series could be actually due to diminished growth of the phytoplankton. A core assumption of the dilution technique is that instantaneous growth is equal in all dilution levels (Landry & Hassett, 1982). However, negative grazing rates, even when nutrient limitation was prevented by nutrient additions, suggest lower growth of phytoplankton in highly diluted treatments (Stoecker et al., 2014, 2015). Studies based on phytoplankton cultures reported a lag phase after extreme dilutions, potentially due to factors such as shock acclimation, lack of condition factors after the dilution, or the presence of inhibitory compounds in the filtered seawater used in the dilutions (Duarte Ferreira et al., 2021; Fredrickson & Strom, 2008; Stoecker et al., 2014). Studies showing lower photosynthetic efficiency in highly diluted treatments indicate the potential occurrence of physiological stress (Stoecker et al., 2014). This is not a generalised pattern since depends on multiple factors of the community and the filtration process (Stoecker et al., 2015). In our experiments, decreased photosynthetic efficiency after the dilutions was only observed in the ANT experiments. Gentle filtration protocols and additional incubation time to let the communities recover after the dilution were applied to diminish the impact of this potential artifact. Additionally, equal dilution factors were applied in all the bottles of the *G. dominans* addition experiments and in the culture-based experiments to rule out this confounding factor as the reason behind the positive relation between grazing and recovery.

Despite the inherent uncertainties associated with studying natural communities, our findings suggest the occurrence of preferential predation of herbivorous protists on stressed phytoplankton cells in microbial planktonic food webs. This provides support to a microbial variant of the controversial healthy herds hypothesis proposed in terrestrial ecology. For our observations to comply with this hypothesis, the preferential removal of the stressed (unfit) cells should translate into a benefit for the overall prey population fitness without impairing the predator population. The phenomenon could also be coined “kill-the-loser”, as opposite to the broadly accepted “kill-the-winner” concept, that names the fact that many predators, viruses and parasites target the most abundant (hence fittest) prey. While the “kill-the-winner” model helps explain the diversity in microbial plankton, where there is no fittest species that takes over and outcompetes all the others, the “kill-the-loser” model would provide an explanation of how populations survive in harsh environments like the high-UV exposed waters of the sunlit surface ocean.

As previously described, while research on the ecological implications of preferentially targeting environmentally stressed individuals remains limited, we found an example suggesting selective parasitic infection of physiologically compromised diatoms as a mechanism to improve population photosynthetic efficiency (Laundon et al., 2021). In the context of microzooplankton grazing, one study reported increased photosynthetic efficiency of a *Synechococcus* strain when a nanoflagellate predator was present, although the observation was not explicitly discussed (Callieri et al., 2016). Our results lend strong support to hypothesis four of the thesis, suggesting that higher grazing pressure can have a positive impact on the recovery processes of stressed phytoplankton assemblages. To our knowledge, this is the first evidence of this phenomenon in microbial plankton communities from natural environments. While acknowledging the inherent limitations of our field and lab-based studies, these findings pave the way for further exploration in this exciting area of research.

REFERENCES

- Abrams, P. A. (2022). Food web functional responses. *Frontiers in Ecology and Evolution*, 10, 984384. <https://doi.org/10.3389/fevo.2022.984384>
- Anderson, R., Kjelleberg, S., McDougald, D., & Jürgens, K. (2011). Species-specific patterns in the vulnerability of carbon-starved bacteria to protist grazing. *Aquatic Microbial Ecology*, 64(2), 105–116. <https://doi.org/10.3354/ame01518>
- Archer, S. D., Ragni, M., Webster, R., Airs, R. L., & Geider, R. J. (2010). Dimethyl sulfoniopropionate and dimethyl sulfide production in response to photoinhibition in *Emiliana huxleyi*. *Limnology and Oceanography*, 55(4), 1579–1589. <https://doi.org/10.4319/lo.2010.55.4.1579>
- Archer, S. D., Stefels, J., Airs, R. L., Lawson, T., Smyth, T. J., Rees, A. P., & Geider, R. J. (2018). Limitation of dimethylsulfoniopropionate synthesis at high irradiance in natural phytoplankton communities of the Tropical Atlantic. *Limnology and Oceanography*, 63(1), 227–242. <https://doi.org/10.1002/lno.10625>
- Arias, A., Saiz, E., & Calbet, A. (2020). Towards an understanding of diel feeding rhythms in marine protists: Consequences of light manipulation. *Microbial Ecology*, 79(1), 64–72. <https://doi.org/10.1007/s00248-019-01390-y>
- Bates, D. M., & Chambers, J. M. (1992). Nonlinear models. In Chapter 10 of *Statistical Models* in S. Wadsworth & Brooks/Cole.
- Bates, D. M., & Watts, D. G. (1988). *Nonlinear regression analysis and its applications*. John Wiley & Sons, Inc. <https://onlinelibrary.wiley.com/doi/book/10.1002/9780470316757>
- Boenigk, J., Matz, C., Jürgens, K., & Arndt, H. (2001). Confusing selective feeding with differential digestion in bacterivorous nanoflagellates. *Journal of Eukaryotic Microbiology*, 48(4), 425–432. <https://doi.org/10.1111/j.1550-7408.2001.tb00175.x>
- Breckels, M. N., Roberts, E. C., Archer, S. D., Malin, G., & Steinke, M. (2011). The role of dissolved infochemicals in mediating predator-prey interactions in the heterotrophic dinoflagellate *Oxyrrhis marina*. *Journal of Plankton Research*, 33(4), 629–639. <https://doi.org/10.1093/plankt/fbq114>
- Brussaard, C., Marie, D., Thyrrhaug, R., & Bratbak, G. (2001). Flow cytometric analysis of phytoplankton viability following viral infection. *Aquatic Microbial Ecology*, 26(2), 157–166. <https://doi.org/10.3354/ame026157>
- Butler, W. L. (1972). On the primary nature of fluorescence yield changes associated with photosynthesis. *Proceedings of the National Academy of Sciences*, 69(11), 3420–3422. <https://doi.org/10.1073/pnas.69.11.3420>
- Calbet, A. (2008). The trophic roles of microzooplankton in marine systems. *ICES Journal of Marine Science*, 65(3), 325–331. <https://doi.org/10.1093/icesjms/fsn013>
- Calbet, A., Isari, S., Martínez, R., Saiz, E., Garrido, S., Peters, J., Borrat, R., & Alcaraz, M. (2013). Adaptations to feast and famine in different strains of the marine heterotrophic dinoflagellates *Gyrodinium dominans* and *Oxyrrhis marina*. *Marine Ecology Progress Series*, 483, 67–84. <https://doi.org/10.3354/meps10291>
- Calbet, A., & Landry, M. R. (1999). Mesozooplankton influences on the microbial food web: Direct and indirect trophic interactions in the oligotrophic open ocean. *Limnology and Oceanography*, 44(6), 1370–1380. <https://doi.org/10.4319/lo.1999.44.6.1370>
- Calbet, A., & Landry, M. R. (2004). Phytoplankton growth, microzooplankton grazing, and carbon cycling in marine systems. *Limnology and Oceanography*, 49(1), 51–57. <https://doi.org/10.4319/lo.2004.49.1.0051>
- Calbet, A., & Saiz, E. (2013). Effects of trophic cascades in dilution grazing experiments: From artificial saturated feeding responses to positive slopes. *Journal of Plankton Research*, 35(6), 1183–1191. <https://doi.org/10.1093/plankt/fbt067>
- Callieri, C., Amalfitano, S., Corno, G., & Bertoni, R. (2016). Grazing-induced *Synechococcus* microcolony formation: Experimental insights from two freshwater phylogenotypes. *FEMS Microbiology Ecology*, 92(11), fiw154. <https://doi.org/10.1093/femsec/fiw154>
- Cherrier, J., Valentine, S., Hamill, B., Jeffrey, W. H., & Marra, J. F. (2015). Light-mediated release of dissolved organic carbon by phytoplankton. *Journal of Marine Systems*, 147, 45–51. <https://doi.org/10.1016/j.jmarsys.2014.02.008>
- Cooney, E. C., Fredrickson, K. A., Bright, K. J., & Strom, S. L. (2019). Contrasting effects of high-intensity photosynthetically active radiation on two bloom-forming dinoflagellates. *Journal of Phycology*, 55(5), 1082–1095. <https://doi.org/10.1111/jpy.12890>
- Cullen, J. J., & MacIntyre, J. G. (1998). Behavior, physiology and the niche of depth-regulating phytoplankton. In *Physiological Ecology of Harmful Algal Blooms: Vol. Vol. G 41*. Springer-Verlag.

- Cunningham, G. B., Strauss, V., & Ryan, P. G. (2008). African penguins (*Spheniscus demersus*) can detect dimethyl sulphide, a prey-related odour. *Journal of Experimental Biology*, 211(19), 3123–3127. <https://doi.org/10.1242/jeb.018325>
- Darroch, L., Lavoie, M., Levasseur, M., Laurion, I., Sunda, W., Michaud, S., Scarratt, M., Gosselin, M., & Caron, G. (2015). Effect of short-term light- and UV-stress on DMSP, DMS, and DMSP lyase activity in *Emiliana huxleyi*. *Aquatic Microbial Ecology*, 74(2), 173–185. <https://doi.org/10.3354/ame01735>
- De Lange, H. J., & Lüring, M. (2003). Effects of UV-B irradiated algae on zooplankton grazing. *Hydrobiologia*, 491(1–3), 133–144. <https://doi.org/10.1023/A:1024485320677>
- Demmig-Adams, B. (1990). Carotenoids and photoprotection in plants: A role for the xanthophyll zeaxanthin. *Biochimica et Biophysica Acta (BBA) - Bioenergetics*, 1020(1), 1–24. [https://doi.org/10.1016/0005-2728\(90\)90088-L](https://doi.org/10.1016/0005-2728(90)90088-L)
- Dolan, J. R., & McKeon, K. (2005). The reliability of grazing rate estimates from dilution experiments: Have we over-estimated rates of organic carbon consumption by microzooplankton? *Ocean Science*, 1(1), 1–7. <https://doi.org/10.5194/os-1-1-2005>
- Duarte Ferreira, G., Romano, F., Medić, N., Pitta, P., Hansen, P. J., Flynn, K. J., Mitra, A., & Calbet, A. (2021). Mixoplankton interferences in dilution grazing experiments. *Scientific Reports*, 11(1), 23849. <https://doi.org/10.1038/s41598-021-03176-0>
- Duffy, M. A., Hall, S. R., Tessier, A. J., & Huebner, M. (2005). Selective predators and their parasitized prey: Are epidemics in zooplankton under top-down control? *Limnology and Oceanography*, 50(2), 412–420. <https://doi.org/10.4319/lo.2005.50.2.0412>
- Edgcomb, V. P. (2021). Eat me, or don't eat me? *Nature Microbiology*, 6(11), 1341–1342. <https://doi.org/10.1038/s41564-021-00992-y>
- Evans, C., Kadner, S. V., Darroch, L. J., Wilson, W. H., Liss, P. S., & Malin, G. (2007). The relative significance of viral lysis and microzooplankton grazing as pathways of dimethylsulfoniopropionate (DMSP) cleavage: An *Emiliana huxleyi* culture study. *Limnology and Oceanography*, 52(3), 1036–1045. <https://doi.org/10.4319/lo.2007.52.3.1036>
- Evans, C., Malin, G., Mills, G. P., & Wilson, W. H. (2006). Viral infection of *Emiliana huxleyi* (Prymnesiophyceae) leads to elevated production of reactive oxygen species. *Journal of Phycology*, 42(5), 1040–1047. <https://doi.org/10.1111/j.1529-8817.2006.00256.x>
- Evans, C., & Wilson, W. H. (2008). Preferential grazing of *Oxyrrhis marina* on virus infected *Emiliana huxleyi*. *Limnology and Oceanography*, 53(5), 2035–2040. <https://doi.org/10.4319/lo.2008.53.5.2035>
- Fields, D. M., Durif, C. M. F., Bjelland, R. M., Shema, S. D., Skiftesvik, A. B., & Browman, H. I. (2011). Grazing rates of *Calanus finmarchicus* on *Thalassiosira weissflogii* cultured under different levels of ultraviolet radiation. *PLoS ONE*, 6(10), e26333. <https://doi.org/10.1371/journal.pone.0026333>
- Fredrickson, K. A., & Strom, S. L. (2008). The algal osmolyte DMSP as a microzooplankton grazing deterrent in laboratory and field studies. *Journal of Plankton Research*, 31(2), 135–152. <https://doi.org/10.1093/plankt/fbn112>
- Fuentes-Lema, A., Sobrino, C., González, N., Estrada, M., & Neale, P. (2015). Effect of solar UVR on the production of particulate and dissolved organic carbon from phytoplankton assemblages in the Indian Ocean. *Marine Ecology Progress Series*, 535, 47–61. <https://doi.org/10.3354/meps11414>
- Galí, M., Ruiz-González, C., Lefort, T., Gasol, J. M., Cardelús, C., Romera-Castillo, C., & Simó, R. (2013). Spectral irradiance dependence of sunlight effects on plankton dimethylsulfide production. *Limnology and Oceanography*, 58(2), 489–504. <https://doi.org/10.4319/lo.2013.58.2.0489>
- Galindo, V., Levasseur, M., Mundy, C. J., Gosselin, M., Scarratt, M., Papakyriakou, T., Stefels, J., Gale, M. A., Tremblay, J.-É., & Lizotte, M. (2016). Contrasted sensitivity of DMSP production to high light exposure in two Arctic under-ice blooms. *Journal of Experimental Marine Biology and Ecology*, 475, 38–48. <https://doi.org/10.1016/j.jembe.2015.11.009>
- Garcés, E., Alacid, E., Reñé, A., Petrou, K., & Simó, R. (2013). Host-released dimethylsulphide activates the dinoflagellate parasitoid *Parvilucifera sinerae*. *ISME Journal*, 7(5), 1065–1068. <https://doi.org/10.1038/ismej.2012.173>
- García-Oliva, O., & Wirtz, K. (2022). Size-dependent and -independent prey selection of dinoflagellates. *Marine Biology*, 169(9), 122. <https://doi.org/10.1007/s00227-022-04102-2>
- Genovart, M., Negre, N., Tavecchia, G., Bistuer, A., Parpal, L., & Oro, D. (2010). The young, the weak and the sick: Evidence of natural selection by predation. *PLoS ONE*, 5(3), e9774. <https://doi.org/10.1371/journal.pone.0009774>

- Gorbunov, M., Shirsin, E., Nikonova, E., Fadeev, V., & Falkowski, P. (2020). A multi-spectral fluorescence induction and relaxation (FIRe) technique for physiological and taxonomic analysis of phytoplankton communities. *Marine Ecology Progress Series*, 644, 1–13. <https://doi.org/10.3354/meps13358>
- Gorbunov, M. Y., & Falkowski, P. G. (2022). Using chlorophyll fluorescence to determine the fate of photons absorbed by phytoplankton in the world's oceans. *Annual Review of Marine Science*, 14(1), 213–238. <https://doi.org/10.1146/annurev-marine-032621-122346>
- Guadayol, Ò., Mendonca, T., Segura-Noguera, M., Wright, A. J., Tassieri, M., & Humphries, S. (2021). Microrheology reveals microscale viscosity gradients in planktonic systems. *Proceedings of the National Academy of Sciences*, 118(1), e2011389118. <https://doi.org/10.1073/pnas.2011389118>
- Guillard, R.R.L. (1975). Culture of phytoplankton for feeding marine invertebrates. In *Culture of marine invertebrates animals* (pp. 29–60). Smith, M.L. and Chanley, M.H., Eds. http://dx.doi.org/10.1007/978-1-4615-8714-9_3
- Gutierrez, S. O., Minchella, D. J., & Bernal, X. E. (2022). Survival of the sickest: Selective predation differentially modulates ecological and evolutionary disease dynamics. *Oikos*, 2022(9), e09126. <https://doi.org/10.1111/oik.09126>
- Hall, S. R., Duffy, M. A., & Cáceres, C. E. (2005). Selective predation and productivity jointly drive complex behavior in host-parasite systems. *The American Naturalist*, 165(1), 70–81. <https://doi.org/10.1086/426601>
- Hamm, C. E., Merkel, R., Springer, O., Jurkojc, P., Maier, C., Prectel, K., & Smetacek, V. (2003). Architecture and material properties of diatom shells provide effective mechanical protection. *Nature*, 421(6925), 841–843. <https://doi.org/10.1038/nature01416>
- Harada, H., Vila-Costa, M., Cebrian, J., & Kiene, R. P. (2009). Effects of UV radiation and nitrate limitation on the production of biogenic sulfur compounds by marine phytoplankton. *Aquatic Botany*, 90(1), 37–42. <https://doi.org/10.1016/j.aquabot.2008.05.004>
- Harrison, J. W., Silsbe, G. M., & Smith, R. E. H. (2015). Photophysiology and its response to visible and ultraviolet radiation in freshwater phytoplankton from contrasting light regimes. *Journal of Plankton Research*, 37(2), 472–488. <https://doi.org/10.1093/plankt/fbv003>
- Harvey, E. L., Jeong, H. J., & Menden-Deuer, S. (2013). Avoidance and attraction: Chemical cues influence predator-prey interactions of planktonic protists. *Limnology and Oceanography*, 58(4), 1176–1184. <https://doi.org/10.4319/lo.2013.58.4.1176>
- Hessen, D., De Lange, H., & Van Donk, E. (1997). UV-induced changes in phytoplankton cells and its effects on grazers. *Freshwater Biology*, 38(3), 513–524. <https://doi.org/10.1046/j.1365-2427.1997.00223.x>
- Holling CS. (1965). The functional response of predators to prey density and its role in mimicry and population regulation. *Memoirs of the Entomological Society of Canada*, 97(S45), 5–60. <https://doi.org/10.4039/entm9745fv>
- Jakobsen, H. H., & Strom, S. L. (2004). Circadian cycles in growth and feeding rates of heterotrophic protist plankton. *Limnology and Oceanography*, 49(6), 1915–1922. <https://doi.org/10.4319/lo.2004.49.6.1915>
- Jakobsen, H., Hansen, P., & Larsen, J. (2000). Growth and grazing responses of two chloroplast-retaining dinoflagellates: Effect of irradiance and prey species. *Marine Ecology Progress Series*, 201, 121–128. <https://doi.org/10.3354/meps201121>
- Jeong, H. J., Yoo, Y. D., Kim, J. S., Seong, K. A., Kang, N. S., & Kim, T. H. (2010). Growth, feeding and ecological roles of the mixotrophic and heterotrophic dinoflagellates in marine planktonic food webs. *Ocean Science Journal*, 45(2), 65–91. <https://doi.org/10.1007/s12601-010-0007-2>
- Jeschke, J., & Tollrian, R. (2005). Effects of predator confusion on functional responses. *Oikos*, 111(3), 547–555. <https://doi.org/10.1111/j.1600-0706.2005.14118.x>
- Keller, M. D., Bellows, W. K., & Guillard, R. R. L. (1989). Dimethyl sulfide production in marine phytoplankton. In *Biogenic sulfur in the environment* (Vol. 393, pp. 167–182). American Chemical Society. <https://doi.org/10.1021/bk-1989-0393.ch011>
- Kennedy, F., McMinn, A., & Martin, A. (2012). Effect of temperature on the photosynthetic efficiency and morphotype of *Phaeocystis antarctica*. *Journal of Experimental Marine Biology and Ecology*, 429, 7–14. <https://doi.org/10.1016/j.jembe.2012.06.016>
- Kiene, R. P., & Slezak, D. (2006). Low dissolved DMSP concentrations in seawater revealed by small-volume gravity filtration and dialysis sampling. *Limnology and Oceanography: Methods*, 4(4), 80–95. <https://doi.org/10.4319/lom.2006.4.80>
- Kinsey, J. D., & Kieber, D. J. (2016). Microwave preservation method for DMSP, DMSO, and acrylate in unfiltered seawater and phytoplankton culture samples. *Limnology and Oceanography: Methods*, 14(3), 196–209. <https://doi.org/10.1002/lom3.10081>

- Kowalewsky, S., Dambach, M., Mauck, B., & Dehnhardt, G. (2006). High olfactory sensitivity for dimethyl sulphide in harbour seals. *Biology Letters*, 2(1), 106–109. <https://doi.org/10.1098/rsbl.2005.0380>
- Kuhlish, C., Shemi, A., Barak-Gavish, N., Schatz, D., & Vardi, A. (2024). Algal blooms in the ocean: Hot spots for chemically mediated microbial interactions. *Nature Reviews Microbiology*, 22(3), 138–154. <https://doi.org/10.1038/s41579-023-00975-2>
- Lana, A., Simó, R., Vallina, S. M., & Dachs, J. (2012). Re-examination of global emerging patterns of ocean DMS concentration. *Biogeochemistry*, 110(1–3), 173–182. <https://doi.org/10.1007/s10533-011-9677-9>
- Landry, M. R., Barber, R. T., Bidigare, R. R., Chai, F., Coale, K. H., Dam, H. G., Lewis, M. R., Lindley, S. T., McCarthy, J. J., Roman, M. R., Stoecker, D. K., Verity, P. G., & White, J. R. (1997). Iron and grazing constraints on primary production in the central equatorial Pacific: An EqPac synthesis. *Limnology and Oceanography*, 42(3), 405–418. <https://doi.org/10.4319/lo.1997.42.3.0405>
- Landry, M. R., & Hassett, R. P. (1982). Estimating the grazing impact of marine micro-zooplankton. *Marine Biology*, 67(3), 283–288. <https://doi.org/10.1007/BF00397668>
- Laundon, D., Mock, T., Wheeler, G., & Cunliffe, M. (2021). Healthy herds in the phytoplankton: The benefit of selective parasitism. *The ISME Journal*, 15(7), 2163–2166. <https://doi.org/10.1038/s41396-021-00936-8>
- Lawrence, C., & Menden-Deuer, S. (2012). Drivers of protistan grazing pressure: Seasonal signals of plankton community composition and environmental conditions. *Marine Ecology Progress Series*, 459, 39–52. <https://doi.org/10.3354/meps09771>
- Li, A., Stoecker, D. K., & Coats, D. W. (2000). Mixotrophy in *Gyrodinium galatheanum* (Dinophyceae): Grazing responses to light intensity and inorganic nutrients. *Journal of Phycology*, 36(1), 33–45. <https://doi.org/10.1046/j.1529-8817.2000.98076.x>
- Li, J., Fenton, A., Kettley, L., Roberts, P., & Montagnes, D. J. S. (2013). Reconsidering the importance of the past in predator–prey models: Both numerical and functional responses depend on delayed prey densities. *Proceedings of the Royal Society B: Biological Sciences*, 280(1768), 20131389. <https://doi.org/10.1098/rspb.2013.1389>
- Livanou, E., Lagaria, A., Psarra, S., & Lika, K. (2017). Dissolved organic matter release by phytoplankton in the context of the Dynamic Energy Budget theory. <https://doi.org/10.5194/bg-2017-426>
- Lopez, L. K., Cortez, M. H., DeBlieux, T. S., Menel, I. A., O'Brien, B., Cáceres, C. E., Hall, S. R., & Duffy, M. A. (2023). A healthy but depleted herd: Predators decrease prey disease and density. *Ecology*, 104(7), e4063. <https://doi.org/10.1002/ecy.4063>
- Martel, C. M. (2006). Prey location, recognition and ingestion by the phagotrophic marine dinoflagellate *Oxyrrhis marina*. *Journal of Experimental Marine Biology and Ecology*, 335(2), 210–220. <https://doi.org/10.1016/j.jembe.2006.03.006>
- Masdeu-Navarro, M., Mangot, J.-F., Xue, L., Cabrera-Brufau, M., Gardner, S. G., Kieber, D. J., González, J. M., & Simó, R. (2022). Spatial and diel patterns of volatile organic compounds, DMSP-derived compounds, and planktonic microorganisms around a tropical scleractinian coral colony. *Frontiers in Marine Science*, 9, 944141. <https://doi.org/10.3389/fmars.2022.944141>
- McParland, E. L., & Levine, N. M. (2019). The role of differential DMSP production and community composition in predicting variability of global surface DMSP concentrations. *Limnology and Oceanography*, 64(2), 757–773. <https://doi.org/10.1002/lno.11076>
- Meunier, C. L., Hantzsche, F. M., Cunha-Dupont, A. Ö., Haafke, J., Oppermann, B., Malzahn, A. M., & Boersma, M. (2012). Intraspecific selectivity, compensatory feeding and flexible homeostasis in the phagotrophic flagellate *Oxyrrhis marina*: Three ways to handle food quality fluctuations. *Hydrobiologia*, 680(1), 53–62. <https://doi.org/10.1007/s10750-011-0900-4>
- Mittag, M. (2001). Circadian rhythms in microalgae. *International Review of Cytology*. Academic Press., 206, 213–247.
- Moeller, H. V., Laufkötter, C., Sweeney, E. M., & Johnson, M. D. (2019). Light-dependent grazing can drive formation and deepening of deep chlorophyll maxima. *Nature Communications*, 10(1), 1978. <https://doi.org/10.1038/s41467-019-09591-2>
- Montagnes, D., Barbosa, A., Boenigk, J., Davidson, K., Jürgens, K., Macek, M., Parry, J., Roberts, E., & Imek, K. (2008). Selective feeding behaviour of key free-living protists: Avenues for continued study. *Aquatic Microbial Ecology*, 53, 83–98. <https://doi.org/10.3354/ame01229>
- Montero, O., Sobrino, C., Parés, G., & Lubián, L. (2002). Photoinhibition and recovery after selective short-term exposure to solar radiation of five chlorophyll c-containing marine microalgae. *Ciencias Marinas*, 28(3), 223–236. <https://doi.org/10.7773/cm.v28i3.229>

- Moran, M. A., Kujawinski, E. B., Schroer, W. F., Amin, S. A., Bates, N. R., Bertrand, E. M., Braakman, R., Brown, C. T., Covert, M. W., Doney, S. C., Dyhrman, S. T., Edison, A. S., Eren, A. M., Levine, N. M., Li, L., Ross, A. C., Saito, M. A., Santoro, A. E., Segrè, D., ... Vardi, A. (2022). Microbial metabolites in the marine carbon cycle. *Nature Microbiology*, 7(4), 508–523. <https://doi.org/10.1038/s41564-022-01090-3>
- Morel, A. (1988). Optical modeling of the upper ocean in relation to its biogenous matter content (case I waters). *Journal of Geophysical Research: Oceans*, 93(C9), 10749–10768. <https://doi.org/10.1029/JC093iC09p10749>
- Nevitt, G. A. (2008). Sensory ecology on the high seas: The odor world of the procellariiform seabirds. *Journal of Experimental Biology*, 211(11), 1706–1713. <https://doi.org/10.1242/jeb.015412>
- Ochs, C. A. (1997). Effects of UV radiation on grazing by two marine heterotrophic nanoflagellates on autotrophic picoplankton. *Journal of Plankton Research*, 19(10), 1517–1536. <https://doi.org/10.1093/plankt/19.10.1517>
- Ochs, C. A., & Eddy, L. P. (1998). Effects of UV-A (320 to 399 nanometers) on grazing pressure of a marine heterotrophic nanoflagellate on strains of the unicellular cyanobacteria *Synechococcus* spp. *Applied and Environmental Microbiology*, 64(1), 287–293. <https://doi.org/10.1128/AEM.64.1.287-293.1998>
- Ostfeld, R. S., & Holt, R. D. (2004). Are predators good for your health? Evaluating evidence for top-down regulation of zoonotic disease reservoirs. *Frontiers in Ecology and the Environment*, 2(1), 13–20. [https://doi.org/10.1890/1540-9295\(2004\)002\[0013:APGFYH\]2.0.CO;2](https://doi.org/10.1890/1540-9295(2004)002[0013:APGFYH]2.0.CO;2)
- Packer, C., Holt, R. D., Hudson, P. J., Lafferty, K. D., & Dobson, A. P. (2003). Keeping the herds healthy and alert: Implications of predator control for infectious disease. *Ecology Letters*, 6(9), 797–802. <https://doi.org/10.1046/j.1461-0248.2003.00500.x>
- Park, M. G., Kim, A., Jeon, B. S., & Kim, M. (2021). Parasite-mediated increase in prey edibility in the predator-prey interaction of marine planktonic protists. *Harmful Algae*, 103, 101982. <https://doi.org/10.1016/j.hal.2021.101982>
- Pausz, C., & Herndl, G. (1999). Role of ultraviolet radiation on phytoplankton extracellular release and its subsequent utilization by marine bacterioplankton. *Aquatic Microbial Ecology*, 18, 85–93. <https://doi.org/10.3354/ame018085>
- Pohnert, G., Steinke, M., & Tollrian, R. (2007). Chemical cues, defence metabolites and the shaping of pelagic interspecific interactions. *Trends in Ecology & Evolution*, 22(4), 198–204. <https://doi.org/10.1016/j.tree.2007.01.005>
- Rijstenbil, J. W. (2002). Assessment of oxidative stress in the planktonic diatom *Thalassiosira pseudonana* in response to UVA and UVB radiation. *Journal of Plankton Research*, 24(12), 1277–1288. <https://doi.org/10.1093/plankt/24.12.1277>
- Roberts, E. C., Legrand, C., Steinke, M., & Wootton, E. C. (2011). Mechanisms underlying chemical interactions between predatory planktonic protists and their prey. *Journal of Plankton Research*, 33(6), 833–841. <https://doi.org/10.1093/plankt/fbr005>
- Robinson, D., Hayes, A., & Couch, S. (2023). broom: Convert statistical objects into tidy tibbles. <https://broom.tidymodels.org/>, <https://github.com/tidymodels/broom>.
- Saló, V., Simó, R., Vila-Costa, M., & Calbet, A. (2009). Sulfur assimilation by *Oxyrrhis marina* feeding on a ³⁵S-DMSP-labelled prey. *Environmental Microbiology*, 11(12), 3063–3072. <https://doi.org/10.1111/j.1462-2920.2009.02011.x>
- Sandhu, S. K., Morozov, A. Yu., Mitra, A., & Flynn, K. (2019). Exploring nonlinear functional responses of zooplankton grazers in dilution experiments via optimization techniques. *Limnology and Oceanography*, 64(2), 774–784. <https://doi.org/10.1002/lno.11073>
- Schmoker, C., Hernández-León, S., & Calbet, A. (2013). Microzooplankton grazing in the oceans: Impacts, data variability, knowledge gaps and future directions. *Journal of Plankton Research*, 35(4), 691–706. <https://doi.org/10.1093/plankt/fbt023>
- Seymour, J. R., Amin, S. A., Raina, J.-B., & Stocker, R. (2017). Zooming in on the phycosphere: The ecological interface for phytoplankton–bacteria relationships. *Nature Microbiology*, 2(7), 17065. <https://doi.org/10.1038/nmicrobiol.2017.65>
- Seymour, J. R., Simó, R., Ahmed, T., & Stocker, R. (2010). Chemoattraction to dimethylsulfoniopropionate throughout the marine microbial food web. *Science*, 329(5989), 342–345. <https://doi.org/10.1126/science.1188418>
- Shemi, A., Alcolombri, U., Schatz, D., Farstey, V., Vincent, F., Rotkopf, R., Ben-Dor, S., Frada, M. J., Tawfik, D. S., & Vardi, A. (2021). Dimethyl sulfide mediates microbial predator–prey interactions between zooplankton and algae in the ocean. *Nature Microbiology*, 6(11), 1357–1366. <https://doi.org/10.1038/s41564-021-00971-3>

- Slezak, D., & Herndl, G. (2003). Effects of ultraviolet and visible radiation on the cellular concentrations of dimethylsulfoniopropionate (DMSP) in *Emiliania huxleyi* (strain L). *Marine Ecology Progress Series*, 246(August), 61–71. <https://doi.org/10.3354/meps246061>
- Slobodkin, L. B. (1974). Prudent predation does not require group selection. *The American Naturalist*, 108(963), 665–678.
- Smriga, S., Fernandez, V. I., Mitchell, J. G., & Stocker, R. (2016). Chemotaxis toward phytoplankton drives organic matter partitioning among marine bacteria. *Proceedings of the National Academy of Sciences*, 113(6), 1576–1581. <https://doi.org/10.1073/pnas.1512307113>
- Sobrino, C., Segovia, M., Neale, P., Mercado, J., García-Gómez, C., Kulk, G., Lorenzo, M., Camarena, T., Van De Poll, W., Spilling, K., & Ruan, Z. (2014). Effect of CO₂, nutrients and light on coastal plankton. IV. Physiological responses. *Aquatic Biology*, 22, 77–93. <https://doi.org/10.3354/ab00590>
- Sommaruga, R. (2003). UVR and its effects on species interactions. In *UV effects in aquatic organisms and ecosystems*.
- Stefels, J. (2000). Physiological aspects of the production and conversion of DMSP in marine algae and higher plants. *Journal of Sea Research*, 43(3–4), 183–197. [https://doi.org/10.1016/S1385-1101\(00\)00030-7](https://doi.org/10.1016/S1385-1101(00)00030-7)
- Stefels, J., Steinke, M., Turner, S., Malin, G., & Belviso, S. (2007). Environmental constraints on the production and removal of the climatically active gas dimethylsulphide (DMS) and implications for ecosystem modelling. *Biogeochemistry*, 83(1–3), 245–275. <https://doi.org/10.1007/s10533-007-9091-5>
- Stefels, J., & van Leeuwe, M. A. (1998). Effects of iron and light stress on the biochemical composition of antarctic *Phaeocystis* sp. (*Prymnesiophyceae*). I. Intracellular DMSP concentrations. *Journal of Phycology*, 34(3), 486–495. <https://doi.org/10.1046/j.1529-8817.1998.340486.x>
- Steiner, P. A., Sintes, E., Simó, R., De Corte, D., Pfannkuchen, D. M., Ivančić, I., Najdek, M., & Herndl, G. J. (2019). Seasonal dynamics of marine snow-associated and free-living demethylating bacterial communities in the coastal northern Adriatic Sea. *Environmental Microbiology Reports*, 11(5), 699–707. <https://doi.org/10.1111/1758-2229.12783>
- Steinke, M., Malin, G., & Liss, P. S. (2002). Trophic interactions in the sea: An ecological role for climate relevant volatiles? *Journal of Phycology*, 38(4), 630–638. <https://doi.org/10.1046/j.1529-8817.2002.02057.x>
- Stoecker, D. K., Nejstgaard, J. C., Madhusoodhanan, R., Pohnert, G., Wolfram, S., Jakobsen, H. H., Šulčius, S., & Larsen, A. (2015). Underestimation of microzooplankton grazing in dilution experiments due to inhibition of phytoplankton growth. *Limnology and Oceanography*, 60(4), 1426–1438. <https://doi.org/10.1002/lno.10106>
- Stoecker, D. K., Weigel, A., & Goes, J. I. (2014). Microzooplankton grazing in the Eastern Bering Sea in summer. *Deep Sea Research part II: Topical studies in oceanography*, 109, 145–156. <https://doi.org/10.1016/j.dsr2.2013.09.017>
- Strom, S. (2001). Light-aided digestion, grazing and growth in herbivorous protists. *Aquatic Microbial Ecology*, 23, 253–261. <https://doi.org/10.3354/ame023253>
- Strom, S., Barberi, O., Mazur, C., Bright, K. J., & Fredrickson, K. (2020). High light stress reduces dinoflagellate predation on phytoplankton through both direct and indirect responses. *Aquatic Microbial Ecology*, 84, 43–57. <https://doi.org/10.3354/ame01924>
- Suggett, D. J., Le Floch, E., Harris, G. N., Leonardos, N., & Geider, R. J. (2007). Different strategies of photoacclimation by two strains of *Emiliania huxleyi* (*Haptophyta*). *Journal of Phycology*, 43(6), 1209–1222. <https://doi.org/10.1111/j.1529-8817.2007.00406.x>
- Sunda, W., Kieber, D. J., Kiene, R. P., & Huntsman, S. (2002). An antioxidant function for DMSP and DMS in marine algae. *Nature*, 418(6895), 317–320. <https://doi.org/10.1038/nature00851>
- Tang, K., & Simó, R. (2003). Trophic uptake and transfer of DMSP in simple planktonic food chains. *Aquatic Microbial Ecology*, 31(2), 193–202. <https://doi.org/10.3354/ame031193>
- Tang, K. W. (2001). Defecation of dimethylsulfoniopropionate (DMSP) by the copepod *Acartia tonsa* as functions of ambient food concentration and body DMSP content. *Journal of Plankton Research*, 23(5), 549–553. <https://doi.org/10.1093/plankt/23.5.549>
- Tarangkoon, W., & Hansen, P. (2011). Prey selection, ingestion and growth responses of the common marine ciliate *Mesodinium pulex* in the light and in the dark. *Aquatic Microbial Ecology*, 62(1), 25–38. <https://doi.org/10.3354/ame01455>
- Temple, S. A. (1987). Do predators always capture substandard individuals disproportionately from prey populations? *Ecology*, 68(3), 669–674. <https://doi.org/10.2307/1938472>
- Thornton, D. C. O. (2014). Dissolved organic matter (DOM) release by phytoplankton in the contemporary and future ocean. *European Journal of Phycology*, 49(1), 20–46. <https://doi.org/10.1080/09670262.2013.875596>

- Tillmann, U. (2004). Interactions between planktonic microalgae and protozoan grazers. *The Journal of Eukaryotic Microbiology*, 51(2), 156–168. <https://doi.org/10.1111/j.1550-7408.2004.tb00540.x>
- Toole, D. A., Slezak, D., Kiene, R. P., Kieber, D. J., & Siegel, D. A. (2006). Effects of solar radiation on dimethylsulfide cycling in the western Atlantic Ocean. *Deep Sea Research Part I: Oceanographic Research Papers*, 53(1), 136–153. <https://doi.org/10.1016/j.dsr.2005.09.003>
- Tyystjärvi, E. (2013). Photoinhibition of photosystem II. In *international review of cell and molecular Biology* (Vol. 300, pp. 243–303). Elsevier. <https://doi.org/10.1016/B978-0-12-405210-9.00007-2>
- Vallina, S. M., & Simó, R. (2007). Strong relationship between DMS and the solar radiation dose over the global surface ocean. *Science*, 315(5811), 506–508. <https://doi.org/10.1126/science.1133680>
- van Donk, E., & Hessen, D. (1995). Reduced digestibility of UV-B stressed and nutrient-limited algae by *Daphnia magna*. *Hydrobiologia*, 307(1–3), 147–151. <https://doi.org/10.1007/BF00032006>
- van Rijssel, M., & Buma, A. (2002). UV radiation induced stress does not affect DMSP synthesis in the marine prymnesiophyte *Emiliana huxleyi*. *Aquatic Microbial Ecology*, 28(2), 167–174. <https://doi.org/10.3354/ame028167>
- Verity, P. G. (1988). Chemosensory behavior in marine planktonic ciliates. *Bulletin of Marine Science*, 43(3), 772–782.
- Verity, P. G. (1991). Feeding in planktonic protozoans: Evidence for non-random acquisition of prey. *The Journal of Protozoology*, 38(1), 69–76. <https://doi.org/10.1111/j.1550-7408.1991.tb04804.x>
- Vincent, W. F., & Neale, P. J. (2000). Mechanisms of UV damage to aquatic organisms. In S. De Mora, S. Demers, & M. Vernet (Eds.), *The Effects of UV Radiation in the Marine Environment* (1st ed., pp. 149–176). Cambridge University Press. <https://doi.org/10.1017/CBO9780511535444.007>
- Vincent, W. F., & Roy, S. (1993). Solar ultraviolet-B radiation and aquatic primary production: Damage, protection, and recovery. *Environmental Reviews*, 1(1), 1–12. <https://doi.org/10.1139/a93-001>
- Visser, A. W., & Kjørboe, T. (2006). Plankton motility patterns and encounter rates. *Oecologia*, 148(3), 538–546. <https://doi.org/10.1007/s00442-006-0385-4>
- Weisse, T., Anderson, R., Arndt, H., Calbet, A., Hansen, P. J., & Montagnes, D. J. S. (2016). Functional ecology of aquatic phagotrophic protists – Concepts, limitations, and perspectives. *European Journal of Protistology*, 55, 50–74. <https://doi.org/10.1016/j.ejop.2016.03.003>
- Williams, P. D. (2008). Unhealthy herds: Some epidemiological consequences of host heterogeneity in predator–host–parasite systems. *Journal of Theoretical Biology*, 253(3), 500–507. <https://doi.org/10.1016/j.jtbi.2008.03.022>
- Wootton, E. C., Zubkov, M. V., Jones, D. H., Jones, R. H., Martel, C. M., Thornton, C. A., & Roberts, E. C. (2007). Biochemical prey recognition by planktonic protozoa. *Environmental Microbiology*, 9(1), 216–222. <https://doi.org/10.1111/j.1462-2920.2006.01130.x>
- Worden, A. Z., Follows, M. J., Giovannoni, S. J., Wilken, S., Zimmerman, A. E., & Keeling, P. J. (2015). Rethinking the marine carbon cycle: Factoring in the multifarious lifestyles of microbes. *Science*, 347(6223), 1257594. <https://doi.org/10.1126/science.1257594>
- Wu, L., Lei, Y., Lan, S., & Hu, C. (2017). Photosynthetic recovery and acclimation to excess light intensity in the rehydrated lichen soil crusts. *PLOS ONE*, 12(3), e0172537. <https://doi.org/10.1371/journal.pone.0172537>
- Wu, M., McCain, J. S. P., Rowland, E., Middag, R., Sandgren, M., Allen, A. E., & Bertrand, E. M. (2019). Manganese and iron deficiency in Southern Ocean *Phaeocystis antarctica* populations revealed through taxon-specific protein indicators. *Nature Communications*, 10(1), 3582. <https://doi.org/10.1038/s41467-019-11426-z>
- Zagarese, H., & Helbling, E. W. (2003). UV effects in aquatic organisms and ecosystems. *Comprehensive series in photochemistry & photobiology - volume 1*. The Royal Society of Chemistry.

**CHAPTER 3 -
SUPPLEMENTARY INFORMATION**

**EXPLORING THE DYNAMICS OF LIGHT STRESS AND GRAZING INTERACTIONS IN
NATURAL COMMUNITIES AND MODEL SYSTEMS**

Queralt Güell-Bujons, Yaiza Castillo, Albert Calbet and Rafel Simó

3.1: Light-stress treatments and responses of four phytoplankton assemblages

Table S3.1 – Characteristics of the stress treatments applied to each experiment. The phytoplankton response is also provided with the values of photosynthetic efficiency (%Fv'/Fm') at the end of the treatments (Exp. = Experiment, Inc. = Incubation, %Fv'/Fm' = percentage of similarity).

Exp. set	Exp.	Inc.time (min)	Average Intensity (W /m ²)	Intensity range max-min (W/m ²)	Dose (Kj/m ²)	Fv'/Fm' (%)
ISO	ISO_1	35	98	150 - 54	203	12
	ISO_2	40	98	150 - 54	284	11
	ISO_3	20	150	150	180	38
MED	MED_1	60	546	806 - 483	1932	55
	MED_2	60	550	825 - 494	1945	56
	MED_3	60	550	840 - 463	1984	69
	MED_4	60	602	787 - 473	2205	79
	MED_5	60	729	802 - 450	2625	62
MEDH	MEDH_1	88	308	591 - 111	1460	25
	MEDH_2	55	520	935 - 203	1553	29
	MEDH_3	55	362	866 - 170	1029	39
	MEDH_4	53	508	937 - 200	1611	27
ANT	ANT_1	93	233	343-48	1314	18
	ANT_2	58	87	302-32	313	45
	ANT_3	31	193	274-128	371	53
	ANT_4	41	242	420-166	611	35
	ANT_5	85	211	342-108	1090	36

Table S3.2 – Results of the One-tailed Welch's significance test for dissolved DMSP values (DMSPd). MEDH_1 is not in the table since the lack of good replicates did not enable the application of the test.

Exp. set	Exp.	Statistic	df	p.value
ISO	ISO_1	-2.03	1.41	0.231
	ISO_2	-2.02	2.10	0.088
	ISO_3	-2.19	2.40	0.069
MED	MED_1	-6.89	3.39	0.002
	MED_2	-10.38	1.61	0.009
	MED_3	-2.87	2.28	0.044
	MED_4	-5.89	3.05	0.005
	MED_5	-7.61	3.94	0.001
MEDH	MEDH_2	0.19	3.73	0.572
	MEDH_3	0.13	3.14	0.548
	MEDH_4	0.22	3.86	0.582

ANT	ANT_1	-2.67	1.54	0.0760
	ANT_2	-1.08	1.49	0.2120
	ANT_3	-4.72	3.10	0.0084
	ANT_4	-13.62	1.64	0.0056

3.2: Microzooplankton grazing on light-stressed and non-stressed phytoplankton

Table S3.3. Regression analysis of log-transformed cell concentration and ANCOVA statistical test results between the slopes of control and stressed communities. (Exp. = Experiment, C=Control, S= Stressed, Treat. = Treatment: C or S, P = Picophytoplankton, N= Nanophytoplankton).

Exp.	Parameter	Estimate	Std.Err	Statistic	p.value	Adj. R2	Treat.	Prey
MEDH_1	Intercept	9.02	0.022	408.18	2.16E-10		C	P
	Slope	-0.025	0.006	-4.48	1.10E-02	0.79	C	P
	Intercept	9.11	0.099	91.90	4.76E-12		S	P
	Slope	-0.110	0.026	-4.24	3.84E-03	0.68	S	P
	Slope:Treat			10.82	7.21E-03		C vs S	P
	Intercept	8.87	0.011	796.48	1.49E-11		C	N
	Slope	-0.004	0.003	-1.54	1.99E-01	0.21	C	N
	Intercept	8.81	0.034	261.22	3.18E-15		S	N
	Slope	-0.014	0.009	-1.64	1.45E-01	0.18	S	N
	Slope:Treat			1.27	2.85E-01		C vs S	N
MEDH_2	Intercept	9.16	0.032	288.42	6.17E-21		C	P
	Slope	0.011	0.011	1.00	3.42E-01	-	C	P
	Intercept	9.35	0.083	113.13	1.11E-12		S	P
	Slope	-0.075	0.024	-3.08	1.77E-02	0.52	S	P
	Slope:Treat			12.86	2.28E-03		C vs S	P
	Intercept	8.45	0.022	384.73	3.46E-22		C	N
	Slope	-0.028	0.007	-3.79	3.57E-03	0.55	C	N
	Intercept	8.59	0.051	168.75	6.77E-14		S	N
	Slope	-0.076	0.015	-5.05	1.49E-03	0.75	S	N
	Slope:Treat			9.41	6.98E-03		C vs S	N
MEDH_3	Intercept	9.08	0.059	154.84	1.28E-22		C	P
	Slope	-0.018	0.018	-1.00	3.34E-01	-	C	P
	Intercept	9.20	0.063	146.07	2.73E-22		S	P
	Slope	-0.123	0.019	-6.52	1.95E-05	0.75	S	P
	Slope:Treat			16.70	3.74E-04		C vs S	P
	Intercept	8.38	0.056	148.79	2.15E-22		C	N
	Slope	-0.070	0.017	-4.13	1.19E-03	0.53	C	N
	Intercept	8.55	0.032	268.24	1.01E-25		S	N
	Slope	-0.152	0.010	-15.91	6.66E-10	0.95	S	N
	Slope:Treat			18.03	2.45E-04		C vs S	N

MEDH_4	Intercept	8.68	0.024	360.13	2.20E-27		C	P
	Slope	-0.019	0.007	-2.65	2.00E-02	0.30	C	P
	Intercept	8.66	0.018	474.11	6.18E-29		S	P
	Slope	-0.039	0.006	-7.04	8.81E-06	0.78	S	P
	Slope:Treat			4.57	4.21E-02		C vs S	P
	Intercept	7.90	0.019	414.83	3.51E-28		C	N
	Slope	-0.046	0.006	-7.96	2.38E-06	0.82	C	N
	Intercept	7.88	0.025	318.88	1.07E-26		S	N
	Slope	-0.052	0.007	-7.03	8.96E-06	0.78	S	N
	Slope:Treat			0.46	5.04E-01		C vs S	N

3.3 Influence of grazing on phytoplankton recovery from light-stress

Table S3.4. Log-linear regression fits of cell concentrations vs time. The ANT set does not have the parameters “statistic” and “p.value” since the dataset was comprised of only two data points (initial and final). (Exp. = Experiment, P = Picophytoplankton, N= Nanophytoplankton, Inc= Incubation).

Exp.	Bottle	Prey	Inc. Time (h)	Estimate (h ⁻¹) (Net growth rates)	Std.Err	Statistic	p. value
MEDH_1	S ₁	P	4.9	-0.111	0.026	-4.26	0.0037
	S _{0.75}	P		-0.066	0.011	-5.95	0.0006
	S _{0.5}	P		-0.094	0.011	-8.35	6.90E-05
	S _{0.25}	P		-0.091	0.025	-3.63	0.0084
	S ₁	N		-0.015	0.009	-1.65	0.1435
	S _{0.75}	N		-0.016	0.012	-1.29	0.2385
	S _{0.5}	N		0.003	0.010	0.29	0.7768
	S _{0.25}	N		0.011	0.001	1.07	0.3189
MEDH_2	S ₁	P	5.7	-0.077	0.024	-3.19	0.0153
	S _{0.75}	P		-0.057	0.012	-4.62	0.0024
	S _{0.5}	P		-0.067	0.021	-3.20	0.0151
	S _{0.25}	P		-0.049	0.012	-4.12	0.0045
	S ₁	N		-0.077	0.014	-5.24	0.0012
	S _{0.75}	N		-0.028	0.011	-2.57	0.0368
	S _{0.5}	N		-0.079	0.006	-13.14	0.0000
	S _{0.25}	N		-0.032	0.016	-1.97	0.0892
ANT_1	S ₁	N	3.6	-0.013	0.001	-	-
	S _{0.5}	N		0.028	0.022	-	-
	S _{0.25}	N		0.031	0.009	-	-
ANT_2	S ₁	N	2.9	-0.016	0.005	-	-
	S _{0.5}	N		0.003	0.003	-	-
	S _{0.25}	N		0.013	0.001	-	-
ANT_3	S ₁	N	8.8	0.005	0.018	-	-

ANT_4	$S_{0.5}$	N	8.6	0.093	0.010	-	-
	$S_{0.25}$	N		0.143	0.016	-	-
	S_1	N		-0.035	0.004	-	-
	$S_{0.5}$	N		-0.020	0.004	-	-
	$S_{0.25}$	N		-0.017	0.005	-	-

Table S3.5. Log-linear regression fits results of cell concentrations vs time. (Exp. = Experiment, P = Picophytoplankton, N= Nanophytoplankton).

Exp	Bottle	Prey	Estimate (h ⁻¹) (Net growth rates)	Std.Err	Statistic	p.value
MEDH_3	S+FSW	P	-0.04	0.008	-5.38	0.0010
	S+G _{1:4}	P	-0.06	0.007	-8.36	7.98E-06
	S+G _{1:2}	P	-0.06	0.010	-5.81	0.00017
	S+G _{1:1}	P	-0.06	0.006	-8.63	5.98E-06
	S+FSW	N	-0.06	0.01	-4.62	2.41E-03
	S+G _{1:4}	N	-0.09	0.01	-8.04	1.13E-05
	S+G _{1:2}	N	-0.10	0.01	-8.82	4.98E-06
	S+G _{1:1}	N	-0.13	0.01	-16.04	1.83E-08
MEDH_4	S+FSW	P	-0.04	0.01	-3.87	3.11E-03
	S+G _{1:4}	P	-0.07	0.01	-5.64	2.16E-04
	S+G _{1:1}	P	-0.03	0.01	-3.86	3.18E-03
	S+FSW	N	-0.04	0.01	-4.29	1.58E-03
	S+G _{1:4}	N	-0.08	0.01	-6.43	7.51E-05
	S+G _{1:1}	N	-0.05	0.01	-4.35	1.45E-03

Table S3.6. Results of the exponential sigmoidal function fit. Two parameters of the function are detailed (p = higher asymptote, r =recovery rate constant). (Exp= Experiment).

Exp.	Bottle	Parameter	Estimate	Std.Err	t.value	p.value	df
MEDH_1	S_1	Higher assym. (p)	0.444	0.007	65.6	<2.00E-16	12
	S_1	Recovery rate contant (r)	4.066	0.424	9.6	5.58E-07	12
	$S_{0.75}$	Higher assym. (p)	0.473	0.006	75.0	<2.00E-16	12
	$S_{0.75}$	Recovery rate contant (r)	3.578	0.349	10.3	2.70E-07	12
	$S_{0.5}$	Higher assym. (p)	0.471	0.007	70.7	<2.00E-16	12
	$S_{0.5}$	Recovery rate contant (r)	3.728	0.358	10.4	2.33E-07	12
	$S_{0.25}$	Higher assym. (p)	0.458	0.007	69.2	<2.00E-16	12
	$S_{0.25}$	Recovery rate contant (r)	3.779	0.364	10.4	2.42E-07	12
MEDH_2	S_1	Higher assym. (p)	0.457	0.008	59.8	3.53E-15	11
	S_1	Recovery rate contant (r)	3.172	0.299	10.6	4.10E-07	11
	$S_{0.75}$	Higher assym. (p)	0.470	0.007	63.6	1.79E-15	11
	$S_{0.75}$	Recovery rate contant (r)	2.871	0.246	11.7	1.54E-07	11
	$S_{0.5}$	Higher assym. (p)	0.473	0.008	61.6	2.56E-15	11
	$S_{0.5}$	Recovery rate contant (r)	2.673	0.234	11.4	1.94E-07	11
	$S_{0.25}$	Higher assym. (p)	0.464	0.006	82.6	<2.00E-16	11

	$S_{0.25}$	Recovery rate contant (r)	2.689	0.179	15.0	1.11E-08	11
MEDH_3	S+FSW	Higher assym. (p)	0.483	0.008	61.0	3.42E-14	10
	S+FSW	Recovery rate contant (r)	0.898	0.195	4.6	0.001	10
	S+G _{1:4}	Higher assym. (p)	0.485	0.006	76.8	3.41E-15	10
	S+G _{1:4}	Recovery rate contant (r)	0.884	0.147	6.0	0.000132	10
	S+G _{1:2}	Higher assym. (p)	0.486	0.006	85.2	1.21E-15	10
	S+G _{1:2}	Recovery rate contant (r)	0.983	0.142	6.9	4.06E-05	10
	S+G _{1:1}	Higher assym. (p)	0.475	0.005	90.2	6.89E-16	10
	S+G _{1:1}	Recovery rate contant (r)	1.065	0.151	7.1	3.46E-05	10
MEDH_4	S+FSW	Higher assym. (p)	0.490	0.007	73.5	8.10E-14	9
	S+FSW	Recovery rate contant (r)	2.531	0.537	4.7	0.001	9
	S+G _{1:4}	Higher assym. (p)	0.481	0.005	101.1	4.60E-15	9
	S+G _{1:4}	Recovery rate contant (r)	2.672	0.342	7.8	2.68E-05	9
	S+G _{1:1}	Higher assym. (p)	0.463	0.007	65.9	2.15E-13	9
	S+G _{1:1}	Recovery rate contant (r)	2.056	0.419	4.9	0.001	9
ANT_1	S_1	Higher assym. (p)	0.398	0.018	22.6	2.26E-05	4
	S_1	Recovery rate contant (r)	2.671	0.489	5.5	0.005	4
	$S_{0.5}$	Higher assym. (p)	0.372	0.014	26.6	1.42E-06	5
	$S_{0.5}$	Recovery rate contant (r)	1.981	0.276	7.2	0.001	5
	$S_{0.25}$	Higher assym. (p)	0.315	0.016	19.3	4.28E-05	5
	$S_{0.25}$	Recovery rate contant (r)	1.536	0.259	5.9	0.004	5
ANT_2	S_1	Higher assym. (p)	0.491	0.006	83.5	4.71E-13	8
	S_1	Recovery rate contant (r)	5.175	0.519	10.0	8.67E-06	8
	$S_{0.5}$	Higher assym. (p)	0.427	0.008	56.7	1.04E-11	8
	$S_{0.5}$	Recovery rate contant (r)	3.144	0.457	6.9	0.0001	8
	$S_{0.25}$	Higher assym. (p)	0.416	0.013	33.1	7.50E-10	8
	$S_{0.25}$	Recovery rate contant (r)	3.580	0.989	3.6	0.0068	8
ANT_3	S_1	Higher assym. (p)	0.358	0.030	11.9	6.66E-06	7
	S_1	Recovery rate contant (r)	2.712	1.022	2.7	0.033	7
	$S_{0.5}$	Higher assym. (p)	0.342	0.030	11.6	2.50E-05	7
	$S_{0.5}$	Recovery rate contant (r)	1.957	0.579	3.4	0.014825	7
	$S_{0.25}$	Higher assym. (p)	0.369	0.049	7.5	0.000292	6
	$S_{0.25}$	Recovery rate contant (r)	1.318	0.459	2.9	0.028	6
ANT_4	S_1	Higher assym. (p)	0.523	0.012	42.4	1.51E-13	11
	S_1	Recovery rate contant (r)	2.079	0.255	8.2	5.40E-06	11
	$S_{0.5}$	Higher assym. (p)	0.474	0.009	50.1	2.47E-14	11
	$S_{0.5}$	Recovery rate contant (r)	2.381	0.237	10.1	6.93E-07	11
	$S_{0.25}$	Higher assym. (p)	0.386	0.006	59.8	3.55E-15	11
	$S_{0.25}$	Recovery rate contant (r)	2.342	0.210	11.2	2.41E-07	11

3.3 ADDITIONAL INFORMATION

G. dominans-specific grazing

Setup 2 (*G. dominans* addition experiments) altered the natural grazing pressure by adding a non-stressed cultured grazer (*G. dominans*). The setup analysed the total grazing observed but additional information could be retrieved from these two experiments (MEDH_3 and MEDH_4). The bottle with only natural grazers (S+FSW) was used to correct the consumption rates in the boosted incubations to obtain the *G. dominans*-specific grazing. The following metrics were used: overall grazing ($g: h^{-1}$) and ingestion rates (ING: $cell \cdot hr^{-1} \cdot grazer^{-1}$). We differentiated between the grazing rates obtained in each bottle (g) and the individual performance of the grazers in each of the proportions used (ING). Grazing and ingestion rates and average prey concentrations were calculated using Frost's (1972) equations. The corrected values provided information on the extra grazing ($g: h^{-1}$) induced by *G. dominans* whilst also evaluating its grazing performance with individual ingestion rates (ING: cells/ind/hr) (Figure S3.1). The analysis considered solely the initial ($t=1h$) and final ($t=4h$) time points. The additional grazing (g) of *G. dominans* was similar between incubations with different grazer proportions in MEDH_3 experiment. While the highest picophytoplankton grazing was detected in the S+G_{1:2} bottle, larger rates were obtained in S+G_{1:1} for the nanophytoplankton. Individual ingestion rates determined 1:2 and 1:4 as the proportions where *G. dominans* performed better depending on the phytoplankton population analysed. The MEDH_4 picophytoplankton results established the 1:2 proportion as the best option to induce grazing (g) and obtain the larger individual *G. dominans* rates. The bottle S+G_{1:1} exhibited lower grazing rates than the incubation with only natural grazers (S+FSW) resulting in negative values. Overall, the lowest addition of *G. dominans* was the optimal choice to ensure higher induced grazing.

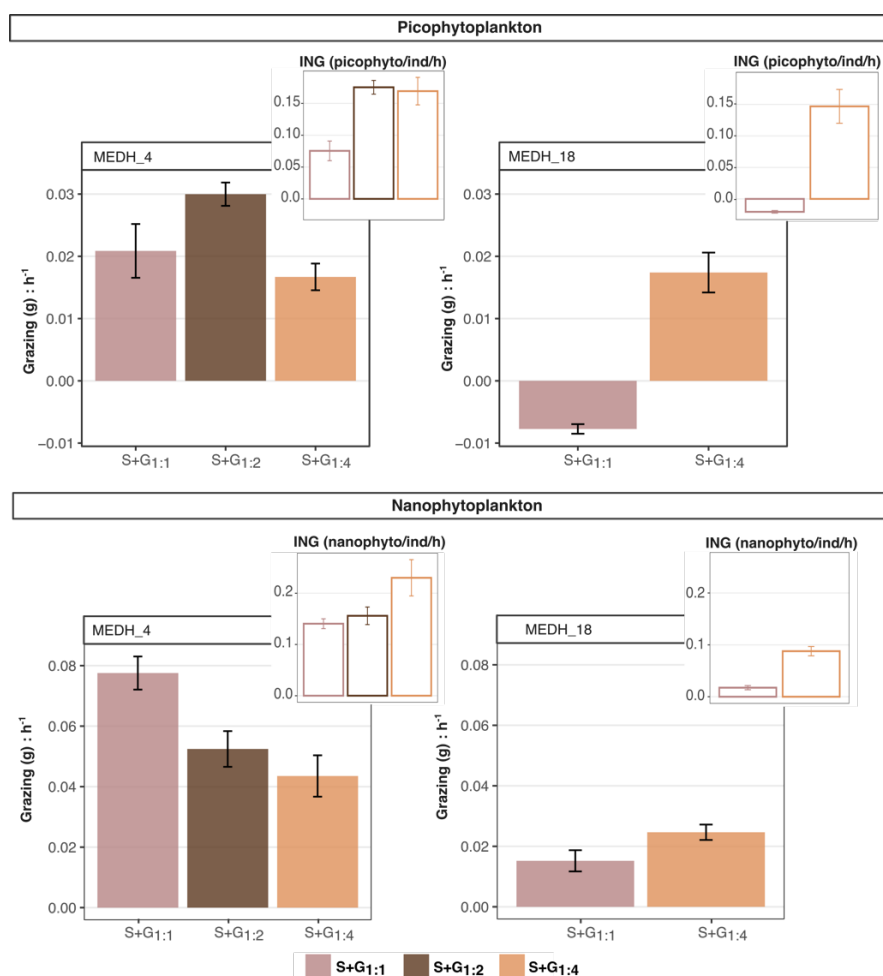


Figure S3.1. The grazing rates ($g: h^{-1}$) and individual ingestion rates (ING: cells/ind/h) of *G. dominans* addition experiments. The filled bars of the main plots represent the grazing rate. The smaller plots with empty bars illustrate the individual ingestion rates of each experiment. Data is given for each bottle (x-axis). Error bars represent the standard error.

ANT_5: Chemical additions experiment

An extra experiment was performed within the ANT set to modify grazing pressure without the need for a dilution series. The approach inoculated three potential chemical cues to cause interferences in chemotactic-driven grazing relationships. The chemicals tested were DMSP, DMS, and acrylate. MQ water was used in the control bottle. When grazing was evaluated, the ANT_5 also presented different net growth rates between control and chemically-treated bottles with either DMSP, DMS, or acrylate (Figure S3.2 A, Table S3.7). The highest grazing occurred in the control bottle where MQ water was added. The incubations with chemical additions presented higher net growth rates, so less grazing was presumed. DMSP and DMS induced similar net growth rates while acrylate addition caused positive rates indicating a modest net growth. Photosynthetic efficiency recovery was assessed by monitoring F_v/F_m' values after the tress treatment. The exponential sigmoidal function fitted to the temporal series of F_v/F_m' data allowed the observation of the recovery dynamics (Figure S3.2 B). The recovery rate constant (r : h^{-1}) described how rapidly saturation was reached. Although recovery dynamics appeared similar between treatments, minor differences were observed between the recovery rate constants (Table S3.8). Remarkably, when net growth rates were aligned with the recovery rate constants, a subtle positive relation was inferred (Figure S3.2 C). The higher rates of both metrics were detected in the control bottle with MQ and the lower ones in the one treated with acrylate. DMSP- and DMS-treated bottles clustered together at the middle range of both metrics. Overall, higher net growth rates matched with higher recovery rates as presented in the main text for most of the experiments of section 3.3.

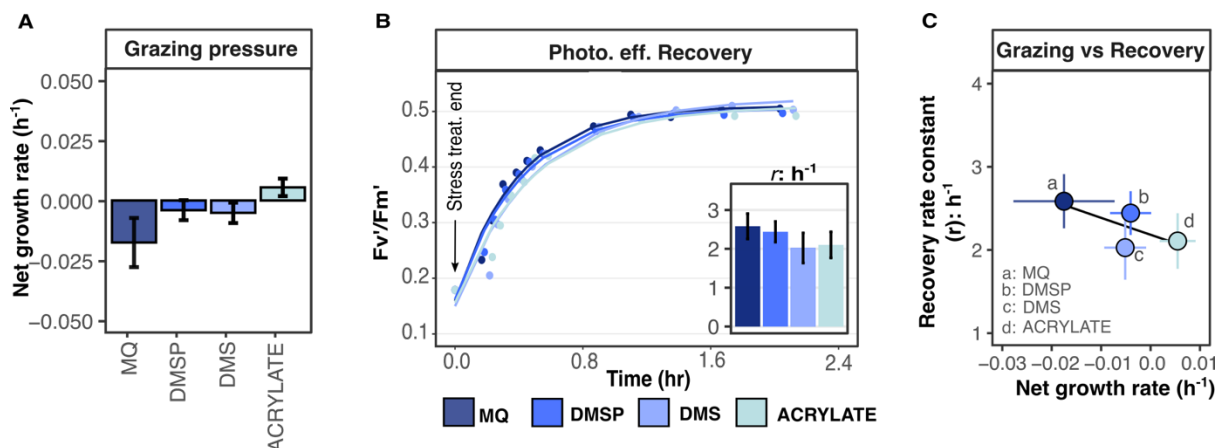


Figure S3.2. (A). Net growth rates of each experimental bottle (x-axis) calculated by a logarithmic model. (B). Temporal series of F_v/F_m' values illustrating the recovery dynamics. The fitted sigmoidal curve is represented over the monitored data. The specific recovery rate constants (r) of each bottle are presented as bars within the small subplot and identified with the colour code. (C). Individual dot plot relating the recovery rate constants (y-axis) with the net growth rates (x-axis). All four bottles were plotted together and represented with individual dots. Model I regression analysis was fit into the data and represented by a straight line.

Table S3.7. Net growth rates of each experimental bottle (x-axis) calculated by a logarithmic model (Exp. = Experiment, N= Nanophytoplankton, Inc= Incubation).

Exp.	Bottle	Prey	Inc. Time (h)	Estimate (h^{-1}) (Net growth rates)	Std.Err
ANT_5	MQ	N	4.5	-0.0175	0.0102
	DMSP	N		-0.0040	0.0042
	DMS	N		-0.0051	0.0042
	ACRYLATE	N		0.0055	0.0036

Table S3.8. Results of the exponential sigmoidal function fit. Two parameters of the function are detailed (p = higher asymptote, r =recovery rate constant). (Exp= Experiment).

Exp.	Bottle	Parameter	Estimate	Std.Err	t.value	p.value	df
ANT_5	MQ	Higher assym. (p)	0.510	0.012	40.9	1.54E-11	9
	MQ	Recovery rate contant (r)	2.581	0.326	7.9	2.39E-05	9
	DMSP	Higher assym. (p)	0.506	0.011	47.5	4.10E-12	9
	DMSP	Recovery rate contant (r)	2.439	0.263	9.3	6.78E-06	9
	DMS	Higher assym. (p)	0.524	0.022	24.1	1.73E-09	9
	DMS	Recovery rate contant (r)	2.023	0.385	5.3	0.000525	9
	ACRYLATE	Higher assym. (p)	0.510	0.017	30.0	2.46E-10	9
	ACRYLATE	Recovery rate contant (r)	2.103	0.334	6.3	0.000143	9

3.4. The relationship of light stress and grazing in a model system: *G. dominans* grazing on *I. galbana*

Table S3.9 Regression analysis on log-transformed cell concentration and ANCOVA statistical test results between slopes of control and stress communities with added *G. dominans* (S+G vs C+G). Regressions on bottles with only control or stressed *I. galbana* (S or C) were only performed at 5h incubation time. (Exp. = Experiment, Inc= Incubation, C=Control, S= Stress, G= *G. dominans*, Rep=Replicate).

Exp.	Inc. Time	Parameter	Estimate	Std.err	Statistic	p.value	Bottle	Rep.
ISO_1	2h	Intercept	8.973	0.061	147.52	6.55E-12	C+G	1
		Slope	-0.493	0.044	-11.10	3.18E-05	C+G	1
		Intercept	8.940	0.027	333.09	5.80E-16	C+G	2
		Slope	-0.452	0.021	-21.76	1.09E-07	C+G	2
		Intercept	9.046	0.017	527.54	3.13E-15	S+G	1
		Slope	-0.237	0.013	-18.92	1.41E-06	S+G	1
		Intercept	9.020	0.016	560.51	1.52E-17	S+G	2
		Slope	-0.271	0.012	-21.71	1.11E-07	S+G	2
		Slope:Bottle			70.34	2.32E-09	C+G vs S+G	all
	5h	Intercept	8.829	0.052	168.89	5.15E-26	C+G	1
		Slope	-0.360	0.017	-21.44	1.15E-12	C+G	1
		Intercept	8.893	0.035	253.50	2.89E-30	C+G	2
		Slope	-0.407	0.012	-35.16	1.41E-16	C+G	2
		Intercept	9.028	0.022	412.28	7.93E-32	S+G	1
		Slope	-0.233	0.007	-33.15	1.90E-15	S+G	1
		Intercept	8.979	0.018	504.57	4.78E-35	S+G	2
		Slope	-0.227	0.006	-38.62	3.17E-17	S+G	2
		Intercept	8.948	0.018	491.91	7.17E-35	C	1

		Slope	0.009	0.006	1.52	1.49E-01	C	1
		Intercept	8.974	0.023	389.06	3.06E-33	C	2
		Slope	0.022	0.008	2.92	1.01E-02	C	2
		Intercept	9.017	0.016	556.21	1.00E-35	S	1
		Slope	0.019	0.005	3.57	2.58E-03	S	1
		Intercept	8.984	0.027	338.26	2.87E-32	S	2
		Slope	0.017	0.009	1.91	7.39E-02	S	2
		Slope:Bottle			167.45	9.01E-20	C+G vs S+G	all
ISO_2	2h	Intercept	10.531	0.031	342.75	4.01E-12	C+G	1
		Slope	-0.120	0.022	-5.54	2.63E-03	C+G	1
		Intercept	10.478	0.010	1062.46	1.73E-19	C+G	2
		Slope	-0.128	0.008	-16.70	6.74E-07	C+G	2
		Intercept	10.508	0.029	360.18	3.13E-12	S+G	1
		Slope	-0.054	0.021	-2.64	4.61E-02	S+G	1
		Intercept	10.493	0.019	562.35	1.48E-17	S+G	2
		Slope	-0.100	0.014	-6.89	2.33E-04	S+G	2
		Slope:Bottle			4.50	4.29E-02	C+G vs S+G	all
	5h	Intercept	10.549	0.024	441.73	1.01E-24	C+G	1
		Slope	-0.136	0.007	-18.52	1.22E-09	C+G	1
		Intercept	10.479	0.014	744.97	1.74E-31	C+G	2
		Slope	-0.124	0.005	-26.72	9.55E-13	C+G	2
		Intercept	10.541	0.020	519.40	1.69E-25	S+G	1
		Slope	-0.090	0.006	-14.40	1.75E-08	S+G	1
		Intercept	10.466	0.024	437.68	1.75E-28	S+G	2
		Slope	-0.061	0.008	-7.69	3.44E-06	S+G	2
		Intercept	10.366	0.021	497.57	2.92E-27	C	1
		Slope	0.004	0.007	0.59	5.69E-01	C	1
		Intercept	10.515	0.038	276.76	6.75E-26	C	2
		Slope	-0.001	0.013	-0.09	9.32E-01	C	2
		Intercept	10.537	0.019	554.78	7.92E-28	S	1
		Slope	-0.005	0.006	-0.76	4.60E-01	S	1
		Intercept	10.490	0.016	644.17	1.15E-30	S	2
		Slope	0.003	0.005	0.64	5.33E-01	S	2
		Slope:Bottle			55.20	1.02E-09	C+G vs S+G	all
ISO_3	2h	Intercept	10.815	0.013	814.02	2.32E-16	C+G	1
		Slope	-0.049	0.010	-5.08	2.26E-03	C+G	1
		Intercept	10.777	0.022	488.99	3.43E-19	C+G	2
		Slope	-0.061	0.018	-3.39	9.43E-03	C+G	2

		Intercept	10.727	0.039	277.58	2.08E-15	S+G	1
		Slope	-0.052	0.030	-1.74	1.25E-01	S+G	1
		Intercept	10.747	0.017	624.89	7.10E-18	S+G	2
		Slope	-0.084	0.013	-6.28	4.12E-04	S+G	2
		Slope:Bottle			0.60	4.43E-01	C+G vs S+G	all
	5h	Intercept	10.828	0.012	880.59	1.60E-23	C+G	1
		Slope	-0.063	0.004	-14.70	1.35E-07	C+G	1
		Intercept	10.761	0.019	578.60	5.16E-26	C+G	2
		Slope	-0.040	0.007	-5.67	1.45E-04	C+G	2
		Intercept	10.712	0.027	401.75	2.25E-22	S+G	1
		Slope	-0.034	0.010	-3.51	5.59E-03	S+G	1
		Intercept	10.710	0.024	445.38	7.23E-19	S+G	2
		Slope	-0.040	0.012	-3.30	1.09E-02	S+G	2
		Intercept	10.767	0.018	606.07	3.68E-24	C	1
		Slope	0.004	0.006	0.57	5.80E-01	C	1
		Intercept	10.785	0.015	715.52	7.00E-25	C	2
		Slope	0.013	0.006	2.28	4.59E-02	C	2
		Intercept	10.648	0.028	381.77	3.74E-22	S	1
		Slope	-0.002	0.010	-0.20	8.46E-01	S	1
		Intercept	10.760	0.022	486.22	3.33E-23	S	2
		Slope	0.010	0.008	1.28	2.29E-01	S	2
		Slope:Bottle			2.98	9.17E-02	C+G vs S+G	all

Table S3.10. Results of the exponential sigmoidal function fit. Two parameters of the function are detailed (p = higher asymptote, r =recovery rate constant). (Exp= Experiment, Rep=Replicate).

Exp.	Bottle	Rep.	Parameter	Estimate	Std.Error	t.value	p.value	df
ISO_1	S	1	Higher assym. (p)	0.432	0.009	48.34	3.48E-12	9
	S	1	Recovery rate contant (r)	2.186	0.142	15.42	8.88E-08	9
	S+G	1	Higher assym. (p)	0.368	0.009	39.46	2.15E-11	9
	S+G	1	Recovery rate contant (r)	2.838	0.292	9.72	4.53E-06	9
	S	2	Higher assym. (p)	0.414	0.009	44.09	7.93E-12	9
	S	2	Recovery rate contant (r)	2.459	0.203	12.14	6.98E-07	9
	S+G	2	Higher assym. (p)	0.369	0.011	33.35	9.66E-11	9
	S+G	2	Recovery rate contant (r)	3.339	0.482	6.93	6.81E-05	9
ISO_2	S	1	Higher assym. (p)	0.380	0.009	40.43	2.57E-13	11
	S	1	Recovery rate contant (r)	3.744	0.484	7.73	9.00E-06	11
	S+G	1	Higher assym. (p)	0.344	0.007	46.16	6.04E-14	11
	S+G	1	Recovery rate contant (r)	4.830	0.646	7.47	1.24E-05	11

	S	2	Higher assym. (p)	0.377	0.008	48.96	3.17E-14	11
	S	2	Recovery rate contant (r)	3.756	0.402	9.35	1.44E-06	11
	S+G	2	Higher assym. (p)	0.349	0.005	65.90	1.22E-15	11
	S+G	2	Recovery rate contant (r)	4.660	0.425	10.96	2.94E-07	11
ISO_3	S	1	Higher assym. (p)	0.487	0.012	39.73	3.51E-05	3
	S	1	Recovery rate contant (r)	3.487	0.635	5.49	1.19E-02	3
	S+G	1	Higher assym. (p)	0.472	0.008	61.77	9.35E-06	3
	S+G	1	Recovery rate contant (r)	3.796	0.474	8.01	4.07E-03	3
	S	2	Higher assym. (p)	0.504	0.013	39.94	3.45E-05	3
	S	2	Recovery rate contant (r)	2.990	0.487	6.14	8.70E-03	3
	S+G	2	Higher assym. (p)	0.508	0.010	49.52	1.81E-05	3
	S+G	2	Recovery rate contant (r)	3.465	0.504	6.88	6.29E-03	3

GENERAL DISCUSSION

This thesis investigated the implications of light stress on phytoplankton in microscale trophic interactions. Four main hypotheses describe a potential sequential process: (i) DMSP triggers positive chemotaxis in herbivore protists; (ii) phytoplankton release DMSP under light-stress; (iii) there is higher grazing on stressed phytoplankton; (iv) higher grazing rates on stressed cells helps the phytoplankton assemblage to recover from stress.

The healthy herds hypothesis

The concept of selective grazing on stressed prey introduces the healthy herds hypothesis (Packer et al., 2003) in marine microbial ecosystems. The idea of preferential predation on individuals whose consumption does not significantly impact the prey population dates back to the last century (Slobodkin, 1974; Temple, 1987). Slobodkin (1974) elaborated on this concept, termed “prudent predation”, in terrestrial environments, examining the hunting behaviour of wolves. He highlighted the wolves’ selective predation on very young, old or weakened animals, which would make them act as “prudent” predators by removing animals with a high likelihood of dying anyway (Slobodkin, 1974). Additionally, he described how the chase was either abandoned or continued depending on the prey response. Selectivity was explained in relation to prey size, behaviour and flavour, recognizing the role of chemicals in triggering preference. Interestingly, he clarified that “prudence” refers to the type of prey selected and not to the quantity of prey taken.

Later studies on the hypothesis focused on the reasons behind the preference towards weak individuals, proposing the ease of capture as a direct influence on selection (Temple, 1987). More recent investigations using large sample sizes and measuring multiple prey traits confirmed non-random killing by predators, and suggested that weaker individuals with specific traits were preferentially targeted (Genovart et al., 2010). Alterations in the prey behaviour were again identified as a critical factor in increasing prey susceptibility.

A significant portion of most recent research explores the relationship between parasitic infections and predation (Duffy et al., 2005; Gutierrez et al., 2022; Packer et al., 2003; Park et al., 2021; Williams, 2008). Selective predation on infected organisms has been substantially investigated also in protists, inferring implications for predator control over parasitic and viral diseases (Duffy et al., 2005; Evans & Wilson, 2008; Packer et al., 2003). However, although less considered, preferential predation on healthy (uninfected) individuals has also been reported and related to host traits and variations in disease response (Gutierrez et al., 2022; Williams, 2008). Regardless of whether predation is enhanced or discouraged on unhealthy, stressed, or infected individuals, there is a consensus that changes in traits and behaviour are key factors shaping predator-prey interactions.

Light stress and phytoplankton grazing

The third chapter of this thesis discusses the consequences of ephemeral light stress on phytoplankton grazing interactions. We hypothesize that light-induced DMSP exudation would alter the chemical signature (“smell” or “flavour”) of the prey. The chemoattraction role of DMSP documented in herbivore protists in Chapter 1 would facilitate the capture of the prey (“ease of capture”) promoting the chase and potentially favouring preferential grazing. The examination of the photosynthetic efficiency recovery aims to provide evidence regarding the benefits of selective predation for the entire phytoplankton assemblage. In terrestrial systems, the advantages of removing sick or weak individuals are assumed to be related to reproductive success and population strength through natural selection (Genovart et al., 2010). However, demonstrating these benefits in protist communities is more challenging. Laundon et al. (2021) provided the first evidence of improved overall health in a diatom population due to the selective targeting of low-fitness diatom cells by a thraustochytrid parasite. Our study in Chapter 3

aligns with this concept, showing a positive correlation between increased grazing rate and faster photosynthetic recovery of the phytoplankton assemblage. Therefore, this thesis provided the first preliminary evidence for the benefits of preferential predation in protist communities.

While the overall story would be strengthened by confirming and aligning all four suggested steps with the healthy herds hypothesis, each of the four can be independently tested and validated, without the other three needing to be met. Each proposition offers an intriguing research objective with significant ecological implications. In this general discussion, I will further explore key concepts and pivotal implications that are highly connected to our study.

The plankton interactome

This thesis links the observation of enhanced grazing on stressed prey to DMSP exudation caused by light stress. However, there is active discussion about the importance of assessing these events in realistic contexts, acknowledging the complex chemical environment present on the microscale (Clerc et al., 2022, 2023; Kuhlisch et al., 2024). Studying microbial chemotaxis is typically approached with simple model systems involving one organism and one infochemical (Kuhlisch et al., 2024 and references therein). This reductionist approach enables the detailed examination of chemotaxis assessing both the chemical gradients and the response of the organisms. While these methods are crucial and have yielded significant knowledge (e.g. Breckels et al., 2011; Harvey et al., 2013; Roberts et al., 2011; Seymour et al., 2010) they provide a limited understanding of the real world by ignoring the actual biotic and abiotic context of natural microbial communities.

Our current understanding of the marine pelagic microscale environments describes them as complex, highly heterogeneous, and dynamic (Stocker, 2012). As a result, dynamic, multi-faceted interactions involving organisms of several trophic levels are expected to occur within a seascape of chemical gradients (Kuhlisch et al., 2024; Stocker & Seymour, 2012). The term "plankton interactome" aptly describes this intricate network of organisms and associations (Kuhlisch et al., 2024; Lima-Mendez et al., 2015). Most of the studies on microbial chemical ecology focus on one interaction restricted in terms of time, space and microbial species. However, some investigations have provided compelling evidence about elaborated chemical interactions. Oxylipins released by diatoms can negatively affect the grazing and growth of heterotrophic protists and influence mesozooplankton behaviour (Kå et al., 2014). These compounds trigger positive chemoattraction of copepods and increase their grazing at low concentrations, but cause their death at high concentrations (Kå et al., 2014). Additionally, decadienal induces the ingestion rate of non-diatom prey by heterotrophic protists, acting as a competitive advantage for diatom producers (Franzè et al., 2018). The haptophyte *Phaeocystis globosa* can distinguish the type of predator present, triggering differential defensive responses: colony formation is enhanced when ciliates grazing on individual cells are present, while it is suppressed under dominance of colony-feeding copepods (Long et al., 2007). Although these behavioural and morphological changes are induced by the sole presence of the grazer, they can influence other interactions and trigger trophic cascades (Kuhlisch et al., 2024). Both in the haptophyte and the diatom examples, tri-trophic interactions or trophic cascades are involved in the system, evidencing the high feasibility of multi-scale responses.

DMSP and DMS are also important candidates for triggering tri-trophic relationships and meso- and large-scale interactions (Steinke et al., 2002). DMSP exudation might initiate a chain of trophic events by generating attractive hot spots (phytoplankton cells, faecal pellets, marine snow aggregates) where microzooplankton grazing is enhanced (as discussed in Chapter 1). Feeding on DMSP-rich particles leads to DMS (and acrylate) production which, in turn, can trigger search behaviour (Steinke et al., 2006) and enhance predation by mesozooplankton (Shemi et al., 2021). The tri-trophic interaction developed will increase microzooplankton mortality and reduce grazing pressure on phytoplankton. The generation

of a grazing hot spot is at the same time a focal point of infochemicals that can affect higher-scale processes such as migration patterns aimed at locating prey and activating a particular feeding mode (Steinke et al., 2002). The volatile properties of DMS, together with its role as a chemoattractant for high-order predators with olfactory foraging, like procellariiform birds, penguins, or seals (Cunningham et al., 2008; Kowalewsky et al., 2006; Nevitt, 2008), can link microenvironment processes to larger-scale behaviours, influencing ecological interactions both in the surface ocean and up in the air (Simó, 2001; Steinke et al., 2002).

In addition to a single compound interacting with different trophic levels, chemical communication also implies a bidirectional exchange of compounds. Chemical arms race and defensive responses are usually developed under these circumstances (Pohnert et al., 2007; Smetacek, 2001). The release of copepodamides, sensed by phytoplankton species such as diatoms and dinoflagellates, induces a chemical response producing the release of domoic acid and saxitoxins, known for their anti-grazer functions (Selander et al., 2019). Our study missed the bidirectional component of the interactions examined because chemical responses induced by additions of grazer were overlooked. However, I participated in an experiment on the production and release of volatile organic compounds by the two partners in a prey-predator interaction, whose information can be found in Annex I.

To better comprehend all these complex, multi-faceted and multi-scale chemical interactions, a holistic view that considers the biotic, environmental, and chemical context is crucial (Kuhlisch et al., 2024). The synergistic effect of DMSP in enhancing chemotaxis towards polysaccharides (Clerc et al., 2023), or the DMSP-fired pathogenic switch of *Sulfitobacter* sp. on *Emiliana huxleyi* (Barak-Gavish et al., 2018, 2023) are two good examples of the importance of the chemical microenvironment. The environmental context, shaped by abiotic factors like light, temperature, nutrient concentrations or pH, directly influences organisms' physiology and behaviour (Archer et al., 2018; Johnson et al., 2022; Kennedy et al., 2012; Righetti et al., 2019; Sobrino et al., 2014; Strom et al., 2020; Sunda et al., 2002). Therefore, the role of these factors in chemotactic interactions cannot be dismissed. The consequences of light-stress events on microplanktonic communities and how phytoplankton stress has consequences for the whole trophic web have been discussed in Chapter 3. Overall, although our study evaluated chemotactic relationships per se in a reductionist manner in Chapter 1, their consequences were either evaluated or discussed from an ecological perspective.

Cell aggregation. Benefit or drawback?

Our research evidences microorganism behaviours like organization, association or congregation. Aggregation is ubiquitous across all forms of marine life from microbes to birds, fishes and dolphins, as a strategy to fulfil social, foraging, defence and reproductive functions (Falgueras-Cano et al., 2022). It emerges as a response to both external forcings and internal dynamics (Levin, 1994), and therefore it is determined by environmental drivers, the relationships within a community, and the physiological needs of the organisms (Falgueras-Cano et al., 2022). In protistan ecology, resource acquisition and defence mechanisms are the two functions most commonly hypothesised to be behind aggregation (Levin, 1994). In both cases, chemical communication is key to initiating and maintaining aggregations.

Heterogeneity at the microscale, characterised by distinct hot spots interconnected by chemical gradients, stimulates aggregation of organisms spanning multiple trophic levels (Pohnert et al., 2007; Steinke et al., 2002; Stocker & Seymour, 2012). Is aggregation advantageous or disadvantageous for microplanktonic organisms? As is typical in scientific inquiries, the answer is complex and context-dependent. Depending on the specific processes under investigation, one may argue for either the drawbacks or the benefits of aggregating. The spatial distribution of resources within a dynamic environment (Stocker, 2012) favours cell congregations as a key surviving mechanism (Cordero & Datta, 2016). In the case of multi-species aggregations, consumption and transformation of resources concurs with ecological interactions. Thus, the colonization of a microenvironment will be determined by

swimming behaviours, chemotactic abilities and surface attachment mechanisms, but the residence time and the organism's success within the aggregation will be highly influenced by quorum sensing, chemical antagonisms, metabolic benefits, and symbiotic relationships (Cordero & Datta, 2016; Gralka et al., 2020).

Within aggregations, both cooperative and competitive interactions emerge. On the one hand, proximity facilitates the exchange of diffusible metabolites with surrounding cells, enabling organic matter transformations through complementary metabolic pathways (Cordero & Datta, 2016; Seymour et al., 2017). Community members can interchange trophic resources and nutrients and use each other's waste products. All these processes can enhance growth and promote anti-predator strategies by collective defensive mechanisms or protective structures (Cordero & Datta, 2016). On the other hand, competition for resources can trigger the exudation of toxic and allelopathic compounds, or favour stress conditions by resource scarcity (Cordero & Datta, 2016; Franzè et al., 2018; Kuhlisch et al., 2024). Reproduction impairments due to intraspecific competition, or the enhanced success and transmission of parasites, pathogens and viruses can also compromise survival in aggregates (Kuhlisch et al., 2024). This may result in growth inhibition of some microorganisms. Additionally, cell congregation implies a high concentration of grazers, which can cause predator interference effects by influencing the ability of individual grazers to ingest prey (Weisse et al., 2016). The drawbacks of responding to hot spots where cells aggregate extend beyond the congregated community. Microbial colonization of an organic matter hot spot may provide an appetizing food option for mesozooplankton organisms capable of finding concentrated prey in a single location (Steinke et al., 2002). Besides causing prey concentration, microbial aggregation transforms the hot spot's environment, inducing the release of secondary metabolites that can in turn act as new chemical gradients. The DMSP/DMS cycle exemplifies how microscale trophic processes driven by chemotaxis to DMSP can scale-up to higher trophic levels due to the volatile properties of evolved DMS and its attractant role for upper-level predators (Kowalewsky et al., 2006; Nevitt, 2008; Steinke et al., 2006). Therefore, aggregation can also expose the colonizer microbes to additional predators by the release of infochemicals. Contemporary literature abounds with studies documenting aggregation patterns in the microscale (e.g. Deuer & Grünbaum, 2006; Harvey et al., 2013; Poulsen et al., 2011; Smriga et al., 2016; Stocker et al., 2008).

Concerning protists and grazing interactions, most of the studies report aggregation in laboratory, culture-based investigations. The implication of chemical signals in the location and congregation mechanisms has been confirmed with protists through microscopic observations (Deuer & Grünbaum, 2006; Harvey et al., 2013, Chapter 1) and micro-fluidic devices (Seymour et al., 2010). Visualization of protist aggregation in prey patches, characterised by fast responses and long residence times, allowed the estimation of higher growth and prey consumption rates for the protists with this ability (Deuer & Grünbaum, 2006; Harvey et al., 2013). Understanding protists' swimming behaviour allowed for a thorough description of their kinetic responses in patches (Fenchel, 2001; Fenchel & Blackburn, 1999). Decreasing swimming velocity, and switching to circular and smaller-pitch helicoidal trajectories result in protists congregation within a food patch (Fenchel & Blackburn, 1999). As a further step to these past observations, in this thesis we were able to also document the swimming behaviour of protistan grazers leaving a chemical patch. Thus, *G. dominans* was strongly attracted to a DMSP point source where it displayed an active search behaviour (Chapter 1). Surprisingly, the dinoflagellate rapidly abandoned the DMSP patch with differential swimming behaviour, changing from convoluted to straight trajectories. We suggest that the absence of actual prey and the inefficient use of DMSP as a substrate were the reasons for avoiding cell accumulation in the chemical patch. Although the trigger for the shape of the outward trajectories remains unknown, the non-accumulation pattern in the absence of food could represent a strategy to evade predation on aggregations. Overall, the results discussed in this thesis support chemotaxis and trophic interactions as key drivers of population/community aggregation.

From micro to macro. A global perspective of microscale processes and their connection with biogeochemical cycles

The cycling of organic matter occurs through both photosynthetic and heterotrophic processes, among which trophic interactions are crucial. While the importance of microscale dynamics in shaping global biogeochemical cycles has been widely recognised (e.g. Clerc et al., 2022; Stocker & Seymour, 2012), a comprehensive understanding of scaling up is still lacking. This field of study encompasses complex relationships, high taxonomic and physiological diversity amongst organisms, and intricate influences of environmental drivers and chemical gradients.

Phototrophy and heterotrophy

The marine biosphere accounts for half of Earth's primary production (Field et al., 1998), with photosynthetic assemblages being the predominant contributors. The comprehensive literature available regarding the fluxes and dynamics of overall marine planktonic primary production contrasts with a still limited knowledge of the identity and ecophysiological diversity of photosynthetic protists (Worden et al., 2015). The variety of protistan morphological structures and physiological requirements advocate for differential dependence on nutrients and elements and distinct responses to environmental factors (Worden et al., 2015). Organisms react to environmental perturbations, undergo stress and respond with coping mechanisms. Amongst the perturbations of environmental conditions that concur, this thesis focused on high solar radiation as a stressor. Natural scenarios leading to exposure to high irradiance conditions include upwelling events, strengthened upper stratification, and cloud cover reduction (Strom et al., 2020). Stratification, where water is retained near the surface under persistent high light (Galí et al., 2013), is likely to gain greater significance in climate warming scenarios owing to the rise in heat fluxes into the ocean (Jackson & Gabric, 2022). Ephemeral or persistent exposure to high solar radiation (and particularly high UV) induces physiological stress, which may lead to reduced photosynthetic performance or damaged cell membranes (Fuentes-Lema et al., 2015; Gorbunov & Falkowski, 2022; Harrison et al., 2015; Sobrino et al., 2004, 2014). Too high doses may end up with irreversible damage and cell death, but periods of reduced sunlight exposure, from vertical mixing to night-time darkness, allow for cell recovery (Franks & Marra, 1994; Harrison et al., 2015; Vincent & Roy, 1993). Our experiments showed variable responses to high light among cultures and natural assemblages of phytoplankton, suggesting that the taxonomic composition and the previous light history were the main influencing factors. The results are in accordance with the highly regionalised responses of photosynthetic assemblages to environmental perturbations (Worden et al., 2015).

Abiotic in situ drivers are interconnected with microscale chemical gradients by inducing physiological responses that lead to the active release or passive exudation of metabolites, conforming the chemical heterogeneous landscape (Cherrier et al., 2015; Fuentes-Lema et al., 2015; Thornton, 2014). As documented in this thesis, light-stress can induce higher concentrations of dissolved DMSP as a potential response to unbalanced growth or compromised membrane permeability. The various responses of the photosynthetic assemblage to stressors generate variability in metabolite exudation (Archer et al., 2018; Moran et al., 2022; Stefels et al., 2007), alter the chemical environment and the partitioning of the particulate and dissolved organic matter (POM and DOM) reservoirs (Cherrier et al., 2015; Fuentes-Lema et al., 2015; Thornton, 2014), and generate variability within the prey pool for grazers (De Lange & Lüring, 2003; Hessen et al., 1997; Strom et al., 2020). All these consequences have important implications in trophic interactions and thus in biogeochemical cycles connecting the cycling of organic matter from photosynthetic to heterotrophic processes.

Heterotrophy oxidises photosynthetic products and remineralises carbon and nutrients. Predators and pathogenic bacteria, parasites and viruses, play an important role in heterotrophy by releasing elements from the particulate fraction (biomass) into the dissolved phase, and making them available to remineralisers (Azam et al., 1983; Worden et al., 2015). Protistan predation is responsible for the consumption of the 49-77% of daily planktonic primary production (Calbet & Landry, 2004; Schmoker

et al., 2013). Microzooplankton (<200 µm) are the main predators in most marine systems but the high variability in their grazing rates and taxonomic composition suggests a diversity in strategies and responses to environmental conditions (Calbet, 2008). This diversity is not represented in current biogeochemical and ecological models (Worden et al., 2015). The lack of complete knowledge about the drivers of prey selection and predation rates, as well as the intricacies of feeding strategies, hinders its full comprehension. Prey selection is known to be driven by prey size (García-Oliva & Wirtz, 2022), biochemical and morphological features (Hamm et al., 2003; Martel, 2006; Meunier et al., 2012), swimming behaviour and turbulent flow (Visser & Kiørboe, 2006), and chemical cues (Pohnert et al., 2007). Environmental stressors are important triggers of prey variability, generating a wide spectrum of stressed individuals with distinct characteristics (Breton et al., 2022; Righetti et al., 2019). The effects of light-stress on photosynthetic organisms are multiple and species- and context-dependent (Vincent & Neale, 2000). Indeed, its consequences on trophic interactions have been seen to be species-specific in culture-based studies (De Lange & Lüring, 2003; Strom et al., 2020). The chapter 3 of the thesis evaluates the consequences of a light-stress event on cultured strains but also on distinct natural communities, with the aim to document a general pattern. The results provide first (yet preliminary) evidence for preferential (faster) consumption of light-stressed phytoplankton. Furthermore, we show that faster consumption results in faster recovery of the prey population photosynthetic efficiency after alleviation of the stress. Although further studies are certainly required to draw conclusions of general applicability, we hope these results will foster research on this topic.

One consequence of exposure to high light is the release of metabolites like DMSP and DMS, which influence the microscale chemical seascape and the prey chemical signature. Chemical cues are important drivers of selective grazing, and DMSP and related compounds are great candidates to influence trophic interactions (Edgcomb, 2021; Shemi et al., 2021; Steinke et al., 2002). The results of chapter 1 document how the same chemical cue can induce different behaviours depending on the grazer feeding mechanism. A strict phago-heterotroph (*G. dominans*) responded to DMSP gradients with a typical exploratory behaviour across the chemical plume, followed by a change to ballistic swimming to rapidly abandon the chemical patch when no prey was found. In contrast, a dinoflagellate with proven osmotrophic capability (*O. marina*) congregated within the chemical patch to take up DMSP as a substrate to satisfy its demand of reduced sulphur. A third dinoflagellate, a mixotroph able to feed via a peduncle (*K. armiger*), showed exploratory behaviour and accumulation within the DMSP patch. This behaviour would allow the protist to increase its proximity to DMSP-leaky particles for feeding via its peduncle or taking advantage of the dissolved substrate via osmotrophy. In brief, grazing selection based on chemotaxis was suggested for the organisms tested and preference to DMSP- or DMS-leaky prey was proposed. Additionally, we related the distinct chemotactic behaviours to each organism's trophic mode, emphasizing the role of patches of dissolved DMSP or DMSP-leaking particles as relevant food resources influencing different heterotrophic strategies.

The carbon cycle

Grazing processes greatly influence the organic matter continuum between the DOM and POM pools, and between recalcitrance and lability (Azam, 1998). Osmotrophs and saprotrophs take advantage of the amalgam of compounds to contribute to the microbial loop and the carbon cycle (Worden et al., 2015). Labile organic matter is rapidly used by bacteria and protists with production of living POM, recirculating the waste products of some organisms into new particulate matter (Cordero & Datta, 2016) that serves as a trophic resource for higher-trophic level organisms. It is not a surprise that the existing diversity of organic compounds is closely associated with an intricate network of heterotrophic capabilities that enable its exploitation (Worden et al., 2015). Currently, new strategies and players in organic matter respiration continue to be discovered such as the emerging significance of marine fungi as eukaryotic saprotrophs (Richards et al., 2012). The diversity of compounds generating gradients in the microscale heterogeneity suggests chemotaxis as a meaningful influencer of the marine carbon cycle. Motility and chemotactic abilities enable bacteria and osmotrophic protists to reach hot spots of

DOM where increased uptake of dissolved carbon is expected (Fenchel & Blackburn, 1999; Stocker, 2012, Chapter 1). This point-sources would trigger an enhanced carbon flux into biomass and finally into the food web. Chemotactic behaviour also impacts particle fluxes and thus carbon sinking from the upper ocean into the deep (Kjørboe & Jackson, 2001; Stocker, 2012). POM degradation in the sunlit ocean is tightly linked to chemical gradients enabling particle colonization events and the development of activity hot spots. Degradation and transformation processes would retain the carbon within the upper ocean, where its flux would be directed to the microbial food webs instead of sinking into the deep ocean (Azam et al., 1983). DMSP involvement in dissolved carbon uptake processes as well as in chemotactic gradients for locating prey and particles, has been also shown and discussed in chapter 1.

The organic sulphur cycle

Understanding the participation of DMSP in the organic matter cycle needs consideration of its important role in the sulphur cycle. DMSP production in the sunlit ocean, mainly by eukaryotic autotrophs, accounts for 5-9% of the total carbon produced by marine photosynthetic organisms (Hopkins et al., 2023). The tight relationship of DMSP synthesis and release with the physiological state of the producing cell (Archer et al., 2018; Simó, 2001; Stefels et al., 2007; Strom et al., 2020) has the potential to connect individuals to inter-organism interactions, including grazing. Intracellular DMSP can be oxidised to intracellular DMSO, cleaved to DMS and lost across cell membranes (Sunda et al., 2002), released as DMSP to the dissolved pool where it is available to bacteria and osmotrophic protists (Ruiz-González et al., 2012; Saló et al., 2009; Stefels et al., 2007; Vila et al., 2004; Vila-Costa et al., 2006) or taken up by higher trophic level organisms as they predate on the DMSP producer (Tang & Simó, 2003; Tang, 2001). Several studies have revealed microzooplankton as a main contributor in grazing prey DMSP (Archer et al., 2002; Simó et al., 2002, 2018), highlighting the influence of ingestion on DMSP dynamics. The fate of the ingested DMSP will depend on the DMSP-assimilation capacity of the predator. If the majority is released into the dissolved pool and degraded by bacteria, grazing enhances the coupling between phytoplankton DMSP and its degradation products, such as DMS and methanethiol (Gao et al., 2020; Kiene, 1996; Tang & Simó, 2003). However, if DMSP is assimilated into the predator's biomass, the carbon and sulphur contents will be re-introduced into the microbial food web and transferred to mesozooplankton. The assimilation efficiency depends on food types and grazer metabolic preferences, and DMSP can be retained in the micrograzer with little assimilation (Saló et al., 2009; Tang & Simó, 2003). Subsequently, the transfer of retained DMSP into higher trophic levels, such as copepods, will also influence the DMSP cycle. Experiments with the copepod *Acartia tonsa* have shown short-time DMSP retention in the gut before release into the food web via faecal particles (Tang, 2001). Thus, prey-DMSP ingestion allows the formation of DMSP-rich particles, that will diffuse DMSP into the dissolved pool.

Bacterial degradation of dissolved DMSP occurs by two main pathways: demethylation (producing methanethiol) and cleavage into DMS and acrylate (Gao et al., 2020). The relative importance of each process is dependent on DMSP concentration (Gao et al., 2020; Kiene et al., 2000) with DMS production upregulated in high DMSP patches. Therefore, chemotaxis to DMSP patches of high concentration may favour DMS production over what would have been predicted from the bulk (average) dissolved DMSP concentration. The conversion of DMSP into DMS is also common in grazing and lysis events by the DMSP lyase enzymes present in many phytoplankton and bacterial species (Alcolombri et al., 2015; Curson et al., 2008; Hopkins et al., 2023; Simó et al., 2018). Thus, DMS release during grazing generates microscale gradients that may trigger chemoattraction of higher-trophic levels organisms, building tri-trophic interactions in microscale hot-spots of predatory activity (Shemi et al., 2021) potentially impacting the final budget of grazed primary production (Steinke et al., 2002).

DMS production is a key step in the organic sulphur cycle and the largest source of marine sulphur to the atmosphere (Hopkins et al., 2023). DMS emissions and subsequent oxidation to sulphate and methanesulfonate aerosols increase cloud albedo by forming cloud condensation nuclei (CCN) and

influence the radiative balance of Earth (Simó, 2001). This is the founding process of the CLAW hypothesis, which postulates that plankton-emitted DMS exerts a negative (regulatory) feedback on climate (Charlson et al., 1987). Enhanced DMS production and emission would increase cloud albedo inducing a sunlight dimming and cooling effect that would, in turn, diminish the biological DMS production. Although the biological climate feedback is still controversial (Quinn & Bates, 2011), the role of DMS in aerosol distribution and CCN formation is well-established (Hopkins et al., 2023; Simó, 2001). This thesis suggests that a comprehensive understanding of the processes controlling DMS-relevant emission from the oceans requires considering chemotaxis to DMSP at the microscale.

Microbial plankton research beyond genomic data

Scientists in the omics era are adept at describing communities and their functions using high throughput sequencing techniques. Describing diversity and metabolic potential in the prokaryotic world is successfully accomplished by mining enzymes and biochemical pathways from genomic and metagenomic databases (Worden et al., 2015). However, although eukaryotes might have diverse metabolisms reflected in their genomes, their interactions and responses to biotic and abiotic factors are much more linked to cellular structures and feeding strategies reflected on distinct behaviours (Worden et al., 2015). The active search and capture processes of prey by raptorial feeding and the ability to digest or domesticate photosynthetic organisms are complex strategies not characterised through genomic sequencing data alone. Thus, we cannot solely rely on a catalogue of sequences if we are to characterize cellular structures, and describe trophic or symbiotic interactions. The bigger size of protists in contrast to those of bacteria and archaea argue for microscopic observations as a powerful tool to describe behaviour (Deuer & Grünbaum, 2006; Fenchel, 2001; Harvey et al., 2013). Current state-of-the-art technologies such as microfluidics or the usage of bioinformatic tools for image analyses have allowed the documentation and deep exploration of chemotactic interactions (Seymour et al., 2010, Chapter 1). This thesis has benefited from novel technologies by combining traditional methods with powerful bioinformatic analysis in chapter 1. Additionally, a novel microfluid-based device for in situ chemotactic experiments (Lambert et al., 2017) was tested in chapter 2, although methodological artifacts and the protocol used for natural communities hindered the obtention of fruitful results. The method applied in chapter 1 (capillary assays with high-resolution video recording) successfully allowed the observation and characterization of chemotactic responses by direct visualization of protist behaviour. Radioisotope incubations allowed to describe metabolic strategies concerning DMSP uptake. No interaction or metabolic pathway was inferred from genomic data, as the organisms used are not sequenced. Still, the application of omics techniques (e.g. metabarcoding, metatranscriptomics) would have been helpful in the experiments of chapters 2 and 3 to identify the main partners involved and their responses to chemical and environmental factors.

To summarize and end this discussion we propose the combination of multi-level studies integrating morphological, physiological, behavioural, genomic and chemical data as the most appropriate approach to target microbial responses and interactions at the microscale. Hence, despite the crucial information provided by culture-based studies on functional responses and intricate interactions with chemical gradients, it is imperative to incorporate natural community experiments conducted under in-situ conditions and embrace their elevated levels of uncertainty.

The general aim of this thesis was fulfilled by combining laboratory studies using cultured species with experiments with natural communities, which provided data on the chemotactic behaviour of herbivore protists and community responses to light-stress events and unveiled the implications for microscale trophic interactions.

GENERAL REFERENCES

- Abrams, P. A. (2022). Food web functional responses. *Frontiers in Ecology and Evolution*, 10, 984384. <https://doi.org/10.3389/fevo.2022.984384>
- Adler J. (1966). Chemotaxis in bacteria. *Science*, 12;153(3737):708-16. doi: 10.1126/science.153.3737.708.
- Adler, J. (1973). A method for measuring chemotaxis and use of the method to determine optimum conditions for chemotaxis by *Escherichia coli*. *Journal of General Microbiology*, 74(1), 77–91. <https://doi.org/10.1099/00221287-74-1-77>
- Alcolombri, U., Ben-Dor, S., Feldmesser, E., Levin, Y., Tawfik, D. S., & Vardi, A. (2015). Identification of the algal dimethyl sulfide-releasing enzyme: A missing link in the marine sulfur cycle. *Science*, 348(6242), 1466–1469. <https://doi.org/10.1126/science.aab1586>
- Allredge, A. L., & Cohen, Y. (1987). Can microscale chemical patches persist in the sea? Microelectrode study of marine snow, fecal pellets. *Science*, 235(4789), 689–691. <https://doi.org/10.1126/science.235.4789.689>
- Allredge, A. L., & Silver, M. W. (1988). Characteristics, dynamics and significance of marine snow. *Progress in Oceanography*, 20(1), 41–82. [https://doi.org/10.1016/0079-6611\(88\)90053-5](https://doi.org/10.1016/0079-6611(88)90053-5)
- Archer, S. D., Ragni, M., Webster, R., Airs, R. L., & Geider, R. J. (2010). Dimethyl sulfoniopropionate and dimethyl sulfide production in response to photoinhibition in *Emiliania huxleyi*. *Limnology and Oceanography*, 55(4), 1579–1589. <https://doi.org/10.4319/lo.2010.55.4.1579>
- Archer, S. D., Smith, G. C., Nightingale, P. D., Widdicombe, C. E., Tarran, G. A., Rees, A. P., & Burkill, P. H. (2002). Dynamics of particulate dimethylsulphoniopropionate during a Lagrangian experiment in the northern North Sea. *Deep Sea Research Part II: Topical Studies in Oceanography*, 49(15), 2979–2999. [https://doi.org/10.1016/S0967-0645\(02\)00067-X](https://doi.org/10.1016/S0967-0645(02)00067-X)
- Archer, S. D., Stefels, J., Airs, R. L., Lawson, T., Smyth, T. J., Rees, A. P., & Geider, R. J. (2018). Limitation of dimethylsulfoniopropionate synthesis at high irradiance in natural phytoplankton communities of the Tropical Atlantic. *Limnology and Oceanography*, 63(1), 227–242. <https://doi.org/10.1002/lno.10625>
- Arias, A., Saiz, E., & Calbet, A. (2020). Towards an understanding of diel feeding rhythms in marine protists: Consequences of light manipulation. *Microbial Ecology*, 79(1), 64–72. <https://doi.org/10.1007/s00248-019-01390-y>
- Ayo, B., Latatu, A., Artolozaga, I., Jürgens, K., & Iriberrí, J. (2009). Factors affecting preference responses of the freshwater ciliate *Uronema nigricans* to bacterial prey. *Journal of Eukaryotic Microbiology*, 56(2), 188–193. <https://doi.org/10.1111/j.1550-7408.2008.00387.x>
- Ayo, B., Txakartegi, A., Baña, Z., Artolozaga, I., & Iriberrí, J. (2010). Chemosensory response of marine flagellate towards L- and D- dissolved free amino acids generated during heavy grazing on bacteria. *International Microbiology*, 13(3), 151–158. <https://doi.org/10.2436/20.1501.01.120>
- Azam, F. (1998). Microbial control of oceanic carbon flux: The plot thickens. *Science, New Series*, 280(5364), 694–696.
- Azam, F., Fenchel, T., Field, J., Gray, J., Meyer-Reil, L., & Thingstad, F. (1983). The ecological role of water-column microbes in the sea. *Marine Ecology Progress Series*, 10, 257–263. <https://doi.org/10.3354/meps010257>
- Azam, F., & Malfatti, F. (2007). Microbial structuring of marine ecosystems. *Nature Reviews Microbiology*, 5(10), 782–791. <https://doi.org/10.1038/nrmicro1747>
- Barak-Gavish, N., Dassa, B., Kuhlisch, C., Nussbaum, I., Brandis, A., Rosenberg, G., Avraham, R., & Vardi, A. (2023). Bacterial lifestyle switch in response to algal metabolites. *eLife*, 12, e84400. <https://doi.org/10.7554/eLife.84400>
- Barak-Gavish, N., Frada, M. J., Ku, C., Lee, P. A., DiTullio, G. R., Malitsky, S., Aharoni, A., Green, S. J., Rotkopf, R., Kartvelishvili, E., Sheyn, U., Schatz, D., & Vardi, A. (2018). Bacterial virulence against an oceanic bloom-forming phytoplankton is mediated by algal DMSP. *Science Advances*, 4(10), eaau5716. <https://doi.org/10.1126/sciadv.aau5716>
- Bar-On, Y. M., & Milo, R. (2019). The biomass composition of the oceans: A blueprint of our blue planet. *Cell*, 179(7), 1451–1454. <https://doi.org/10.1016/j.cell.2019.11.018>
- Beardall, J., Stojkovic, S., & Larsen, S. (2009). Living in a high CO₂ world: Impacts of global climate change on marine phytoplankton. *Plant Ecology & Diversity*, 2(2), 191–205. <https://doi.org/10.1080/17550870903271363>
- Bidle, K. D. (2015). The molecular ecophysiology of programmed cell death in marine phytoplankton. *Annual Review of Marine Science*, 7(1), 341–375. <https://doi.org/10.1146/annurev-marine-010213-135014>
- Blackburn, N., & Fenchel, T. (1999). Modelling of microscale patch encounter by chemotactic protozoa. *Protist*, 150(3), 337–343. [https://doi.org/10.1016/S1434-4610\(99\)70034-9](https://doi.org/10.1016/S1434-4610(99)70034-9)

- Breckels, M. N., Roberts, E. C., Archer, S. D., Malin, G., & Steinke, M. (2011). The role of dissolved infochemicals in mediating predator-prey interactions in the heterotrophic dinoflagellate *Oxyrrhis marina*. *Journal of Plankton Research*, 33(4), 629–639. <https://doi.org/10.1093/plankt/fbq114>
- Breton, E., Goberville, E., Sautour, B., Ouadi, A., Skouroliahou, D.-I., Seuront, L., Beaugrand, G., Kléparski, L., Crouvoisier, M., Pecqueur, D., Salmeron, C., Cauvin, A., Poquet, A., Garcia, N., Gohin, F., & Christaki, U. (2022). Multiple phytoplankton community responses to environmental change in a temperate coastal system: A trait-based approach. *Frontiers in Marine Science*, 9, 914475. <https://doi.org/10.3389/fmars.2022.914475>
- Brown, E. R., Cepeda, M. R., Mascuch, S. J., Poulson-Ellestad, K. L., & Kubanek, J. (2019). Chemical ecology of the marine plankton. *Natural Product Reports*, 36(8), 1093–1116. <https://doi.org/10.1039/C8NP00085A>
- Brussaard, C., Marie, D., Thyrhaug, R., & Bratbak, G. (2001). Flow cytometric analysis of phytoplankton viability following viral infection. *Aquatic Microbial Ecology*, 26(2), 157–166. <https://doi.org/10.3354/ame026157>
- Butler, W. L. (1972). On the primary nature of fluorescence yield changes associated with photosynthesis. *Proceedings of the National Academy of Sciences*, 69(11), 3420–3422. <https://doi.org/10.1073/pnas.69.11.3420>
- Calbet, A. (2008). The trophic roles of microzooplankton in marine systems. *ICES Journal of Marine Science*, 65(3), 325–331. <https://doi.org/10.1093/icesjms/fsn013>
- Calbet, A., & Landry, M. R. (2004). Phytoplankton growth, microzooplankton grazing, and carbon cycling in marine systems. *Limnology and Oceanography*, 49(1), 51–57. <https://doi.org/10.4319/lo.2004.49.1.0051>
- Calbet, A., & Saiz, E. (2005). The ciliate-copepod link in marine ecosystems. *Aquatic Microbial Ecology*, 38, 157–167. <https://doi.org/10.3354/ame038157>
- Calbet, A., & Saiz, E. (2013). Effects of trophic cascades in dilution grazing experiments: From artificial saturated feeding responses to positive slopes. *Journal of Plankton Research*, 35(6), 1183–1191. <https://doi.org/10.1093/plankt/fbt067>
- Caron, D. A., Countway, P. D., Jones, A. C., Kim, D. Y., & Schnetzer, A. (2012). Marine protistan diversity. *Annual Review of Marine Science*, 4(1), 467–493. <https://doi.org/10.1146/annurev-marine-120709-142802>
- Charette, M., & Smith, W. (2010). The volume of Earth's ocean. *Oceanography*, 23(2), 112–114. <https://doi.org/10.5670/oceanog.2010.51>
- Charlson, R. J., Lovelock, J. E., Andreae, M. O., & Warren, S. G. (1987). Oceanic phytoplankton, atmospheric sulphur, cloud albedo and climate. *Nature*, 326(6114), 655–661. <https://doi.org/10.1038/326655a0>
- Chase, J. M., Abrams, P. A., Grover, J. P., Diehl, S., Chesson, P., Holt, R. D., Richards, S. A., Nisbet, R. M., & Case, T. J. (2002). The interaction between predation and competition: A review and synthesis. *Ecology Letters*, 5(2), 302–315. <https://doi.org/10.1046/j.1461-0248.2002.00315.x>
- Cherrier, J., Valentine, S., Hamill, B., Jeffrey, W. H., & Marra, J. F. (2015). Light-mediated release of dissolved organic carbon by phytoplankton. *Journal of Marine Systems*, 147, 45–51. <https://doi.org/10.1016/j.jmarsys.2014.02.008>
- Clerc, E. E., Raina, J.-B., Keegstra, J. M., Landry, Z., Pontrelli, S., Alcolombri, U., Lambert, B. S., Anelli, V., Vincent, F., Masdeu-Navarro, M., Sichert, A., De Schaetzen, F., Sauer, U., Simó, R., Hehemann, J.-H., Vardi, A., Seymour, J. R., & Stocker, R. (2023). Strong chemotaxis by marine bacteria towards polysaccharides is enhanced by the abundant organosulfur compound DMSP. *Nature Communications*, 14(1), 8080. <https://doi.org/10.1038/s41467-023-43143-z>
- Clerc, E. E., Raina, J.-B., Peaudecerf, F. J., Seymour, J. R., & Stocker, R. (2022). Survival in a sea of gradients: Bacterial and archaeal foraging in a heterogeneous ocean. In L. J. Stal & M. S. Cretoiu (Eds.), *The Marine Microbiome* (Vol. 3, pp. 47–102). Springer International Publishing. https://doi.org/10.1007/978-3-030-90383-1_2
- Cooney, E. C., Fredrickson, K. A., Bright, K. J., & Strom, S. L. (2019). Contrasting effects of high-intensity photosynthetically active radiation on two bloom-forming dinoflagellates. *Journal of Phycology*, 55(5), 1082–1095. <https://doi.org/10.1111/jpy.12890>
- Cordero, O. X., & Datta, M. S. (2016). Microbial interactions and community assembly at microscales. *Current Opinion in Microbiology*, 31, 227–234. <https://doi.org/10.1016/j.mib.2016.03.015>
- Crenshaw, H. C. (1993). Orientation by helical motion--III. Microorganisms can orient to stimuli by changing the direction of their rotational velocity. *Bulletin of Mathematical Biology*, 55(1), 231–255.
- Cullen, J. J., & MacIntyre, J. G. (1998). Behavior, physiology and the niche of depth-regulating phytoplankton. In *Physiological Ecology of Harmful Algal Blooms: Vol. Vol. G 41*. Springer-Verlag.
- Cunningham, G. B., Strauss, V., & Ryan, P. G. (2008). African penguins (*Spheniscus demersus*) can detect dimethyl sulphide, a prey-related odour. *Journal of Experimental Biology*, 211(19), 3123–3127. <https://doi.org/10.1242/jeb.018325>

- Curson, A. R. J., Rogers, R., Todd, J. D., Brearley, C. A., & Johnston, A. W. B. (2008). Molecular genetic analysis of a dimethylsulfoniopropionate lyase that liberates the climate-changing gas dimethylsulfide in several marine α -proteobacteria and *Rhodobacter sphaeroides*. *Environmental Microbiology*, 10(3), 757–767. <https://doi.org/10.1111/j.1462-2920.2007.01499.x>
- Darroch, L., Lavoie, M., Levasseur, M., Laurion, I., Sunda, W., Michaud, S., Scarratt, M., Gosselin, M., & Caron, G. (2015). Effect of short-term light- and UV-stress on DMSP, DMS, and DMSP lyase activity in *Emiliana huxleyi*. *Aquatic Microbial Ecology*, 74(2), 173–185. <https://doi.org/10.3354/ame01735>
- De Lange, H. J., & Lüring, M. (2003). Effects of UV-B irradiated algae on zooplankton grazing. *Hydrobiologia*, 491(1–3), 133–144. <https://doi.org/10.1023/A:1024485320677>
- Deuer, S. M., & Grünbaum, D. (2006). Individual foraging behaviors and population distributions of a planktonic predator aggregating to phytoplankton thin layers. *Limnology and Oceanography*, 51(1), 109–116. <https://doi.org/10.4319/lo.2006.51.1.0109>
- Dolan, J. R., & McKeon, K. (2005). The reliability of grazing rate estimates from dilution experiments: Have we over-estimated rates of organic carbon consumption by microzooplankton? *Ocean Science*, 1(1), 1–7. <https://doi.org/10.5194/os-1-1-2005>
- Duarte Ferreira, G., Romano, F., Medić, N., Pitta, P., Hansen, P. J., Flynn, K. J., Mitra, A., & Calbet, A. (2021). Mixoplankton interferences in dilution grazing experiments. *Scientific Reports*, 11(1), 23849. <https://doi.org/10.1038/s41598-021-03176-0>
- Duffy, M. A., Hall, S. R., Tessier, A. J., & Huebner, M. (2005). Selective predators and their parasitized prey: Are epidemics in zooplankton under top-down control? *Limnology and Oceanography*, 50(2), 412–420. <https://doi.org/10.4319/lo.2005.50.2.0412>
- Edgcomb, V. P. (2021). Eat me, or don't eat me? *Nature Microbiology*, 6(11), 1341–1342. <https://doi.org/10.1038/s41564-021-00992-y>
- Evans, C., & Wilson, W. H. (2008). Preferential grazing of *Oxyrrhis marina* on virus infected *Emiliana huxleyi*. *Limnology and Oceanography*, 53(5), 2035–2040. <https://doi.org/10.4319/lo.2008.53.5.2035>
- Falgueras-Cano, J., Falgueras-Cano, J. A., & Moya, A. (2022). Aggregated distribution as an explanation for the paradox of plankton and collective animal behavior. *Biology*, 11(10), 1477. <https://doi.org/10.3390/biology11101477>
- Falkowski, P. (2012). Ocean Science: The power of plankton. *Nature*, 483(7387), S17–S20. <https://doi.org/10.1038/483S17a>
- Falkowski, P. G., Fenchel, T., & Delong, E. F. (2008). The microbial engines that drive Earth's biogeochemical cycles. *Science*, 320(5879), 1034–1039. <https://doi.org/10.1126/science.1153213>
- Fenchel, T. (2001). How dinoflagellates swim. *Protist*, 152(4), 329–338. <https://doi.org/10.1078/1434-4610-00071>
- Fenchel, T., & Blackburn, N. (1999). Motile chemosensory behaviour of phagotrophic protists: Mechanisms for and efficiency in congregating at food patches. *Protist*, 150(3), 325–336. [https://doi.org/10.1016/S1434-4610\(99\)70033-7](https://doi.org/10.1016/S1434-4610(99)70033-7)
- Field, C. B., Behrenfeld, M. J., Randerson, J. T., & Falkowski, P. (1998). Primary production of the biosphere: Integrating terrestrial and oceanic components. *Science*, 281(5374), 237–240. <https://doi.org/10.1126/science.281.5374.237>
- Fields, D. M., Durif, C. M. F., Bjelland, R. M., Shema, S. D., Skiftesvik, A. B., & Browman, H. I. (2011). Grazing rates of *Calanus finmarchicus* on *Thalassiosira weissflogii* cultured under different levels of ultraviolet radiation. *PLoS ONE*, 6(10), e26333. <https://doi.org/10.1371/journal.pone.0026333>
- Flintrop, C. M., Rogge, A., Miksch, S., Thiele, S., Waite, A. M., & Iversen, M. H. (2018). Embedding and slicing of intact in situ collected marine snow. *Limnology and Oceanography: Methods*, 16(6), 339–355. <https://doi.org/10.1002/lom3.10251>
- Franks, P., & Marra, J. (1994). A simple new formulation for phytoplankton photo-response and an application in a wind-driven mixed-layer model. *Marine Ecology Progress Series*, 111, 143–153. <https://doi.org/10.3354/meps111143>
- Franzè, G., Pierson, J. J., Stoecker, D. K., & Lavrentyev, P. J. (2018). Diatom-produced allelochemicals trigger trophic cascades in the planktonic food web. *Limnology and Oceanography*, 63(3), 1093–1108. <https://doi.org/10.1002/lno.10756>
- Froneman, P., Pakhomov, E., Perissinotto, R., Laubscher, R., & McQuaid, C. (1997). Dynamics of the plankton communities of the Lazarev Sea (Southern Ocean) during seasonal ice melt. *Marine Ecology Progress Series*, 149, 201–214. <https://doi.org/10.3354/meps149201>

- Fuentes-Lema, A., Sobrino, C., González, N., Estrada, M., & Neale, P. (2015). Effect of solar UVR on the production of particulate and dissolved organic carbon from phytoplankton assemblages in the Indian Ocean. *Marine Ecology Progress Series*, 535, 47–61. <https://doi.org/10.3354/meps11414>
- Galí, M., Simó, R., Pérez, G. L., Ruiz-González, C., Sarmiento, H., Royer, S.-J., Fuentes-Lema, A., & Gasol, J. M. (2013). Differential response of planktonic primary, bacterial, and dimethylsulfide production rates to static vs. dynamic light exposure in upper mixed-layer summer sea waters. *Biogeosciences*, 10(12), 7983–7998. <https://doi.org/10.5194/bg-10-7983-2013>
- Gao, C., Fernandez, V. I., Lee, K. S., Fenizia, S., Pohnert, G., Seymour, J. R., Raina, J.-B., & Stocker, R. (2020). Single-cell bacterial transcription measurements reveal the importance of dimethylsulfoniopropionate (DMSP) hotspots in ocean sulfur cycling. *Nature Communications*, 11(1), 1942. <https://doi.org/10.1038/s41467-020-15693-z>
- García-Oliva, O., & Wirtz, K. (2022). Size-dependent and -independent prey selection of dinoflagellates. *Marine Biology*, 169(9), 122. <https://doi.org/10.1007/s00227-022-04102-2>
- Gebühr, C., Sheward, R. M., Herrle, J. O., & Bollmann, J. (2021). Strain-specific morphological response of the dominant calcifying phytoplankton species *Emiliana huxleyi* to salinity change. *PLOS ONE*, 16(2), e0246745. <https://doi.org/10.1371/journal.pone.0246745>
- Genovart, M., Negre, N., Tavecchia, G., Bistuer, A., Parpal, L., & Oro, D. (2010). The young, the weak and the sick: Evidence of natural selection by predation. *PLoS ONE*, 5(3), e9774. <https://doi.org/10.1371/journal.pone.0009774>
- Gerritsen, J. (1980). Adaptive responses to encounter problems. In *ecology and evolution of zooplankton communities: Vol. Special Symposium Vol. 3*. University Press of New England.
- Gorbunov, M., Shirsin, E., Nikonova, E., Fadeev, V., & Falkowski, P. (2020). A multi-spectral fluorescence induction and relaxation (FIRe) technique for physiological and taxonomic analysis of phytoplankton communities. *Marine Ecology Progress Series*, 644, 1–13. <https://doi.org/10.3354/meps13358>
- Gorbunov, M. Y., & Falkowski, P. G. (2022). Using chlorophyll fluorescence to determine the fate of photons absorbed by phytoplankton in the world's oceans. *Annual Review of Marine Science*, 14(1), 213–238. <https://doi.org/10.1146/annurev-marine-032621-122346>
- Gralka, M., Szabo, R., Stocker, R., & Cordero, O. X. (2020). Trophic interactions and the drivers of microbial community assembly. *Current Biology*, 30(19), R1176–R1188. <https://doi.org/10.1016/j.cub.2020.08.007>
- Guadayol, Ò., Mendonca, T., Segura-Noguera, M., Wright, A. J., Tassieri, M., & Humphries, S. (2021). Microrheology reveals microscale viscosity gradients in planktonic systems. *Proceedings of the National Academy of Sciences*, 118(1), e2011389118. <https://doi.org/10.1073/pnas.2011389118>
- Guasto, J. S., Rusconi, R., & Stocker, R. (2012). Fluid mechanics of planktonic microorganisms. *Annual Review of Fluid Mechanics*, 44(1), 373–400. <https://doi.org/10.1146/annurev-fluid-120710-101156>
- Gutierrez, S. O., Minchella, D. J., & Bernal, X. E. (2022). Survival of the sickest: Selective predation differentially modulates ecological and evolutionary disease dynamics. *Oikos*, 2022(9), e09126. <https://doi.org/10.1111/oik.09126>
- Hamm, C. E., Merkel, R., Springer, O., Jurkojc, P., Maier, C., Prectel, K., & Smetacek, V. (2003). Architecture and material properties of diatom shells provide effective mechanical protection. *Nature*, 421(6925), 841–843. <https://doi.org/10.1038/nature01416>
- Harrison, J. W., Silsbe, G. M., & Smith, R. E. H. (2015). Photophysiology and its response to visible and ultraviolet radiation in freshwater phytoplankton from contrasting light regimes. *Journal of Plankton Research*, 37(2), 472–488. <https://doi.org/10.1093/plankt/fbv003>
- Harvey, E. L., Jeong, H. J., & Menden-Deuer, S. (2013). Avoidance and attraction: Chemical cues influence predator-prey interactions of planktonic protists. *Limnology and Oceanography*, 58(4), 1176–1184. <https://doi.org/10.4319/lo.2013.58.4.1176>
- Hay, M. E. (2009). Marine chemical ecology: Chemical signals and cues structure marine populations, communities, and ecosystems. *Annual Review of Marine Science*, 1(1), 193–212. <https://doi.org/10.1146/annurev.marine.010908.163708>
- Hazelbauer, G. L. (2012). Bacterial chemotaxis: The early years of molecular studies. *Annual Review of Microbiology*, 66(1), 285–303. <https://doi.org/10.1146/annurev-micro-092611-150120>
- Hessen, D., De Lange, H., & Van Donk, E. (1997). UV-induced changes in phytoplankton cells and its effects on grazers. *Freshwater Biology*, 38(3), 513–524. <https://doi.org/10.1046/j.1365-2427.1997.00223.x>
- Holling CS. (1965). The functional response of predators to prey density and its role in mimicry and population regulation. *Memoirs of the Entomological Society of Canada*, 97(S45), 5–60. <https://doi.org/10.4039/entm9745fv>

- Hopkins, F. E., Archer, S. D., Bell, T. G., Suntharalingam, P., & Todd, J. D. (2023). The biogeochemistry of marine dimethylsulfide. *Nature Reviews Earth & Environment*, 4(6), 361–376. <https://doi.org/10.1038/s43017-023-00428-7>
- Isao, K., Hara, S., Terauchi, K., & Kogure, K. (1990). Role of sub-micrometre particles in the ocean. *Nature*, 345(6272), 242–244. <https://doi.org/10.1038/345242a0>
- Jackson, R., & Gabric, A. (2022). Climate change impacts on the marine cycling of biogenic sulfur: A review. *Microorganisms*, 10(8), 1581. <https://doi.org/10.3390/microorganisms10081581>
- Jakobsen, H. H., & Strom, S. L. (2004). Circadian cycles in growth and feeding rates of heterotrophic protist plankton. *Limnology and Oceanography*, 49(6), 1915–1922. <https://doi.org/10.4319/lo.2004.49.6.1915>
- Jennings, H.S. (1906). *Behavior of the lower organisms*. Columbia University Press.
- Jeong, H. J., Yoo, Y. D., Kim, J. S., Seong, K. A., Kang, N. S., & Kim, T. H. (2010). Growth, feeding and ecological roles of the mixotrophic and heterotrophic dinoflagellates in marine planktonic food webs. *Ocean Science Journal*, 45(2), 65–91. <https://doi.org/10.1007/s12601-010-0007-2>
- Johnson, R., Langer, G., Rossi, S., Probert, I., Mammone, M., & Ziveri, P. (2022). Nutritional response of a coccolithophore to changing pH and temperature. *Limnology and Oceanography*, 67(10), 2309–2324. <https://doi.org/10.1002/lno.12204>
- Kâ, S., Carotenuto, Y., Romano, G., Hwang, J.-S., Buttino, I., & Ianora, A. (2014). Impact of the diatom-derived polyunsaturated aldehyde 2-trans,4-trans decadienal on the feeding, survivorship and reproductive success of the calanoid copepod *Temora stylifera*. *Marine Environmental Research*, 93, 31–37. <https://doi.org/10.1016/j.marenvres.2013.07.009>
- Keegstra, J. M., Carrara, F., & Stocker, R. (2022). The ecological roles of bacterial chemotaxis. *Nature Reviews Microbiology*, 20(8), 491–504. <https://doi.org/10.1038/s41579-022-00709-w>
- Keeling, P. J., & Burki, F. (2019b). Progress towards the Tree of Eukaryotes. *Current Biology*, 29(16), R808–R817. <https://doi.org/10.1016/j.cub.2019.07.031>
- Keller, M. D., Bellows, W. K., & Guillard, R. R. L. (1989). Dimethyl sulfide production in marine phytoplankton. In *Biogenic Sulfur in the Environment* (Vol. 393, pp. 167–182). American Chemical Society. <https://doi.org/10.1021/bk-1989-0393.ch011>
- Kennedy, F., McMinn, A., & Martin, A. (2012). Effect of temperature on the photosynthetic efficiency and morphotype of *Phaeocystis antarctica*. *Journal of Experimental Marine Biology and Ecology*, 429, 7–14. <https://doi.org/10.1016/j.jembe.2012.06.016>
- Kiene, R. P. (1996). Production of methanethiol from dimethylsulfoniopropionate in marine surface waters. *Marine Chemistry*, 54(1–2), 69–83. [https://doi.org/10.1016/0304-4203\(96\)00006-0](https://doi.org/10.1016/0304-4203(96)00006-0)
- Kiene, R. P., Linn, L. J., & Bruton, J. A. (2000). New and important roles for DMSP in marine microbial communities. *Journal of Sea Research*, 43(3–4), 209–224. [https://doi.org/10.1016/S1385-1101\(00\)00023-X](https://doi.org/10.1016/S1385-1101(00)00023-X)
- Kjørboe, T. (2000). Colonization of marine snow aggregates by invertebrate zooplankton: Abundance, scaling, and possible role. *Limnology and Oceanography*, 45(2), 479–484. <https://doi.org/10.4319/lo.2000.45.2.0479>
- Kjørboe, T., & Jackson, G. A. (2001). Marine snow, organic solute plumes, and optimal chemosensory behavior of bacteria. *Limnology and Oceanography*, 46(6), 1309–1318. <https://doi.org/10.4319/lo.2001.46.6.1309>
- Kjørboe, T., Saiz, E., Tiselius, P., & Andersen, K. H. (2018). Adaptive feeding behavior and functional responses in zooplankton. *Limnology and Oceanography*, 63(1), 308–321. <https://doi.org/10.1002/lno.10632>
- Kjørboe, T., Tang, K., Grossart, H.-P., & Ploug, H. (2003). Dynamics of microbial communities on marine snow aggregates: Colonization, growth, detachment, and grazing mortality of attached bacteria. *Applied and Environmental Microbiology*, 69(6), 3036–3047. <https://doi.org/10.1128/AEM.69.6.3036-3047.2003>
- Klawonn, I., Van den Wyngaert, S., Parada, A. E., Arandia-Gorostidi, N., Whitehouse, M. J., Grossart, H. P., Dekas, A.E. (2021). Characterizing the “fungal shunt”: Parasitic fungi on diatoms affect carbon flow and bacterial communities in aquatic microbial food webs. *Proc. Natl. Acad. Sci. U.S.A.* 118. doi: 10.1073/pnas.2102225118
- Kóhidai, László, Lemberkovics, Eva, & Csaba, György. (1995). Molecule dependent chemotactic responses of *Tetrahymena pyriformis* elicited by volatile oils. *Acta Protozoologica*, 34, 181–185.
- Korolik, V., & Ottemann, K. M. (2018). Two spatial chemotaxis assays: The nutrient-depleted chemotaxis assay and the agarose-plug-bridge assay. In M. Manson (Ed.), *Bacterial Chemosensing. Methods in Molecular Biology* (Vol. 1729, pp. 23–31). Humana Press. https://doi.org/10.1007/978-1-4939-7577-8_3
- Kowalewsky, S., Dambach, M., Mauck, B., & Dehnhardt, G. (2006). High olfactory sensitivity for dimethyl sulphide in harbour seals. *Biology Letters*, 2(1), 106–109. <https://doi.org/10.1098/rsbl.2005.0380>

- Kuhlisch, C., Shemi, A., Barak-Gavish, N., Schatz, D., & Vardi, A. (2024). Algal blooms in the ocean: Hot spots for chemically mediated microbial interactions. *Nature Reviews Microbiology*, 22(3), 138–154. <https://doi.org/10.1038/s41579-023-00975-2>
- Lambert, B. S., Raina, J.-B., Fernandez, V. I., Rinke, C., Siboni, N., Rubino, F., Hugenholtz, P., Tyson, G. W., Seymour, J. R., & Stocker, R. (2017). A microfluidics-based in situ chemotaxis assay to study the behaviour of aquatic microbial communities. *Nature Microbiology*, 2(10), 1344–1349. <https://doi.org/10.1038/s41564-017-0010-9>
- Landry, M. R., & Hassett, R. P. (1982). Estimating the grazing impact of marine micro-zooplankton. *Marine Biology*, 67(3), 283–288. <https://doi.org/10.1007/BF00397668>
- Lane, N. (2015). The unseen world: Reflections on Leeuwenhoek (1677) 'Concerning little animals'. *Philosophical Transactions of the Royal Society B: Biological Sciences*, 370(1666), 20140344. <https://doi.org/10.1098/rstb.2014.0344>
- Laundon, D., Mock, T., Wheeler, G., & Cunliffe, M. (2021). Healthy herds in the phytoplankton: The benefit of selective parasitism. *The ISME Journal*, 15(7), 2163–2166. <https://doi.org/10.1038/s41396-021-00936-8>
- Lawrence, C., & Menden-Deuer, S. (2012). Drivers of protistan grazing pressure: Seasonal signals of plankton community composition and environmental conditions. *Marine Ecology Progress Series*, 459, 39–52. <https://doi.org/10.3354/meps09771>
- Leick, V., & Helle, J. (1983). A quantitative assay for ciliate chemotaxis. *Analytical Biochemistry*, 135(2), 466–469. [https://doi.org/10.1016/0003-2697\(83\)90713-3](https://doi.org/10.1016/0003-2697(83)90713-3)
- Levandowsky, M., Cheng, T., Kehr, A., Kim, J., Gardner, L., Silvern, L., Tsang, L., Lai, G., Chung, C., & Prakash, E. (1984). Chemosensory responses to amino acids and certain amines by the ciliate *Tetrahymena*: A flat capillary assay. *The Biological Bulletin*, 167(2), 322–330. <https://doi.org/10.2307/1541279>
- Levin, S.A. (1994). Patchiness in marine and terrestrial systems: From individuals to populations. *Philosophical Transactions of the Royal Society of London. Series B: Biological Sciences*, 343(1303), 99–103. <https://doi.org/10.1098/rstb.1994.0013>
- Lima-Mendez, G., Faust, K., Henry, N., Decelle, J., Colin, S., Carcillo, F., Chaffron, S., Ignacio-Espinosa, J. C., Roux, S., Vincent, F., Bittner, L., Darzi, Y., Wang, J., Audic, S., Berline, L., Bontempi, G., Cabello, A. M., Coppola, L., Cornejo-Castillo, F. M., ... Raes, J. (2015). Determinants of community structure in the global plankton interactome. *Science*, 348(6237), 1262073. <https://doi.org/10.1126/science.1262073>
- Long, J. D., Smalley, G. W., Barsby, T., Anderson, J. T., & Hay, M. E. (2007). Chemical cues induce consumer-specific defenses in a bloom-forming marine phytoplankton. *Proceedings of the National Academy of Sciences*, 104(25), 10512–10517. <https://doi.org/10.1073/pnas.0611600104>
- Martel, C. M. (2006). Prey location, recognition and ingestion by the phagotrophic marine dinoflagellate *Oxyrrhis marina*. *Journal of Experimental Marine Biology and Ecology*, 335(2), 210–220. <https://doi.org/10.1016/j.jembe.2006.03.006>
- McParland, E. L., & Levine, N. M. (2019). The role of differential DMSP production and community composition in predicting variability of global surface DMSP concentrations. *Limnology and Oceanography*, 64(2), 757–773. <https://doi.org/10.1002/lno.11076>
- Meunier, C. L., Hantzschke, F. M., Cunha-Dupont, A. Ö., Haafke, J., Oppermann, B., Malzahn, A. M., & Boersma, M. (2012). Intraspecific selectivity, compensatory feeding and flexible homeostasis in the phagotrophic flagellate *Oxyrrhis marina*: Three ways to handle food quality fluctuations. *Hydrobiologia*, 680(1), 53–62. <https://doi.org/10.1007/s10750-011-0900-4>
- Montagnes, D., Barbosa, A., Boenigk, J., Davidson, K., Jürgens, K., Macek, M., Parry, J., Roberts, E., & Imek, K. (2008). Selective feeding behaviour of key free-living protists: Avenues for continued study. *Aquatic Microbial Ecology*, 53, 83–98. <https://doi.org/10.3354/ame01229>
- Moran, M. A., Kujawinski, E. B., Schroer, W. F., Amin, S. A., Bates, N. R., Bertrand, E. M., Braakman, R., Brown, C. T., Covert, M. W., Doney, S. C., Dyhrman, S. T., Edison, A. S., Eren, A. M., Levine, N. M., Li, L., Ross, A. C., Saito, M. A., Santoro, A. E., Segrè, D., ... Vardi, A. (2022). Microbial metabolites in the marine carbon cycle. *Nature Microbiology*, 7(4), 508–523. <https://doi.org/10.1038/s41564-022-01090-3>
- Nahon, S., Charles, F., Lantoine, F., Vétion, G., Escoubeyrou, K., Desmalades, M., & Pruski, A. M. (2010). Ultraviolet radiation negatively affects growth and food quality of the pelagic diatom *Skeletonema costatum*. *Journal of Experimental Marine Biology and Ecology*, 383(2), 164–170. <https://doi.org/10.1016/j.jembe.2009.12.006>
- Nevitt, G. A. (2008). Sensory ecology on the high seas: The odor world of the procellariiform seabirds. *Journal of Experimental Biology*, 211(11), 1706–1713. <https://doi.org/10.1242/jeb.015412>

- Obiol Plana, A. (2022). Return of the marine heterotrophic flagellates: Diversity, distribution and gene expression patterns. Universitat Politècnica de Catalunya.
- Ochs, C. A. (1997). Effects of UV radiation on grazing by two marine heterotrophic nanoflagellates on autotrophic picoplankton. *Journal of Plankton Research*, 19(10), 1517–1536. <https://doi.org/10.1093/plankt/19.10.1517>
- Ochs, C. A., & Eddy, L. P. (1998). Effects of UV-A (320 to 399 Nanometers) on grazing pressure of a marine heterotrophic nanoflagellate on strains of the unicellular cyanobacteria *Synechococcus* spp. *Applied and Environmental Microbiology*, 64(1), 287–293. <https://doi.org/10.1128/AEM.64.1.287-293.1998>
- Packer, C., Holt, R. D., Hudson, P. J., Lafferty, K. D., & Dobson, A. P. (2003). Keeping the herds healthy and alert: Implications of predator control for infectious disease. *Ecology Letters*, 6(9), 797–802. <https://doi.org/10.1046/j.1461-0248.2003.00500.x>
- Park, M. G., Kim, A., Jeon, B. S., & Kim, M. (2021). Parasite-mediated increase in prey edibility in the predator-prey interaction of marine planktonic protists. *Harmful Algae*, 103, 101982. <https://doi.org/10.1016/j.hal.2021.101982>
- Paterson, H. L., Knott, B., & Waite, A. M. (2007). Microzooplankton community structure and grazing on phytoplankton, in an eddy pair in the Indian Ocean off Western Australia. *Deep Sea Research Part II: Topical Studies in Oceanography*, 54(8–10), 1076–1093. <https://doi.org/10.1016/j.dsr2.2006.12.011>
- Peduzzi, P., & Herndl, G. J. (1992). Zooplankton activity fueling the microbial loop: Differential growth response of bacteria from oligotrophic and eutrophic waters. *Limnology and Oceanography*, 37(5), 1087–1092. <https://doi.org/10.4319/lo.1992.37.5.1087>
- Pfeffer, W. (1884). Locomotorische Richtungsbewegungen durch Chemische Reize. *Untersuchungen Aus Dem Botanischen Institut in Tübingen*, 1, 363–482.
- Pohnert, G., Steinke, M., & Tollrian, R. (2007). Chemical cues, defence metabolites and the shaping of pelagic interspecific interactions. *Trends in Ecology & Evolution*, 22(4), 198–204. <https://doi.org/10.1016/j.tree.2007.01.005>
- Pomeroy, L., Williams, P., Azam, F., & Hobbie, J. (2007). The microbial loop. *Oceanography*, 20(2), 28–33. <https://doi.org/10.5670/oceanog.2007.45>
- Pomeroy, R. Lawrence. (1974). The ocean's food web, a changing paradigm. *BioScience*, 24(9), 499–504. <https://doi.org/10.2307/1296885>
- Poulsen, L., Moldrup, M., Berge, T., & Hansen, P. (2011). Feeding on copepod fecal pellets: A new trophic role of dinoflagellates as detritivores. *Marine Ecology Progress Series*, 441, 65–78. <https://doi.org/10.3354/meps09357>
- Quinn, P. K., & Bates, T. S. (2011). The case against climate regulation via oceanic phytoplankton sulphur emissions. *Nature*, 480(7375), 51–56. <https://doi.org/10.1038/nature10580>
- Raina, J.B., Lambert, B. S., Parks, D. H., Rinke, C., Siboni, N., Bramucci, A., Ostrowski, M., Signal, B., Lutz, A., Mendis, H., Rubino, F., Fernandez, V. I., Stocker, R., Hugenholtz, P., Tyson, G. W., & Seymour, J. R. (2022). Chemotaxis shapes the microscale organization of the ocean's microbiome. *Nature*, 605(7908), 132–138. <https://doi.org/10.1038/s41586-022-04614-3>
- Raina, J.B., Tapiolas, D., Willis, B. L., & Bourne, D. G. (2009). Coral-associated bacteria and their role in the biogeochemical cycling of sulfur. *Applied and Environmental Microbiology*, 75(11), 3492–3501. <https://doi.org/10.1128/AEM.02567-08>
- Richards, T. A., Jones, M. D. M., Leonard, G., & Bass, D. (2012). Marine fungi: Their ecology and molecular diversity. *Annual Review of Marine Science*, 4(1), 495–522. <https://doi.org/10.1146/annurev-marine-120710-100802>
- Righetti, D., Vogt, M., Gruber, N., Psomas, A., & Zimmermann, N. E. (2019). Global pattern of phytoplankton diversity driven by temperature and environmental variability. *Science Advances*, 5(5), eaau6253. <https://doi.org/10.1126/sciadv.aau6253>
- Roberts, E. C., Legrand, C., Steinke, M., & Wootton, E. C. (2011). Mechanisms underlying chemical interactions between predatory planktonic protists and their prey. *Journal of Plankton Research*, 33(6), 833–841. <https://doi.org/10.1093/plankt/fbr005>
- Roberts, E. C., Wootton, E. C., Davidson, K., Jeong, H. J., Lowe, C. D., & Montagnes, D. J. S. (2011). Feeding in the dinoflagellate *Oxyrrhis marina*: Linking behaviour with mechanisms. *Journal of Plankton Research*, 33(4), 603–614. <https://doi.org/10.1093/plankt/fbq118>
- Ruiz-González, C., Galí, M., Sintes, E., Herndl, G. J., Gasol, J. M., & Simó, R. (2012). Sunlight effects on the osmotrophic uptake of DMSP-sulfur and leucine by polar phytoplankton. *PLoS ONE*, 7(9), e45545. <https://doi.org/10.1371/journal.pone.0045545>

- Saló, V., Simó, R., Vila-Costa, M., & Calbet, A. (2009b). Sulfur assimilation by *Oxyrrhis marina* feeding on a ^{35}S -DMSP-labelled prey. *Environmental Microbiology*, 11(12), 3063–3072. <https://doi.org/10.1111/j.1462-2920.2009.02011.x>
- Schmoker, C., Hernández-León, S., & Calbet, A. (2013). Microzooplankton grazing in the oceans: Impacts, data variability, knowledge gaps and future directions. *Journal of Plankton Research*, 35(4), 691–706. <https://doi.org/10.1093/plankt/fbt023>
- Selander, E., Berglund, E. C., Engström, P., Berggren, F., Eklund, J., Harðardóttir, S., Lundholm, N., Grebner, W., & Andersson, M. X. (2019). Copepods drive large-scale trait-mediated effects in marine plankton. *Science Advances*, 5(2), eaat5096. <https://doi.org/10.1126/sciadv.aat5096>
- Seymour, J. R., Amin, S. A., Raina, J.-B., & Stocker, R. (2017). Zooming in on the phycosphere: The ecological interface for phytoplankton–bacteria relationships. *Nature Microbiology*, 2(7), 17065. <https://doi.org/10.1038/nmicrobiol.2017.65>
- Seymour, J. R., Simó, R., Ahmed, T., & Stocker, R. (2010). Chemoattraction to dimethylsulfoniopropionate throughout the marine microbial food web. *Science*, 329(5989), 342–345. <https://doi.org/10.1126/science.1188418>
- Shemi, A., Alcolombri, U., Schatz, D., Farstey, V., Vincent, F., Rotkopf, R., Ben-Dor, S., Frada, M. J., Tawfik, D. S., & Vardi, A. (2021). Dimethyl sulfide mediates microbial predator–prey interactions between zooplankton and algae in the ocean. *Nature Microbiology*, 6(11), 1357–1366. <https://doi.org/10.1038/s41564-021-00971-3>
- Sherr, E. B., & Sherr, B. F. (2002). Significance of predation by protists in aquatic microbial food webs. *Antonie van Leeuwenhoek*, 81, 193–308.
- Sheyn, U., Rosenwasser, S., Ben-Dor, S., Porat, Z., & Vardi, A. (2016). Modulation of host ROS metabolism is essential for viral infection of a bloom-forming coccolithophore in the ocean. *The ISME Journal*, 10(7), 1742–1754. <https://doi.org/10.1038/ismej.2015.228>
- Sibbald, M., Albright, L., & Sibbald, P. (1987). Chemosensory responses of a heterotrophic microflagellate to bacteria and several nitrogen compounds. *Marine Ecology Progress Series*, 36(1975), 201–204. <https://doi.org/10.3354/meps036201>
- Sieburth, J. M. (1960). Acrylic acid, an 'antibiotic' principle in *Phaeocystis* blooms in Antarctic waters. *Science*, 132, 676–677. <https://doi.org/10.1126/science.132.3428.676>
- Simó, R. (2001). Production of atmospheric sulfur by oceanic plankton: Biogeochemical, ecological and evolutionary links. *Trends in Ecology & Evolution*, 16(6), 287–294. [https://doi.org/10.1016/S0169-5347\(01\)02152-8](https://doi.org/10.1016/S0169-5347(01)02152-8)
- Simó, R., Archer, S. D., Pedrós-Alió, C., Gilpin, L., & Stelfox-Widdicombe, C. E. (2002). Coupled dynamics of dimethylsulfoniopropionate and dimethylsulfide cycling and the microbial food web in surface waters of the North Atlantic. *Limnology and Oceanography*, 47(1), 53–61. <https://doi.org/10.4319/lo.2002.47.1.0053>
- Simó, R., & Pedrós-Alió, C. (1999). Role of vertical mixing in controlling the oceanic production of dimethyl sulphide. *Nature*, 402(6760), 396–399. <https://doi.org/10.1038/46516>
- Simó, R., Saló, V., Almeda, R., Movilla, J., Trepát, I., Saiz, E., & Calbet, A. (2018). The quantitative role of microzooplankton grazing in dimethylsulfide (DMS) production in the NW Mediterranean. *Biogeochemistry*, 141(2), 125–142. <https://doi.org/10.1007/s10533-018-0506-2>
- Slezak, D., Puskarić, S., & Herndl, G. (1994). Potential role of acrylic acid in bacterioplankton communities in the sea. *Marine Ecology Progress Series*, 105, 191–197. <https://doi.org/10.3354/meps105191>
- Slobodkin, L. B. (1974). Prudent predation does not require group selection. *The American Naturalist*, 108(963), 665–678.
- Smetacek, V. (2001). A watery arms race. *Nature*, 411(6839), 745–745. <https://doi.org/10.1038/35081210>
- Smriga, S., Fernandez, V. I., Mitchell, J. G., & Stocker, R. (2016). Chemotaxis toward phytoplankton drives organic matter partitioning among marine bacteria. *Proceedings of the National Academy of Sciences*, 113(6), 1576–1581. <https://doi.org/10.1073/pnas.1512307113>
- Sobrinho, C., Montero, O., & Lubián, L. M. (2004). UV-B radiation increases cell permeability and damages nitrogen incorporation mechanisms in *Nannochloropsis gaditana*. *Aquatic Sciences*, 66(4), 421–429. <https://doi.org/10.1007/s00027-004-0731-8>
- Sobrinho, C., Segovia, M., Neale, P., Mercado, J., García-Gómez, C., Kulk, G., Lorenzo, M., Camarena, T., Van De Poll, W., Spilling, K., & Ruan, Z. (2014). Effect of CO₂, nutrients and light on coastal plankton. IV. Physiological responses. *Aquatic Biology*, 22, 77–93. <https://doi.org/10.3354/ab00590>
- Spero, H. J. (1984). Chemosensory capabilities in the phagotrophic dinoflagellate *Gymnodinium fungiforme*. *Journal of Phycology*, 21(2), 181–184. <https://doi.org/10.1111/j.0022-3646.1985.00181.x>

- Stefels, J. (2000). Physiological aspects of the production and conversion of DMSP in marine algae and higher plants. *Journal of Sea Research*, 43(3–4), 183–197. [https://doi.org/10.1016/S1385-1101\(00\)00030-7](https://doi.org/10.1016/S1385-1101(00)00030-7)
- Stefels, J., Dacey, J. W. H., & Elzenga, J. T. M. (2009). In vivo DMSP-biosynthesis measurements using stable-isotope incorporation and proton-transfer-reaction mass spectrometry (PTR-MS). *Limnology and Oceanography: Methods*, 7(8), 595–611. <https://doi.org/10.4319/lom.2009.7.595>
- Stefels, J., Steinke, M., Turner, S., Malin, G., & Belviso, S. (2007). Environmental constraints on the production and removal of the climatically active gas dimethylsulphide (DMS) and implications for ecosystem modelling. *Biogeochemistry*, 83(1–3), 245–275. <https://doi.org/10.1007/s10533-007-9091-5>
- Steiner, P. A., Sintes, E., Simó, R., De Corte, D., Pfannkuchen, D. M., Ivančić, I., Najdek, M., & Herndl, G. J. (2019). Seasonal dynamics of marine snow-associated and free-living demethylating bacterial communities in the coastal northern Adriatic Sea. *Environmental Microbiology Reports*, 11(5), 699–707. <https://doi.org/10.1111/1758-2229.12783>
- Steinke, M., Malin, G., & Liss, P. S. (2002). Trophic interactions in the sea: An ecological role for climate relevant volatiles? *Journal of Phycology*, 38(4), 630–638. <https://doi.org/10.1046/j.1529-8817.2002.02057.x>
- Steinke, M., Stefels, J., & Stamhuis, E. (2006). Dimethyl sulfide triggers search behavior in copepods. *Limnology and Oceanography*, 51(4), 1925–1930. <https://doi.org/10.4319/lo.2006.51.4.1925>
- Stocker, R. (2012). Marine microbes see a sea of gradients. *Science*, 338(6107), 628–633. <https://doi.org/10.1126/science.1208929>
- Stocker, R., & Seymour, J. R. (2012). Ecology and physics of bacterial chemotaxis in the ocean. *Microbiology and Molecular Biology Reviews*, 76(4), 792–812. <https://doi.org/10.1128/MMBR.00029-12>
- Stocker, R., Seymour, J. R., Samadani, A., Hunt, D. E., & Polz, M. F. (2008). Rapid chemotactic response enables marine bacteria to exploit ephemeral microscale nutrient patches. *Proceedings of the National Academy of Sciences*, 105(11), 4209–4214. <https://doi.org/10.1073/pnas.0709765105>
- Stoecker, D. K., Neistgaard, J. C., Madhusoodhanan, R., Pohnert, G., Wolfram, S., Jakobsen, H. H., Šulčius, S., & Larsen, A. (2015). Underestimation of microzooplankton grazing in dilution experiments due to inhibition of phytoplankton growth. *Limnology and Oceanography*, 60(4), 1426–1438. <https://doi.org/10.1002/lno.10106>
- Strom, S. (2001). Light-aided digestion, grazing and growth in herbivorous protists. *Aquatic Microbial Ecology*, 23, 253–261. <https://doi.org/10.3354/ame023253>
- Strom, S., Barberi, O., Mazur, C., Bright, K. J., & Fredrickson, K. (2020). High light stress reduces dinoflagellate predation on phytoplankton through both direct and indirect responses. *Aquatic Microbial Ecology*, 84, 43–57. <https://doi.org/10.3354/ame01924>
- Strom, S. L., Benner, R., Ziegler, S., & Dagg, M. J. (1997). Planktonic grazers are a potentially important source of marine dissolved organic carbon. *Limnology and Oceanography*, 42(6), 1364–1374. <https://doi.org/10.4319/lo.1997.42.6.1364>
- Sunda, W., Kieber, D. J., Kiene, R. P., & Huntsman, S. (2002). An antioxidant function for DMSP and DMS in marine algae. *Nature*, 418(6895), 317–320. <https://doi.org/10.1038/nature00851>
- Suschek, C. V., Briviba, K., Bruch-Gerharz, D., Sies, H., Kröncke, K. D., & Kolb-Bachofen, V. (2001). Even after UVA-exposure will nitric oxide protect cells from reactive oxygen intermediate-mediated apoptosis and necrosis. *Cell Death & Differentiation*, 8(5), 515–527. <https://doi.org/10.1038/sj.cdd.4400839>
- Suttle, C. A. (2007). Marine viruses—Major players in the global ecosystem. *Nature Reviews Microbiology*, 5(10), 801–812. <https://doi.org/10.1038/nrmicro1750>
- Tang, K., & Simó, R. (2003). Trophic uptake and transfer of DMSP in simple planktonic food chains. *Aquatic Microbial Ecology*, 31(2), 193–202. <https://doi.org/10.3354/ame031193>
- Tang, K. W. (2001). Defecation of dimethylsulfoniopropionate (DMSP) by the copepod *Acartia tonsa* as functions of ambient food concentration and body DMSP content. *Journal of Plankton Research*, 23(5), 549–553. <https://doi.org/10.1093/plankt/23.5.549>
- Tarangkoon, W., & Hansen, P. (2011). Prey selection, ingestion and growth responses of the common marine ciliate *Mesodinium pulex* in the light and in the dark. *Aquatic Microbial Ecology*, 62(1), 25–38. <https://doi.org/10.3354/ame01455>
- Taylor, J. R., & Stocker, R. (2012). Trade-offs of chemotactic foraging in turbulent water. *Science*, 338(6107), 675–679. <https://doi.org/10.1126/science.1219417>
- Temple, S. A. (1987). Do predators always capture substandard individuals disproportionately from prey populations? *Ecology*, 68(3), 669–674. <https://doi.org/10.2307/1938472>

- Teng, Z.-J., Wang, P., Chen, X.-L., Guillonneau, R., Li, C.-Y., Zou, S.-B., Gong, J., Xu, K.-W., Han, L., Wang, C., Scanlan, D. J., Chen, Y., & Zhang, Y.-Z. (2021). Acrylate protects a marine bacterium from grazing by a ciliate predator. *Nature Microbiology*, 6(11), 1351–1356. <https://doi.org/10.1038/s41564-021-00981-1>
- Thornton, D. C. O. (2014). Dissolved organic matter (DOM) release by phytoplankton in the contemporary and future ocean. *European Journal of Phycology*, 49(1), 20–46. <https://doi.org/10.1080/09670262.2013.875596>
- Thume, K., Gebser, B., Chen, L., Meyer, N., Kieber, D. J., & Pohnert, G. (2018). The metabolite dimethylsulfoxonium propionate extends the marine organosulfur cycle. *Nature*, 563(7731), 412–415. <https://doi.org/10.1038/s41586-018-0675-0>
- Tyssebotn, I. M. B., Kinsey, J. D., Kieber, D. J., Kiene, R. P., Rellinger, A. N., & Motard-Côté, J. (2017). Concentrations, biological uptake, and respiration of dissolved acrylate and dimethylsulfoxide in the northern Gulf of Mexico. *Limnology and Oceanography*, 62(3), 1198–1218. <https://doi.org/10.1002/lno.10495>
- Tyystjärvi, E. (2013). Photoinhibition of photosystem II. In *international review of cell and molecular biology* (Vol. 300, pp. 243–303). Elsevier. <https://doi.org/10.1016/B978-0-12-405210-9.00007-2>
- Vallina, S. M., & Simó, R. (2007). Strong relationship between DMS and the solar radiation dose over the global surface ocean. *Science*, 315(5811), 506–508. <https://doi.org/10.1126/science.1133680>
- Vila, M., Simó, R., Kiene, R. P., Pinhassi, J., González, J. M., Moran, M. A., & Pedrós-Alió, C. (2004). Use of microautoradiography combined with Fluorescence In Situ Hybridization to determine dimethylsulfoniopropionate incorporation by marine bacterioplankton taxa. *Applied and Environmental Microbiology*, 70(8), 4648–4657. <https://doi.org/10.1128/AEM.70.8.4648-4657.2004>
- Vila-Costa, M., Simó, R., Harada, H., Gasol, J. M., Slezak, D., & Kiene, R. P. (2006). Dimethylsulfoniopropionate uptake by marine phytoplankton. *Science*, 314(5799), 652–654. <https://doi.org/10.1126/science.1131043>
- Vincent, W. F., & Neale, P. J. (2000). Mechanisms of UV damage to aquatic organisms. In S. De Mora, S. Demers, & M. Vernet (Eds.), *The Effects of UV Radiation in the Marine Environment* (1st ed., pp. 149–176). Cambridge University Press. <https://doi.org/10.1017/CBO9780511535444.007>
- Vincent, W. F., & Roy, S. (1993). Solar ultraviolet-B radiation and aquatic primary production: Damage, protection, and recovery. *Environmental Reviews*, 1(1), 1–12. <https://doi.org/10.1139/a93-001>
- Visser, A. W., & Kjørboe, T. (2006). Plankton motility patterns and encounter rates. *Oecologia*, 148(3), 538–546. <https://doi.org/10.1007/s00442-006-0385-4>
- Weisse, T., Anderson, R., Arndt, H., Calbet, A., Hansen, P. J., & Montagnes, D. J. S. (2016). Functional ecology of aquatic phagotrophic protists – Concepts, limitations, and perspectives. *European Journal of Protistology*, 55, 50–74. <https://doi.org/10.1016/j.ejop.2016.03.003>
- Wiggins, H. L., & Rappoport, J. Z. (2010). An agarose spot assay for chemotactic invasion. *BioTechniques*, 48(2), 121–124. <https://doi.org/10.2144/000113353>
- Williams, P. D. (2008). Unhealthy herds: Some epidemiological consequences of host heterogeneity in predator–host–parasite systems. *Journal of Theoretical Biology*, 253(3), 500–507. <https://doi.org/10.1016/j.jtbi.2008.03.022>
- Wolfe, G. V., Steinke, M., & Kirst, G. O. (1997). Grazing-activated chemical defence in a unicellular marine alga. *Nature*, 387(6636), 894–897. <https://doi.org/10.1038/43168>
- Worden, A. Z., Follows, M. J., Giovannoni, S. J., Wilken, S., Zimmerman, A. E., & Keeling, P. J. (2015). Rethinking the marine carbon cycle: Factoring in the multifarious lifestyles of microbes. *Science*, 347(6223), 1257594. <https://doi.org/10.1126/science.1257594>
- Xue, L., Kieber, D. J., Masdeu-Navarro, M., Cabrera-Brufau, M., Rodríguez-Ros, P., Gardner, S. G., Marrasé, C., & Simó, R. (2022). Concentrations, sources, and biological consumption of acrylate and DMSP in the tropical Pacific and coral reef ecosystem in Mo'orea, French Polynesia. *Frontiers in Marine Science*, 9, 911522. <https://doi.org/10.3389/fmars.2022.911522>
- Zagarese, H., & Helbling, E. W. (2003). UV effects in aquatic organisms and ecosystems. Volume 1. *Comprehensive series in photochemical & photobiological sciences*. The Royal Society of Chemistry.
- Zheng, Y., Wang, J., Zhou, S., Zhang, Y., Liu, J., Xue, C.-X., Williams, B. T., Zhao, X., Zhao, L., Zhu, X.-Y., Sun, C., Zhang, H.-H., Xiao, T., Yang, G.-P., Todd, J. D., & Zhang, X.-H. (2020). Bacteria are important dimethylsulfoniopropionate producers in marine aphotic and high-pressure environments. *Nature Communications*, 11(1), 4658. <https://doi.org/10.1038/s41467-020-18434-4>
- Zimmer, R., & Butman, C. (2000). Chemical signaling processes in the marine environment. *The Biological Bulletin*, 198(2), 168–187. <https://doi.org/10.2307/1542522>

CONCLUSIONS

1. The integration of the microcapillary assay with advanced image analysis tools offers an excellent platform for investigating protist swimming behaviour and their spatial distribution in response to chemical gradients diffusing from a point source. The possibility to observe real-time behaviours both inside and outside of the capillaries increases our understanding of the influence of chemical cues on feeding strategies.
2. DMSP acted as a strong chemoattractor for the three herbivore protists tested (*Karlodinium armiger*, *Oxyrrhis marina* and *Gyrodinium dominans*). However, the different feeding strategies of the protists elicited distinct behaviours in response to DMSP gradients, confirming its multi-function chemotactic role. DMSP may enhance prey encounter and ingestion, induce aggregation in nutritious hot spots and serve as a source of reduced sulphur in protists with osmotrophic capabilities.
3. The distinct behaviours reflected how each organism perceives, interprets and uses DMSP. *O. marina* displayed circular tracks irrespective of the swimming direction to maximize the stay within the DMSP patch and take up DMSP when no prey was found. DMSP triggered a search behaviour in *K. armiger* and *G. dominans*, that was reflected in more convoluted inwards trajectories. Subsequently, *K. armiger* temporarily aggregated within the DMSP patch in order to take up dissolved DMSP, but low satiation levels and the absence of prey caused the organism to eventually leave the patch returning to ballistic swimming. *G. dominans*, being a strict phago-heterotroph without osmotrophic capabilities, did not accumulate and rapidly abandoned the DMSP patch after unsuccessful prey search, returning also to ballistic swimming.
4. The chemoattractant role of DMS was confirmed for *O. marina* and revealed for the first time for *G. dominans*. However, when compared to that of DMSP, DMS chemoattraction was weak and less consistent in the conditions and concentrations tested.
5. The role of acrylate as a repellent or attractor for herbivore protists was not confirmed. Consequently, acrylate cannot be defined as an infochemical for the three protists tested.
6. The in-situ chemotaxis assay (ISCA) method, designed to target the chemotactic responses of in situ bacterial communities, did not yield successful results with microplankton natural assemblages. To address the challenge posed by low cell concentrations, alternative methods are required to quantify and characterize the organisms within the wells. Filtered seawater (FSW) from in situ samples must be used to prepare the cue dilutions, to ensure no salinity-driven density gradients between the cue source and the in-situ water, but filtration artifacts may result in the alteration of chemical gradients.
7. The response of phytoplankton photosynthetic efficiency to ephemeral episodes of high solar radiation depends on the previous light-exposure history of the phytoplankton assemblage. Similarly, DMSP release as a light-stress response is primarily influenced by the phytoplankton assemblage composition over the level of stress experienced.
8. Experiments with natural communities showed faster microzooplankton grazing on phytoplankton that had been exposed to light-stress. In a model system with cultivated strains, conversely, *G. dominans* grazed faster on “healthy” (not high light exposed) *I. galbana*.

9. The model system with cultured strains behaved differently from the studied natural communities. Hence, the risk of choosing model systems to study general microbial responses to environmental perturbations is that they may present species or strain-specific behaviour.
10. Short-term incubations (<9h) are the optimal to observe differential grazing patterns after a light-stress event that might induce chemotaxis-related responses.
11. Introducing a cultured grazer to natural communities offers a viable option for altering the grazing pressure, alternative to the serial dilution technique.
12. The monitoring of the photosynthetic efficiency is a non-destructive, fast and informative technique to supervise the fitness of natural photosynthetic assemblages during short-term stress treatments and recovery phases.
13. All treated phytoplankton assemblages recovered from stress, yet with different kinetics. Grazing rates positively correlated with the rate of photosynthetic efficiency recovery. Preferential grazing on the most stressed individuals would explain the patterns by removing the individuals with the lowest photosynthetic efficiency. Additionally, the preference for the stressed cells could be mediated by the chemoattraction to DMSP or other exudates.
14. The positive relationship between grazing and recovery in the model system, where no preferential consumption of the stressed individuals was inferred, suggests the influence of, as yet unknown, additional factors.
15. This thesis offers preliminary evidence that selective protistan grazing enhances the recovery of the short-term overall fitness of phytoplankton prey populations. Our observations align with the healthy herds hypothesis, and pave the path for

ANNEX I –

VOLATILE ORGANIC COMPOUNDS RELEASED BY *Oxyrrhis marina* GRAZING ON *Isochrysis galbana*

Charel Wohl, Queralt Güell-Bujons, Yaiza M. Castillo, Albert Calbet and Rafel Simó

Oceans (2023). <https://doi.org/10.3390/oceans4020011>

Article

Volatile Organic Compounds Released by *Oxyrrhis marina* Grazing on *Isochrysis galbana*

Charel Wohl *, Queralt Güell-Bujons, Yaiza M. Castillo, Albert Calbet and Rafel Simó *

Department of Marine Biology and Oceanography, Institut de Ciències del Mar, ICM-CSIC, Barcelona 08003, Catalonia, Spain; queraltguell@icm.csic.es (Q.G.-B.); yaiza@icm.csic.es (Y.M.C.); acalbet@icm.csic.es (A.C.)

*Correspondence: cwohl@icm.csic.es (C.W.); rsimo@icm.csic.es (R.S.)

Abstract: A range of volatile organic compounds (VOCs) have been found to be released during zooplankton grazing on microalgae cultivated for commercial purposes. However, production of grazing-derived VOCs from environmentally relevant species and their potential contribution to oceanic emissions to the atmosphere remains largely unexplored. Here, we aimed to qualitatively explore the suite of VOCs produced due to grazing using laboratory cultures of the marine microalga *Isochrysis galbana* and the herbivorous heterotrophic dinoflagellate *Oxyrrhis marina* with and without antibiotic treatment. The VOCs were measured using a Vocus proton-transfer-reaction time-of-flight mass spectrometer, coupled to a segmented flow coil equilibrator. We found alternative increases of dimethyl sulphide by up to 0.2 nmol dm⁻³ and methanethiol by up to 10 pmol dm⁻³ depending on the presence or absence of bacteria regulated by antibiotic treatment. Additionally, toluene and xylene increased by about 30 pmol dm⁻³ and 10 pmol dm⁻³, respectively during grazing only, supporting a biological source for these compounds. Overall, our results highlight that VOCs beyond dimethyl sulphide are released due to grazing, and prompt further quantification of this source in budgets and process-based understanding of VOC cycling in the surface ocean.

Keywords: volatile organic compounds; grazing; Vocus; PTR-MS; *Isochrysis galbana*; *Oxyrrhis marina*

1. Introduction

Biological processes in the world's oceans produce a plethora of volatile organic compounds (VOCs) that can be released

to the atmosphere [1]. In seawater, VOCs can act as a source of energy and carbon for bacteria [2,3] or as messenger molecules in microbial interactions [4–7].

Many of these compounds are released through the interaction between members of the microbiota. One of these processes is grazing by microzooplankton (herbivore protists) on photosynthetic protists (microalgae) [8]. Additionally, bacterial activity can be a source [9–12] or a sink [8] of VOCs to the water column and strongly influence the volatile profile associated with certain phytoplankton [13].

A range of VOCs have been found to be emitted during grazing on species during cultivation for commercial purposes [14]. One study found that, amongst others, pentane, 2- and 3-methylfuran, 3-methylhexane and 3-pentanone were produced as a consequence of the rotifer *Brachionus plicatilis* grazing on the alga *Microchloropsis salina* [15]. The ecological roles of these compounds remained speculative, but the authors suspected that these compounds act as grazer deterrents or allelochemicals, and are generated as by-products of oxidative stress [15]. Sauer et al. [16] reported that monoterpenes decreased and a compound of likely molecular formula C₄H₇N and NH₃ increased temporarily as a grazer of the genus *Tetrahymena* consumed the cyanobacteria *Synechococcus elongatus* in the culture. They hypothesised that the decrease in monoterpenes was due to loss in algal biomass, while the transient peaks in nitrogen-containing compounds could be due to a defence mechanism [16]. Previous experiments had shown the release of β-cyclocitral and β-ionone upon grazing of a rotifer on the phytoplankton *M. gaditana* [17] and *M. salina* [18]. Recently, β-cyclocitral and β-ionone have also been observed in grazed cyanobacterial cultures and their non-grazed control culture [19]. These two compounds belong to a class of compounds coined apocarotenoids, which originate from the degradation of the photosynthetic pigment β-carotene [20]. The roles of these two compounds in algae is rather unknown, but in terrestrial plants β-cyclocitral fulfils allelopathic roles related to stress

signalling [20]. For short periods, β -cyclocitral has been found to increase swimming velocities of *Daphnia magna* [21], illustrating a potential role in chemical signalling.

One thoroughly investigated example of a gas produced from grazing in the ocean is dimethyl sulphide (DMS). DMS is produced through the action of bacterial or phytoplanktonic lyases on the precursor molecule dimethylsulfoniopropionate (DMSP) [22]. DMSP is largely produced by phytoplankton, with production rates that vary widely between phytoplankton species. Phytoplankton species can be divided into high and low DMSP producers [23–25]. Beyond grazing, algal DMSP is released into seawater through exudation, physiological stress, cell death by autolysis or viral lysis [26–28]. DMSP and its lyase degradation products, DMS and acrylate, have been shown to influence microzooplankton grazing. Although contradictory outcomes of the net effect, attraction or repulsion, have been reported [29–31]. DMSP is also degraded by bacteria into methanethiol [32], which is a much more poorly studied VOC, largely due to the difficulty of measuring dissolved methanethiol in seawater. Our current understanding is that most DMSP follows the degradation pathway into methanethiol while only a smaller fraction is transformed to DMS [33,34]. The production of methanethiol is thought to partially depend on bacterial sulphur demand, where bacteria would preferentially produce DMS if their sulphur demand is satisfied [35]. Methanethiol on the other hand seems to be an intermediate, produced during incorporation of sulphur from DMSP into cellular macromolecules [33]. Sea-to-air fluxes and seawater measurements suggest that methanethiol concentrations are approximately 20% of the DMS concentration [36–38], but this ratio can vary hugely [39]. This is because bacterial consumption is much faster for methanethiol than for DMS [32,40,41]. Beyond methanethiol and DMS, a number of sulphur-containing VOCs have recently been measured from an induced phytoplankton bloom [36].

Evidence exists for the production of benzene, toluene and xylene from axenic phytoplankton cultures and mesocosm studies [42]. This points to a biological source in seawater, supported by field measurements in the ocean [43,44]. Toluene is produced by some naturally occurring bacteria [45], including bacteria isolated from surface seawater in Antarctica [10]. An enzyme has been identified in bacteria that is responsible for toluene production [46]. However, very little is known about the actual oceanic biological production mechanisms as hitherto benzene, toluene and xylene have been labelled as anthropogenic pollutants [47]. Their largest source to the atmosphere is from anthropogenic activity, such as fuel evaporation and combustion, spillage, solvent use, refining of gasoline, landfill wastes and coal-fired stations [48]. Fuel spillage is also a source of benzene, toluene and xylene to the seawater [49]. The largest sink of these simple aromatics in seawater is probably bacterial consumption [50,51].

All in all, the floor was ripe to further explore the suite of VOCs produced from microzooplankton grazing and bacterial activity. In this experiment, we aimed to focus on compounds and phytoplankton species that are relevant for marine biogeochemistry. Thus, we decided to measure the VOCs produced in grazing experiments at high resolution using proton-transfer-reaction time-of-flight mass spectrometry (PTR-ToF-MS) coupled to a segmented flow coil equilibrator (SFCE). We adopted a mass scanning approach for an untargeted exploration of compounds, followed by high-time resolution monitoring of specific ions of target VOCs identified during the exploration. Our objective was to work with a highly simplified monospecific predator grazing on a DMSP-containing prey, making use of the bacteria naturally abundant in the culture. We used the marine heterotrophic dinoflagellate *Oxyrrhis marina* as a model grazer, and the haptophyte microalga *Isochrysis galbana* as the prey. In contrast to previous studies, we used an environmentally relevant prey in our experiments, rather than species cultivated for commercial interest. Haptophytes are environmentally relevant as they may account for 30–50% of the total photosynthetic standing stock in the oceans [52]. *Isochrysis galbana* is a well-characterised species known to produce large amounts of DMSP [28] while lacking DMSP lyase to cleave DMSP into DMS [53]. *Oxyrrhis marina* is frequently used as a model grazer [54] because of its voracious feeding which is generally well studied [55]. Although it is not typically found in the open ocean, *O. marina* is widely distributed in coastal habitats of the Northern Hemisphere, south of 63°N [56]. *Isochrysis galbana* and *O. marina* were also chosen because they readily grow up to high cell concentrations under antibiotic treatment. We used antibiotics to elucidate what compounds were produced as a direct consequence of the grazing activity or as products of bacterial processing. Short experimental timescales were implemented to avoid potential bottle effects or lab air to culture VOC exchange and allow for comparison between cultures [56]. By continuously measuring VOCs from a

phytoplankton culture as it was grazed down over the course of approximately five hours, we expected to detect the VOCs produced during grazing that could be of most interest for atmospheric chemistry.

2. Materials and Methods

2.1. Phytoplankton and Microzooplankton Cultures

The microzooplankton strain *O. marina* (ICM-ZOO-OM001) was originally isolated by A. Calbet in 1996 from the NW Mediterranean coast [55]. The prey chosen for growing the culture was *Rhodomonas salina* strain K-0294 in exponential growth phase. *Rhodomonas salina* is a weak DMSP producer [57]. By growing the grazer on a low-DMSP producer, we aim to keep DMSP concentrations in the grazer reasonably low and thus avoid potential interferences with our experiment. The prey used in the grazing experiment was *I. galbana* strain CCMP 1323. The three cultures were cultivated in autoclaved filtered seawater, which was supplemented with f/2 nutrients for the two microalgae. The growing phase prior to the experiment was performed on a 14:10 h light to dark cycle, at 19 °C and 50 $\mu\text{mol m}^{-2} \text{s}^{-1}$ of light, similar to Li et al. [28]. The cell concentration of the cultures and cell volume were monitored using a MultisizerTM 3 Coulter Counter (Beckman Coulter, Indianapolis, United States). Two batches of the grazer and two of the prey were grown for each culture. One was treated twice with a mix of three antibiotics: kanamycin (Merck K1377) at 1000 mg dm^{-3} , neomycin (Merck N6386) at 250 mg dm^{-3} , and penicillin G (Merck P3032) at 1000 mg dm^{-3} , one time at the start of the culture and again 24–48 h before the experiments. *Oxyrrhis marina* was starved for three days before the grazing experiments, until most of their vacuoles were empty and no prey was found in the culture as verified by microscopy. *Isochrysis galbana* was grown to an exponential growth phase for the grazing experiment.

2.2. The Grazing Experiment

Cultures of the grazer, *O. marina*, and the exponentially growing prey, *I. galbana*, were mixed on the day of the experiment in dark glass bottles of 2.5 dm^{-3} . Two mixtures, one with and one without antibiotic treatment, are coined here “grazing cultures”. As soon as possible after mixing grazer and prey, grazing cultures with and without antibiotic treatment were measured alternately for VOCs over five hours by passing the culture through an SFCE equilibrator coupled to a Vocus PTR-ToF-MS (see Appendix) [58]. Through frequent, repeat measurements of the same grazing cultures over time we aim to increase statistical significance of our observations. These repeat measurements essentially replace biological replicates, which were not possible to achieve because of workload, large number of cells for VOC analysis and requirement of multiple SFCE-PTR-ToF-MS for true replication. Replicate experiments done one after another would have involved using other batches of cultures.

Additionally, at the beginning of the experiment and hourly thereafter, we measured VOCs in each of the cultures of grazer and prey in isolation as well as in the culture medium alone, kept in 0.5 dm^{-3} dark bottles, to check for possible contamination from lab air. Time zero hereafter is defined as the timepoint at which we began the VOC measurements. The cultures measured during the experiment were all diluted in the same batch of autoclaved filtered seawater carefully syphoned in the sampling glass bottles to avoid atmospheric contamination prior to the experiment. Starting cell concentrations of each component in the individual grazer and prey cultures were chosen to be nearly equal to the cell concentrations of each component in the grazing culture to allow direct comparison of VOC concentrations in the grazing and parent cultures. Starting concentrations of *I. galbana* were around $5\text{--}6 \times 10^4 \text{ cells cm}^{-3}$ and starting concentrations of *O. marina* were approximately $3\text{--}4 \times 10^3 \text{ cells cm}^{-3}$.

2.3. Auxiliary Measurements

During the grazing experiments, we took samples for Coulter Counter and Flow Cytometry to document cell concentration and cell volume at times 0, 15, 30, 60, 90, 120, and 300 min after mixing prey and grazer. Samples for epifluorescence microscopy were also collected at times 0, 60, 120, and 300 min to obtain further evidence of the grazing process and quantify the number of *O. marina* cells that had ingested prey. Microscopy samples were fixed with 10% glutaraldehyde and counterstained with 0.5 mg dm^{-3} DAPI (4'-6-diamidino-2-phenylindole). Images were automatically acquired using a Zeiss Axio Imager Z2m epifluorescence microscope (Carl Zeiss, Germany) connected to a Zeiss camera (AxioCamHR, Carl Zeiss MicroImaging, S.L., Barcelona, Spain) at 630x magnification through the

AxioVision 4.8 software. The DAPI signal was observed using the UV filter set (370/40 nm excitation, 425/46 emission, and FT 395 beam splitter), while the cell's chlorophyll was observed using a filter set specific for chlorophyll (585/35 nm excitation, 615 LP emission, and FT 570 beam splitter). All pictures were taken using the same intensities and exposure times (15 ms for DAPI and 10 ms for chlorophyll). Nutrient concentrations (total nitrate plus nitrite, ammonia, silicate, and phosphate) were measured at time zero and after five hours in the parent cultures. Nutrients in the grazing cultures were additionally measured after 120 min.

2.4. Measurement of Dissolved VOCs

A commercially available Vocus PTR-ToF-MS (PTR-TOF-MS; TOFWERK AG, Thun, Switzerland, Vocus Scout) [58] was coupled to an SFCE equilibrator [59]. Details on the Vocus operation and settings, humidity considerations and data processing are provided in Appendix A.

The inlet of the SFCE equilibrator consisted of an 80 cm PFA tube (outer diameter 6.35 mm, wall thickness, 1.19 mm), which was used to draw samples from the bottom of glass bottles containing the cultures—exactly the same as discrete VOC sampling with the SFCE. We manually rapidly switched between measurement of the different cultures by moving the sampling tube from one bottle to another. Each culture or culture medium was measured for about 3 min which gave a stable signal of 2 min. Between samples, we briefly measured Milli-Q water to distinguish samples during data post-processing. Cultures were gently swirled approximately every 15 min to avoid sedimentation of the microorganisms.

The SFCE equilibrator was reproduced as before [59] with a few noteworthy modifications: (a) a 15 m long segmented flow tube was used to achieve a high degree of equilibration of less soluble compounds (e.g., isoprene); (b) the zero air carrier gas was supplied from a zero air generator (Vocus PTR Clean Air System: ZeroAir, TOFWERK AG, Thun, Switzerland) and the flow was controlled by daily flow-checked needle valves; and (c) the water flow into the equilibrator was reduced to $20.5 \text{ cm}^3 \text{ min}^{-1}$ to reduce the culture volume requirement for this experiment. This resulted in operating the water flow-controlling peristaltic pump at 27 rounds per minute which should have been gentle enough to avoid damage to the microorganisms and subsequent artefactual gas release. The equilibrator headspace air was transported to the main inlet of the Vocus via a 1.2 m PFA tube (outer diameter 3.18 mm, wall thickness, 0.77 mm) equipped with a vent to the atmosphere for excess air flow.

Equilibrator headspace mole fractions were calculated from a multi-compound gas standard. From that, dissolved concentrations were calculated assuming full equilibration of gases more soluble in water than benzene and toluene and accounting for the reduced water flow rate in the purging factor. More details are provided in the Appendix A5.

To test for significance, we use the repeated measures ANOVA test [60] applying it to pairwise comparisons of time series. We chose this statistical test because it allows to test for significant differences of the same repeatedly measured sample, thus accounting for repeat measurements not being statistically independent. To account for differences in time resolution, which are incompatible with the ANOVA test, higher resolution time series were subsampled to the nearest located measurement of the lower resolution time series. In the text, we state the p -value to give the significance level and chose a significance threshold of 0.1 to account for the high dynamicity of the study system.

3. Results

3.1. Biological Results for Culture Grazing

Isochrysis galbana cell concentrations decreased rapidly in both the antibiotically and non-antibiotically treated grazing culture over the first 90 min (Figure 1a). The decrease was slower afterwards (Figure 1a) (O_I_B culture, *I. galbana* cell concentrations vs time: linear regression slope \pm 95% confidence interval; 0 to 90 min -371 ± 285 , 90 to 300 min -65 ± 59). The same pattern was reflected in the ingestion rates (Figure 1b), with the particularity that they were on average 21% lower without antibiotics (O_I_B culture, ingestion rates vs time: linear regression slope \pm 95% confidence interval; 0 to 90 min -0.036 ± 0.036 , 90 to 300 min -0.006 ± 0.030). Coulter Counter measurements confirmed that the cell concentrations of *O. marina* (Figure 1a) did not increase substantially during the five-hour experiment. The average cell volume of *O. marina* rapidly increased during the first 90 min and at a slower rate

thereafter (Figure 1c). Microscopy images of *I. galbana* cells inside *O. marina* were further used to confirm that the *O. marina* cells were actively ingesting the selected prey during our experiment (Appendix B). These fluorescence microscopy images showed that a single cell of *O. marina* had ingested multiple *I. galbana* cells. They also showed that at time zero, already 66% of the *O. marina* cells had prey inside i.e., monitoring of the experiment started with the grazing already in progress. By 120 min, 95% of the *O. marina* cells contained prey as determined by microscopy. Overall, these observations suggest that there was very intense grazing from the onset of the experiment until approximately 90 min. Then onwards, grazing was slower, while *O. marina* cells did not start to divide yet.

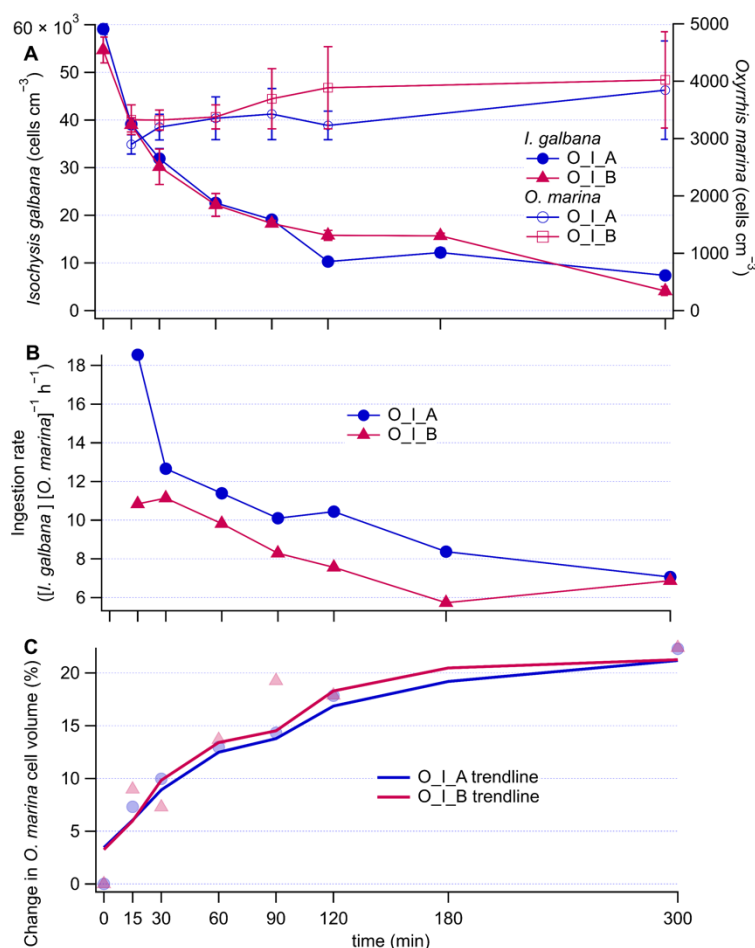


Figure 1. Time series of *I. galbana* (prey) and *O. marina* (grazer) concentrations (A), ingestion rates (B), and percent increase of *O. marina* cell volume (C) relative to the initial time point. In the legends, O stands for *O. marina*, I for *I. galbana*, A for antibiotic treatment and B for no antibiotic treatment. Error bars represent measurement noise from repeat measurements of the same sample.

Nutrient measurements (Appendix C) confirmed that over the course of the experiment, phytoplankton did not deplete the nutrients supplied in the culture media. Ammonium concentrations substantially increased in the grazing culture without antibiotic treatment (about 2-fold) and in the *I. galbana* culture without antibiotic treatment (about 70-fold). This is likely because bacteria present in the cultures produced ammonia from nitrogen-containing organic matter released during prey growth and grazing-induced prey cell lysis [61,62]. In contrast, ammonium concentrations in antibioticly treated cultures of *I. galbana* and *O. marina* remained essentially constant over the course of the experiment. Only a very small increase in ammonia concentration (20%) was observed in the grazing culture treated with antibiotics.

Microscopy results and flow cytometry indicate that bacterial cell concentrations were on the order of 10^6 to 10^4 cells cm^{-3} in all cultures, even in those with antibiotic treatment. However, aliquots of the antibioticly-treated cultures plated on agar plates did not show bacterial growth. Similarly, the changes in ammonium concentrations suggest that the bacteria present in the antibioticly-treated cultures were largely inactive. Some of the bacteria observed in the cultures by microscopy and flow cytometry could be antibioticly resistant or inactive bacterial cells or debris. It seems likely that

microscopy and flow cytometry count inactive or dead bacteria, which leads to overestimates of the living bacterial cell counts.

3.2. Mass Spectral Characteristics to Identify Organic Compounds from Grazing

Figure 2 shows a mass spectrum of the grazing culture without antibiotics. This mass spectrum was calculated as the difference between the spectrum at the end of the experimental period ($t = 300$ min) minus that at the beginning ($t = 0$ min). The data are presented as the percentage of the total number of ion-impacts measured by the Vocus detector per second. The numbers do not add up to one hundred in the figure, because prominent peaks related to instrument operation have been set to zero to facilitate interpretation. In the case of measuring the equilibrator headspace, the magnitude of the signal of each individual compound is mostly influenced by the compound's solubility, where more volatile compounds display a higher signal. Thus, this mass spectrum is a reasonable way to explore the more volatile compounds produced in the grazing culture with bacteria.

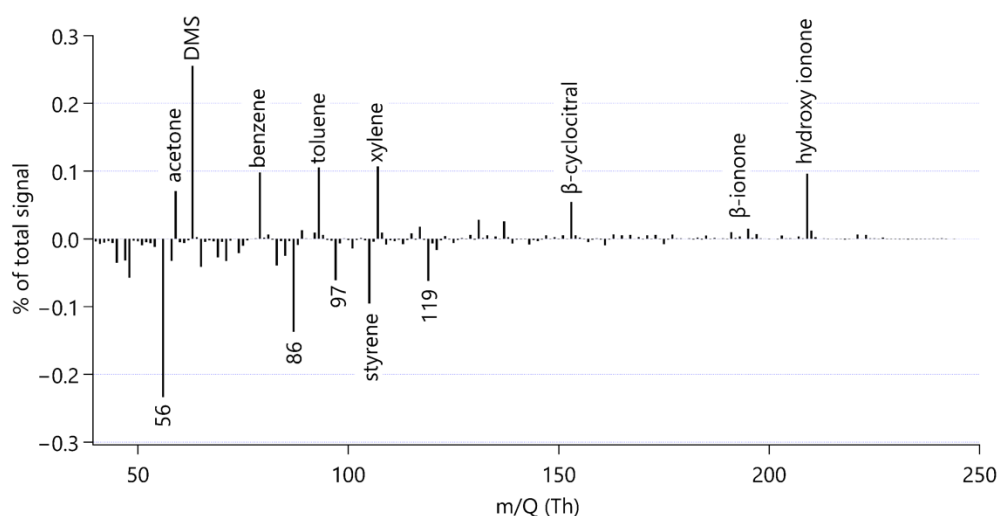


Figure 2. Mass spectrum calculated as the difference between the end of the experimental period ($t = 300$ min) minus the beginning ($t = 0$ min) of the grazing culture without antibiotic treatment (O_I_B). Identified and discussed peaks are labelled with the compound name or nominal mass. To simplify the interpretation of the spectrum, prominent peaks due to water clusters and some of their isotopes have been set to zero in this graph, namely nominal masses m/Q 55, 57, 73 and 91. Similarly, a prominent peak due to the artefactual acetone-water cluster at m/Q 77 and the instrument parameter NO^+ at m/Q 46 are set to zero.

Each bar in Figure 2 represents a different compound measured by the Vocus. This illustrates that the instrument can detect many VOCs in the headspace of a phytoplankton culture, some of which are of very low intensity and not discussed here.

Figure 2 is useful to visually scan for VOCs emitted or consumed during grazing, where potential production is indicated by a prominent positive bar. In our time series analysis, we will focus on compounds which; (a) increased during the experiment; (b) can be identified reliably; and (c) were detected at relatively high intensity.

Notable increases in ion intensity were observed for ions at nominal mass m/Q 59, 63, 79, 93 and 107. By matching high resolution peaks with expected masses based on elemental formula, these peaks were attributed to acetone, dimethyl sulphide, benzene, toluene and the sum of xylenes respectively, in line with common mass assignments [63]. We did not observe other peaks at these nominal masses. The instrument cannot distinguish isomers and thus we cannot tell what isomer of xylene (*o*-, *m*- or *p*-) or ethylbenzene is present in the sample. Hence, we are reporting this signal as “Xylenes” (see Appendix A4).

By comparing the time series of the grazing culture with those of the culture media alone, we concluded that the increase in acetone and benzene during our experiment was probably due to a flux of these gases from lab air into the culture. Mole fractions of these two gases can be very high in indoor air [64]

and we do not expect any changes in concentration in the culture media alone. Consequently, our results do not appear to support a grazing source for acetone and benzene. Similarly, we could not observe an increase in the acetaldehyde signal due to grazing. Future experiments measuring these gases produced from lab cultures should also focus on rigorously avoiding or quantifying lab air to culture exchange to avoid false positive reporting. For example, Reese et al. [12] had to exclude many peaks from their analysis that were associated with the culture media and the sampling device. Furthermore, Rocco et al. [42] subtracted a background of benzene, toluene and xylene from their culture media.

We additionally recognised an isolated peak at m/Q 49.011, which we identified as methanethiol following the mass assignments of Pagonis et al. [63] and Kilgour et al. [36]. The identity of this peak was additionally confirmed by comparing the peak observed in the experiment and from evasion calibrations of methanethiol by dissolving sodium methanethiolate in seawater [65].

Three ions of m/Q 153.107, m/Q 193.158 and m/Q 209.165 increased in intensity during the experiment. We assigned the molecular formulae $C_{10}H_{16}OH^+$, $C_{13}H_{20}OH^+$ and $C_{13}H_{20}O_2H^+$ to the three ions, respectively, using Tofware software package (ver. 3.2.5, www.tofwerk.com/tofware) developed by Tofwerk and Aerodyne Research Inc. (www.aerodyne.com). This software suggests the most likely elemental formula of a peak given its high-resolution mass. Based on that, we suspect that these ions correspond to α - or β -cyclocitral (CAS number 432-25-7), α - or β -ionone (CAS number 79-77-6) and hydroxy ionone. Note that the Vocus PTR-MS cannot distinguish between isomers of these compounds. These compounds have been identified as common products of carotene degradation in plants [66] and also in algae [5,13,13,18]. Other researchers using PTR-MS alongside GC-MS for identification have identified these peaks as β -cyclocitral, β -ionone and hydroxy ionone [66,67]. In agreement with observations by García-Plazaola et al. [66], we removed influences from the peaks $C_8H_8O_3H^+$, $C_{12}H_8H^+$ and $C_9H_{16}N_2H^+$ from the β -cyclocitral peak using the Tofware software.

By comparing the time courses of cyclocitral, ionone and hydroxy ionone ions in the different cultures, we could not identify a production mechanism as they increased in all cultures over the course of the experiment, but not in the culture media (Appendix D). As there was no difference in concentration between the cultures, a production mechanism could not be inferred. Therefore, although we can confirm the release of α - or β -cyclocitral (CAS number 432-25-7), α - or β -ionone (CAS number 79-77-6) and hydroxy ionone from these microorganism strains (see Appendix D), our results do not allow a more in-depth discussion.

Figure 2 also shows that some ion intensities decreased during the experiment. This could be because bacteria are a sink for these VOCs [68,69], or these compounds may be lost/outgassed to the atmosphere during sampling. We observed notable net decreases in compounds at nominal masses m/Q 56, 86, 97, 105 and 119, which could not be reliably assigned. Mass 86 could potentially be 3-pentanone, which has previously been observed to be emitted from the microzooplankter *Brachionus plicatilis* grazing on the phytoplankter *Microchloropsis salina* [15]. For the rest of this analysis, we will focus on compounds with a net production during grazing, but it is important to keep in mind that microorganisms are not only sources but also sinks of VOCs.

3.3. Time Series Analysis

In the grazing experiment without antibiotics, the DMS concentrations increased rapidly by $0.08 \text{ nmol dm}^{-3}$ during the first 40 min, coinciding with the fastest consumption of the prey, and continued increasing at a slower, constant pace thereafter attaining a total increase in concentration of 0.2 nmol dm^{-3} (Figure 3a). The culture of *I. galbana* alone without antibiotics also displayed an increase of DMS concentration of $0.17 \text{ nmol dm}^{-3}$, yet significantly less than the grazing culture (repeated measures ANOVA comparing grazing culture without antibiotics and *I. galbana* culture without antibiotics, $p = 0.005$). Conversely, the antibiotic treatment of both the grazing culture and *I. galbana* culture alone resulted in no substantial increase in DMS concentration. However, antibiotic treatment only resulted in a significant difference in the case of the grazing culture (repeated measures ANOVA, comparing antibiotically treated and non-antibiotically treated; grazing culture, $p = 0.06$, *I. galbana* culture $p = 0.175$). No increase was observed in the *O. marina* cultures, even though a slight decrease occurred in the presence of antibiotics, which resulted in a significant difference between the two *O. marina* cultures

(repeated measures ANOVA, comparing antibiotically treated and non-antibiotically treated; *O. marina* culture $p = 0.07$).

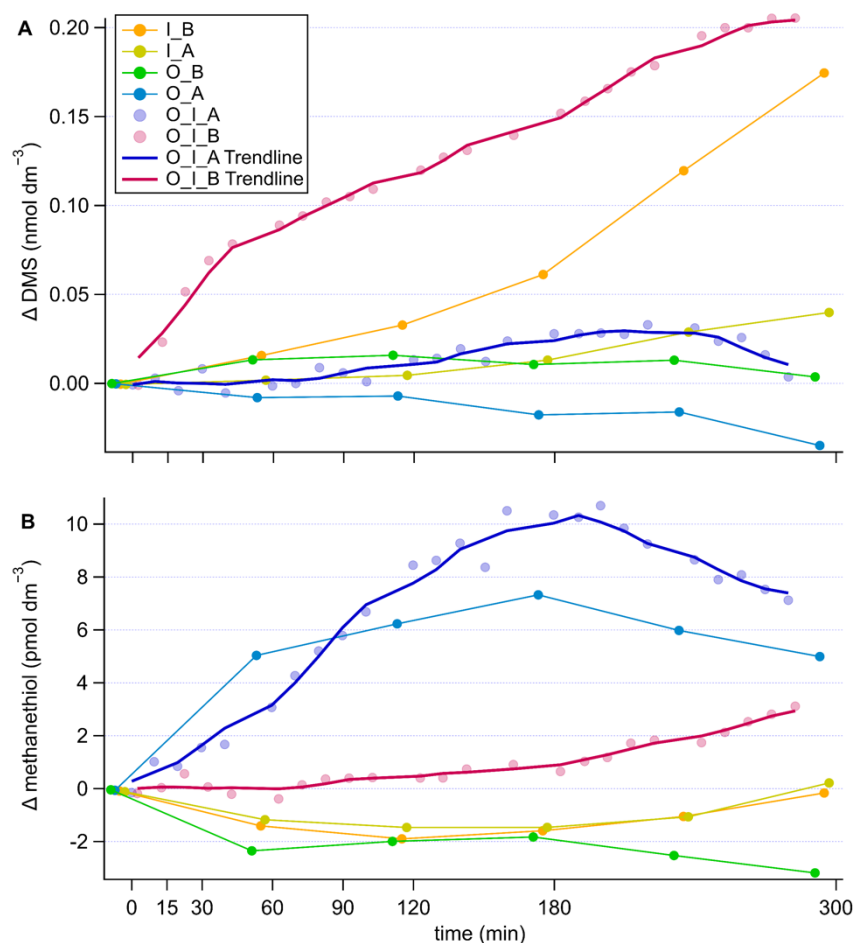


Figure 3. Timeseries of changes in DMS (A) and methanethiol (B) concentration in the different cultures, corrected for the culture medium blank. Components of the cultures are abbreviated as follows, O: *O. marina*, I: *I. galbana*, A: antibiotic treatment, B: no antibiotic treatment. In the grazing cultures, with more frequent data points, the 5-point running average trendlines are shown to help visually tease out trends.

The patterns of methanethiol were somewhat opposite to those of DMS (Figure 3b). In the grazing culture without antibiotics, methanethiol concentrations remained constant during the first 60 min of intense grazing and increased slightly (by 3 pmol dm⁻³) thereafter. In the presence of antibiotics, methanethiol increased immediately from the onset of the measurement period, both in the grazing and the *O. marina* cultures to around 7 pmol dm⁻³ by the end of the experiment. This led to significant differences between the antibiotically treated and non-antibiotically treated cultures containing the grazer (repeated measures ANOVA antibiotically treated and non-antibiotically treated *O. marina* culture, $p = 0.075$, grazing cultures antibiotically treated and non-antibiotically treated $p = 0.094$). Without antibiotics, methanethiol decreased slightly in the *O. marina* culture. No remarkable pattern was found in the *I. galbana* cultures, irrespective of antibiotics.

The aromatic compounds toluene and xylenes showed concentration increases by about 30 pmol dm⁻³ and 10 pmol dm⁻³ respectively only in the grazing cultures and after a lag of approximately 120 min from the onset of the measurement period (Figure 4). This resulted in poor significance levels (repeated measures ANOVA, comparing *I. galbana* culture to grazing culture with and without antibiotic treatment, toluene $p = 0.231$, $p = 0.532$, xylene $p = 0.304$, $p = 0.606$). This time lag was about 30 min longer for toluene in the presence of antibiotics (Figure 4a), an effect that was not recorded for xylenes (Figure 4b). No substantial change in concentration was observed in the cultures of the grazer or the prey alone, irrespective of antibiotic treatment.

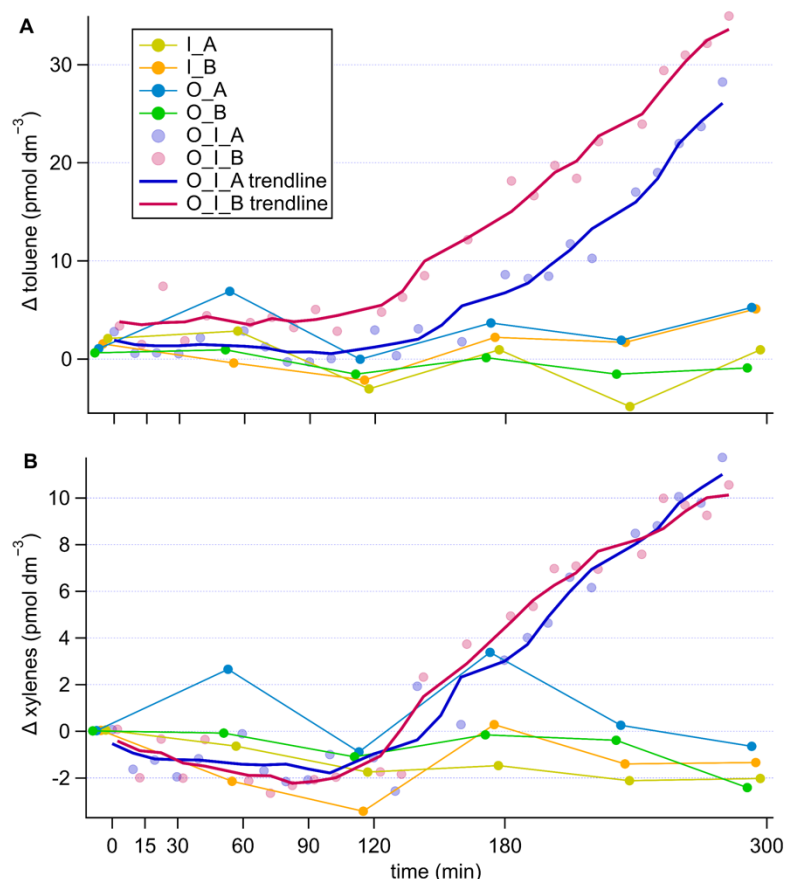


Figure 4. Timeseries of changes in toluene (A) and xylenes (B) concentrations in the different cultures, corrected for the culture medium blank. Components of the cultures are abbreviated as follows, O: *O. marina*, I: *I. galbana*, A: antibiotic treatment, B: no antibiotic treatment. In the grazing cultures, with more frequent data points, the 5-point running average trendlines are shown to help visually tease out trends.

4. Discussion

4.1. Advantages of Our Experimental Design and Measurement Setup

In most previous studies, VOCs produced by cultures were measured either in the bottle headspace or after bubbling the culture and injecting the sparging gas into a PTR-MS [42,70,71] or a purge and trap gas chromatography/mass spectrometry system [13]. In our experiment, culture volumes were passed through a segmented flow equilibrator, which allowed quick and sensitive measurements. Our setup has the following advantages: (a) we have characterised the degree of equilibration for many compounds and achieved a high level of equilibration for a broad range of VOCs, which results in high sensitivity; (b) the analytical system has a rapid response time of about 30 s; and (c) the segmented flow headspace air is only exposed to very inert PFA, making this setup ideal for the detection of compounds that readily stick to or react with other materials (such as methanethiol, which can be lost to stainless steel [37]); PFA is considered to be the most inert commercially available material for reactive gas measurement [72,73].

With our experimental design, we aimed to distinguish what VOCs were produced due to grazing activity and bacterial processing compared to the grazer and the prey alone. Our use of frequent, rapid response measurements, along with measurements of the grazer and prey alone, allowed us to relate the production of VOCs to the most plausible source using statistics. Furthermore, by measuring the VOCs instantly released from grazing over a relatively short time span, we reduced experimental artefacts, such as lab-air to culture VOC exchange or biological bottle effects.

4.2. Grazing Activity

Concentrations of grazer and prey were chosen to lead to near complete consumption of *I. galbana* cells over the course of the experiment. Rapid decreases in cell concentrations of *I. galbana*, especially during the first 90 min (Figure 1a), confirmed the instant response of the grazer to the presence of the prey

with high ingestion rates, as expected for a starved *O. marina* culture [55]. A decrease in ingestion rates over the time course of the experiment is due to (a) a reduction in the encounter rates of grazer and prey as prey concentration decreases, and (b) *O. marina* satiation over time [55]. We observed on average 21% lower ingestion rates in the non-antibiotically treated grazing culture. This could be due to (a) small differences in the starting concentrations of *O. marina* affecting competition for prey and (b) *O. marina* probably grazing on bacteria thus alleviating grazing pressure [74]. *Oxyrrhis marina* has been found to feed and grow on bacteria alone [74]. The increase in volume of *O. marina* cells during the experiment (Figure 1c) is related to prey accumulation inside digestive vacuoles. The *O. marina* cell volume increased by 2% more in the grazing cultures without antibiotics, despite lower ingestion rates in this grazing culture (Figure 1b,c), which could be attributed to ingestion of bacteria as well as *I. galbana* [74]. Notably, over the course of the experiment, the grazing cultures contained both intact cells of non-eaten *I. galbana* in exponential growth and grazed cell debris (Figure 1a). *Oxyrrhis marina* cell concentrations did not change substantially during the experiment (Figure 1a), indicating that the grazer cells were mostly actively ingesting and digesting prey and less actively dividing.

4.3. Sulphur Compounds

Grazing enhanced DMS production compared to *I. galbana* alone, and DMS concentrations increased faster at the beginning of the grazing experiment, coinciding with faster ingestion rates (Figure 3a). Wolfe et al. [56] also observed rapid production of DMS as *O. marina* was grazing on the high DMSP producer *Emiliania huxleyi*. The very low DMS production in the antibiotically-treated culture confirms that bacteria are key to the production of DMS and that neither *I. galbana* nor *O. marina* possess the relevant enzymes to cleave algal-released DMSP. This is in line with observations by Saló et al. [75] and Niki et al. [53] who found that neither of those organisms possess the ability to cleave DMSP. The DMS increase in the *I. galbana* culture without antibiotics was likely due to bacterial cleavage of the DMSP released by the microalga through exudation or cell death. Li et al. [28] observed an ‘acclimatisation period’ of *I. galbana* after transfer into culture media resulting in higher DMS concentrations per cell at day 1 compared to day 6 of their experiment. A similar process likely occurred at the onset of our *I. galbana* cultures, but DMS production was observed only when bacteria were present (no antibiotic treatment).

Relatively large accumulations of methanethiol were observed only in the *O. marina*-containing cultures treated with antibiotics (Figure 3b). There is a strong indication that bacteria were net methanethiol consumers in our experiment and antibiotics efficiently arrested consumption and allowed accumulation. The evidence for this is that methanethiol concentrations increased by only half as much in the grazing culture without antibiotics, and even decreased in the *O. marina* culture without antibiotics. Therefore, in our experiments, bacteria seem to be a net sink of methanethiol, while they are a net source of DMS. This is in good agreement with previous observations of rapid bacterial methanethiol consumption [33], and points to marine bacteria as critical players in the regulation of methanethiol concentrations in the surface ocean, being not only sources, but also sinks of methanethiol.

More surprising is the observation of methanethiol production in the *O. marina* cultures with antibiotics. It is not totally clear why this is the case. Because methanethiol sources in seawater are poorly understood, we cannot thoroughly describe the reasons behind this observation. It could be that the grazer produced methanethiol because it had been grown feeding on a low DMSP producer (*R. salina*). There is reported evidence that *O. marina* incorporates sulphur from DMSP-containing prey [75]. Given that the *O. marina* cells were starved before the experiment, it is possible that they kept producing methanethiol as a transient metabolite to sulphur assimilation from DMSP, similar to bacteria [35], and some was lost through membrane diffusion. The ecological significance of this process remains speculative. *Oxyrrhis marina* grown on a low DMSP producer (*Dunaliella tertiolecta*) has previously been shown to release small amounts of DMS [56], so it seems possible that it could also release methanethiol—another DMSP breakdown product. Overall, the experiment suggests that DMSP degrading bacteria as well as microzooplankton may be biological sources of methanethiol in the pelagic ocean, with bacteria being the main biological sink. This highlights the need for a better process-based understanding of marine methanethiol cycling, especially in light of its non-negligible contribution to the oceanic emission of sulphur to the atmosphere [37].

4.4. Aromatic Compounds

The results of the experiment (Figure 4) suggest that toluene and xylenes were released into seawater because of grazing, whereas benzene was not associated with grazing. Additionally, bacteria slightly enhanced toluene production in the grazing cultures. There was a notable lag time to the production of these aromatic compounds compared to that of DMS. The increase in toluene and xylene in the grazing cultures seems to coincide with the increase in methanethiol in the same culture after about 120 min, potentially pointing towards common production mechanism. The observation that the increase in concentration occurred during the second half of the experiment, coinciding with lower ingestion rates, suggests that there are intermediate steps between grazing and toluene/xylenes production. This could indicate that toluene and xylenes are released during digestion of the prey, yet a detailed biochemical mechanism or ecological relevance of this process cannot be speculated at this point. In any case, our experiment provides further evidence for a biological source of toluene and xylenes in seawater, and points to the intervention of grazing and bacteria as a possible explanation for why in situ concentrations of toluene correlate more poorly with chlorophyll *a* than benzene concentrations [44]. Much work remains to be done to elucidate the marine biological sources of these aromatic VOCs that are important for atmospheric chemistry [44].

5. Conclusions

Grazing by *O. marina* on *I. galbana* was shown to produce up to 0.2 nmol dm⁻³ DMS in this culture by release of DMSP from grazing and subsequent bacterial cleavage into DMS. The grazer also produced up to 10 pmol dm⁻³ methanethiol, potentially from a DMSP-containing diet, however, in the presence of bacteria, methanethiol was rapidly consumed thus preventing accumulation. Toluene and xylenes were also produced by grazing, leading to increases by about 30 pmol dm⁻³ and 10 pmol dm⁻³ over the controls. There was a distinct time lag of about 120 min that suggested intermediate steps in their production. Our results prompt to further identify the VOCs produced during grazing on phytoplankton, and to quantify this source in budgets and process-based understanding of VOCs in the surface ocean. Ultimately, this will help to quantify the impact of grazing on ocean emissions of VOCs and atmospheric chemistry.

Author Contributions: Conceptualization, C.W., Q.G.-B. and R.S.; data curation, C.W.; funding acquisition, R.S.; investigation, C.W., Q.G.-B., Y.M.C. and A.C.; methodology, C.W., Q.G.-B. and R.S.; project administration, R.S.; resources, R.S.; supervision, R.S.; visualization, C.W.; writing—original draft, C.W.; writing—review and editing, Q.G.-B., Y.M.C., A.C. and R.S. All authors have read and agreed to the published version of the manuscript.

Funding: The SUMMIT project is funded by the European Research Council (ERC) under the European Union's Horizon 2020 research and innovation programme (Project ERC-2018-AdG 834162 SUMMIT to RS, Grant Agreement No. 834162). The ICM-CSIC received funding from the Spanish government through the 'Severo Ochoa Centre of Excellence' accreditation (CEX2019-000928-S).

Institutional Review Board Statement: Not applicable

Informed Consent Statement: Not applicable.

Data Availability Statement: Data used in this paper were acquired during the experiment and are not currently archived in a data repository. Please contact us if you are interested in the data.

Acknowledgments: We would like to thank the Simó Lab members for helpful discussions and administrative support. Many thanks to Ana Sotomayor and Claudia Traboni for providing *Rhodomonas salina* for feeding the *O. marina* culture. We are also very thankful to Veronika Pospisilova and Felipe Lopez-Hilfiker from Tofwerk for excellent instrument support.

Conflicts of Interest: The authors declare no conflict of interest.

Appendix

Appendix A. Details Regarding the Operation of the PTR-MS and SFCE

Appendix A.1. Vocus Settings

The focussing ion-molecule reactor (FIMR) (Vocus Reactor) was operated at 2 mbar. The Vocus front and back voltages were 600 V and 24 V, respectively, giving an axial voltage of 576 V. The quadrupole around the FIMR was set to 500 V and the frequency was 2.22×10^6 Hz. The temperature in the reactor was 50 °C. Using these measured FIMR settings, we calculated an electric field strength (E/N) of 134 Td ($1 \text{ Td} = 1 \times 10^{-17} \text{ V cm}^2$). However, due to the location of the sensor measuring the FIMR pressure and the application of an RF field, the true electric field strength experienced by the product ions (protonated VOCs) was somewhat different. Hence, it is best practice to estimate the E/N in a Vocus instrument using the fragmentation pattern of α -pinene [58,76]. By comparing published fragmentation patterns to our observed fragmentation ratio, we determined the true electric field strength to be 80 ± 5 Td. Therefore, the electric field applied during this experiment was very low, allowing for relatively soft ionisation and less fragmentation. To keep the total ion current measured by the detector below 10^7 ions per second and thus prolong detector lifetime, the BSQ voltage was set to 275 V. This changes the flight path of ions of low molecular weight and makes that only a small fraction of highly abundant hydronium ions, lower mass hydronium ion water clusters and their isotopes were transmitted to the detector. At the same time, this reduced transmission of all ions of molecular weight of less than m/Q 59 as determined by transmission curves generated from a multi-compound gas standard. This reduced transmission was accounted for in the calculation of the methanethiol (m/Q 49) concentrations. During the experiment, the Vocus was operated to scan masses up to m/Q 250.

Appendix A.2. Vocus Calibrations

The Vocus was calibrated on the day of the experiment using a multi-compound gas standard (nominal concentration 500 nmol mol⁻¹; methanol, acetaldehyde, acetone, isoprene, DMS, benzene, toluene, m-xylene, α -pinene in nitrogen, Apel-Riemer Environmental, Inc., Miami, Florida, USA). The gas standard was serially diluted in zero air from a Vocus zero air unit (Vocus PTR Clean Air System 2020: ZeroAir, ToFwerk, Thun, Switzerland) using two build-in mass flow controllers, which injected the calibrant gas through a 16th inch tube at the Vocus inlet. At the cited FIMR settings, we assessed the contribution of fragmenting toluene to the benzene signal to be less than 2% using liquid standards measured in the SFCE equilibrator.

Appendix A.3. Vocus Humidity Considerations

Equilibrator headspace air was laden with humidity at around 20 °C. Previous generations of PTR-MS instruments used to display a dependence of the signal to sample humidity [77] which had to be considered when coupling to the SFCE equilibrator [59]. Compared to previous PTR-MS instruments, the Vocus uses a very high flow of water vapor from a water reservoir into the H₃O⁺ ion source (20 sccm compared to 1–2 sccm on previous generations). This results in an extremely high amount of hydronium ions, their clusters and water vapor concentration in the FIMR. Krechmer et al. [58] showed that the Vocus does not display a humidity dependence of the signal as the flow of sample air into the FIMR does not substantially alter the humidity therein. Experimentally, we were able to confirm that our instrument does not display a humidity dependence of the signal for the compounds contained in our gas standard and at the humidities expected in equilibrator headspace air. We note that Novak et al. [37] suggested a humidity dependence of methanethiol in their Vocus, which was probably due to a metal tee piece used in their atmospheric sampling line. Our calibrations with liquid standards of methanethiol did not obviously suggest any such artefact, probably because the SFCE equilibrator does not contain any metal pieces.

Appendix A.4. Vocus Data Processing

The Vocus data files were processed using Tofware version 3.2.5, run in Igor 9.0.1.2. To do the high-resolution peak fitting, we used the PTR library published by Pagonis et al. [63] and integrated it into our Tofware peak list using only ions identified by PTR instruments listed by Pagonis et al. [63]. If there was a peak we could not identify using the Pagonis et al. [63] library, we used the library from Yáñez-

Serrano et al. [78] or compounds listed in García-Plazaola et al. [66]. This peak list was used to de-isotope the mass spectrum. Details on the peak identification for each individual peak are further provided in the results section.

The xylene signal is reported here as the sum of xylene isomers (*o*-, *m*-, *p*-Xylene and ethylbenzene) based on the following reasoning: The Vocus and SFCE sensitivity depends on the hydronium reaction rate constant and the compound's solubility. The hydronium reaction rate constant of the Xylene isomers ranges between $(2.26\text{--}2.32) \cdot 10^{-9} \text{ cm}^3 \text{ s}^{-1}$ (range: 2% of the average rate of the four isomers) [79], while the solubility of these compounds is poorly constrained and the range of estimates overlaps. Hence we use the Vocus sensitivity and water solubility of *m*-xylene [80] (solubility by Karl et al. [81], temperature dependence by Staudinger and Roberts [82]) to calculate the dissolved concentration in seawater. To calculate dissolved methanethiol concentrations, we used the solubility and temperature dependence recommended by Burkholder et al. [83].

The limit of detection was calculated as three times the measurement noise. Measurement noise, in turn, was calculated as the standard deviation of repeated zero air measurements, as recommended by the Vocus PTR-ToF-MS manufacturer. This gave the following rounded results, presented as measurement noise followed by the limit of detection separated by a comma; DMS 0.0001, 0.0004 nmol dm⁻³, methanethiol 0.05, 0.18 pmol dm⁻³, toluene 0.12, 0.41 pmol dm⁻³, xylene 0.05, 0.17 pmol dm⁻³. Small differences between three times the listed measurement noise and the limit of detection are due to rounding numbers.

Appendix A.5. SFCE Calibrations

The SFCE equilibrator was calibrated frequently for a period leading up to the experiment day using liquid standards for evasion calibrations. This was used to confirm consistent near-complete equilibration in the segmented flow tube. The advantage of a high degree of equilibration compared to partial equilibration is that the degree of equilibration is more robust and does not have to be monitored continuously for example by using an internal standard. The following compounds were calibrated using liquid standards; DMS, methanethiol, isoprene, acetone, acetic acid, dimethyl disulphide and toluene. The compounds contained in the gas standard canister (methanol, acetaldehyde, acetone, isoprene, DMS, benzene, toluene, *m*-xylene, α -pinene) were additionally calibrated for by invasion calibrations. These compounds were chosen due to their relatively low toxicity, ready availability, and range in solubility/volatility. Low solubility is defined here as a low value of the Henry's dimensionless water-over-air solubility. Of these compounds, isoprene has the lowest solubility.

By demonstrating near-full equilibration of isoprene in the SFCE equilibrator using the longer equilibration tube, we were able to confirm that compounds of higher solubility also fully equilibrate, due to the effect of solubility on the air-sea exchange transfer velocity (low solubility compounds take longer to fully equilibrate than high solubility compounds due to lower air-sea transfer velocities [84]). By conducting evasion calibrations for acetic acid, we are able to verify that the Vocus and the SFCE equilibrator are inert enough to detect compounds of extremely low volatility [73].

We note that these calibrations were done at a water flow of $40 \text{ cm}^3 \text{ min}^{-1}$, while the experiment was carried out at a water flow of $20.5 \text{ cm}^3 \text{ min}^{-1}$. Last minute adaptations related to culture growth required us to use this lower water flow. Given that we have full equilibration of isoprene at $40 \text{ cm}^3 \text{ min}^{-1}$, we also expect this to be the case at the lower water flow rate, which allows for a longer equilibration time. The measured dissolved concentrations were finally computed using published solubility values with which we found agreement in our calibrations and accounting for the reduced water flow using the purging factor [59].

For compounds we directly calibrate for (standard gas canister, evasion or invasion i.e., DMS, methanethiol, benzene, toluene and xylene), we expect the uncertainty to be less than 15%.

Appendix B. Microscopy Images

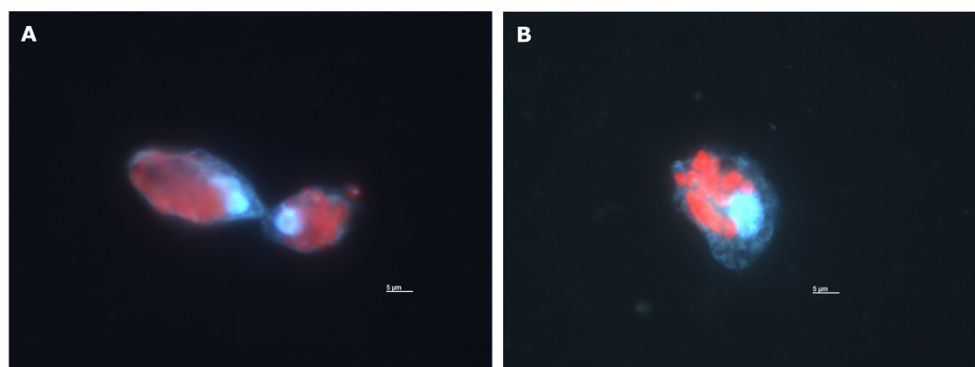


Figure A1. Fluorescence microscopy image of *O. marina* cells after grazing on *I. galbana* at the incubation timepoint of 120 min from the antibioticly treated culture (A) and the non-antibiotically treated culture (B). Blue fluorescence: *O. marina* DNA stained by DAPI (4',6-diamidino-2-phenylindole). Red fluorescence: Autofluorescence of *I. galbana* chlorophyll *a*. Both images show *O. marina* with several ingested cells of *I. galbana*. Small blue dots in (B) are probably bacteria.

Appendix C. Nutrient Measurements

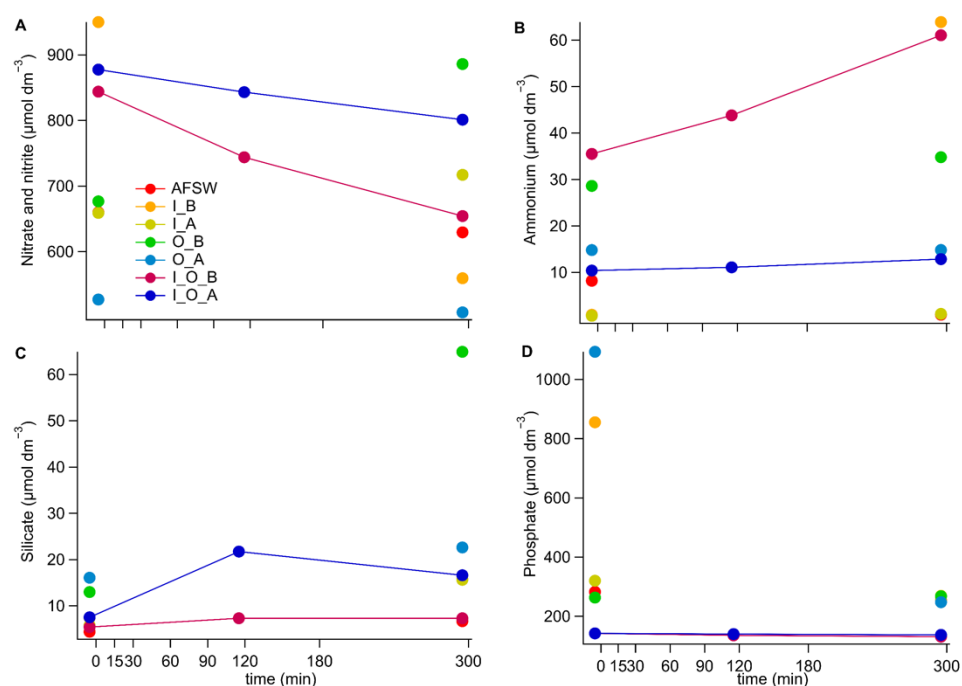


Figure A2. Nutrient concentrations of total nitrate and nitrite (A), ammonium (B), dissolved silicate (C) and phosphate (D) measured in the different cultures over the course of the grazing experiment. The content of the cultures is abbreviated as follows; O: for *O. marina*, I: for *I. galbana*, A: for antibiotic treatment and B: for no antibiotic treatment, AFSW: autoclaved filtered seawater, which is the culture medium for all cultures.

Appendix D. Norisoprenoid Time Series

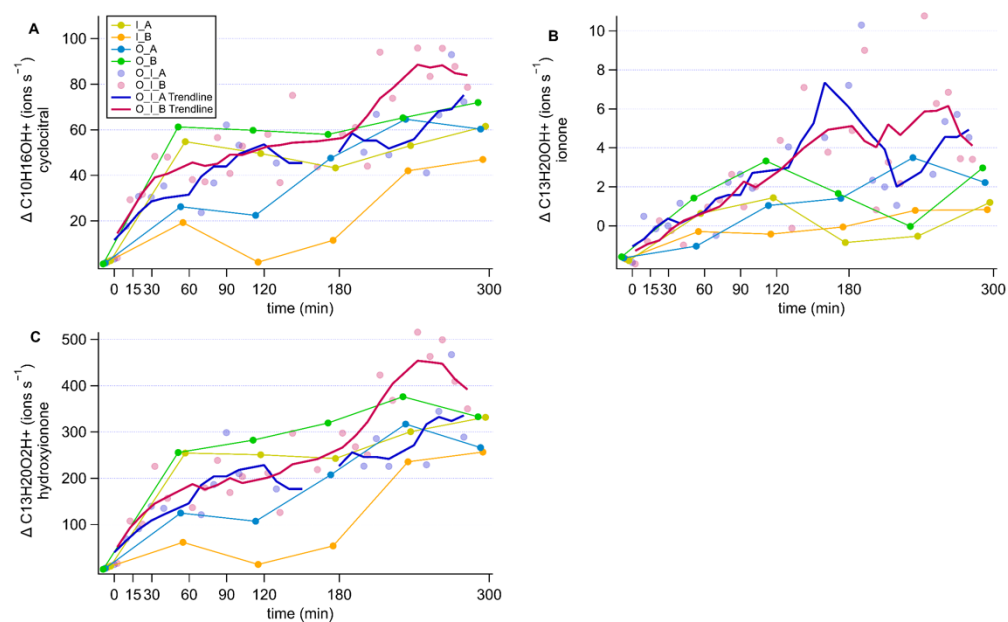


Figure A3. Timeseries of the changes in norisoprenoid concentrations expressed in ions s⁻¹. Each panel represents a different compound; β-cyclocitral (A), β-ionone (B) and hydroxy ionone (C). Components of the culture are abbreviated as; O: *O. marina*, I: *I. galbana*, A: antibiotic treatment, B: no antibiotic treatment.

References

1. Carpenter, L.J.; Archer, S.D.; Beale, R. Ocean-Atmosphere Trace Gas Exchange. *Chem. Soc. Rev.* **2012**, *41*, 6473. <https://doi.org/10.1039/c2cs35121h>.
2. Dixon, J.L.; Hopkins, F.E.; Stephens, J.A.; Schäfer, H. Seasonal Changes in Microbial Dissolved Organic Sulfur Transformations in Coastal Waters. *Microorganisms* **2020**, *8*, 337. <https://doi.org/10.3390/microorganisms8030337>.
3. Sargeant, S.L.; Colin Murrell, J.; Nightingale, P.D.; Dixon, J.L. Basin-Scale Variability of Microbial Methanol Uptake in the Atlantic Ocean. *Biogeosciences* **2018**, *15*, 5155–5167. <https://doi.org/10.5194/bg-15-5155-2018>.
4. Pohnert, G.; Steinke, M.; Tollrian, R. Chemical Cues, Defence Metabolites and the Shaping of Pelagic Interspecific Interactions. *Trends Ecol. Evol.* **2007**, *22*, 198–204. <https://doi.org/10.1016/j.tree.2007.01.005>.
5. Achyuthan, K.E.; Harper, J.C.; Manginell, R.P.; Moorman, M.W. Volatile Metabolites Emission by in Vivo Microalgae—An Overlooked Opportunity? *Metabolites* **2017**, *7*, 39. <https://doi.org/10.3390/metabo7030039>.
6. Zuo, Z. Why Algae Release Volatile Organic Compounds—The Emission and Roles. *Front. Microbiol.* **2019**, *10*, 491. <https://doi.org/10.3389/fmicb.2019.00491>.
7. Jüttner, F.; Watson, S.B.; von Elert, E.; Köster, O. β -Cyclocitral, a Grazer Defence Signal Unique to the Cyanobacterium *Microcystis*. *J. Chem. Ecol.* **2010**, *36*, 1387–1397. <https://doi.org/10.1007/s10886-010-9877-0>.
8. Simó, R.; Saló, V.; Almeda, R.; Movilla, J.; Trepát, I.; Saiz, E.; Calbet, A. The Quantitative Role of Microzooplankton Grazing in Dimethylsulfide (DMS) Production in the NW Mediterranean. *Biogeochemistry* **2018**, *141*, 125–142. <https://doi.org/10.1007/s10533-018-0506-2>.
9. Lawson, C.A.; Seymour, J.R.; Possell, M.; Suggett, D.J.; Raina, J.B. The Volatilomes of *Symbiodiniaceae*-Associated Bacteria Are Influenced by Chemicals Derived From Their Algal Partner. *Front. Mar. Sci.* **2020**, *7*, 106. <https://doi.org/10.3389/fmars.2020.00106>.
10. Romoli, R.; Papaleo, M.C.; De Pascale, D.; Tutino, M.L.; Michaud, L.; Logiudice, A.; Fani, R.; Bartolucci, G. Characterization of the Volatile Profile of Antarctic Bacteria by Using Solid-Phase Microextraction-Gas Chromatography-Mass Spectrometry. *J. Mass Spectrom.* **2011**, *46*, 1051–1059. <https://doi.org/10.1002/jms.1987>.
11. Moore, E.R.; Davie-Martin, C.L.; Giovannoni, S.J.; Halsey, K.H. Pelagibacter Metabolism of Diatom-Derived Volatile Organic Compounds Imposes an Energetic Tax on Photosynthetic Carbon Fixation. *Environ. Microbiol.* **2020**, *22*, 1720–1733. <https://doi.org/10.1111/1462-2920.14861>.
12. Reese, K.L.; Rasley, A.; Avila, J.R.; Jones, A.D.; Frank, M. Metabolic Profiling of Volatile Organic Compounds (VOCs) Emitted by the Pathogens *Francisella Tularensis* and *Bacillus Anthracis* in Liquid Culture. *Sci. Rep.* **2020**, *10*, 9333. <https://doi.org/10.1038/s41598-020-66136-0>.
13. Koteska, D.; Sanchez Garcia, S.; Wagner-Döbler, I.; Schulz, S. Identification of Volatiles of the Dinoflagellate *Prorocentrum Cordatum*. *Mar. Drugs* **2022**, *20*, 371. <https://doi.org/10.3390/md20060371>.
14. Deore, P.; Beardall, J.; Noronha, S. A Perspective on the Current Status of Approaches for Early Detection of Microalgal Grazing. *J. Appl. Phycol.* **2020**, *32*, 3723–3733. <https://doi.org/10.1007/s10811-020-02241-x>.
15. Fisher, C.L.; Lane, P.D.; Russell, M.; Maddalena, R.; Lane, T.W. Low Molecular Weight Volatile Organic Compounds Indicate Grazing by the Marine Rotifer *Brachionus Plicatilis* on the Microalgae *Microchloropsis Salina*. *Metabolites* **2020**, *10*, 1–20. <https://doi.org/10.3390/metabo10090361>.
16. Sauer, J.S.; Simkovsky, R.; Moore, A.N.; Camarda, L.; Sherman, S.L.; Prather, K.A.; Pomeroy, R.S. Continuous Measurements of Volatile Gases as Detection of Algae Crop Health. *Proc. Natl. Acad. Sci. USA* **2021**, *118*, e2106882118. <https://doi.org/10.1073/pnas.2106882118>.
17. Reese, K.L.; Fisher, C.L.; Lane, P.D.; Jaryenneh, J.D.; Jones, A.D.; Frank, M.; Lane, T.W. Abiotic and Biotic Damage of Microalgae Generate Different Volatile Organic Compounds (Vocs) for Early Diagnosis of Algal Cultures for Biofuel Production. *Metabolites* **2021**, *11*, 707. <https://doi.org/10.3390/metabo11100707>.
18. Reese, K.L.; Fisher, C.L.; Lane, P.D.; Jaryenneh, J.D.; Moorman, M.W.; Jones, A.D.; Frank, M.; Lane, T.W. Chemical Profiling of Volatile Organic Compounds in the Headspace of Algal Cultures as Early Biomarkers of Algal Pond Crashes. *Sci. Rep.* **2019**, *9*, 13866. <https://doi.org/10.1038/s41598-019-50125-z>.
19. Nguyen, D.D.; Sauer, J.S.; Camarda, L.P.; Sherman, S.L.; Prather, K.A.; Golden, S.S.; Pomeroy, R.; Dorrestein, P.C.; Simkovsky, R. Grazer-Induced Changes in Molecular Signatures of Cyanobacteria. *Algal Res.* **2022**, *61*, 102575. <https://doi.org/10.1016/j.algal.2021.102575>.
20. Havaux, M. β -Cyclocitral and Derivatives: Emerging Molecular Signals Serving Multiple Biological Functions. *Plant Physiol. Biochem.* **2020**, *155*, 35–41. <https://doi.org/10.1016/j.plaphy.2020.07.032>.
21. Watson, S.B.; Jüttner, F.; Köster, O. Daphnia Behavioural Responses to Taste and Odour Compounds: Ecological Significance and Application as an Inline Treatment Plant Monitoring Tool. *Water Sci. Technol.* **2007**, *55*, 23–31. <https://doi.org/10.2166/wst.2007.158>.
22. Simó, R. Production of Atmospheric Sulfur by Oceanic Plankton: Biogeochemical, Ecological and Evolutionary Links. *Trends Ecol. Evol.* **2001**, *16*, 287–294. [https://doi.org/10.1016/S0169-5347\(01\)02152-8](https://doi.org/10.1016/S0169-5347(01)02152-8).

23. Keller, M.D. Dimethyl Sulfide Production and Marine Phytoplankton: The Importance of Species Composition and Cell Size. *Biol. Oceanogr.* **1988**, *6*, 375–382. <https://doi.org/10.1080/01965581.1988.10749540>.
24. McParland, E.L.; Levine, N.M. The Role of Differential DMSP Production and Community Composition in Predicting Variability of Global Surface DMSP Concentrations. *Limnol. Oceanogr.* **2019**, *64*, 757–773. <https://doi.org/10.1002/lno.11076>.
25. Stefels, J.; Steinke, M.; Turner, S.; Malin, G.; Belviso, S. Environmental Constraints on the Production and Removal of the Climatically Active Gas Dimethylsulphide (DMS) and Implications for Ecosystem Modelling. *Biogeochemistry* **2007**, *83*, 245–275. <https://doi.org/10.1007/s10533-007-9091-5>.
26. Archer, S.D.; Gilbert, F.J.; Nightingale, P.D.; Zubkov, M.V.; Taylor, A.H.; Smith, G.C.; Burkill, P.H. Transformation of Dimethylsulphonioacetate to Dimethyl Sulphide during Summer in the North Sea with an Examination of Key Processes via a Modelling Approach. *Deep-Sea Res. Part II* **2002**, *49*, 3067–3101. [https://doi.org/10.1016/S0967-0645\(02\)00072-3](https://doi.org/10.1016/S0967-0645(02)00072-3).
27. Stefels, J. Physiological Aspects of the Production and Conversion of DMSP in Marine Algae and Higher Plants. *J. Sea Res.* **2000**, *43*, 183–197. [https://doi.org/10.1016/S1385-1101\(00\)00030-7](https://doi.org/10.1016/S1385-1101(00)00030-7).
28. Li, C.; Yang, G.; Pan, J.; Zhang, H. Experimental Studies on Dimethylsulfide (DMS) and Dimethylsulfoniopropionate (DMSP) Production by Four Marine Microalgae. *Acta Oceanol. Sin.* **2010**, *29*, 78–87. <https://doi.org/10.1007/s13131-010-0052-9>.
29. Breckels, M.N.; Roberts, E.C.; Archer, S.D.; Malin, G.; Steinke, M. The Role of Dissolved Infochemicals in Mediating Predator-Prey Interactions in the Heterotrophic Dinoflagellate *Oxyrrhis Marina*. *J. Plankton Res.* **2011**, *33*, 629–639. <https://doi.org/10.1093/plankt/fbq114>.
30. Seymour, J.; Simó, R.; Ahmed, T.; Stocker, R. Chemoattraction to Dimethylsulfoniopropionate Throughout the Marine Microbial Food Web. *Science* **2010**, *329*, 342–345. <https://doi.org/10.1126/science.1188418>.
31. Teng, Z.J.; Qin, Q.L.; Zhang, W.; Li, J.; Fu, H.H.; Wang, P.; Lan, M.; Luo, G.; He, J.; McMin, A.; et al. Biogeographic Traits of Dimethyl Sulfide and Dimethylsulfoniopropionate Cycling in Polar Oceans. *Microbiome* **2021**, *9*, 207. <https://doi.org/10.1186/s40168-021-01182-y>.
32. Kiene, R.P. Production of Methanethiol from Dimethylsulfoniopropionate in Marine Surface Waters. *Mar. Chem.* **1996**, *54*, 69–83. [https://doi.org/10.1016/0304-4203\(96\)00006-0](https://doi.org/10.1016/0304-4203(96)00006-0).
33. Kiene, R.P.; Linn, L.J. The Fate of Dissolved Dimethylsulfoniopropionate (DMSP) in Seawater: Tracer Studies Using ³⁵S-DMSP. *Geochim. Cosmochim. Acta* **2000**, *64*, 2797–2810. [https://doi.org/10.1016/S0016-7037\(00\)00399-9](https://doi.org/10.1016/S0016-7037(00)00399-9).
34. Wirth, J.S.; Wang, T.; Huang, Q.; White, R.H.; Whitman, W.B. Dimethylsulfoniopropionate Sulfur and Methyl Carbon Assimilation in *Ruegeria* Species. *mBio* **2020**, *11*, e00329-20. <https://doi.org/10.1128/mBio.00329-20>.
35. Sun, J.; Todd, J.D.; Thrash, J.C.; Qian, Y.; Qian, M.C.; Temperton, B.; Guo, J.; Fowler, E.K.; Aldrich, J.T.; Nicora, C.D.; et al. The Abundant Marine Bacterium *Pelagibacter* Simultaneously Catabolizes Dimethylsulfoniopropionate to the Gases Dimethyl Sulfide and Methanethiol. *Nat. Microbiol.* **2016**, *1*, 6–11. <https://doi.org/10.1038/nmicrobiol.2016.65>.
36. Kilgour, D.B.; Novak, G.A.; Sauer, J.S.; Moore, A.N.; Dinasquet, J.; Amiri, S.; Franklin, E.B.; Mayer, K.; Winter, M.; Morris, C.K.; et al. Marine Gas-Phase Sulfur Emissions during an Induced Phytoplankton Bloom. *Atmos. Chem. Phys.* **2022**, *22*, 1601–1613. <https://doi.org/10.5194/acp-22-1601-2022>.
37. Novak, G.A.; Kilgour, D.B.; Jernigan, C.M.; Vermeuel, M.P.; Bertram, T.H. Oceanic Emissions of Dimethyl Sulfide and Methanethiol and Their Contribution to Sulfur Dioxide Production in the Marine Atmosphere. *Atmos. Chem. Phys.* **2022**, *22*, 6309–6325. <https://doi.org/10.5194/acp-22-6309-2022>.
38. Lawson, S.J.; Law, C.S.; Harvey, M.J.; Bell, T.G.; Walker, C.F.; De Bruyn, W.J.; Saltzman, E.S. Methanethiol, Dimethyl Sulfide and Acetone over Biologically Productive Waters in the Southwest Pacific Ocean. *Atmos. Chem. Phys.* **2020**, *20*, 3061–3078. <https://doi.org/10.5194/acp-20-3061-2020>.
39. Gros, V.; Bonsang, B.; Sarda-Estève, R.; Nikolopoulos, A.; Metfies, K.; Wietz, M.; Peeken, I. Concentrations of dissolved dimethyl sulfide (DMS), methanethiol and other trace gases in context of microbial communities from the temperate Atlantic to the Arctic Ocean. *Biogeosciences* **2022**, *20*, 851–867. <https://doi.org/10.5194/bg-20-851-2023>, 2023.
40. Kiene, R.P.; Bates, T.S. Biological Removal of Dimethyl Sulphide from Sea Water. *Nature* **1990**, *345*, 702–705. <https://doi.org/10.1038/258748a0>.
41. Simo, R.; Pedros-Alio, C.; Malin, G.; Grimalt, J.O. Biological Turnover of DMS, DMSP and DMSO in Contrasting Open-Sea Waters. *Mar. Ecol. Prog. Ser.* **2000**, *203*, 1–11. <https://doi.org/10.3354/meps203001>.
42. Rocco, M.; Dunne, E.; Peltola, M.; Barr, N.; Williams, J.; Colomb, A.; Safi, K.; Saint-Macary, A.; Marriner, A.; Deppeler, S.; et al. Oceanic Phytoplankton Are a Potentially Important Source of Benzenoids to the Remote Marine Atmosphere. *Commun. Earth Environ.* **2021**, *2*, 175. <https://doi.org/10.1038/s43247-021-00253-0>.
43. Sauer, T.C. Volatile Organic Compounds in Open Ocean and Coastal Surface Waters. *Org. Geochem.* **1981**, *3*, 91–101. [https://doi.org/10.1016/0146-6380\(81\)90003-6](https://doi.org/10.1016/0146-6380(81)90003-6).

44. Wohl, C.; Li, Q.; Cuevas, C.A.; Fernandez, R.P.; Yang, M.; Saiz-Lopez, A.; Simó, R. Marine Biogenic Emissions of Benzene and Toluene and Their Contribution to Secondary Organic Aerosols over the Polar Oceans. *Sci. Adv.* **2023**, *9*, eadd9031. <https://doi.org/10.1126/sciadv.add9031>.
45. Lemfack, M.C.; Gohlke, B.O.; Toguem, S.M.T.; Preissner, S.; Piechulla, B.; Preissner, R. MVOC 2.0: A Database of Microbial Volatiles. *Nucleic Acids Res.* **2018**, *46*, D1261–D1265. <https://doi.org/10.1093/nar/gkx1016>.
46. Beller, H.R.; Rodrigues, A.V.; Zargar, K.; Wu, Y.W.; Saini, A.K.; Saville, R.M.; Pereira, J.H.; Adams, P.D.; Tringe, S.G.; Petzold, C.J.; et al. Discovery of Enzymes for Toluene Synthesis from Anoxic Microbial Communities. *Nat. Chem. Biol.* **2018**, *14*, 451–457. <https://doi.org/10.1038/s41589-018-0017-4>.
47. Cabrera-Perez, D.; Taraborrelli, D.; Sander, R.; Pozzer, A. Global Atmospheric Budget of Simple Monocyclic Aromatic Compounds. *Atmos. Chem. Phys.* **2016**, *16*, 6931–6947. <https://doi.org/10.5194/acp-16-6931-2016>.
48. Kansal, A. Sources and Reactivity of NMHCs and VOCs in the Atmosphere: A Review. *J. Hazard. Mater.* **2009**, *166*, 17–26. <https://doi.org/10.1016/j.jhazmat.2008.11.048>.
49. Khalid, F.E.; Lim, Z.S.; Sabri, S.; Gomez-Fuentes, C.; Zulkharnain, A.; Ahmad, S.A. Bioremediation of Diesel Contaminated Marine Water by Bacteria: A Review and Bibliometric Analysis. *J. Mar. Sci. Eng.* **2021**, *9*, 155. <https://doi.org/10.3390/jmse9020155>.
50. Han, D.; Ma, W.; Chen, D. Determination of Biodegradation Process of Benzene, Toluene, Ethylbenzene and Xylenes in Seabed Sediment by Purge and Trap Gas Chromatography. *Chin. J. Anal. Chem.* **2006**, *34*, 1361–1365. [https://doi.org/10.1016/S1872-2040\(07\)60006-1](https://doi.org/10.1016/S1872-2040(07)60006-1).
51. Wakeham, S.G.; Canuel, E.A.; Doering, P.H. Geochemistry of Volatile Organic Compounds in Seawater: Mesocosm Experiments with ¹⁴C-Model Compounds. *Geochim. Cosmochim. Acta* **1986**, *50*, 1163–1172. [https://doi.org/10.1016/0016-7037\(86\)90399-6](https://doi.org/10.1016/0016-7037(86)90399-6).
52. Liu, H.; Probert, I.; Uitz, J.; Claustre, H.; Aris-Brosou, S.; Frada, M.; Not, F.; de Vargas, C. Extreme Diversity in Noncalcifying Haptophytes Explains a Major Pigment Paradox in Open Oceans. *Proc. Natl. Acad. Sci. USA* **2009**, *106*, 12803–12808. <https://doi.org/10.1073/pnas.0905841106>.
53. Niki, T.; Kunugi, M.; Otsuki, A. DMSP-Lyase Activity in Five Marine Phytoplankton Species: Its Potential Importance in DMS Production. *Mar. Biol.* **2000**, *136*, 759–764. <https://doi.org/10.1007/s002279900235>.
54. Montagnes, D.J.S.; Lowe, C.D.; Roberts, E.C.; Breckels, M.N.; Boakes, D.E.; Davidson, K.; Keeling, P.J.; Slamovits, C.H.; Steinke, M.; Yang, Z.; et al. An Introduction to the Special Issue: *Oxyrrhis Marina*, a Model Organism? *J. Plankton Res.* **2011**, *33*, 549–554. <https://doi.org/10.1093/plankt/fbq121>.
55. Calbet, A.; Isari, S.; Martínez, R.A.; Saiz, E.; Garrido, S.; Peters, J.; Borrat, R.M.; Alcaraz, M. Adaptations to Feast and Famine in Different Strains of the Marine Heterotrophic Dinoflagellates *Gyrodinium Dominans* and *Oxyrrhis Marina*. *Mar. Ecol. Prog. Ser.* **2013**, *483*, 67–84. <https://doi.org/10.3354/meps10291>.
56. Wolfe, G.V.; Sherr, E.B.; Sherr, B.F. Release and Consumption of DMSP from *Emiliania Huxleyi* during Grazing by *Oxyrrhis Marina*. *Mar. Ecol. Prog. Ser.* **1994**, *111*, 111–120. <https://doi.org/10.3354/meps111111>.
57. Keller, M.D.; Korjoff-Bellows, W. Physiological Aspects of the Production of Dimethylsulfoniopropionate (DMSP) by Marine Phytoplankton. *Biol. Environ. Chem. DMSP Relat. Sulfonium Compd.* **1996**, 131–142, doi:10.1007/978-1-4613-0377-0_12.
58. Krechmer, J.; Lopez-Hilfiker, F.; Koss, A.; Hutterli, M.; Stoermer, C.; Deming, B.; Kimmel, J.; Warneke, C.; Holzinger, R.; Jayne, J.; et al. Evaluation of a New Reagent-Ion Source and Focusing Ion-Molecule Reactor for Use in Proton-Transfer-Reaction Mass Spectrometry. *Anal. Chem.* **2018**, *90*, 12011–12018. <https://doi.org/10.1021/acs.analchem.8b02641>.
59. Wohl, C.; Capelle, D.; Jones, A.; Sturges, W.T.; Nightingale, P.D.; Else, B.G.T.; Yang, M. Segmented Flow Coil Equilibrator Coupled to a Proton Transfer Reaction Mass Spectrometer for Measurements of a Broad Range of Volatile Organic Compounds in Seawater. *Ocean Sci.* **2019**, *15*, 925–940. <https://doi.org/10.5194/os-15-925-2019>.
60. Schober, P.; Vetter, T.R. Repeated Measures Designs and Analysis of Longitudinal Data: If at First You Do Not Succeed—Try, Try Again. *Anesth. Analg.* **2018**, *127*, 569–575. <https://doi.org/10.1213/ANE.0000000000003511>.
61. Zehr, J.P.; Kudela, R.M. Nitrogen Cycle of the Open Ocean: From Genes to Ecosystems. *Annu. Rev. Mar. Sci.* **2011**, *3*, 197–225. <https://doi.org/10.1146/annurev-marine-120709-142819>.
62. Pajares, S.; Ramos, R. Processes and Microorganisms Involved in the Marine Nitrogen Cycle: Knowledge and Gaps. *Front. Mar. Sci.* **2019**, *6*, 739. <https://doi.org/10.3389/fmars.2019.00739>.
63. Pagonis, D.; Sekimoto, K.; de Gouw, J. A Library of Proton-Transfer Reactions of H₃O⁺ Ions Used for Trace Gas Detection. *J. Am. Soc. Mass Spectrom.* **2019**, *30*, 1330–1335. <https://doi.org/10.1007/s13361-019-02209-3>.
64. Weisel, C.P.; Alimokhtari, S.; Sanders, P.F. Indoor Air VOC Concentrations in Suburban and Rural New Jersey. *Environ. Sci. Technol.* **2008**, *42*, 8231–8238. <https://doi.org/10.1021/es8005223>.

65. Carrión, O.; Pratscher, J.; Curson, A.R.J.; Williams, B.T.; Rostant, W.G.; Colin Murrell, J.; Todd, J.D. Methanethiol-Dependent Dimethylsulfide Production in Soil Environments. *ISME J.* **2017**, *11*, 2379–2390. <https://doi.org/10.1038/ismej.2017.105>.
66. García-Plazaola, J.I.; Portillo-Estrada, M.; Fernández-Marín, B.; Kännaste, A.; Niinemets, Ü. Emissions of Carotenoid Cleavage Products upon Heat Shock and Mechanical Wounding from a Foliose Lichen. *Environ. Exp. Bot.* **2017**, *133*, 87–97. <https://doi.org/10.1016/j.envexpbot.2016.10.004>.
67. Peinado, I.; Mason, M.; Romano, A.; Biasioli, F.; Scampicchio, M. Stability of β -Carotene in Polyethylene Oxide Electrospun Nanofibers. *Appl. Surf. Sci.* **2016**, *370*, 111–116. <https://doi.org/10.1016/j.apsusc.2016.02.150>.
68. de Bruyn, W.J.; Clark, C.D.; Harrison, A.W.; Senstad, M.; Hok, S. The Degradation of Acetaldehyde in Estuary Waters in Southern California, USA. *Environ. Sci. Pollut. Res.* **2021**, *28*, 35811–35821. <https://doi.org/10.1007/s11356-021-13232-x>.
69. Herr, A.E.; Kiene, R.P.; Dacey, J.W.H.; Tortell, P.D. Patterns and Drivers of Dimethylsulfide Concentration in the Northeast Subarctic Pacific across Multiple Spatial and Temporal Scales. *Biogeosciences* **2019**, *16*, 1729–1754. <https://doi.org/10.5194/bg-16-1729-2019>.
70. Kameyama, S.; Hiroshi Tanimoto, T.; Inomata, S.; Suzuki, K.; Komatsu, D.D.; Hirota, A.; Konno, U.; Tsunogai, U. Application of PTR-MS to an Incubation Experiment of the Marine Diatom *Thalassiosira Pseudonana*. *Geochim. J.* **2011**, *45*, 355–363. <https://doi.org/10.2343/geochemj.1.0127>.
71. Davie-Martin, C.L.; Giovannoni, S.J.; Behrenfeld, M.J.; Penta, W.B.; Halsey, K.H. Seasonal and Spatial Variability in the Biogenic Production and Consumption of Volatile Organic Compounds (VOCs) by Marine Plankton in the North Atlantic Ocean. *Front. Mar. Sci.* **2020**, *7*, 611870. <https://doi.org/10.3389/fmars.2020.611870>.
72. Deming, B.L.; Pagonis, D.; Liu, X.; Day, D.A.; Talukdar, R.; Krechmer, J.E.; De Gouw, J.A.; Jimenez, J.L.; Ziemann, P.J. Measurements of Delays of Gas-Phase Compounds in a Wide Variety of Tubing Materials Due to Gas–Wall Interactions. *Atmos. Meas. Tech.* **2019**, *12*, 3453–3461.
73. Pagonis, D.; Krechmer, J.E.; De Gouw, J.; Jimenez, J.L.; Ziemann, P.J.; De Gouw, J.; Jimenez, J.L.; Ziemann, P.J. Effects of Gas–Wall Partitioning in Teflon Tubing and Instrumentation on Time-Resolved Measurements of Gas-Phase Organic Compounds. *Atmos. Meas. Tech.* **2017**, *10*, 4687–4696. <https://doi.org/10.5194/amt-10-4687-2017>.
74. Jeong, H.J.; Seong, K.A.; Yoo, Y.D.; Kim, T.H.; Kang, N.S.; Kim, S.; Park, J.Y.; Kim, J.S.; Kim, G.H.; Song, J.Y. Feeding and Grazing Impact by Small Marine Heterotrophic Dinoflagellates on Heterotrophic Bacteria. *J. Eukaryot. Microbiol.* **2008**, *55*, 271–288. <https://doi.org/10.1111/j.1550-7408.2008.00336.x>.
75. Saló, V.; Simó, R.; Vila-Costa, M.; Calbet, A. Sulfur Assimilation by *Oxyrrhis Marina* Feeding on a ^{35}S -DMSP-Labelled Prey. *Environ. Microbiol.* **2009**, *11*, 3063–3072. <https://doi.org/10.1111/j.1462-2920.2009.02011.x>.
76. Materić, D.; Lanza, M.; Sulzer, P.; Herbig, J.; Bruhn, D.; Gauci, V.; Mason, N.; Turner, C. Selective Reagent Ion-Time of Flight-Mass Spectrometry Study of Six Common Monoterpenes. *Int. J. Mass Spectrom.* **2017**, *421*, 40–50. <https://doi.org/10.1016/j.ijms.2017.06.003>.
77. de Gouw, J.A.; Warneke, C. Measurements of Volatile Organic Compounds In the Earth's Atmosphere Using Proton-Transfer-Reaction Mass Spectrometry. *Mass Spectrom. Rev.* **2007**, *26*, 223–257. <https://doi.org/10.1002/mas>.
78. Yáñez-Serrano, A.M.; Filella, I.; LLusià, J.; Gargallo-Garriga, A.; Granda, V.; Bourtsoukidis, E.; Williams, J.; Seco, R.; Cappellin, L.; Werner, C.; et al. GLOVOCs—Master Compound Assignment Guide for Proton Transfer Reaction Mass Spectrometry Users. *Atmos. Environ.* **2021**, *244*, 117929. <https://doi.org/10.1016/j.atmosenv.2020.117929>.
79. Zhao, J.; Zhang, R. Proton Transfer Reaction Rate Constants between Hydronium Ion (H_3O^+) and Volatile Organic Compounds. *Atmos. Environ.* **2004**, *38*, 2177–2185. <https://doi.org/10.1016/j.atmosenv.2004.01.019>.
80. Sander, R. Compilation of Henry's Law Constants (Version 4.0) for Water as Solvent. *Atmos. Chem. Phys.* **2015**, *15*, 4399–4981. <https://doi.org/10.5194/acp-15-4399-2015>.
81. Karl, T.; Yeretzyan, C.; Jordan, A.; Lindinger, W. Dynamic Measurements of Partition Coefficients Using Proton-Transfer-Reaction Mass Spectrometry (PTR-MS). *Int. J. Mass Spectrom.* **2003**, *223*, 383–395.
82. Staudinger, J.; Roberts, P.V. A Critical Compilation of Henry's Law Constant Temperature Dependence Relations for Organic Compounds in Dilute Aqueous Solutions. *Chemosphere* **2001**, *44*, 561–576. [https://doi.org/10.1016/S0045-6535\(00\)00505-1](https://doi.org/10.1016/S0045-6535(00)00505-1).
83. Burkholder, J.B.; Sander, S.P.; Abbatt, J.P.D.; Barker, J.R.; Huie, R.E.; Kolb, C.E.; Kurylo, M.J.; Orkin, V.L.; Wilmouth, D.M.; Wine, P.H.; et al. *Chemical Kinetics and Photochemical Data for Use in Atmospheric Studies, Evaluation No. 19*; JPL Publications: Pasadena, CA, USA, 2019; Volume 15–10, pp. 5–153.
84. Liss, P.S.; Slater, P.G. Flux of Gases across the Air-Sea Interface. *Nature* **1974**, *247*, 181–184. <https://doi.org/10.1038/247181a0>.

Disclaimer/Publisher's Note: The statements, opinions and data contained in all publications are solely those of the individual author(s) and contributor(s) and not of MDPI and/or the editor(s). MDPI and/or the editor(s) disclaim responsibility for any injury to people or property resulting from any ideas, methods, instructions or products referred to in the content.